The role of the Vip1 kinase family member Asp1 in the morphogenesis of the fission yeast *Schizosaccharomyces pombe*

Inaugural dissertation

for the attainment of the title of doctor

in the Faculty of Mathematics and Natural Sciences

at the Heinrich Heine University Düsseldorf

presented by

Anand Babu Vangala

from Kazipeta, India

Düsseldorf, July 2018

from the Institute for Functional Genome Research of Microorganisms, Eukaryotic Microbiology

at the Heinrich Heine University Düsseldorf

Published by permission of the
Faculty of Mathematics and Natural Sciences at
Heinrich Heine University Düsseldorf

Supervisor: Prof. Dr. Ursula Nicole Fleig
Co-supervisor: Prof. Dr. Johannes Hegemann

Date of oral examination:

Contents

Summary
1. Introduction 8
1.1 Fungi - a boon and a bane 9
1.2 Fungal morphogenesis 10
1.2.1 Morphogenesis in yeast cell form 10
1.2.2 Morphogenesis in hyphal growth form 11
1.3 The fission yeast *Schizosaccharomyces pombe* as a model organism 12
1.4 Polarized growth in *S. pombe* 13
1.5 Morphogenetic machinery essential for morphogenesis 14
1.5.1 Role of the cytoskeleton in fungal morphogenesis 14
1.5.2 Role of landmark proteins and polarity factors in morphogenesis 16
1.5.3 Signal transduction associated with morphogenesis in fungi 16
1.6 Morphogenic machinery in *S. pombe* 17
1.7 Fungal dimorphism as an important pathogenic trait 19
1.7.1 Environmental factors that regulate dimorphism/dimorphic switch 20
1.8 Dimorphic switch in *S. pombe* and the signaling pathway required for the switch 22
1.9 Adhesins facilitate adhesion or adherence to the substrate or host tissues 23
1.10 Adhesins and the transcriptional network that govern *S. pombe* adhesion and invasion 25
1.11 What are Inositol pyrophosphates? 27
1.11.1 Structure of inositol pyrophosphates 27
1.11.2 Intracellular generation of inositol pyrophosphates 28
1.11.3 Modes of operations of inositol pyrophosphates 31
1.11.4 Inositol pyrophosphates are involved in diverse cellular functions 32
1.11.5 Structure of Vip1 kinases 34
1.11.6 Asp1 variants generated different levels of inositol pyrophosphates 37
1.11.7 Inositol pyrophosphate levels influence several cellular processes in *S. pombe* 39
1.12 Aim of this work 41
2. Materials and Methods 36
2.1. Reagents 37
2.2. Restriction endonucleases 38
2.3. Other enzymes 39
2.4. Equipment 39

2.5. Kits 39
2.6. Other materials and Plastic wear 39
2.7. Plasmids 40
2.8. Strains 42
2.8.1 *S. pombe* strains 42
2.8.2. *S. cerevisiae* strains 47
2.8.3. *E. coli* Strain 47
2.9. Oligo Nucleotides 47
2.10. Antibodies 52
2.11. Media and growth conditions for *S. pombe* 52
2.12. Media and growth conditions for *S. cerevisiae* 54
2.13. DNA methods 55
2.14. Transformation of *E. coli* 56
2.15. Plasmid isolation from *E. coli* 56
2.16 PCR 57
2.17 *In vitro* ligation 57
2.18. Yeast transformation methods: *S. pombe* 58
2.19 *S. cerevisiae* plasmid isolation 59
2.20 Mating of *S. pombe* 60
2.21 Random spore analysis 60
2.22. Tetrad analysis 60
2.23 Invasive growth analysis 61
2.24. Yeast two hybrid 61
2.25 Protein extraction from *S. pombe* 62
2.26 Determination of protein concentration using Bradford's assay 62
2.27. Strain construction 63
2.28. Luciferase assays 64
3. Results 66
3.1 Extrinsic signals that govern invasive growth 67
3.1.1. Lower temperatures induce the formation of invasively forming colonies 68
3.1.2. Excess iron induces invasive colonies in the absence of Asp1 70
3.1.3. Different growth media did not influence the number of invasive colonies 72
3.2. Inositol pyrophosphates levels and invasive growth 74

3.2.1. Intracellular 1,5-IP_8 levels are correlated with the number of invasive colonies ...74
3.2.2 Expression of *asp1*$^+$ and *asp1*$^{1-364}$ by *nmt1*$^+$ promoter variants ...74
3.2.3 The *asp1*$^+$ and *asp*$^{1-364}$ are differentially expressed by *nmt1*$^+$ promoter variants ...74
3.2.4 IPP levels generated by *asp1*$^{1-364}$ has to be altered for increased invasive growth .76
3.2.5 Invasive growth assay as a dissection of the Asp1 pyrophosphatase function ...79
3.3 Potential targets of Asp1 and invasive growth ...85
3.3.1 Adhesins ...85
3.3.2. Adhesin Gsf2 is a possible target of Asp1 ...85
3.3.3 Increase of *gsf2*$^+$ levels alter the number of invasively growing colonies ...88
3.3.4 Positive regulators of the adhesin Gsf2 expression are required for invasive growth ...90
3.3.5 Asp1 generated 1,5-IP_8 regulate the Gsf2 expression level ...94
3.3.6 The *gsf2*$^+$ promoter is inactive by the expression of *asp1*$^{365-920}$ ...96
3.3.7 Asp1 regulate the *gsf2*$^+$ expression level analyzed by Luciferase assay ...98
3.4 Asp1 interacts with four proteins in a yeast two-hybrid screen ...100
3.4.1 Asp1 does not interact with Asp1$^{1-364}$ and Asp1$^{365-920}$ domain ...100
3.4.2 Yeast two-hybrid screen identified four potential interactors ...101
3.4.3 SPAC1071.05: histidine protein methyltransferase ...102
3.4.4 Met10 interacts with Asp1 and *met10*Δ strain displayed increased invasive growth ...104
3.4.5 Absence of Asp1 generated 1,5-IP_8 increase the heat tolerance ...106
3.4.6 SPBC725.03 pyridoxamine 5'- phosphate oxidase ...109
3.4.7 SPCC4B3.05c uroporphyrinogen decarboxylase (Hem12) ...111
4. Discussion ...113
4.1 Inositol pyrophosphates are essential for morphogenesis ...114
4.2 Environmental stress govern the dimorphic switch in fungi ...114
4.3 Intracellular inositol pyrophosphate levels regulate the frequency of invasive colonies ...118
4.4 Gsf2 adhesin promoter activity is regulated by the intracellular levels of 1,5-IP_8 ...122
4.5 The *hpm1*Δ, *hem12*Δ strains displayed no difference in number of invasive colonies 125
4.5.1 The *met10*Δ strain exhibited an increased in the number of invasive colonies ...126
5. References ...128
6. Abbreviations ...143
7. List of Figures ...145

8. List of Tables 147
9. Publications 148
10. Acknowledgements 149
11. Statutory Declaration 151

Summary

The medical advancements in the last decades like, treatment of cancer by chemotherapy and the management of organ transplantation via immune suppressive medication have led to a massive increase of serious infections by pathogenic fungi. A vital virulence trait of life-threatening pathogenic fungi is their ability to undergo morphological transitions in response to external clues. Such an alteration in growth form is a conserved feature present in all fungi including the non-pathogenic model yeasts. Thus, elucidation of conserved molecular pathways essential for the dimorphic switch will contribute to understand fungal virulence mechanisms.

We have used the fission yeast *Schizosaccharomyces pombe* to identify the molecular regulators of this switch and were the first to demonstrate that **i**nositol **p**yro**p**hosphates (IPPs) generated by the Asp1 protein are essential for the dimorphic switch. Inositol pyrophosphates are conserved high energy signaling molecules. Asp1-like proteins are present in all eukaryotes and possess a dual domain structure consisting of an N-terminal "rimK"/ATP-grasp superfamily domain that generates 1,5-IP_8 and a C-terminal domain with pyrophosphatase activity that specifically dephosphorylates 1,5-IP_8 to 5-IP_7. IPPs regulate a variety of cellular activities ranging from the human antiviral response to plant defense mechanisms against pathogens. It was shown that a correlation exists between the amount of 1,5-IP_8 and the ability to switch. In the current study, it was identified that lower temperature and iron at toxic concentrations together with nutrient limitation can enhance the switching process.To understand exactly how 1,5-IP_8 regulate the dimorphic switch, I analyzed adhesins as possible targets and identified the adhesin Gsf2 as one of the essential components required for Asp1 mediated dimorphic switch. Upregulation of *gsf2*$^+$ increased the number of invasively growing colonies, but only in the presence of 1,5-IP_8. Next, it was analyzed, if 1,5-IP_8 regulate Gsf2 adhesin expression, and later identified to be true. The absence of cellular 1,5-IP_8 negatively influenced *gsf2*$^+$ expression and higher levels positively influenced *gsf2*$^+$ expression. All the transcriptional activators that regulate Gsf2 adhesin are identified to be essential for the Asp1 mediated dimorphic switch. A yeast two-hybrid screen identified that, Met10 interacts with Asp1 and negatively regulates Asp1 pyrophosphatase activity *in vitro* and localizes to mitochondria *in vivo*. Surprisingly *met10Δ* strain did not show any difference in the IP_8 levels *in vivo*. It can be hypothesized that Met10 acts as a negative regulator upstream of Asp1 to regulate the dimorphic switch as *met10Δ* strain showed enhanced number of invasively growing colonies.

1. Introduction

1.1 Fungi - a boon and a bane

Fungi form a distinct kingdom apart from animals and plants. Plants produce energy through photosynthesis whereas, animals get energy by consuming these plants. Fungi derive nutrients through very distinct processes by degrading both animals and plants (mainly saprophytes). This contributes to the maintenance and balance of ecosystems, nutrients and carbon cycling. Fungi directly became a part of our life, as fungi are found in most of the foods, we eat such as cheese, bread, and edible mushrooms and indirectly by utilizing the products produced by them after fermentation. Furthermore, these fungi are a significant source of medical products such as antibiotics; the first discovered antibiotic penicillin was produced in fungi. Fungi are beneficial for food and other products such as commercial dyes. Fungi vary widely in size and shape, from unicellular, microscopic organisms to the largest organism present on earth today.

Although fungi are beneficial for mankind in several ways, they can also be life-threatening. In the recent decades, severe systemic fungal infections have increased exponentially. Development of clinical treatments such as organ transplantation, cancer therapy by use of immunosuppressive agents and large spectrum antibiotics are associated with an increasing threat to fungal infections. Resistance to antifungal drugs is mainly caused by the frequent use of antifungal therapies (Perfect & Casadevall, 2006, d'Enfert & Hube, 2007). In immunocompromised patient's opportunistic pathogenic fungi belonging to the genera, *Candida, Cryptococcus*, and *Aspergillus* cause infections via invasion, which leads to superficial mucosal or skin infections or deeply rooted mycoses that infect organs (Richardson, 2005). Unfortunately, antifungal agents are becoming less effective at these pathogenic species and display increased resistance to drugs.

Infection of plants by fungi is considered as a major problem in agriculture. *Magnaporthe oryzae* a plant pathogen is responsible for lowering the yield in rice up to 10-30% per annum; a loss that could feed up to 60 million people (Pennisi, E.2010). No traditional or chemical approaches have been successful in controlling this disease as the fungus can adapt, mutate, and evolve resistance to multiple varieties of rice (Pennisi E 2010). *M. oryzae* can undergo various morphological changes in order to infiltrate and infect rice cell (Fernandez J et al., 2017).

Overcoming the host defense systems by several virulence factors such as expression of proteins, enzymes, and toxins are associated with pathogenicity and can be the cause of diseases (Tomee and Kauffman, 2000). The assumed fungal virulence factors might have evolved, serving them to survive against extreme conditions and thereby facilitating them to cause diseases (Justyna Karkowska-Kuleta et al., 2009). Adaptation to the host environment is very crucial for their survival and assimilation. This can be achieved by morphological alterations and expression of virulence factors. Morphogenetic switching, expression and secretion of special proteins such as hydrolytic enzymes and toxins are few of the several virulence factors that facilitate pathogenicity. The recognition and elucidation of aforesaid virulence traits and their processes involved in pathogenesis will further aid in the development of novel efficient antifungal treatments.

1.2 Fungal morphogenesis

Morphogenesis is a biological process through which an organism attains its size, shape, and growth. The major morphogenetic characteristic of fungi is their cell polarity, where the cell wall expands through deposition of cell wall components to confined places on the cell wall. Morphogenesis in fungi is often activated by external cellular factors and accomplished by internal genetic factors. Cell polarity is regulated by an intrinsic system consisting mainly of the actin and microtubule cytoskeleton and cell polarity proteins. To initiate morphogenetic change fungi must respond to extrinsic clues. These external clues can be environmental conditions such as temperature CO_2, O_2, and the host immune system (for pathogenic fungi). Pathogenic fungi also require external signals to initiate morphogenesis. Both these external and internal clues are merged into a single response and trigger the morphogenesis (Boyce K. J. et al., 2015). Fungi can grow as single cell yeast and multicellular hyphae. Hyphae are long filamentous structures that can branch and are also called mycelia. Yeast and hyphae growth forms display distinct growth modes.

1.2.1 Morphogenesis in yeast cell form

Fungi growing as unicellular yeast reproduce asexually by budding or fission (Martin et al., 2014). The three basic functions that enable polarized growth are first; the generation of an axis of growth, second; the maintenance of cell polarity and third; depolarization by regulated mechanisms. The equilibrium between these three mechanisms generates fungal cell shapes (Lin X et al., 2015). One form of cell polarity is defined as the limitation of growth zones to certain regions in the cell. Cytoskeletal proteins such as actin cables,

microtubules, and polarity factors form the key and vital components of the intrinsic polarity system. External signals can stimulate this intrinsic polarity system and reshape the polarized growth (Siegrist & Doe, 2007). Cell differentiation, the formation of tissues and organs are the outcomes of differential cell polarity (Bryant & Mostov 2008). Polarized growth is observed in axons of the nerve cells. The tip at which the receptors signals activate, the actin, microtubules and other accessory proteins are accumulated, and the growth is promoted in the direction of the external signal (Quinn and Wadsworth, 2008).

In *Saccharomyces cerevisiae*, yeast mother cells, grow non-polar in the initial phases of cell growth through non-polar isotropic expansion until the symmetry is distorted with the aid of preexisting spatial landmarks. Subsequently, a cellular axis is generated for the development of structures like buds. *S. cerevisiae* employs landmark proteins to recruit the component required for morphogenesis through GTPase modules to a specific location in the cell (Chant 1999, Lin X et al., 2015). Whereas, *Schizosaccharomyces pombe* uses polarity factors combined with the microtubule-based delivery system to establish polarity (Martin 2009). The second type of symmetry distortion occurs without the utilization of pre-existing land-mark proteins but encompasses multiple feedback loops that guide the Cdc42 GTPase to a specific position on the cell surface (Wedlich-Soldner et al., 2003, Johnsonet al., 2011, Freisinger et al., 2013).

Once the polarity axis has been established it has to be stabilized for appropriate cell-surface expansion and deposition of the cell wall materials to the restricted growth zone. In fungi, the growth site is comprised of vesicles and surrounded by endocytic zones. In *S. pombe* microtubules are arranged along the cell length and facilitate vesicle movement towards the growth zone (Lin X et al., 2015). Depolarization occurs after the growth has occurred in a regulated mechanism. In *S. cerevisiae,* depolarization is established with the aid of the apical-to-isotropic switch (Bi and Park 2012).

1.2.2 Morphogenesis in hyphal growth form

Hyphae are multicellular structures in which the distortion of symmetry leads to the formation of the initial structure called germ tube, that later progresses to hyphae. It was assumed that spontaneous polarization occurs in the fungi that form hyphae. No evidence was available that the spatial landmark proteins determine the growth site. However, it was shown that the secondary germ tube occurs at the opposite side to the first germ tube (Harris 1999).

The extreme form of polarized growth in hyphae forming fungi is found at the growing tip, with continuously elongated cells bound to each other at the ends (Fischer et al, 2008). It is at the growing tip where the initial growing site is established and continues the retention of the growth regulators and polarity factors (Riquelme et al., 2003, Steinberg, 2007). The fungal tip growth zone recruits all the secretory and endocytic vesicles, actin filaments, microtubules and other associated proteins and coordinates the transport of vesicles, proteins, and mRNAs to the hyphal tip (Fischer et al., 2008, Steinberg 2007). The hyphae continue to grow with an apical extension and apical body. The apical body also called Spitzenkörper is located at the tip of the hyphae and determines the shape of the hyphae and the direction of hyphal growth (Girbardt 1957, Sudbery 2011a). A characteristic feature for this growth zone at apical body is the accumulation of secretory and endocytic vesicles, ribosomes and microfilaments, and all these proteins together coordinate the transport of vesicles, proteins, and mRNAs from and to the hyphal tip (Fischer et al, 2008, Steinberg, 2007, Harris et al. 2005, Verdin et al., 2009). Extrinsic signals affect the orientation of the hyphae (Brand & Gow, 2009).

The basic principles and molecular mechanisms of polarized growth are conserved and are found in almost all fungi (Fischer et al, 2008). Changes in the plasma membrane composition could also be a mechanism for establishing polarity in yeast and hyphae. They also have the ability to switch between a unicellular form and a multi-cellular, hyphal-like growth form in response to extrinsic signals.

1.3 The fission yeast *Schizosaccharomyces pombe* as a model organism

Schizosaccharomyces pombe was initially isolated by Paul Linder in 1893. *S. pombe* served as an excellent model organism in studies related to cell cycle, microtubules and actin, cytoskeleton compartmentation, protein phosphorylation and RNA splicing (Fantes and Hoffman, 2016). *S. pombe* belongs to the kingdom Fungi and Phylum Ascomycota. It was one of the top ten eukaryotic organisms to be completely sequenced (Wood et al., 2002). P.Linder described it as novel ascus forming a cylindrical shaped cell which divides by diagonal fission (Linder P 1893). *S. pombe* acquired its name “fission yeast” because of its mode of division, unlike *S. cerevisiae,* which divides by budding. Several processes have been studied since its isolation making it one of the well-studied eukaryotic organisms. Genome sequencing revealed that *S. pombe* contains 13.8 Mb of genetic information in three chromosomes with sizes 5.7, 4.6, and 3.5 Mb respectively (Wood et al., 2002). This 13.8Mb

genome contains 5118 genes (Pombase.org). *S. pombe* has several conserved genes that have significant similarities with human diseases and half of these being cancer-related, makes it an interesting organism to study (Wood et al., 2002).

1.4 Polarized growth in *S. pombe*

The fission yeast *Schizosaccharomyces pombe* has a cylindrical cell shape, divides via fission and grows in a highly polarized manner during the entire cell cycle (Martin, 2009). In yeast form, *S. pombe* measures 7-14 µm in length and 3-4µm in diameter. *S. pombe* cylindrical shape is maintained by restricting growth to specified zones at the cell cortex defined as polarized growth. In the cell cycle, polarized growth is regulated in a chronological manner.

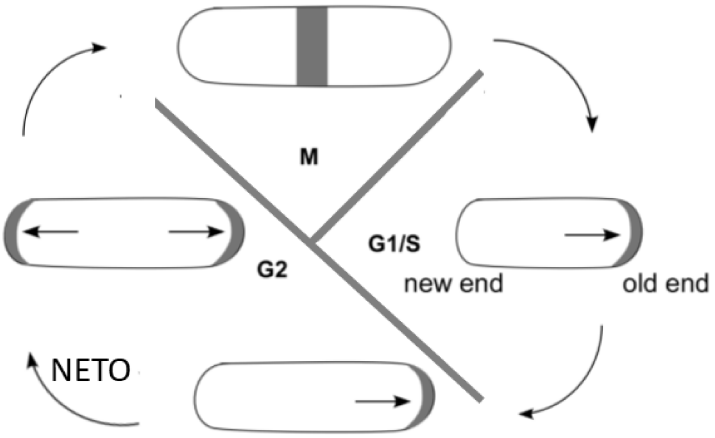

Figure 1: The cell cycle and polarized growth of *S. pombe* during the cell cycle. In *S. pombe*, growth occurs either at the cell poles or at the division site. The activity of the growth zones changes during the course of the cell cycle. After cytokinesis, the daughter cells grow monopolar at the old cell ends. In the G2 phase of the cell cycle, the new cell end is activated as a growth zone (**N**ew **E**nd **T**ake **O**ff), and bipolar growth takes place until entry into mitosis. In late mitosis, another growth zone is formed in the middle of the cell, the division septum, Dark gray: Growth Zones.

In *S. pombe* growth is accomplished by conveying and embedding the new cell wall material in the existing cell wall. This is achieved by either growth at the cell cortex or at the site of cell division that is present at the cell center in the form of the medial contractile ring /septum. The medial contractile ring generates the constricting force to separate one cell into two cells. Accordingly, three distinct growth zones can be defined: the two cell cortexes and the zone of the division. The activity of these growth zones changes according to the course of the cell cycle (Figure 1). The main growth phase of *S. pombe* is in the G2 phase of the cell cycle. After cytokinesis, growth is restricted to the old cell end that is already present and is

referred to as the old end (Figure 1, Mitch & Nurse 1985). The growth at the old end lasts until the end of S-phase. Once the cell attains a size of 8-9 µm the growth occurs at the new tip in a bipolar fashion. This shift of growth from the older end to the new end is termed as **N**ew **E**nd **T**ake **O**ff (NETO, Figure 1, Mitchison et al., 1985). NETO permits the localization of the growth machinery and allows growth at the new end together with the old end. The bipolar cells grow from now on, until the cell has reached the length of 14 µm, and starts mitosis (Fante, 1977). After reaching a length of 14µm before cytokinesis the whole growth machinery is targeted to the site of division. In the cell cycle at the end of mitosis, in the G1 phase, a new zone is created at the center of the cell called the septum (Figure 1). After cell division, the daughter cells growth will return to the old cell end and continue to grow monopolar.

1.5 Morphogenetic machinery essential for morphogenesis

Yeasts and filamentous fungi possess several kinds of machinery that can influence morphogenesis. Vesicle trafficking, cytoskeleton, positional markers, signal transduction, morphotype, niche adaptations are few of the types of machineries fungi use for morphogenesis. Fungal species exhibit several morphological transitions. Cell physiology and structural changes are accompanied by severe cell responses. The fungal morphogenesis is a highly coordinated process and corresponds to the adaptive response against stress and changing environments. This morphological flexibility of fungi permits them to quickly adapt to the changing environmental conditions. Species morphological adaptation and signaling appears to be the direct consequence of fungi to survive harsh conditions (Lin X et al., 2015). Identification of the cellular components controlling fungal morphogenesis can offer specific understanding into fungal life cycles and pathogenesis. Different morphogenetic machineries required for morphogenesis is explained in brief in the following sections.

1.5.1 Role of the cytoskeleton in fungal morphogenesis

Structures comprising polar cytoskeletal elements such as actin filaments and microtubules are the workhorse for morphogenesis, besides GTPase module. In *S. cerevisiae* the actin cytoskeleton is involved in cell polarity, and microtubules are associated with nuclear chromosome segregation. The *S. cerevisiae* actin cytoskeleton is encompassed of actin patches; actin cables and the actomyosin ring (Moseley JB et al., 2006). Actin patches are composed of a network that is nucleated by the Arp2/3 complex. Actin cables are composed of parallel bundles of actin filaments and are nucleated by formin; the actomyosin

ring consists of formin nucleated actin filaments and has a role in cytokinesis. The Rho GTPases are known to regulate the assembly of different kinds of actin structures (Moseley JB et al., 2006).

In contrast, in the fission yeast and other filamentous fungi such as *U. maydis* microtubules play a crucial role in the determination of cell shape and polarized growth. These fungi also possess similar actin structures than that found in *S. cerevisiae,* and they also play an important role in polarized growth. In fission yeast, microtubules regulate the actin assembly and thereby determine the shape of the cell (Chang F et al., 2005). In *U. maydis*, polarized growth was observed in the absence of microtubules and the actin cytoskeleton, but rescued the growth at a reduced rate (Steinberg G. 2007). In few other filamentous fungi, it was observed that the absence of microtubules failed to transport nuclei to the hyphae (Fuchs U et al., 2005). It was shown in *U. maydis* that microtubules are essential for the transport of several RNA binding proteins that are involved in polarized growth (Zarnack K et al., 2007). Microtubules are also essential for the bidirectional transport of endosomes in *U maydis* and are required for efficient recycling and the generation of fast polar growth. Combined disruption of actin and microtubule-dependent transport completely blocked the growth in *S. cerevisiae* and *U. maydis* (Schuchardt I, et al., 2005).

Together with microtubules and the actin cytoskeleton, septins play an essential role in morphogenesis. Septins are GTP binding proteins. These septins can develop structures like filaments and are involved in different cellular functions such as cytokinesis and membrane transport (Lindsey R 2006). Septins form a ring at the vicinity of the neck at the bud and serve as a barrier between mother cell and the bud for mitotic exit and cell polarization proteins in *S.cerevisiae* (Faty M. et al., 2002). Septins are highly conserved from yeast to animal cells and are important for dendritic spine development (Tada T et al., 2007). In *S. pombe*, septins were found to be crucial for efficient cell separation instead of cell division. In *U. maydis* cells, deletion of these septins led to elongated cells and switch to a fission-like division instead of budding (Boyce KJ et al., 2005).

In the current study, I have used *S. pombe* as a model organism and have explained the morphogenetic machinery in this organism. This polarized growth is driven by a combination of the microtubule and actin cytoskeleton, and cell polarity proteins (Terenna et al, 2008). In *S. pombe*, the actin cytoskeleton is needed for growth and cell polarity, the microtubule cytoskeleton is required for maintaining and positioning of new growth zones,

and cell polarity proteins serve as spatial markers for the actin and microtubule cytoskeleton, which determine the cell shape and affect the spatial organization of the cytoskeleton (Terenna et al., 2008).

These finding suggests that the aforementioned morphogenetic components are essential for morphogenesis in fungi. Multiple proteins and multiple pathways, together with several feedback mechanisms contribute to morphogenesis. All the components are might not be essential morphogenesis but a collective teamwork would result in a better effectiveness, robustness in this process i.e. morphogenesis (Chang & Martin, 2009, Terenna et al, 2008).

1.5.2 Role of landmark proteins and polarity factors in morphogenesis

The polarized growth of fungi requires the actin and microtubule cytoskeletons together with landmark proteins. Landmark proteins mark the growing cell-end and play a vital role in the maintenance and development of growth zones. The absence of these cell-end markers resulted in a changed cell shape and hyphal morphology. *S. cerevisiae* and *S. pombe* landmark proteins have a similar function of as observed in other filamentous fungi. *S.cerevisiae* cell surface protein Axl2 and other septin-associated proteins such as Bud3 and Bud4 together specify the budding pattern. Whereas, other *S. cerevisiae* cell surface proteins such as Bud9, Bud8, Rax2, and Rax1 are involved in the bipolar growth pattern (Chant 1999). The landmark proteins initiate the local activation of Cdc42 with the help of Ras-like GTPase Bud1 (Bi and Park 2012). Mod5 a plasma membrane-anchored protein in *S.pombe* serves as a target for the microtubules to deliver Tea1 (Snaith and Sawin 2003). This process aids the correct positioning of microtubules followed by accumulation of formin complexes that enable the formation of microfilaments (Martin 2009).

1.5.3 Signal transduction associated with morphogenesis in fungi

Ras, Rho, Cdc42, and Rac are small that regulate fungal morphogenesis. These GTPases function in coordination with the cytoskeleton and the transport of vesicles to organize polarized growth. Studies in yeasts have shown that these small GTPases work in a chronological order. Studies in *S. cerevisiae* and *S. pombe* have shown that Ras GTPases operate ahead of Cdc42 to regulate polarized growth. Small GTPases, such as Ras, Rho, and Cdc42, do not function alone, but function in a chronological order (Chang et al., 1994). The Ras1-Cdc24 signaling pathway was also shown to regulate cell polarization and budding in *C. neoformans* (Zhao et al., 1995). In *C. neoformans*, it was shown that in the absence of

functional GTPases, the cells cannot efficiently re-polarize their actin cytoskeleton (Alspaugh et al., 2000, Nichols et al., 2007). Several studies have been shown that GTPases are conserved from yeast to humans and function as a key signaling molecule in polarity establishment (Park and Bi 2007). These data imply the small GTPase modules play a vital role in morphogenesis.

1.6 Morphogenic machinery in *S. pombe*

The actin cytoskeleton, microtubules, and other polarity factors are key players in morphogenesis (Martin & Chang 2005, Moseley & Nurse 2009). The components required for the growth are to be transported to different locations within the cell during different stages of the cell cycle. In *S. pombe,* monopolar to bipolar growth transition requires dynamic structures like microtubules. These cytoskeletal structures are composed of polymers of tubulin. These cytoskeletal structures act as means of transport of growth components (Martin 2009). In interphase cells, four to five bundles of microtubules are oriented along the long axis of the cell (Piel & Tran 2009, Terenna et al., 2008). Microtubules are polar structures encompassing one slow-growing minus end and a fast-growing plus end. The minus ends of antiparallel microtubules meet in the center of the cell close to the nuclear membrane. The dynamic plus end of the microtubules polymerizes from the cell center towards the cell ends (Drummond & Cross, 2000). The minus ends radiate from the nuclear envelope and originates from the microtubule organizing centers (MTOCs) (Tran et al., 2001 Hagan 1998). Once the microtubules reach the end of the cell they pause for one to two minutes (dwell time), undergo a catastrophic event and depolymerize. +Tip proteins control the plus end dynamics of the microtubules. Mal3 (EB1 family), Tea2 (kinesin), Tip1 (CLIP-170) are typical examples of the +TIP proteins (Browning et al., 2000, Brunner and Nurse 2000, Beinhauer et al., 1997). The polarity factor Tea1 with the help of Tip1 binds to the microtubule and forms a complex along with Tea4 and this complex is transported to the cell end. The Tea1/Tea4 complex is transported to the cell end via microtubules where Tea1 anchors to Mod5 prenylated protein (Snaith & Sawin, 2003). Tea4 recruits an actin nucleator For3 that is essential for actin assembly (Martin et al., 2005, Snaith et al., 2005, Snaith and Sawin, 2003). Microtubules and polarity factors are essential for correct positioning of growth zones and polarity, Absence of these proteins results in abnormal cell shapes and misplaced growth zones.

At the cell, the end Tea1/Tea4 complex also recruits the polarity factor Rho-GTPase Cdc42. These are small GTPases belonging to the Ras superfamily. These molecules can exist in two forms one being the active GTP bound form and the inactive GDP bound form. These activities are regulated positively by guanine exchange factors (GEF) and negatively by GTPase activating proteins (GAP's) (Iden & Collard, 2008). Pom1 kinase a member of the DYRK "dual specificity" family that can regulate functions in cell development is recruited by the Tea1/Tea4 complex to the cell ends (Bahler & Nurse, 2001, Bahler & Pringle, 1998, Becker & Joost 1999, Behrens & Nurse 2002). Pom1 prevents localization of Cdc42 GAPs at the cell pole and causes the activation of Cdc42 (Tatebe et al., 2008). It was also found that Pom1 was cell cycle regulated as monopolar cells have less Pom1 kinase activity compared to bipolar cells (Bahler & Nurse, 2001).

Formin (For3) and actin monomers binding the protein Bud6 are recruited by the Tea1/Tea4 complex (Feierbach et al., 2004, Glynn et al., 2001). Upon recruitment, For3 is activated by Bud6 and Cdc42 resulting in the formation of vesicle, actin cables and the establishment of a new growth zone (Martin et al., 2007). The Tea1/Tea4 complex is localized to the cell ends during the monopolar growth (Martin et al., 2005, Mata & Nurse, 1997, Tatebe et al., 2005).

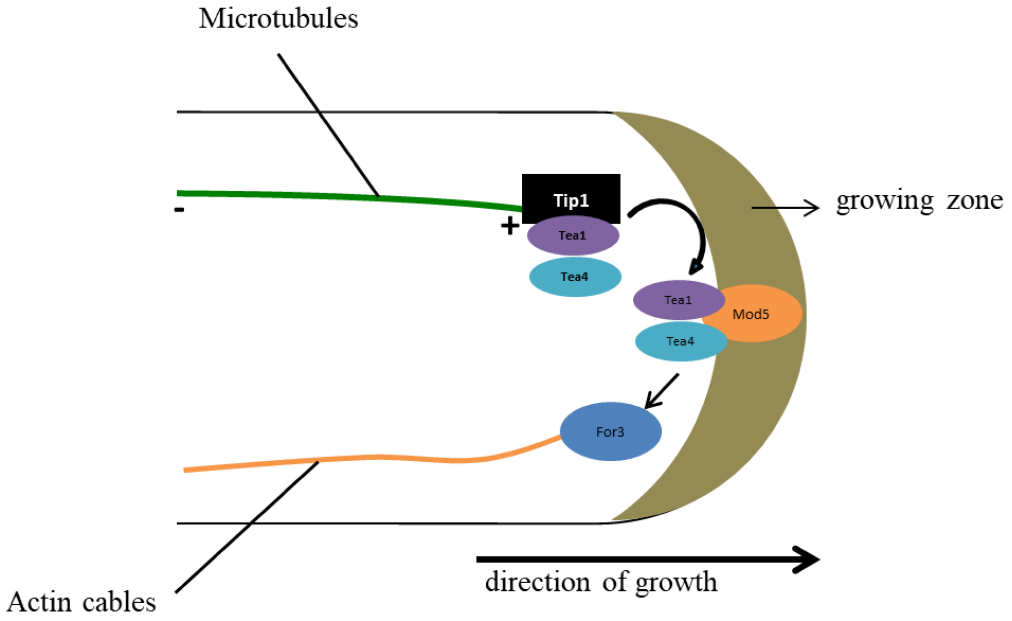

Figure 2: The organization of an *S. pombe* growth zone and the role of actin and microtubule skeleton. Actin and microtubule skeleton together with other components are required for the polarized growth. The microtubules carry the essential polarity factors at the plus end towards the cell ends. The tea1/tea4 complex provides the marking of the potential growth zones by binding to the membrane protein Mod5. This enables the polarity factors

like Bud6 or For3 to be recruited. Cdc42 together with Bud6 and For3 starts the formation of actin cables.

1.7 Fungal dimorphism as an important pathogenic trait

Some fungi have the ability to switch between single cell yeast forms to multi-cellular structures. This switching between various morphologic forms is extensively spread all over the fungal kingdom. This switching ability of the fungi especially in pathogenic fungi enhances the adaptation and colonization of the host environment. Unlike multi-cellular eukaryotes, in which the major sections of cells are surrounded with moderately changing environments, fungi are confronted with unpredictable environmental changes. Fungal dimorphism refers to the switch from yeast to hyphae or vice versa. Morphogenetic changes are required to counteract such changing environmental conditions. *Blastomyces dermatitidis* a pathogenic Ascomycota exists as mycelia in soil whereas, in the host they adapt budding lifestyle a pathogenic form of this fungus in response to temperature (Maresca & Kobayashi, 1989; Nemecek et al., 2006). It is a specialized morphogenetic adaptation allowing colonization of a host. *U. maydis* switch from yeast to pathogenic filamentous form in response to nuclear conidiation and plant signals (Bolker M. et al., 1995). In plant pathogenic fungi *Ophiostoma ulmi* the mycelial growth form is essential for the penetration of the plant cells and the yeast form helps in the dispersal of the fungi to other parts of the plant via xylem vessels (Kulkarni and Nickerson 1981).

Dimorphism is an environmentally controlled reversible process and is observed in most dimorphic fungi (Romano, 1966). Environmentally controlled reversibility was observed in opportunistic pathogen *C. albicans* where this fungus can alter its morphology to and fro in response to environmental changes whereas, this switch is not reversible in *U. maydis*. In *C. albicans* this adaptation is crucial for virulence (Sanchez-Martinez & Perez-Martin, 2001). Ancestral fungi looked like protists and to colonize terrestrial habitats fungi have emerged to grow as hyphae as a dominant growth form but still many filamentous fungi also display yeast like morphogenesis during development (Cole et al., 1979, Jones et al., 2011, Stajich et al., 2009). Specific ecological habitats prefer hyphal growth and the other prefer yeast growth. Yet many members retained the capacity to undergo a transition between yeast and hyphal or pseudohyphal growth (Harris 2011a, b). Morphogenetic change to the other growth form is effective to confront and surpass physical barriers. Hyphal cells are efficient in infiltrating the barriers and expanding the colony via several processes such as

phototropism, gravitropism, and aerotropism (Moore et al., 1996, Aoki et al., 1998, Brand et al., 2007). On the other hand, yeasts like cells are exceptional at growth, stress tolerance, and dispersal.

The fungal dimorphism is associated with changes in cell division/growth behavior and reorganization of the internal polarity system. This switching also allows changes in the cell wall composition and thereby altering the cell wall properties (Klein & Tebbets, 2007, Palecek et al., 2002). These alterations are caused by several environmental stimuli such as nutrient stress, changes in pH and O_2 levels (Berman, 2006, Nadal et al., 2008).

The yeast form of pathogenic fungi such as, *H. capsulatum, B. dermatitis, and P. brasiliensis*, has increased expression of α-1,3-glucan in the cell wall in comparison to the mycelial growth form which shields the fungi from the host immune response (Kanetsuna and Carbonell 1971). Pathogenic yeast cells also secrete special proteins to survive the host immune system. *Histoplasma* secretes the calcium-binding protein (Cbp1) to acquire calcium and survive within the phagolysosomes of the host cells (Batanghari et al., 1998). Other pathogenic fungi such as, *B. dermatitis* secretes the adhesin Bad1 which suppresses the inflammatory response of the host system (Finkel-Jimenez et al., 2002). *C. albicans* in the hyphal growth exhibit hyphal-specific factors such as adhesins (Als3), hyphal regulated gene (Hyr1), and cell surface protein (Hwp1) instead of β-glucan to escape the host immune response as well as to adhere to the host tissues (Staab et al., 1999, Gantner et al., 2005, Luo et al., 2010). *Aspergillus fumigates* exhibit hydrophobins and melanin that masks the yeast cells to escape the host immune system (Aimanianda et al., 2009, Volling et al., 2011).

S. pombe being a non-pathogenic and well-established model organism has been an excellent model system to study this transition from single cell yeast form to pseudo or true hyphal form. *S. pombe* is also used to investigate the effect of various environmental conditions and molecular components that are required for the transition from unicellular to pseudo-hyphae forms.

1.7.1 Environmental factors that regulate dimorphism/dimorphic switch

Fungi must be capable of sensing and adapting to the external environments. The adenylate cyclase Cyr1acts as an assembly point for most of the hyphae inducing signals (Bahn and Sundstrom 2001, Rocha et al., 2001, Hogan and Sundstrom 2009, Zou et al., 2009). In *C. albicans* hypoxia condition is a prerequisite for the fungal form of the pathogen

(Lu et al., 2013) *C. albicans* convert CO_2 to HCO_3 and regulate morphogenesis by activation of adenylyl cyclase Cyr1 and furthermore activate the downstream targets of the cAMP-PKA pathway (Klengel et al., 2005).

N-acetylglucosamine (GlcNAc) is a monosaccharide and a derivative of glucose that stimulate the transition of *C. albicans* from yeast to hyphae via the cAMP-PKA pathway (Castilla et al., 1998, Gunasekera et al., 2010). GlcNAc has also been shown as a potent inducer to initiate transition from yeast to hyphae in pathogenic fungi such as *H. capsulatum* and *B.dermatitis* (Gilmore et al., 2013). In opportunistic fungi like *C. albicans* the yeast cells can transform into hyphal form in response to several environmental factors such as presence of blood-serum, GlcNAc or specific amino acids (Simonetti et al., 1974, Maidan et al., 2005a), as well as upon contact with innate immune cells like macrophages or neutrophils (Lorenz et al., 2004).

Extra-cellular pH is another environmental trigger that initiates fungal morphogenesis. Fungal-specific signaling occurring via the Rim101/PacC pathway controls the fungal transition in response to pH. The Rim101/PacC pathway was found to be conserved in pathogenic fungi. *C. albicans* grows as yeast in acidic conditions and can induce hyphal growth form when shifted to alkaline or neutral environmental conditions (Li and Mitchell 1997, Davis et al., 2000). In *A. fumigatus*, the Rim/Pal signaling cascade is required for pathogenesis (Bignell 2012).

In fungi, thermal homeostasis occurring via heat shock proteins is required to respond to the environmental change in temperatures (Nicholls et al., 2009). Host or temperature induced signals have to be transduced via signaling pathways and lead to changes in the gene expression. The fungi able to transit from one morphological form to other in response to temperatures are called thermally dimorphic fungi. These thermally dimorphic fungi are special as they can cause disease in both normal and deceased immune-compromised patients. Temperature is the predominant stimuli that can influence the transition of fungi and additionally supported by CO_2, pH and other external factors. In yeast nitrogen starvation stimulates the expression of *flo8*$^+$ the gene required for the flocculation in liquid cultures and expression of filamentation specific genes (Kobayashi et al., 1996, Rupp, et al., 1999).

1.8 Dimorphic switch in *S. pombe* and the signaling pathway required for the switch

Fungi are able to switch from unicellular to multi-cellular structures. This phenomenon of switching growth forms is referred to as the dimorphic switch. These invasive multi-cellular hyphae can invade the substrate whereas, the yeast form is non-invasive. This switch acts as a virulent trait in pathogenic fungi and provides additional features compared to the yeast form. For the first time in *S. pombe* formation of invasive structures were observed by Amoah-Buahin et al., 2005 as shown in Figure 3.

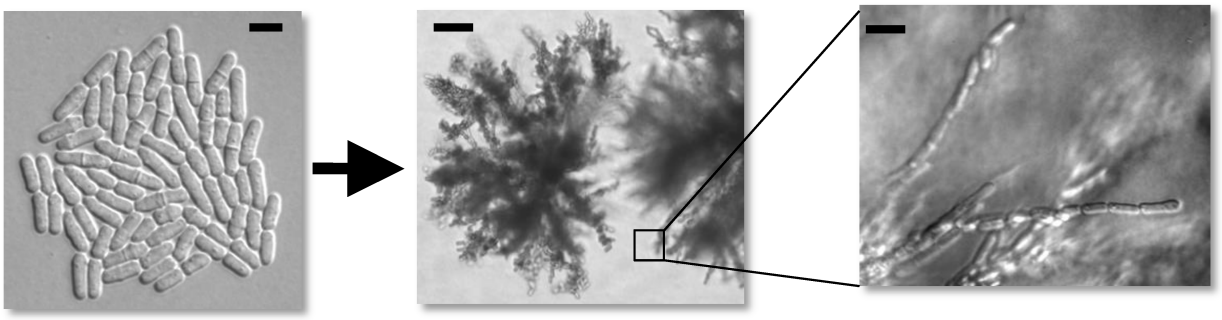

Figure 3: **Dimorphic switch in *S. pombe***. Fission yeast normally grows as a unicellular yeast form. *S. pombe* inoculated at high cell density and incubation for a longer period of time can switch to invasive pseudo-hyphae. Yeast form, bar: 10µm, invasive pseudo-hyphae, bar: 50µm (left), 10µm (right).

In *S. pombe* invasive protrusions are formed around the edge of the cell spot which possibly might be due to the absence of nutrients at the center of the spot and present in excess at the outer edge of the colony. Long filaments of cells which grow away from the colony encompassing cells separated by septae were observed microscopically. This morphology seems to be pseudo-hyphae rather than true hyphae. The center of the colony consisted of cells that were growing invasively, whereas, the long chains of cells were found at the edges of the colonies (Figure 3). In *S. pombe,* the switch is induced by poor environmental conditions such as limited environmental nutrients and is assumed to be a scavenging response in search of nutrients (Madhani et al., 1998, Pöhlmann et al., 2010).

The sensing of the nutrient limitation triggers the morphological changes associated with the dimorphic switch. The changes are transmitted via the cAMP/PKA pathway but neither through the MAPK kinase pathway nor Sty1/Spc1 stress response pathway nor the

Pmk1/Spm1 cell-integrity pathway. The signal transduction occurs via the cAMP/PKA pathway, as deletion of genes encoding the components of this pathway such as heterotrimeric G protein Gpa2 and adenylate cyclase Cyr1 were unable to make the switch (Amoah-Buahin et al., 2005, Pöhlmann et al., 2010).

In several eukaryotes, cAMP is used as a secondary messenger to adapt to external conditions. It was shown that the cAMP level was reduced in response to nitrogen and carbon depletion and leads to inactivation of the cAMP-dependent protein kinase (PKA) (Mochizuki and Yamamoto 1992, Isshiki et al., 1992). This reduction in the cAMP levels induces the generation of glucose from certain non-carbohydrate carbon substrates such as proteins and lipids (Hoffman and Winston, 1991). Starvation of nitrogen sources also induces sexual differentiation in fission yeast (Yamamoto et al., 1997). In *S. pombe* in response to nutrient sensing, the heterotrimeric G-protein (Gpa2) is activated by a seven transmembrane protein Git3 (Isshiki et al., 1992, Welton and Hoffman 2000, Hoffman, 2005). Gpa2 activation induces adenylate cyclase Cyr1/Git2 activity that catalyzes the production of cAMP from ATP (Kawamukai et al., 1991). Thus, generated cAMP associates with Cgs1, a regulatory subunit of the PKA, permitting the subunit Pka1 to be released from the complex with Cgs1 and exerting the kinase activity and thereby allowing the target genes to enter the nucleus and activation of genes required for the switch (Maeda et al., 1994, Devoti et al., 1991).

1.9 Adhesins facilitate adhesion or adherence to the substrate or host tissues

The property of fungi to adhere to host or to other abiotic surfaces is crucial for colonization and damage of the host tissue. Adherence of fungal pathogens to the host tissue is the prerequisite for host invasion. The human pathogenic fungi can adhere tightly to different surfaces such as the human skin, endothelial and epithelial mucosal tissues. This adherence to the host tissue is considered as the first step for the establishment of infections. Pathogenic fungi can also adhere to abiotic surfaces such as catheters, cardiac valves and dental prostheses (Busscher HJ et al., 2010, Ramage G, et al., 2006). Hyphal formation and adhesion are basically related, as contact of *C. albicans* to the host surface stimulate the hyphal formation and immediate expression of genes associated with hyphal adhesins. These processes further enhance the adhesive properties of *C. albicans.* Cell to cell adhesion is also required for mating when two cells of opposite mating type come close to each other and adhere for conjugation and cellular fusion. Asexual aggregation occurs to form large clumps/flocculation in response to nutrient starvation or stressful environments. Flocculation

is most of the time cell density-dependent i.e. when the culture reaches stationary phase cells start to aggregate. This phenomenon occurs to protect the inner cells within the clump from unfavorable environmental conditions and to regrow upon reaching favorable conditions (Verstrepen & Klis, 2006). In the cell substrate adhesion, the fungi adhere to the biotic or abiotic surfaces. Adherence to the surface makes the cells attached to a fixed source of nutrition. The above-mentioned phenomena protect cells from external conditions and increase their chances of survival (Verstrepen & Klis, 2006). This adherence process requires special cell-surface proteins/glycol proteins called adhesins/flocculins/agglutinins (Dranginis et al., 2007). These adhesins have been described in detail in both model yeasts such as *S. cerevisiae*, as well as in pathogenic yeast *C. albicans* (Piet W. J. de Groot et al., 2013).

These adhesins are described as flocculins in *S. cerevisiae,* Agglutinins in *C. albicans*; Epa proteins (epithelial adhesins) in *Candida glabrata* (Teunissen and Steensma, 1995, Cormack et al., 1999, Hoyer, 2001 and Kaur et al., 2005). In *C. albicans* 90% of the cell wall mass is mannose residues that are added by N-glycosylation or O-glycosylation's and are glycosylphosphatidylinositol (GPI) anchored (Piet W. J. de Groot et al., 2013). The majority of the fungal adhesins are GPI-modified cell wall proteins. The key structure of GPI protein precursors comprises of conserved features that can be identified using various bioinformatics tools. These adhesin proteins are cell wall proteins. The conserved features of GPI-modified cell wall proteins are a signal peptide at the N-terminus that facilitates the entry into the endoplasmic reticulum, and a C-terminal peptide for anchoring to the lipid in the membrane of the endoplasmic reticulum. Mature GPI-modified cell wall proteins are large proteins with a modular structure containing an N-terminus region that is exposed to the outer regions and is essential for binding of molecules or ligands present on the other cells that are essential for interaction. It is followed by a tandem repeats of serine/threonine-rich variable domains at the C-terminal (Kobayashi et al., 1998, Veelders et al., 2010).

Sugar molecules on glycoproteins on the cell walls of other cells are required for the binding of these adhesins (Verstrepen & Klis, 2006). The flocculation is caused by the binding of adhesins to galactosyl groups of cell wall glycoproteins. It has been demonstrated that galactose is the main sugar required for the flocculation and invasion in *S. pombe* (Matsuzawa et al., 2011). Binding of adhesins to cell wall glycoproteins of adjacent cells and cell-cell adhesion requires galactose and since agar is a polymer of galactose, cells binding to the agar surface could be mediated by the same mechanism (Matsuzawa et al., 2011).

Adhesion and invasion do not occur constitutively but needs to be triggered by harsh environmental conditions such as nutrient limitation and stress (Verstrepen & Klis, 2006).

1.10 Adhesins and the transcriptional network that govern *S. pombe* adhesion and invasion

S. pombe adhesins contain a ligand binding domain at their C-terminus in contrast to previously identified adhesins that possess that at their N-terminus (Linder T, Gustafsson CM 2008) *S. pombe* adhesins do not contain a visible glycosylphosphatidylinositol (GPI) membrane anchor signal that mediates their adhesion to the cell wall. In *S. pombe,* 12 putative adhesins were identified *in silico* (Linder T, Gustafsson CM 2008). One adhesin Pfl5 displayed homology with *S. cerevisiae* Flo11 a key adhesin required for adhesion (Guo et al., 2000). The activity of these adhesins depends on Ca^{2+} ions (Verstrepen & Klis, 2006). On addition of EDTA, the flocculation can be inhibited (Tanaka et al., 1999). The family of adhesins found in the pathogenic yeast *C. albicans* contains a conserved agglutinin-like sequence (Als), tandem repeats and contains ligand binding domains at the C-terminus like the GLEYA domain as seen in flocculins in *S. cerevisiae* (Linder T, Gustafsson CM 2008). Conserved domains similar to Als conserved repeats were found in almost all *S. pombe* adhesins (Linder T, Gustafsson CM 2008). Glycosylphosphatidylinositol (GPI) anchors are not present in any of the *S. pombe* adhesins other than Pfl1/Gsf2 (Linder T, Gustafsson CM 2008, Matsuzawa et al., 2011). This adhesin Gsf2 was not identified *in silico* by Linder T et al., 2008. The Gsf2 adhesin has a modular structure similar to that observed in other fungi. Gsf2 consists of an N-terminal signal sequence followed by tandem repeats of eight 78 amino acid long sequences and eight 44-amino acid long repeats followed by a C-terminal GPI anchor (Matsuzawa et al., 2011).

Most of the adhesins previously identified by Linder T, Gustafsson CM 2008 *in silico* were characterized as **P**ombe **Fl**occulins (Pfl's). Eun-Joo Gina Kwon et al., in 2012 has published these as the potential adhesins required for flocculation in *S. pombe*. These adhesins were abbreviated as Pfl followed by number 1-9, where the number denotes the degree of flocculation when overexpressed in a wild-type strain. Pfl1 has the highest degree of flocculation whereas, Pfl9 has the least degree of flocculation. SPAPB2C8.01 was the only adhesin identified *in silico* but was not identified in the study by Eun-Joo Gina Kwon et al., in 2012 as a flocculin. Mam3 and Map4 are cell surface proteins that have been identified to have adhesive properties and are demonstrated to have a role in mating (Mata and Bahler,

2006; Sharifmoghadam et al., 2006). The study by Eun-Joo Gina Kwon et al., in 2012 has considered only the genes that were upregulated in two strains that displayed enhanced flocculation, first the overexpression of MADS-box transcription factor *mbx2*$^{+}$, and second, deletion of Zn(2)-Cys(6) transcription repressor Rfl1 (*rfl1*Δ). Gsf2/Pfl1 was identified as the dominant adhesin required for flocculation. Overexpression of Pfl1 led to the formation of large size clumps/flocs (Eun-Joo Gina Kwon et al., 2012). Overexpression of other adhesins also led to the formation of flocs but only to a certain extent but was identified to have an additive effect when two different adhesins were expressed together in the same strain (Eun-Joo Gina Kwon et al., 2012).

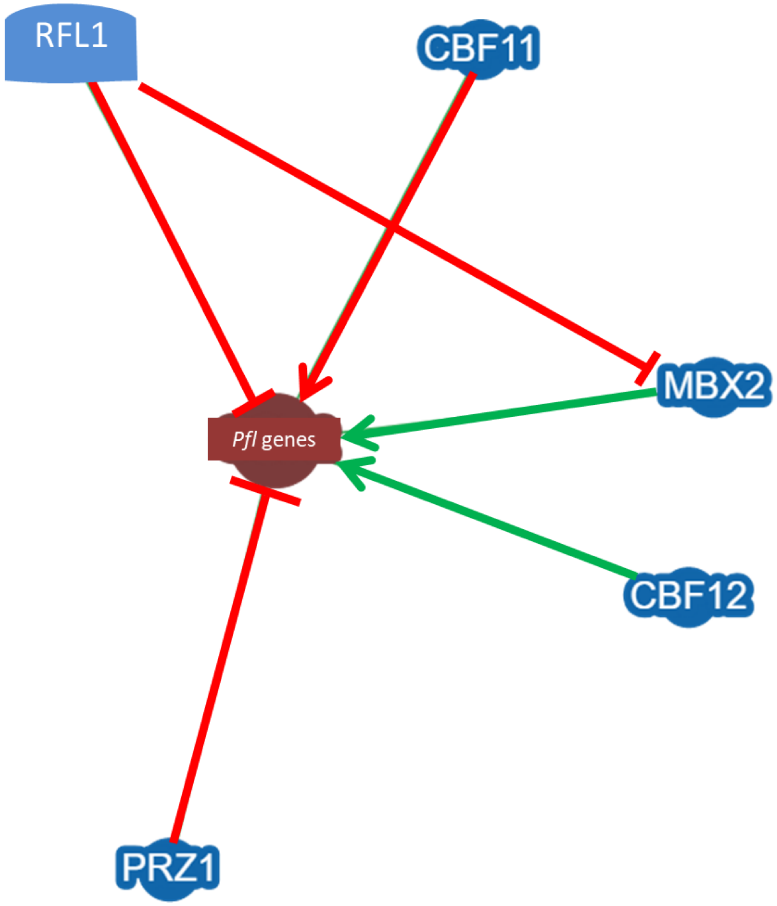

Figure 4: A model depicting the transcriptional regulatory network regulating adhesins in *S. pombe*. Positive regulations are indicated by green arrows and negative regulations are indicated by red bars. The network interactions were obtained from BioGRID[3.4] and modified.

In the study by Eun-Joo Gina Kwon et al., in 2012 the authors have demonstrated *S. pombe* flocculation is regulated by multiple transcription factors that regulate flocculins by ChIP-chip analysis. In the study by Eun-Joo Gina Kwon et al., in 2012, Mbx2, Rfl1, Cbf12, Cbf11, were identified as the transcriptional regulators. Overexpression of transcription

regulators, *mbx2*$^{+}$, *cbf12*$^{+}$, and deletion of *cbf11*$^{+}$ can induce flocculation were already demonstrated in earlier studies (Matsuzawa T et al., 2011, Prevorovsky M et al., 2009). These transcription regulators were observed to regulate expression of the adhesins (Pfl1-Pfl9) and other cell wall remodeling enzymes such as Gas2, Psu1, and SPAC4H3.03c etc. (Eun-Joo Gina Kwon et al., 2012). The transcriptional network governing the *S. pombe* adhesin genes is shown in Figure 4. Some of the transcription factors are shown to be autoregulated and also regulate other transcription factors that regulate flocculation (Eun-Joo Gina Kwon et al., 2012). The green arrows represent positive regulators and red bars represent negative regulators. The network shown in Figure 4 reveals that the flocculation in *S. pombe* is controlled by complex of different transcriptional regulators and their targets genes have a role in flocculation and cell wall remodeling.

1.11 What are Inositol pyrophosphates?

Inositol pyrophosphates were initially identified in the slime mold *Dictyostelium discoideum* and later were found to be present in all eukaryotes (Europe-Finner et al., 1991). Inositol pyrophosphates are high energy molecules as they contain pyrophosphate bonds. These molecules are highly conserved in eukaryotes and regulate a variety of cellular processes like the response to salt stress in *S. cerevisiae*, the jasmonate defense in *Arabidopsis thaliana*, and the interferon response in humans (Dubois et al., 2002, Saiardi et al., 2005, York et al., 2005, Pulloor et al., 2014). Inositol pyrophosphates were identified to regulate the dimorphic switch in *S. pombe* and as a microtubule modulator (Pöhlmann et al., 2010, Pöhlmann et al., 2014). Lately Wild et al., 2016 has proposed intracellular phosphate homeostasis regulation by these inositol pyrophosphate molecules via recognizing inorganic phosphate levels (Pi). Inositol pyrophosphates are required for the morphogenetic response that could occur due to various extrinsic signals (Lev et al., 2015, Pöhlmann et al., 2010, Pöhlmann et al., 2014).

1.11.1 Structure of inositol pyrophosphates

An inositol ring forms the core structure of inositol phosphates. The inositol molecules containing several phosphates as a result of phosphorylation are designated as inositol polyphosphates. The number of phosphate groups in these molecules ranges from two phosphate groups as seen in inositol bisphosphate (IP_2) to eight phosphates groups in bis-diphosphoinositol tetrakisphosphate (IP_8). In inositol pyrophosphates, the inositol ring is mono-phosphorylated at all the carbon positions and has at least one pyrophosphate group at

specific positions on the inositol ring (IP_7 and IP_8). IP_7 and IP_8 are included in inositol polyphosphates, but they represent inositol pyrophosphates due to the presence of one or two di-phosphate groups. Such a high number of phosphate groups make these molecules high in phosphates than carbons. In this current study, the abbreviations used to depict these molecules are **IP** (**I**nositol **P**yrophosphates) and followed by the number of phosphate groups attached to the inositol ring (Figure 5; IP_6, IP_7, and IP_8). For example, 5-IP_7 stands for an inositol ring with six phosphate groups at six carbons and one pyrophosphate or diphosphate group at position 5 and 1-IP_7 represents an inositol ring with a pyrophosphate group at position 1 (Figure 5). Different families of enzymes that generate these molecules are described in detail in a later section

1.11.2 Intracellular generation of inositol pyrophosphates

Inositol pyrophosphates are small intra-cellular molecules that originate from *myo*-inositol. *Myo*-inositol serves as the structural basis of secondary messengers in eukaryotes as well as for the key component in the phosphatidylinositol (PI) and phosphatidylinositol phosphate (PIP) and Phosphatidylinositol (4,5) Biphosphate (PIP_2), (Di Paolo & De Camilli, 2006). It was proposed that the stereochemistry of D-*myo*-inositol ring signifies a signaling scaffold with a potential to "encode" 64 unique signaling states (York, 2005).

The generation of inositol pyrophosphates starts with the hydrolysis of phosphatidylinositol 4,5-biphosphate $PI(4,5)P_2$ located in the plasma membrane, by Phospholipase C leading to the release of IP_3 which after subsequent phosphorylation by different inositol polyphosphate kinases results in IP_4 and IP_5 (Odom et al., 2000; Saiardi et al., 2001). Ipk1 kinase phosphorylates at position 2 of IP_5 to generate IP_6 also known as phytic acid (York et al., 1999).

Two families of enzymes that catalyze the generation of these inositol pyrophosphates are IP_6 kinases (IP6Ks) and diphosphoinositol pentakisphosphate kinases (PPIP5Ks) (Saiardi et al., 1999, Draskovic et al., 2008, Mulugu et al., 2007, Fridy et al., 2007, Lin X et al., 2009). Kcs1 in *S. cerevisiae* and *S. pombe* is an IP6 kinase (IP6Ks) and Vip1 in *S. cerevisiae* and Asp1 in *S. pombe* are diphosphoinositol pentakisphosphate kinases (PPIP5Ks) from now on called Vip1 kinases. The IP6Ks via their 5-kinase activity generate 5-IP_7 using IP_6 as a substrate (Draskovic et al., 2008; Saiardi et al., 1999). These IP_6 kinases are also present in

humans and catalyze the generation of inositol pyrophosphates (IP_6 to 5-IP_7; Draskovic et al., 2008).

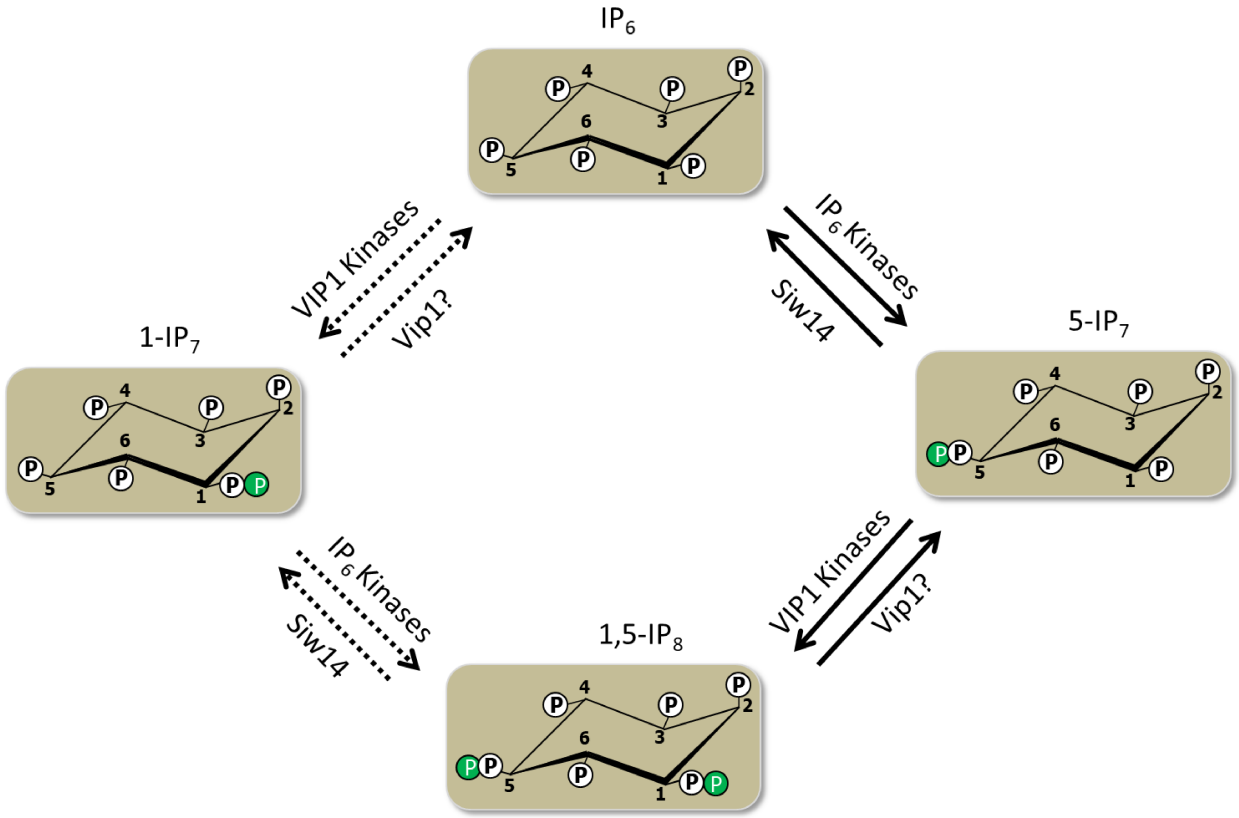

Figure 5: Generation of inositol pyrophosphates. IP_6 kinases generate 5-IP_7 using IP_6 as substrate and then this 5-IP_7 is used as a substrate by Vip1 kinases to generate 1,5-IP_8. (The solid arrows represent the pathway likely to be found *in vivo* and question marks: unidentified). Siw14 metabolizes 5-IP_7 to IP_6 (Elizabeth A. Steidle et al., 2016)

Vip1 kinases can generate 1-IP_7 from IP_6 through their 1-kinase activity. Several studies have proposed that Vip1 kinases can also generate 1,5-IP_8 using 5-IP_7 as substrate (Fridy et al., 2007, Lin X et al., 2009,Mulugu et al., 2007, Wang et al., 2011). In 2007, a study by Mulugu et al. has shown Vip1 as an IP_6 kinase in a strain lacking the *kcs1*$^+$ gene, thereby eliminating the substrate of Vip1. But in a later study by Onnebo et al., 2009 it was demonstrated in a *vip1*Δ strain that that Vip1 kinase activity generates IP_8. A recent study from our lab, has shown that the Vip1 kinase family protein Asp1 in *S. pombe* generates 1,5-IP_8 (Marina Pascual et al., 2018). Vip1, Asp1 and PPIP5K1 and PPIP5K2 are Vip1 kinases in *S. cerevisiae*, *S. pombe* and humans respectively. In the recent years, a couple of studies performed on different organisms such as *C. neoformans, A. thaliana*, and human cells demonstrated that Vip1 family members generate IP_8 (Gu et al., 2016, Laha et al., 2015, Lev

et al., 2015). The extensively studied classes of inositol pyrophosphates are 1-IP_7, 5-IP_7 and 1,5-IP_8. Vip1 family members are highly conserved from yeast to humans.

In yeast and humans, the IP_6 concentration varies from 15-60 µM, whereas, the IP_7 concentration lies at a much lower level at 0.5-5µM (Ingram et al., 2003, Shears et al., 2011). IP_8 levels are found to be only 20% of the total IP_7 present in the human cell (Shears et al., 2011). The major pools of inositol pyrophosphates in both yeasts and humans consists of 5-IP_7 and 1,5-IP_8 rather than 1-IP_7 (Gu et al., 2017, Lin X et al., 2009). In a recent publication from our lab, it was shown in *S. pombe* that Asp1 can generate 1,5-IP_8. It was observed that IP_6 was the most abundant species found in the *S. pombe* followed by IP_7 and IP_8. IP_8 was found to be the least abundant of all the inositol pyrophosphates found in *S. pombe* (Marina Pascual et al., 2018).

Another family of enzymes involved in the inositol pyrophosphate metabolism is nudix hydrolases (Ddp1). This family of proteins has phosphohydrolase activity, cleave diphosphate groups and lack specificity towards inositol pyrophosphates (McLennan, 2006, Safrany et al., 1998, Safrany et al., 1999, Shears, 2009, Lonetti et al., 2011). So, inositol pyrophosphates can be generated by subsequent phosphorylation by IP_6 kinases and Vip1 like proteins, and can be dephosphorylated by nudix hydrolases. Fluorides have been shown to inhibit nudix hydrolases addition of Sodium fluoride (NaF) to the cells enhanced the intra-cellular levels of inositol pyrophosphate. In a study in 2016 conducted by Elizabeth A. Steidle et al., it was shown that Siw14 has a specific pyrophosphatase activity towards 5-IP_7. It was demonstrated both *in vivo* and *in vitro* that Siw14 exclusively cleaves the β-phosphate from 5-diphosphoinositol pentakisphosphate (5-IP_7) (Elizabeth A. Steidle et al., 2016).

The relative level of these inositol pyrophosphate molecules can be altered under varying environmental conditions. In *A. thaliana,* jasmonate-mediated stress response increased IP_8 levels (Laha et al., 2015). These inositol pyrophosphates makeup only up to 2-5% of the total inositol pool in mammalian cells but are involved in a large number of cellular processes (Bennett et al., 2006). The turnover of IP_5 to IP_6 is very slow whereas, the turnover of IP_6 to inositol pyrophosphates is very quick. In this way, it was shown that up to half of the IP_6 reservoir is metabolized to inositol pyrophosphates depending on the cell type every hour (Glennon and Shears, 1993, Menniti et al., 1993). In primary hepatocytes, it was also calculated that IP_7 turn over ten times in a 40 minute period (Glennon & Shears, 1993). In *D. discoideum* and mammalian cells, it was demonstrated that the stress response increased

IP_8 levels (Luo et al., 2003, Choi et al., 2007, Pesesse et al., 2004). Although these molecules are present in lower concentrations but regulate several processes which give a hint that these molecules could act as signaling molecules (Burton et al., 2009, Shears 2009).

1.11.3 Modes of operations of inositol pyrophosphates

Inositol pyrophosphate molecules are mostly referred to as high energy molecules due to the presence of pyrophosphate bonds. The energy released by hydrolysis of the pyrophosphate bond is higher than the hydrolysis of an ATP molecule (Laussmann et al., 1996; Burton et al, 2009). Due to such a high energy release, these inositol pyrophosphates might serve as phosphate donors. There are two general mechanisms of action of inositol pyrophosphates: firstly pyrophosphorylation of target proteins and secondly direct binding to the target proteins (Wu et al., 2016).

In vitro studies showed that inositol pyrophosphate can pyro-phosphorylate proteins directly, by a non-enzymatic reaction (Bhandari et al., 2007 Saiardi et al., 2004). The target consists of a specific pre- phosphorylated serine residue. The inositol pyrophosphate can transfer the ß-phosphate group to the pre-phosphorylated serine residue i.e. pyro-phosphorylation of the target protein occurs (Bhandari et al., 2007b, Saiardi et al., 2004). Interferon regulatory factor IRF3 was shown to be pyro-phosphorylated *in vitro* (Pulloor et al., 2014). This phenomenon could not be detected *in vivo* yet, so this point still remains to be elucidated (Shears, 2009, Yang et al., 2008, York & Hunter, 2004). *In vitro* analysis using cell, free phosphorylation assays demonstrated interferon regulatory factor IRF3 is pyrophosphorylated. PPIP5K silenced cells displayed reduced IRF3 pyrophosphorylation. It was observed that a pyrophosphorylation of the protein subunit AP3B1 is involved in the HIV-1 release by 5-IP_7 and a pyrophosphorylation of RNA polymerase I subunits in *S. cerevisiae* by 5-IP_7 can occur (Azevedo et al., 2009, Thota et al., 2015).

The other kind of inositol pyrophosphate action via direct binding is observed in the *S. cerevisiae* Pho80/Pho85/Pho81 complex. Pho4 is the transcription factor that regulates the *PHO* genes. Under phosphate-rich conditions, Pho4 is phosphorylated by the Cdk complex Pho80/Pho85, which results in cytoplasmic localization and inhibits expression of *PHO* genes (O'Neill et al., 1996). Under phosphate deficient conditions the Cdk inhibitor Pho81 inhibits the Pho80/Pho85 kinase activity and abolishes the phosphorylation of Pho4. Un-phosphorylated Pho4 enters the nucleus and activates the *PHO* genes. IP_7 binds reversibly to

the Pho80/Pho85 complex and mediates the inhibition of Pho85. This allows the Pho4 transcription factor to express *PHO* genes (Lee et al., 2008, Lee et al., 2007). It was demonstrated that inositol pyrophosphates regulate phosphate homeostasis in relation to the synthesis of the energy molecule poly-P and this occurs by binding of inositol pyrophosphate molecules to the SPX domain-containing proteins in *S. cerevisiae* (Auesukaree et al., 2005, Azevedo and Saiardi, 2017, Gerasimaite et al., 2017, Wild et al., 2016).

1.11.4 Inositol pyrophosphates are involved in diverse cellular functions

Inositol pyrophosphates regulate diverse cellular process in fungi, plants, and animals. IRF3 phosphorylation by 1-IP_7 triggers an innate immune response in mammalian cell lines and Insulin secretion is distorted in mice lacking IP6K1 are few examples of how inositol pyrophosphates regulated various cellular processes in mammals (Pulloor et al., 2014, Bhandari et al., 2008, Chakraborty et al., 2010). In yeast, Kcs1 generated inositol pyrophosphates regulate telomere length and DNA recombination (Luo et al., 2002, Saiardi et al., 2005, York et al., 2005). Inositol pyrophosphates were also shown to regulate the jasmonate-regulated defense against wounds in *Arabidopsis*. These molecules are also involved in the response to external stimuli. A 10-25 fold increase in the inositol pyrophosphate concentration was observed in slime mold *D. discoideum.* During starvation, the cAMP signaling molecules act as signaling molecules to induce aggregation (Laussmann et al., 2000). A 10 fold increase in the IP_7 levels and 20-30 fold increase in IP_8 levels were observed during this process (Laussmann et al., 2000, Luo et al., 2003). Inositol pyrophosphate concentration in *D. discoideum* was 10 fold higher compared to mammalian cells and yeast under nutrient-rich conditions (Laussmann et al., 2000). Presences of multiple phosphate groups is an important characteristic of these molecules and are likely to play a role in cell signaling (Burton et al., 2009, Shears et al., 2009).

Sorbitol-induced hyperosmotic stress or heat stress resulted in 10-25 fold increase in the IP_7 levels in mammalian cells (Choi et al., 2007, Pesesse et al., 2004). Mouse embryonic fibroblasts (MEFs) stimulated with insulin-like growth factor 1 (IGF-1) produced less IP_8 that results in an increased signal transduction pathway(Akt signaling) (Chakraborty et al., 2010, Chakraborty et al., 2011). It was shown in *S. cerevisiae*, that the intra-cellular IP_7 concentration increases in response to low phosphate, whereas, a decrease in IP_7 levels were observed in oxidative stress by H_2O_2 (Lee et al., 2007, Onnebo & Saiardi, 2009). The aforementioned studies revealed that intracellular levels of inositol pyrophosphates can be

altered by external and internal signals and thereby acting as signaling molecules (Burton et al., 2009, Chakraborty et al., 2011, Shears et al., 2009). Inositol pyrophosphates generated by Vip1 kinase family in *S. pombe*, *A. nidulans, U. maydis* are essential for the polarized growth and modulate the microtubule cytoskeleton. In another study from our lab, it was demonstrated that these molecules are essential for several processes involved in mitosis such as bipolar spindle assembly, chromatid biorientation, and chromosome missegregation (Topolski B et al., 2016).

In *S. pombe* changes in cell shape is dependent on these high energy molecules due to extrinsic signals. In *S. pombe* it has also been shown that these molecules are crucial in the microtubule cytoskeleton maintenance and morphogenetic switch. In *S. pombe,* absence of inositol pyrophosphates led to an increase in aneuploidy cells (Pöhlmann et al., 2010, Pöhlmann et al., 2014, Topolski B et al., 2016).

Inositol pyrophosphates generated by the IP_6 kinase in *C. neoformans* are essential for the proper growth and cell wall integrity. A *kcs1*Δ strain produced less melanin which is essential for susceptibility towards oxidative stress induced by macrophages and UV light (Lev S et al., 2015). In *C. neoformans* it was demonstrated that these molecules are essential for the fungal acclimatization to the host body, immune recognition and also to cause of disease in the host (Lev S et al., 2015).

VIH1 and VIH2 are functional PPIP5K enzymes that generate inositol pyrophosphates in *A. thaliana.* It was shown that *A. thaliana* VIH1 and VIH2 can complement a VIP1 deletion in *S. cerevisiae*. VIH2 generates inositol pyrophosphates in response to methyl jasmonate perception and triggers jasmonate-regulated plant defense against insect herbivores and necrotrophic fungal pathogens (Debabrata Laha et al., 2015). *In silico* docking, experiments displayed high affinity of inositol pyrophosphates to the F-box protein COL1-jasmonate co-receptor complex which is the important component of the jasmonate-regulated plant defense mechanism (Debabrata Laha et al., 2015).

In a study by Pulloor et al., 2014, a pathway synthesizing inositol pyrophosphates was identified as a positive regulator of the genes that regulate transcriptional induction of type-I interferon response that occurs through RIG-I (pattern recognition receptor that detects RNA viruses). In the study by Pulloor et al., 2014, it was identified for the efficient phosphorylation of IRF3 and regulation of cellular infection by Sendai and influenza A

viruses requires inositol pyrophosphates synthesis pathway. The potential mechanism underlying the phosphoryl transfer could be through protein pyrophosphorylation that involves interferon signaling (Pulloor et al., 2014).

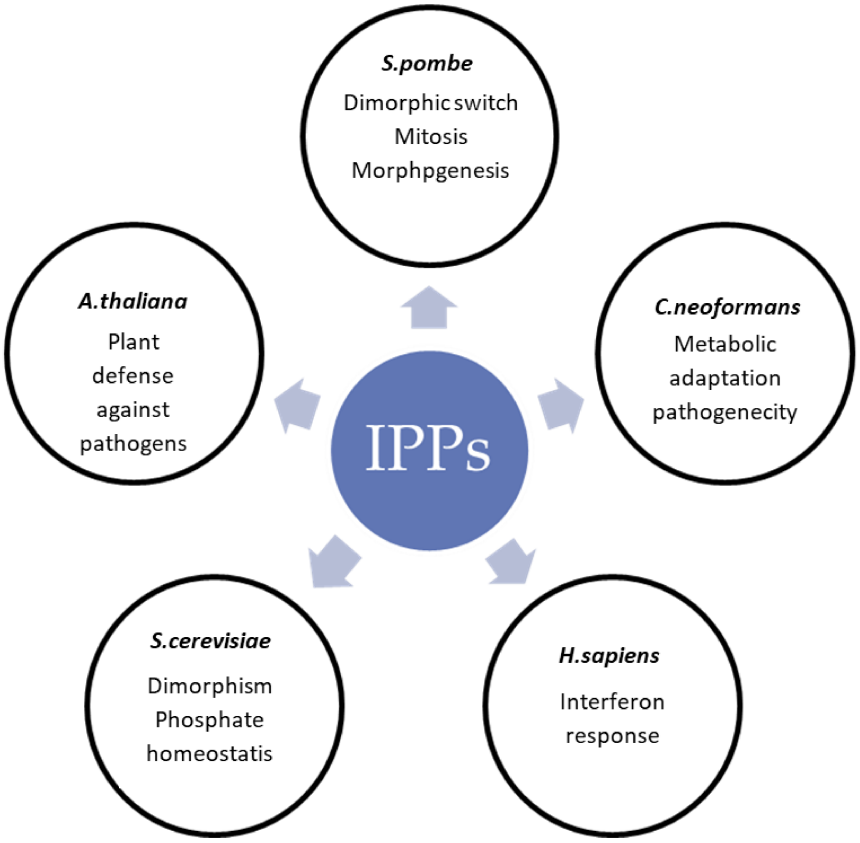

Figure 6: Diagrammatic representation of functions of inositol pyrophosphates in different organisms and their diverse cellular process (Pöhlmann J. et al.,(2012,2014), Lev S et al.,(2015), Debabrata L et al.,(2015), Pulloor NK et al.,(2014).

1.11.5 Structure of Vip1 kinases

Asp1 belongs to a conserved Vip1 inositol polyphosphate kinase family. Vip1 was described initially in *S. cerevisiae* and members of this family are present in all organisms from yeast to mammals (Choi et al., 2007, Fridy et al., 2007, Mulugu et al., 2007). It was discovered in *S. cerevisiae* when *kcs1* was deleted that the predominant inositol pyrophosphates observed were IP_6 and 1-IP_7 but not 5-IP_7. In these circumstances, Vip1 utilizes IP_6 as substrate and generates 1-IP_7. *S. cerevisiae* Vip1 and *S. pombe* Asp1 have almost similar sequence identity (55 %, Feoktistova et al., 1999).

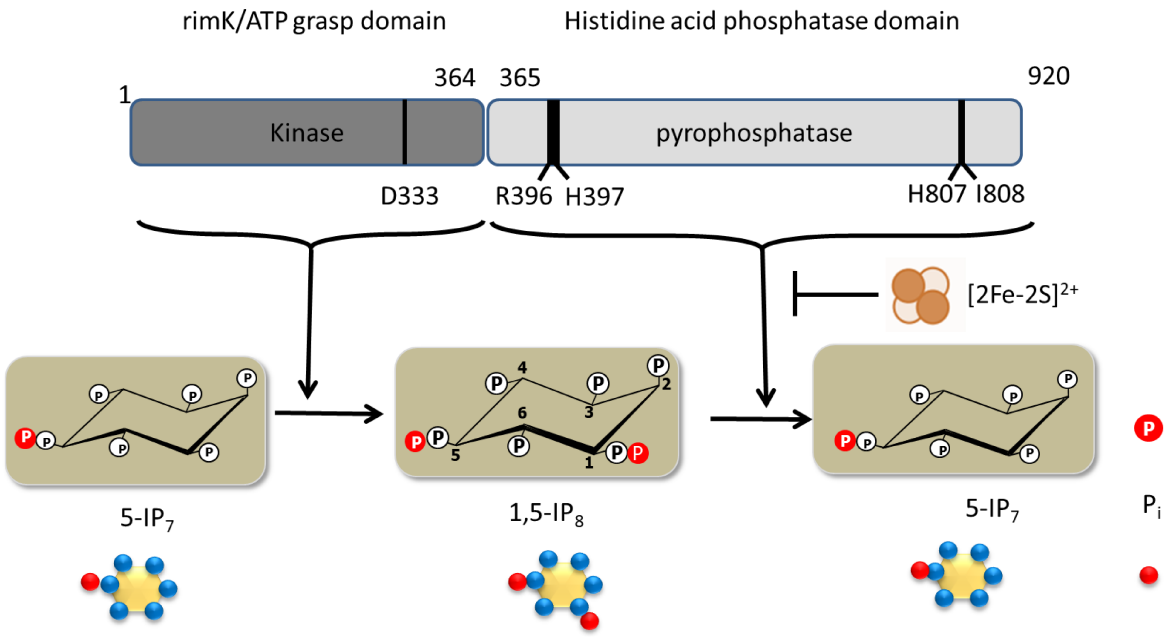

Figure 7: Diagrammatic representation of the structure of Vip1 inositol polyphosphates kinase family. They contain an N-terminal "Rimk / ATP-grasp" superfamily domain which is enzymatically active and can generate inositol pyrophosphates. The C-terminal domain has homology to acid histidine phosphatases and has pyrophosphatase activity. The amino acids numbers represent the start and end of the two domains starting from the N-terminus. The C-terminal domain can hydrolyze the inositol pyrophosphates generated by the N-terminal domain to IP_6 and P_i *in vitro* and 1,5-IP_8 to 1-IP_7 *in vivo* (Marina Pascual et al., 2018*)*. This enzymatic activity can be inhibited by binding of Fe-S cluster *in vitro* (Wang, H et al., 2015). The picture depicts the symbolic representation of IP_7 and IP_8. The red colored dot represents the pyrophosphate and the blue dots represent the phosphate group at six carbon ring of the inositol.

Vip1 kinases are bifunctional enzymes and have a conserved two domain structure consisting of an N-terminal “RimK/ATP-grasp domain” and a C-terminal pyrophosphatase domain with high homology to “acid phosphatases” (Figure 7, Mulugu et al., 2007). The N-terminal domain can bind to ATP and catalyzes the generation of inositol pyrophosphates (Choi et al., 2007; Fridy et al., 2007, Lin X et al., 2009, Mulugu et al., 2007 Pöhlmann et al., 2014). For the catalytic activity of the N-terminal kinase domain, the aspartic acid residue at position 333 in *S. pombe* is essential and exchange to alanine at this position led to the loss of the kinase activity (Mulugu et al., 2007, Pöhlmann et al., 2010, Marina Pascual et al., 2018).

The C-terminal domain has similarities to histidine acid phosphatases which are also found in phytases. Phytases are a group of enzymes that hydrolyze the phosphomonoester bonds from phytic acid or IP_6 and release the inorganic monophosphates (Mullaney & Ullah, 2003). Histidine acid phosphatases have two conserved motifs, firstly RHXXR and second

HD. In Asp1, the first conserved domain RHXXR lies at the amino acid positions 396-400 and the second conserved HD domain at positions 807-808. In *S. pombe* Asp1 in the second motif HD the aspartate residue next to the histidine is substituted to isoleucine (HI) and misled the scientists thinking that the C-terminus of Vip-1 kinases is inactive (Fridy et al., 2007, Gokhale et al., 2011). The aspartate residue in the second motif of Vip1 family members was substituted, with isoleucine, valine, or alanine (Fridy et al, 2007). For the enzymatic function of acid phosphatases, the two histidine motifs are essential and the arginine residues in the first motif form a phosphate pocket. The histidine residue is phosphorylated during the enzymatic reaction and the two arginines stabilize the phosphate through electrostatic interaction (Rigden, 2008). The histidine present in the second motif along with the aspartate residue donates the proton that is bound to the phosphate group. In phytases of *E. coli,* substitution of aspartate residue decreased the catalytic activity over 100-fold (Ostanin et al., 1992).

The enzymatic activity of the C-terminus was not revealed until recent years. An *in vivo* study from our lab in 2014 has demonstrated that the C-terminal domain of Asp1 has a negative effect on the amount of inositol pyrophosphates generated by the N-terminal domain. A very recent study from our lab has shown that C-terminal domain *in vivo* has pyrophosphatase activity (Pöhlmann et al., 2014, Marina Pascual et al., 2018). Relying upon the two studies mentioned above it can be affirmed that the C-terminal of Asp1 has a pyrophosphatase activity.

The Asp1 kinase domain generated inositol pyrophosphates can be hydrolyzed to IP_6 and inorganic phosphate (P_i) by the C-terminal pyrophosphatase domain (Huanchen Wang et al., 2015, Marina Pascual et al., 2018). It was shown *in vitro,* this activity is specific for 1-diphosphate in both 1-IP_7 and 1,5-IP_8. It was also shown that, recombinant Asp1 C-terminal domain ($Asp1^{371-920}$) contained iron and sulfide at a stoichiometry of 2 atoms per Asp1 molecule when reconstituted under anaerobic conditions. The $[2Fe\text{-}2S]^{2+}$ cluster inhibits the phosphatase activity of Asp1 which leads to the increase in the activity of the N-terminal domain (Huanchen Wang et al., 2015). The *in vitro* enzymatic activity of the C-terminal domain in human VIP1 kinases was demonstrated to be specific for 1- diphosphates in both 1-IP_7 and 1,5-IP_8 and this can be inhibited by the addition of inorganic Pi(Gu et al., 2017).

1.11.6 Asp1 variants generated different levels of inositol pyrophosphates

As mentioned in the previous section, the conserved domains in both kinase and pyrophosphatase domains are important for kinase and pyrophosphatase activity respectively. Substitution of the aspartate residue at position 333 to alanine ($Asp1^{D333A}$) led to complete loss of kinase activity and the mutant was unable to generate 1-IP_7 *in vitro* and 1,5-IP_8 *in vivo* (Pöhlmann et al., 2014, Marina Pascual et al., 2018). Pyrophosphatase domain harbor a conserved histidine residue at position 397 and substitution to alanine ($Asp1^{H397A}$) led to the loss of the pyrophosphatase activity (Pöhlmann et al., 2014, Marina Pascual et al., 2018). $Asp1^{H397A}$ was able to generate 1,5-IP_8 *in vivo* and the levels were found to be higher than that of the wild-type Asp1 strain. Protein levels in the corresponding strains (*asp1*$^{+}$, *asp1*^{D333A}, and *asp1*^{H397A}strains) were not altered due to these mutations (Pöhlmann et al., 2010). But these alterations led to changes in the enzymatic activity in comparison to the wild-type Asp1 (Pöhlmann et al., 2014, Marina Pascual et al., 2018).

Generation of inositol pyrophosphates by Asp1 variants was analyzed both *in vitro* and *in vivo* in two studies from our working group. *In vivo* studies measured the amount of IP_6, IP_7, and IP_8 in different *asp1* variants strains mentioned above, through radiolabeled (^3H) inositol and HPLC elution profiles. *In vitro* studies were analyzed using PAGE analysis.

Asp1 *in vitro* generated inositol pyrophosphates (IP_7) in an ATP dependent manner and activity was dosage dependent (Pöhlmann et al., 2014). *In vivo* analysis indicated that Asp1 generated 1,5-IP_8. $Asp1^{D333A}$ *in vitro* was unable to generate inositol pyrophosphates although an equal amount of protein was used in comparison to Asp1. $Asp1^{D333A}$ *in vivo* was unable to generate any 1,5-IP_8 but the increase in the amount of 5-IP_7 was observed. *In vivo* studies have shown that this was similar to the *asp1Δ* strain.

$Asp1^{H397A}$ appears to generate a higher amount of inositol pyrophosphates *in vitro* compared to Asp1. *In vitro* analysis has shown that after a period of ten hours $Asp1^{H397A}$ generates almost twice as much inositol pyrophosphates than wild-type Asp1. In the later, *in vivo* studies, it was demonstrated that this domain has pyrophosphatase activity and it can dephosphorylate 1,5-IP_8 to 5-IP_7. The $Asp1^{H397A}$ variant *in vivo* generated almost two-fold higher levels of IP_8 than the wild-type strain. *In vitro* analysis has shown that affinity of Asp1 and $Asp1^{H397A}$ towards IP_6 was found to be similar whereas, $Asp1^{H397A}$ has 36% higher rate of reaction compared to Asp1 (Pöhlmann et al., 2014).

Asp1 kinase domain *in vitro* ($Asp1^{1-364}$) also exhibited similar output as the $Asp1^{H397A}$ variant. This is due to the complete absence of the Asp1 pyrophosphatase domain ($Asp1^{365-920}$) (Pöhlmann et al., 2014, Marina Pascual et al., 2018).*In vivo* analysis of wild-type strain expressing the $Asp1^{1-364}$ domain displayed an increase of four-fold in IP_7 level and a two-fold increase in 1,5-IP_8 levels.

In vivo analysis have shown that expression of the C-terminal domain ($Asp1^{365-920}$) led to increase in the levels of 5-IP_7 and diminished the levels of 1,5-IP_8 (Marina Pascual et al., 2018). It was demonstrated that the addition of the $Asp1^{365-920}$ domain to the *in vitro* assay resulted in the reduction in inositol pyrophosphates level generated by Asp1 and no significant difference in the levels of IP_6 (Pöhlmann et al., 2014). These two studies demonstrated that the C-terminal domain of Asp1 can dephosphorylate inositol pyrophosphates generated by the N-terminal domain by the pyrophosphatase activity.

Strain	**Plasmid expression**	***In vitro* IP_7 levels**	***In vivo* 1,5-IP_8 levels in relation to IP_6**	***In vivo* IP_7 levels in relation to IP_6**
$asp1^{+}$	-	1x	1x	1x
$asp1^{D333A}$	-	0x	0.12x	6.26(5-IP_7)
$asp1^{H397A}$	-	2x	2x	n.d
*asp1*Δ	-	0	0.11x	4.56
$asp1^{+}$	$asp1^{1-364}$	2x	2x	4x(1-IP_7)
$asp1^{+}$	$asp1^{365-920}$	0	0.4x	9.3
$asp1^{+}$	$asp1^{365-920/H397A}$	1x	5.3x	1.8

Table 1: Inositol pyrophosphate levels generated by Asp1 variant strain in *vivo* and *in vitro*. (Pöhlmann et al., 2014, Marina Pascual et al., 2018)

The variants used in the current study and all the results observed previously, were due to the change in the IP_8 levels generated by different variants of Asp1.

1.11.7 Inositol pyrophosphate levels influence several cellular processes in *S. pombe*

Asp1 was identified as a key regulator of the actin nucleation Arp2/3 complex (Feoktistova et al., 1999). Deletion of *asp1*$^{+}$ resulted in several abnormalities in the cell such as aberrant actin cytoskeleton organization, abnormal cell morphology, and temperature sensitivity. Morphological defects at 19°C and 36°C and dislocated F-actin structures were also observed (Feoktistova et al., 1999). The *asp1*Δ strain exhibited sensitivity to osmotic stress and were highly sensitive to Ca^{+} and a low pH. Polarized growth is established via intrinsic signals and regulated by microtubules and actin cytoskeleton and these can be modulated by extrinsic signals.

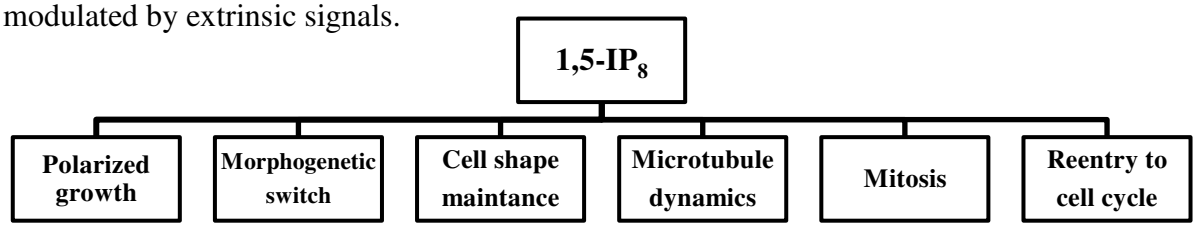

Figure 8: Asp1 generated inositol pyrophosphates regulated cellular processes in *S. pombe*

The Asp1 variant strains displayed varying levels of resistance when exposed to microtubule depolymerizing drug thiabendazole (TBZ). The *asp1*^{D333A} strain was more sensitive to TBZ compared to the wild-type *asp1*$^{+}$, strain, whereas, the *asp1*^{H397A} strain displayed the highest resistance to TBZ (Pöhlmann et al., 2010).

An increase in the cellular levels of inositol pyrophosphates leads to flocculation, a cell-cell adhesion, and cell-substrate adhesion and invasion (dimorphic switch). The *asp1*^{H397A} strain displayed heavy flocculation while cultivating in full media and the wild-type Asp1 strain displayed rarely any flocs. The *asp1*^{D333A} and *asp1*Δ strains did not display any flocs (Pöhlmann et al., 2010). Expression of *asp1*$^{+}$*, asp1*^{H397A}*, and asp1*$^{1-364}$ in an *asp1*Δ strain resulted in flocculation which depicts the functional kinase domain is essential for flocculation (Pöhlmann et al., 2010). Microscopic analysis of the invasive cells displayed pseudo-hyphae or a chain of cells attached to one another (Pöhlmann et al., 2010). The change of growth from the unicellular yeast form to pseudohyphal growth form was a consequence of changed polarized growth as invasively growing cells are predominantly monopolar. The invasively growing cells grew predominately at the old ends after cytokinesis. Cells expressing inositol pyrophosphates displayed invasive growth and an increase in these molecules further enhanced the ability to form invasive colonies. The cells

lacking Asp1 generated inositol pyrophosphates reduced the ability to form normal cylindrical shape after reentering from the G0 phase, implying the importance of IPPs in establishing the polarized growth (Pöhlmann et al., 2010).

Inositol pyrophosphates act as an important modulator for polarized growth. Accurate polarized growth is achieved by the appropriate functioning of the microtubules and actin cytoskeleton function (Chang, F. 2001, Martin, S. G. 2009, Piel, M., and P.T.Tran. 2009). Microtubule mutant *mal3*Δ and *tea1*Δ strains exhibited more invasive colonies than the wild-type strain (Pöhlmann et al., 2010). In the *act1*Δ*, sop2*Δ*, and arp3*Δ actin cytoskeleton mutant strains the ability to grow invasively is lost (Pöhlmann et al., 2010). Disorganized interphase microtubules, an increase in the interphase microtubules that depolymerized at the lateral cortex/cytoplasm and not at the cell tip are some of the defects observed in *S. pombe* that were incurred by the absence of inositol pyrophosphates (Pöhlmann et al., 2014). It was also demonstrated that residence time of microtubules at the cell tip was also regulated by inositol pyrophosphates (Pöhlmann et al., 2014). Inositol pyrophosphates were also shown to modulate the mitotic spindle and chromosome segregation fidelity (Topolski et al., 2016).

1.11.8 Inositol pyrophosphate levels influence several cellular processes in other fungi

In *A. nidulans* the lack of inositol pyrophosphates reduced the ability of the spores to generate a second germ tube and produced branching hyphae. This phenomenon requires microtubules for the correct growth zone selection (Pöhlmann et al., 2014). In *A. nidulans* absence or reduced levels of intracellular inositol pyrophosphates generated by VlpA the microtubule cytoskeleton together with microtubule dynamics at the hyphal tip was altered. In *U. maydis* deletion of Vip1 homolog *Umasp1,* displayed abnormal cell morphology and reduced the proliferation during yeast-like growth, and exhibited high sensitivity towards microtubule depolymerizing drug TBZ. Furthermore *Umasp1Δ* strain formed large buds and displayed depolymerized microtubules. The levels of UmAsp1 were reduced in hyphae, pointing towards reduced protein amount after filament induction (Pöhlmann et al., 2014).

The above-mentioned studies indicate the importance of these high energy molecules and their contribution in diverse cellular functions. As these molecules are identified in all eukaryotes and are shown to have several critical functions, it is necessary to understand the proper functioning of these molecules and to dissect the mechanisms underlying how these molecules modulate their target proteins.

1.12 Aim of this work

The main goal of this project is to decipher the role of Asp1 generated inositol pyrophosphates in the regulation of dimorphic switch. In particular to identify the potential targets of Asp1 those are essential for the switch.

In the initial section of my thesis I want to identify different environmental stimuli that can influence Asp1 mediated dimorphic switch. In the second section of the thesis, I want to identify if an increase in the inositol pyrophosphate concentrations can increase the ability of dimorphic switch linearly.

Further, I want to use invasive growth analysis to compare the *in vivo* measurements that took place during the course of work. In the third section, the aim is to identify the target proteins of Asp1 that are essential for the dimorphic switch. Our targeted proteins are the adhesins that are essential to adhere to the substrate and the transcriptional factors that govern these adhesins. Once identified, we wanted to know, how Asp1 generated inositol pyrophosphates can regulate these molecules. Furthermore I want to understand with which domain of Asp1 does the physical interactors interact and identify their role in the dimorphic switch.

2. Materials and Methods

2.1. Reagents

Chemical	company
3-(N-Morpholino)-Propansulfonsäure (MOPS)	Sigma
4-Nitrophenylphosphat	Sigma
5-Bromo-4-chloro-3-Indolyl-Phosphat (BCIP)	Sigma
5-Bromo-4-Chloro-3-indoxyl-β-D-galactopyranoisid (X-Gal)	Serva (Heidelberg)
Acetic acid	Riedel-deHaën
Acrylamide (37,5:1)	Roth
Adenine	Roth
Agarose: SeaKem LE	Biozym
Ammonium acetate	Roth
Ammonium chloride	Roth
Ammoniumperoxodisulfate (APS)	Merck
Ammonium sulfate	Roth
Ampicillin	Grünenthal
Arginine	Roth
Bacto Agar	Difco
Bacto Trypton	Difco
Bovines Serum albumin (BSA)	Sigma-Aldrich
Bradford Reagent	Bio-Rad
Bromphenolblue	Fluka
Calcium chloride	Sigma
Chloroform	Roth
Concanavalin A	Sigma
Dimethyl sulfoxide (DMSO)	Sigma
Dinatrium-Ethylendiamintetraacetate (EDTA)	AppliChem
di-Natriumhydrogenphosphate (Na2HPO4)	J.T. Baker
Dithiothreitol (DTT)	Roth
Ethanol technical (96 %)	J.T. Baker
Ethidium bromide (10mg/ml)	Roth
Ethylenglycol-bis (β-Aminoethylether) N,N,N,',N'-Tetra acetate	Sigma
Geneticinsulfate (G418)	Calbiochem
Glucose Monohydrate	Roth
Glutamic acid	Sigma
Glycerin	Roth
Glycine	Roth
Histidine	Roth
Isopropanol	Roth
Isopropyl-β-D-thiogalactopyranosid (IPTG)	Stehelin (Basel)
Leucine	Roth
Lithium acetate (LiOAc)	Roth
Lysine	Roth
Magnesium chloride(MgCl2 + 6 H2O)	Roth
Magnesium sulfate	Sigma
Manga sulfate	Sigma
Methanol	Riedel-de Haën
Nitro Blue Tetrazolium (NBT)	Sigma

Nourseothricin	Jena Bio science
Paraffin	Caesar & Loretz
Paraformaldehyde	Sigma
Peptone	Difco
Phenol	Roth
Phenylmethylsulfonylfluorid (PMFS)	Serva
Piperazin-N,N`-bis (2-ethansulfonsäure) (PIPES)	Sigma
Polyethylenglycol 4000 (PEG)	Sigma
Poly-L-Lysine	Sigma
Potassium acetate	Merck
Potassium chloride (KCl)	Roth
Potassium dihydrogen phosphate (KH2PO4)	Merck
Potassium phthalate	Sigma
Salmon fish sperm DNA	Sigma-Aldrich
Sodium acetate (NaOAc)	Roth
Sodiumazide (NaN3)	Sigma
Sodium chloride (NaCl)	J.T. Baker
Sodium citrate	Fluka
Sodiumdodecylsulphate (SDS)	Roth
Sodium fluoride (NaF)	Sigma
Sodium hydroxide (NaOH)	Roth
Sodium-Pantothenacid	Sigma
Sodium phosphate	Sigma
Sodium sulfate	Merck
Sorbitol	Roth
Tetramethylethylendiamine (TEMED)	Merck
Thiabendazole (TBZ)	Sigma
Thiamine	Sigma
Trishydroxymethylaminomethane (Tris)	Roth
Triton X-100	Sigma
Uracil	Sigma
Vaseline	Caesar & Loretz
Hydrogen peroxide	AppliChem
Xylencyanolblue	Serva
Yeast extract	Difco
Zinc sulfate	Sigma
β-Glycerophosphate	Sigma

2.2. Restriction endonucleases

Enzyme	**Sequence of restriction**	**Company**
NotI	GC ↓GGCCGC	Fermentas
XhoI	C ↓TCGAG	Fermentas
Hind III	A↓AGCTT	Fermentas
EcoRI	G↓AATTC	Fermentas
NdeI	CA↓TATG	Fermentas
EcoRV	GAT↓ATC	Fermentas
*Bam*HI	G↓GATCC	Fermentas
XcMI	CCANNNNN↓NNNNTGG	New England Bio labs

2.3. Other enzymes

- β-Glucuronidase Sigma-Aldrich(Roche)
- Pfu-DNA-Polymerase(Invitrogen)
- Pfx-DNA-Polymerase(Fermentas)
- Proteinase K(Roche)
- RNase A Sigma (Sigma Aldrich)
- Taq-DNA-Polymerase (U. Fleig)
- Zymolase-(Seikagaku)
- Lysozyme Sigma(Aldrich)
- T4 DNA Ligase-(Fermentas)

2.4. Equipment

Centrifuge X3R	Thermo Scientific
Nanodrop Spectrophotometer	PEQLAB
Neubauer cell counting chamber	Marienfeld
PCR-Thermocycler	Biorad, MJ
Precellys Homogenizer	PEQLAB
Speed-Vac- Vacuum-Concentrator	Savant
Axiostar Plus Microscope	Zeiss
MSM 300 Micromanipulator	Singer Instruments
Incubators	Thermo scientific

2.5. Kits

Plasmid Midi Kit-Qiagen,
Qia Quick Gel Extraction Kit(Qiagen)
Qia Quick PCR Purification Kit (Qiagen)
Matchmaker GAL4 Two-Hybrid System 3 (Clontech)
Glo-lysis buffer 1x (Promega)

2.6. Other materials and Plastic wear

Complete Protease Inhibitor Cocktail	Roche
Cover slips	Diagonal
dNTP Set	Thermoscientific
Eppendorf tubes	Eppendorf
Filter paper Western blot	VWR
Glass beads (0.4 – 0.6 mm Ø)	Sartorius
Immersion oil 518F	Zeiss

cuvettes (10 x 4 x 45mm)	Sarstedt
Object slides (76 x 26 mm)	Diagonal
Petri dishes 150 mm Ø	Sarstedt
PVDF Transfer Membrane	Thermo Scientific
15 ml centrifugation falcon	Sarstedt
50 ml centrifugation falcon	Sarstedt

2.7. Plasmids

Number	Plasmid	Reference
163	*pAF1* (AmpR) PCR-template plasmid (Gene deletion with *his3*$^{+}$)	U. Fleig
177	*KLG 1153-GFP- kan*^{R} PCR-template plasmid for KanR	U. Fleig
260	pREP81-*asp1*$^{+}$*LEU2, AmpR,*	K. Gould Nr. 1174
261	pREP41-*asp1*$^{+}$*LEU2, AmpR,*	K. Gould Nr. 1175
270	pJR2-3XL *LEU2*, *Amp*^{R}, pREP3X, *nmt1*	U. Fleig
274	pJR2-41XL - *LEU2*, Amp^{R}, entspricht pREP41X,	J.C.Ribas
278	pJR2-81XL *LEU2*, *Amp*^{R}, pREP81X	J.C.Ribas
537	pGADT7 *AmpR, LEU2, ADH1* Promotor, *GAL4 AD*	Yeast 2 hybrid Clontech
538	pGBKT7 *KanR, TRP1, ADH1* Promotor, *GAL4 BD*	Yeast 2 hybrid Clontech
539	pGADT7-*asp1*$^{+}$	U. Fleig
586	pGBKT7-53 KanR, TRP1, ADH1 Promotor, GAL4 BD	Clontech
587	pGBKT7-LaminC KanR, TRP1, ADH1 Promotor, GAL4 BD	Clontech
653	pGBKT7-asp1+	U. Fleig
659	pREP4XU::NLS-GFP *AmpR,*	U. Fleig
672	pJR2-3XL *-asp1 1-364 AmpR,*	U. Fleig
674	pGADT7-T control vector yeast-2-hybrid	Clontech
770	pJR2-3XL-*asp11-364-GFP AmpR,*	U. Fleig
882	pJR2-3XL-*asp1+ LEU2*, *AmpR*,	U. Fleig
885	pJR2-3XL-*asp1365-920-GFP AmpR,*	U. Fleig
887	pJR2-3XL-*asp1+-GFP AmpR,*	U. Fleig
916	pJR2-3XL-*asp1* 365-920 *AmpR,*	U. Fleig
1012	pREP4XU::NES-GFP *AmpR,*	U. Fleig
1024	pREP4XU-asp1^{+}-NLS-GFP, *AmpR,*	this study
1025	pREP4XU-asp1$^{1\text{-}364aa}$-NLS-GFP *AmpR,*	this study

1027	pREP4XL-NLS-GFP, LEU2 *AmpR,*	this study
1028	pREP4XL-NES-GFP, LEU2, *AmpR,*	this study
1031	pGADT7-asp1$^{1\text{-}364aa}$	this study
1032	pGADT7-asp1$^{365\text{-}920aa}$	this study
1033	pGBKT7-asp1$^{1\text{-}364aa}$	this study
1034	pGBKT7-asp1$^{365\text{-}920aa}$	this study
1041	pREP4XL-Asp1-NLS-GFP, LEU2 *AmpR,*	this study
1042	pREP4XL-Asp1$^{1\text{-}364aa}$-NLS-GFP, LEU2 *AmpR,*	this study
1043	pREP4XL-Asp1$^{365\text{-}920aa}$-NLS-GFP, LEU2 *AmpR,*	this study
1044	pREP4XL-Asp1-NES-GFP, LEU2 *AmpR,*	this study
1045	pREP4XL-Asp1$^{1\text{-}364aa}$-NES-GFP, LEU2 *AmpR,*	this study
1046	pREP4XL-Asp1$^{365\text{-}920aa}$NES-GFP, LEU2 *AmpR,*	this study
1053	*KLG 1153-GFP- kan^{R}* Kassette-+Ars+Trp+Cen (plasmid 177)	this study
1054	*KLG 1153-GFP- kan^{R}* Kassette-Ars+Trp+Cen+NLS-GFP::Kan^{R}	this study
1055	*KLG 1153-GFP- kan^{R}* Kassette-Ars+Trp+Cen+NLS::Kan^{R}	this study
1056	*KLG 1153-GFP- kan^{R}* Kassette-Ars+Trp+Cen+NES-GFP::Kan^{R}	this study
1057	*KLG 1153-GFP- kan^{R}* Kassette-Ars+Trp+Cen+NES::Kan^{R}	this study
1059	pJR2-3XL-*asp1^{I808D}, AmpR,*	U. Fleig
1071	pJR2-3XL-*asp1^{H807A}, AmpR,*	U. Fleig
1072	pJR2-3XL-*asp1^{R400A}, AmpR,*	U. Fleig
1083	pJR2-41XL Asp1$^{1\text{-}364}$*LEU2*, Amp^{R},	this study
1084	pJR2-81XL Asp1$^{1\text{-}364}$ *LEU2*, *Amp*^{R},	this study
1097	pJR2-3XL-*asp1$^{365\text{-}920aa,I808D}$ Amp*^{R},	U. Fleig
1099	pJR2-3XL-*asp1^{S674A} Amp*^{R},	U. Fleig
1105	Y9, (SPAC1071.05) Yeast 2 hybrid vector	Clontech
1106	Y14 (SPBC725.03) Yeast 2 hybrid vector	Clontech
1113	Y47,(SPCC584.01c), Yeast 2 hybrid vector	Clontech
1115	Y54, (SPCC594.01), Yeast 2 hybrid vector	Clontech
1157	pJR2-3XL-*asp1^{S674E} Amp*^{R},	U. Fleig
1179	pJR2-3XL-*asp1^{I808N} Amp*^{R},	U. Fleig
1180	pJR2-3XL-*asp1^{I808V} Amp*^{R},	U. Fleig
1146	pREP4XL-Asp1$^{365\text{-}920aa\text{-}\ H397A}$-NLS-GFP	this study

2.8. Strains

2.8.1 *S. pombe* strains

Strain Number	Genotype	Reference
605	*his3-D1, ade6-M210, leu1-32, ura4-D18, h⁻*	K. Gould 425
771	*asp1-pk-GFP::ura4⁺, ade6-M210, ura4-D18, his3-D1, leu1-32, h⁻*	tagging 605
1156	*asp1Δ::kanR, his3-D1, ade6-M216, leu1-32, ura4-D18, h-*	U. Fleig
1511	*asp1^{D333A}::kan^{R}, his3-D1, ade6-M210, leu1-32, ura4-D18, h⁺*	Tagging 605, 2 backcross 605 btn. 606
1579	*asp1^{H397A}::kan^{R}, his3-D1, ade6-M210, leu1-32, ura4-D18, h⁺*	tagging 605, 2 backcrosses 605/606
1580	*asp1^{D333A}-GFP::ura4⁺, his3-D1, ade6-M210, leu1-32, ura4-D18, h⁺*	tagging 1511
1726	*asp1^{H397A}::kanR, SPBC1289.15Δ::his3⁺, leu1-32, ade6-M210, his3-D1, ura4-D18, h⁺*	Deletion von SPBC1289.15 in Stamm 1579
1728	*asp1^{H397A}::kan^{R}, SPAC186.01Δ::his3⁺, leu1-32, ade6-M210, his3-D1, ura4-D18, h⁺*	Deletion von SPAC186.01 in Stamm 1579
2079	*asp1^{H397A}-GFP::ura4⁺, ade6-M210, his3-D1, leu1-32, ura4-D18, h⁺*	tagging 1579
2169	*asp1^{H397A}::kan^{R}, gsf2::ura4⁺, leu1-32, ura4-D18, ade6-210, his3-D1, h⁺*	deletion 1579
2197	*gsf2::ura4⁺, leu1-32, ura4-D18, ade6-210, his3-D1*	2169x605
2232	*mbx2Δ::ura4⁺, ura4-D18, leu1-32, his3-D1, ade6-M210, h⁻*	Deletion 605
2233	*mbx2Δ::ura4⁺, asp1^{H397A}::kan^{R}, ura4-D18, leu1-32, his3-D1, ade6-M210, h⁺*	Deletion 1579
2452	*asp1-NLS-GFP::kan^{R}, ade6-M210, ura4-D18, his3-D1, leu1-32, h⁻*	605 tagging
2480	*asp1-NES-GFP::Kan^{R} his3-D1, ade6-M210, leu1-32, ura4-D18, h*	605 tagging original
2481	*asp1-NES-GFP::Kan^{R} his3-D1, ade6-M210, leu1-32, ura4-D18, h⁻*	605 tagging original
2482	*asp1-NES-GFP::Kan^{R} his3-D1, ade6-M210, leu1-32, ura4-D18, h⁻*	605 tagging original
2649	*hpm1Δ ::"GFP"::kan^{R}, his3-D1, ade6-M210, leu1-32, ura4-D18, h+*	606x2582
2649	*hpm1Δ ::"GFP"::kan^{R}, his3-D1, ade6-M210, leu1-32, ura4-D18, h+*	606x2582
2650	*hpm1ΔΔ ::"GFP"::kan^{R}, his3-D1, ade6-M210, leu1-32, ura4-D18, h+*	606x2582

2650	*hpm1Δ ::"GFP"::kan^{R}, his3-D1, ade6-M210, leu1-32, ura4-D18, h+*	606x2582
2651	*SPBC725.03Δ::"GFP"::kan^{R}, his3-D1, ade6-M210, leu1-32, ura4-D18, h-*	606x2586
2651	*SPBC725.03Δ::"GFP"::kan^{R}, his3-D1, ade6-M210, leu1-32, ura4-D18, h-*	606x2586
2652	*SPBC725.03Δ::"GFP"::kan^{R}, his3-D1, ade6-M210, leu1-32, ura4-D18, h+*	606x2586
2652	*SPBC725.03Δ::"GFP"::kan^{R}, his3-D1, ade6-M210, leu1-32, ura4-D18, h+*	606x2586
2653	*hpm1Δ::"GFP"::kan^{R}, asp1^{D333A}::kan^{R} , his3-D1, ade6-M210, leu1-32, ura4-D18, h-*	1511x2582
2653	*hpm1Δ::"GFP"::kan^{R}, asp1^{D333A}::kan^{R} , his3-D1, ade6-M210, leu1-32, ura4-D18, h-*	1511x2582
2654	*hpm1Δ::"GFP"::kan^{R}, asp1^{D333A}::kan^{R} , his3-D1, ade6-M210, leu1-32, ura4-D18, h+*	1511x2582
2654	*hpm1Δ::"GFP"::kan^{R}, asp1^{D333A}::kan^{R} , his3-D1, ade6-M210, leu1-32, ura4-D18, h+*	1511x2582
2655	*SPBC725.03Δ::"GFP"::kan^{R}, his3-D1, ade6-M210, leu1-32, ura4-D18, h-*	1511x2586
2655	*SPBC725.03Δ::"GFP"::kan^{R}, his3-D1, ade6-M210, leu1-32, ura4-D18, h-*	1511x2586
2656	*SPBC725.03Δ::"GFP"::kan^{R}, his3-D1, ade6-M210, leu1-32, ura4-D18, h+*	1511x2586
2656	*SPBC725.03Δ::"GFP"::kan^{R}, his3-D1, ade6-M210, leu1-32, ura4-D18, h+*	1511x2586
2657	*SPCC794.10Δ ::kan^{R}, asp1^{D333A}::kan^{R} , his3-D1, ade6-M210, leu1-32, ura4-D18, h-*	1511x2588
2657	*SPCC794.10Δ ::kan^{R}, asp1^{D333A}::kan^{R} , his3-D1, ade6-M210, leu1-32, ura4-D18, h-*	1511x2588
2658	*SPCC794.10Δ ::kan^{R}, asp1^{D333A}::kan^{R} , his3-D1, ade6-M210, leu1-32, ura4-D18, h-*	1511x2588
2658	*SPCC794.10Δ ::kan^{R}, asp1^{D333A}::kan^{R} , his3-D1, ade6-M210, leu1-32, ura4-D18, h-*	1511x2588
2659	*hpm1Δ ::"GFP"::kan^{R}, asp1^{H397A}::kan^{R} , his3-D1, ade6-M210, leu1-32, ura4-D18, h-*	1579x2582
2659	*hpm1Δ ::"GFP"::kan^{R}, asp1^{H397A}::kan^{R} , his3-D1, ade6-M210, leu1-32, ura4-D18, h-*	1579x2582
2660	*hpm1Δ ::"GFP"::kan^{R}, asp1^{H397A}::kan^{R} , his3-D1, ade6-M210,*	1579x2582

	leu1-32, ura4-D18, h-	
2660	*hpm1Δ ::"GFP"::kan^{R}, asp1^{H397A}::kan^{R} , his3-D1, ade6-M210, leu1-32, ura4-D18, h-*	1579x2582
2661	*SPBC725.03Δ::"GFP"::kan^{R}, asp1^{H397A}::kan^{R} , his3-D1, ade6-M210, leu1-32, ura4-D18, h*	1579x2586
2661	*SPBC725.03Δ::"GFP"::kan^{R}, asp1^{H397A}::kan^{R} , his3-D1, ade6-M210, leu1-32, ura4-D18, h*	1579x2586
2662	*SPBC725.03Δ::"GFP"::kan^{R}, his3-D1, asp1^{H397A}::kan^{R,} ade6-M210, leu1-32, ura4-D18, h*	1579x2586
2662	*SPBC725.03Δ::"GFP"::kan^{R}, his3-D1, asp1^{H397A}::kan^{R,} ade6-M210, leu1-32, ura4-D18, h*	1579x2586
2663	*gsf2 promoter::GFP::KanR, ade6-M210, leu1-32, ura4-D18, h-*	605 tagging and back cross
2663	*gsf2 promoter::GFP::KanR, ade6-M210, leu1-32, ura4-D18, h-*	605 tagging and back cross
2664	*gsf2 promoter::GFP::KanR, ade6-M210, leu1-32, ura4-D18, h-*	605 tagging and back cross
2664	*gsf2 promoter::GFP::KanR, ade6-M210, leu1-32, ura4-D18, h-*	605 tagging and back cross
2665	*gsf2 promoter::GFP::KanR, asp1^{D333A}::kan^{R} ade6-M210, leu1-32, ura4-D18, h-*	1511x2663
2665	*gsf2 promoter::GFP::KanR, asp1^{D333A}::kan^{R} ade6-M210, leu1-32, ura4-D18, h-*	1511x2663
2666	*gsf2 promoter::GFP::KanR, asp1^{D333A}::kan^{R} ade6-M210, leu1-32, ura4-D18, h+*	1511x2663
2666	*gsf2 promoter::GFP::KanR, asp1^{D333A}::kan^{R} ade6-M210, leu1-32, ura4-D18, h+*	1511x2663
2667	*gsf2 promoter::GFP::KanR, asp1^{H397A}::kan^{R} , ade6-M210, leu1-32, ura4-D18, h+*	1579x2663
2667	*gsf2 promoter::GFP::KanR, asp1^{H397A}::kan^{R} , ade6-M210, leu1-32, ura4-D18, h+*	1579x2663
2668	*gsf2 promoter::GFP::KanR, asp1^{H397A}::kan^{R} , ade6-M210, leu1-32, ura4-D18, h+*	1579x2663
2668	*gsf2 promoter::GFP::KanR, asp1^{H397A}::kan^{R} , ade6-M210, leu1-32, ura4-D18, h+*	1579x2663
2680	*mbx2Δ::ura4^{+}, ura4-D18, leu1-32, his3-D1, ade6-M210, h^{+}*	606x2232
2680	*mbx2Δ::ura4^{+}, ura4-D18, leu1-32, his3-D1, ade6-M210, h^{+}*	606x2232
2681	*gsf2 promoter::GFP::KanR, mbx2Δ::ura4^{+}, ura4-D18, leu1-32, his3-D1, ade6-M210, h^{-}*	2680x2663
2681	*Gsf2 promoter::GFP::KanR, mbx2Δ::ura4^{+}, ura4-D18, leu1-32, his3-D1, ade6-M210, h^{-}*	2680x2663
2730	*cbf12Δ::natR, ura4D-18, leu1-32, ade-M210 h^{+}*	Martin Prevorovsky et

		al., 2009 MP01
2730	*cbf12Δ::natR, ura4D-18, leu1-32, ade-M210 h*$^{+}$	Martin Prevorovsky et al., 2009 MP01
2731	*cbf11Δ::KanR, ura4D-18, leu1-32, ade-M210 h*$^{+}$	Martin Prevorovsky et al ,. 2009 MP05
2731	*cbf11Δ::KanR, ura4D-18, leu1-32, ade-M210 h*$^{+}$	Martin Prevorovsky et al ,.2009 MP05
2732	*cbf12::EGFP-KanR, ura4D-18, leu1-32, ade-M210 h*$^{-}$	Martin Prevorovsky et al., 2009 MP12
2732	*cbf12::EGFP-KanR, ura4D-18, leu1-32, ade-M210 h*$^{-}$	Martin Prevorovsky et al., 2009 MP12
2738	*rfl1Δ::kanR ade6-M21? leu1-32 ura4-D18 h+*	FY23718
2738	*rfl1Δ::kanR ade6-M21? leu1-32 ura4-D18 h+*	FY23718
2739	*cbf11Δ::KanR, Gsf2 promoter::GFP::KanR, ura4D-18, leu1-32, ade-M210 h*$^{+}$	2731 x 2663
2739	*cbf11Δ::KanR, Gsf2 promoter::GFP::KanR, ura4D-18, leu1-32, ade-M210 h*$^{-}$	2731 x 2663
2740	*cbf11Δ::KanR, Gsf2 promoter::GFP::KanR, ura4D-18, leu1-32, ade-M210 h*$^{+}$	2731 x 2663
2740	*cbf11Δ::KanR, Gsf2 promoter::GFP::KanR, ura4D-18, leu1-32, ade-M210 h*$^{-}$	2731 x 2663
2741	*rfl1Δ::kanR, Gsf2 promoter::GFP::KanR, ura4D-18, leu1-32 ade-M-2 h+*	2738 x 2663
2741	*rfl1Δ::kanR, Gsf2 promoter::GFP::KanR, ura4D-18, leu1-32 ade-M-210 h+*	2738 x 2663
2742	*rfl1Δ::kanR, Gsf2 promoter::GFP::KanR, ura4D-18, leu1-32 ade-M-21 h+*	2738 x 2663
2742	*rfl1Δ::kanR, Gsf2 promoter::GFP::KanR, ura4D-18, leu1-32 ade-M-21 h+*	2738 x 2663
2760	*ura4-D18 ori1 ade6-216 imr1R::ura4*$^{+}$ *Leu1D::CBR-hph, h*$^{+}$ *((CBR) **C**lick **B**eetle **R**ed luciferase integrated at Leu1 locus with Leu1 promoter Parental strain SPB80*	Yukiko shimada et al.,(SPB1231)
2760	*ura4-D18 ori1 ade6-216 imr1R::ura4*$^{+}$ *Leu1D::CBR-hph, h*$^{+}$ *((CBR) **C**lick **B**eetle **R**ed luciferase integrated at Leu1 locus with Leu1 promoter Parental strain SPB80*	Yukiko shimada et al.,(SPB1231)
2762	*gsf2 promoter::**CBG68**::KanR, ade6-M210, leu1-32, ura4-D18, h- (**C**lick **B**eetle **G**reen luciferase)*	Back cross to 606
2762	*gsf2 promoter::**CBG68**::KanR, ade6-M210, leu1-32, ura4-D18, h- (**C**lick **B**eetle **G**reen luciferase)*	Back cross to 606
2797	*gsf2 promoter::**CBG68**::KanR, Leu1D::CBR-hph, ori1, leu1-32, ura4-D18, ade6-216 h*$^{+}$	2760 x 2762
2797	*gsf2 promoter::**CBG68**::KanR, Leu1D::CBR-hph, ori1, leu1-32, ura4-D18, ade6-216 h*$^{+}$	2760 x 2762

2798	*gsf2 promoter::**CBG68**::KanR, Leu1D::CBR-hph, ori1, imr1R::ura4^{+}, leu1-32, ura4-D18, ade6-216 h^{+}*	2760 x 2762
2798	*gsf2 promoter::**CBG68**::KanR, Leu1D::CBR-hph, ori1, imr1R::ura4^{+}, leu1-32, ura4-D18, ade6-216 h^{+}*	2760 x 2762
2799	*gsf2 promoter::**CBG68**::KanR, Asp1^{D333A}::kan^{R}, ade6-M210, leu1-32, ura4-D18, h^{-}*	1511x 2762
2799	*gsf2 promoter::**CBG68**::KanR, Asp1^{D333A}::kan^{R}, ade6-M210, leu1-32, ura4-D18, h^{-}*	1511x 2762
2800	*gsf2 promoter::**CBG68**::KanR, Asp1^{D333A}::kan^{R}, ade6-M210, leu1-32, ura4-D18, h^{+}*	1511 x 2762
2800	*gsf2 promoter::**CBG68**::KanR, Asp1^{D333A}::kan^{R}, ade6-M210, leu1-32, ura4-D18, h^{+}*	1511 x 2762
2801	*gsf2 promoter::**CBG68**::KanR, Asp1^{H397A}::kan^{R}, ade6-M210, leu1-32, ura4-D18, h^{-}*	1579x 2762
2801	*gsf2 promoter::**CBG68**::KanR, Asp1^{H397A}::kan^{R}, ade6-M210, leu1-32, ura4-D18, h^{-}*	1579x 2762
2802	*gsf2 promoter::**CBG68**::KanR, Asp1^{H397A}::kan^{R}, ade6-M210, leu1-32, ura4-D18, h*	1579x 2762
2802	*gsf2 promoter::**CBG68**::KanR, Asp1^{H397A}::kan^{R}, ade6-M210, leu1-32, ura4-D18, h^{-}*	1579x 2762
2835	*gsf2 promoter::**CBG68**::KanR, ade6-M216, leu1-32, ura4-D18, his3-D1 h+*	2762 x 606
2835	*gsf2 promoter::**CBG68**::KanR, ade6-M216, leu1-32, ura4-D18, his3-D1 h+*	2762 x 606
2836	*leu1D::CBR-hph, imr1R::ura4^{+} oriI, leu1-32, ade6-210, h^{-}*	2760 x 605
2836	*leu1D::CBR-hph, imr1R::ura4^{+} oriI, leu1-32, ade6-210, h^{-}*	2760 x 605
2837	*asp1Δ::KanR, Leu1D::CBR-hph, imr1R::ura4$^{+,}$ oriI, leu1-32, his3-D1 ade6-216, h^{+}*	2760 x 1156
2837	*asp1Δ::KanR, Leu1D::CBR-hph, imr1R::ura4$^{+,}$ oriI, leu1-32, his3-D1 ade6-216, h^{+}*	2760 x 1156
2838	*asp1Δ::KanR, Leu1D::CBR-hph, imr1R::ura4^{+}, oriI, leu1-32, ura4-D18 ade6-216 h^{+}*	2760 x 1156
2838	*asp1Δ::KanR, Leu1D::CBR-hph, imr1R::ura4^{+}, oriI, leu1-32, ura4-D18 ade6-216 h^{+}*	2760 x 1156
2839	*asp1^{H397A}::kan^{R}, Leu1D::CBR-hph, imr1R::ura4^{+}, oriI, leu1-32, ade6-M210, h^{+}*	2148 x 2760
2839	*asp1^{H397A}::kan^{R}, Leu1D::CBR-hph, imr1R::ura4^{+}, oriI, leu1-32, ade6-M210, h^{+}*	2148 x 2760
2840	*asp1^{H397A}::kan^{R}, Leu1D::CBR-hph, imr1R::ura4^{+}, oriI leu1-32,*	2148 x 2760

	ade6-M210, h^{-}	
2840	*asp1*^{H397A}*::kan*^{R}*, Leu1D::CBR-hph, imr1R::ura4*$^{+}$*, oriI leu1-32, ade6-M210, h*$^{-}$	2148 x 2760
2841	*asp1*^{H397A}*::kan*^{R}*, cbf12Δ::natR, leu1-32, ura4-D18, his3-D1, ade6-M210, h*$^{+}$	2148 x 2730
2841	*asp1*^{H397A}*::kan*^{R}*, cbf12Δ::natR, leu1-32, ura4-D18, his3-D1, ade6-M210, h*$^{+}$	2148 x 2730
2842	*asp1*^{H397A}*::kan*^{R}*, cbf12Δ::natR, leu1-32, ura4-D18, his3-D1, ade6-M210, h*$^{-}$	2663 x 606
2842	*asp1*^{H397A}*::kan*^{R}*, cbf12Δ::natR, leu1-32, ura4-D18, his3-D1, ade6-M210, h*$^{-}$	2663 x 606
2843	*gsf2 promoter::GFP::KanR, ade6-M210, leu1-32, ura4-D18, his3-D1, h+*	2663 x 606
2843	*gsf2 promoter::GFP::KanR, ade6-M210, leu1-32, ura4-D18, his3-D1, h+*	2663 x 606

YGRC = Yeast Genetic Resource Center, Japan

2.8.2. *S. cerevisiae* strains

Strain Name	**Genotype**	**reference**
CEN.PK2	MATa/MATα ura3-52/ura3-52 trp1-289/trp1-289 leu2-3,112/leu2-3,112 his3Δ1/his3Δ1	J. Hegemann
AH109	*MATa trp1-901 leu2-3 112 ura3-52 his3-200 gal4Δ gal80Δ LYS2::GAL1UAS-GAL1TATA-HIS3 GAL2UAS-GAL2TATA-ADE2 URA3::MEL1UAS-MEL1TATA-lacZ*	Clontech

2.8.3. *E. coli* Strain

XL-1 blue *recA1, lac-, endA1, gyrA46, thi, hsdR17, supE44, relA1, F' [proAB+, lacIq ,lacZΔ M15, Tn(tetr)]* –Stratagene

2.9. Oligo Nucleotides

261	BD sequencing	ACGTGTCTTGTAGTTCCC
290	KanR start	ATTCCAACATGGATGCTG
423	Asp1 tagging verify reverse	TCGCGAATCATTTTGGCGCC
519	asp1 sequence forward	CGAAAGTTTGGAATAGAAATC
520	asp1 sequence reverse	GACTCTGAGGCAATTTGAGA

531	Asp1 tagging verify reverse	TTTTCGTTTTAAAACCTAAGAGTC
672	*asp1*^{D333A} verify	GTCAGTCGTATGTGATTGC
673	*asp1*^{H397A} verify	GTCGGAGTCCTGCGTGC
674	*asp1*^{H397A} reverse	GTTCAGAATATTCCGACATG
677	*asp1*$^{+}$ tagging verify forward	GTATACTTGAATCAGGACTACC
777	*asp1*$^{+}$ tagging verify forward	CACCGGATTCAGTCGTCACTC
783	*asp1*$^{+}$ tagging verify forward	CGAGATTCTGATCATGCTTC
821	KanR forward	ATGGGTAAGGAAAAGACTCA
827	KanR reverse	CTCGTCATCAAAATCACTCG
884	*asp1*Δverify	GTATTCTGGGCCTCCATGTCG
1124	BD sequencing	TTTTCGTTTTAAAACCTAAGAGTC
1409	Asp1 tagging verify forward	GCCCGTACATTTAGCCCATA
1543	Gsf2 verification forward	TCTCTGTTGAAACTACGAGC
167	*asp1*-Kinase in Activation domain	GAGGCCCCAAGGGGTTATGCTAGTTATGCGGCCGCTGCAGTTAATGATTC AAAATGCAAGTC
167	*asp1* $^{1-364}$ in Activation domain	GCGGGGTTTTTCAGTATCTACGATTCATCTGCAGCTCGAGTTAATGACGT TCGGCAACATGAAAC
1675	*asp1* $^{365-920}$ in activation domain	CGCCGCCATGGAGTACCCATACGACGTACCAGATTACGCTAGACGGAAT CGTGTACCTTC
1731	*asp1*$^{+}$ NLS Forward primer	AAACTCGAGATGATTCAAAATGCAAGTCA
1732	*asp1*$^{+}$NLS Reverse primer	AAAGCGGCCGCTATTAATGTTAACAGGAATAA
1733	*asp1* $^{1-364}$ + NLS reverse prime	AAAGCGGCCGCTATGACGTTCGGCAACATGAAA
1743	*leu2* replacing Ura^{4+} Forward prim	AAGCTTAGCTACAAATCCCACTGGCTATATGTATGCATTTAAGCTTGTCG ATCGACTACG
1744	*leu2* replacing Ura^{4+} reverse primer	AAGCTTGTGATATTGACGAAACTTTTTGACATCTAATTTAAAGCTTGTCG AGGAGAACTT
1755	asp1 $^{365-920}$ Forward for NLS and NES	AAACTCGAGATGAGACGGAATCGTGTACCTTCA
1758	NLS-GFP::kanR	ACGCTGCAGGTCGACGGATCCCCGGGTTAATTAACGCGGAATTAATTCCC GAGCCTCCAAAAAAGAAGAGAAAGGTCGAATTGGGTACCGCCAGTAAA

		GGAGAAGAACTTTTCACTGGAG
1759	NLS::kanR	ACGCTGCAGGTCGACGGATCCCCGGGTTAATTAACGCGGAATTAATTCCC GAGCCTCCAAAAAAGAAGAGAAAGGTCGAATTGGGTACCGCCTAACCAC TTCTAAATAAGCGAATTTCTT
1760	NES-GFP::kanR	ACGCTGCAGGTCGACGGATCCCCGGGTTAATTAACAACAGCAATGAATT AGCCTTGAAATTAGCAGGTCTTGATATCAACAAGACAGAAAGTAAAGGA GAAGAACTTTTCACTGGAGTTG
1761	NES::kanR	ACGCTGCAGGTCGACGGATCCCCGGGTTAATTAACAACAGCAATGAATT AGCCTTGAAATTAGCAGGTCTTGATATCAACAAGACAGAATAACCACTTC TAAATAAGCGAATTTCTTATG
1867	*pfl3* deletion forward	GAACTTCTGGATCAAAAGTGCAAAAGCTTTATTTATGTATATTGTGTTTT ACGATTGATTGATACAGAGATTCGCGGAACTTTTCTTTACTATTGCACTT
1868	*pfl3* deletion reverse	AAAGCAACAATTAACGACTGTAGAATTTTTTATTTTTTAACTCACAAAAC ACCAGTACGCGATAGAGAATTCTCGCGAGCAAAGCTAACGAATCTTTAA T
1869	*pfl3* ver forward	TTTTGGTTTTTTATGTTCGA
1870	*pfl3* ver reverse	AAAAATAGGATAATGATTTA
1871	SPAPB2C8.01 del forward	GTTTTTTTCCTATAATATATATCCCCAATCTTTCATACACTTTATTACTTCG GCGTTTGTTTGCTTAACTTCTTAGTAAATTTTCTTTACTATTGCACTT
1872	SPAPB2C8.01 del reverse	ACAAAACCAAAAATTTACCAGATGTCGAGTTTTTATATTGGCAACTTGAC ACTTTGCACAATGTCATGATACCAAAAGGAAAAGCTAACGAATCTTTAAT
1873	SPAPB2C8.01 del forward	AACATGTGACATATAGTGATAC
1874	SPAPB2C8.01 del reverse	GAATTATCCACCGTACTCTC
1881	*mam3* deletion forward	AATACTTTCTTTTCTTCTTCTTTGAAAAACATTATTAATTATAATTTTTCTT TTATCGCTTGATCTTCCCATAATTCGTCTTTTCTTTACTATTGCACTT
1882	*mam3* deletion reverse	CGATAAATTAACAATAAAGATTTAAGAAAATAACACGATTTTAATTAAT ATGTAAAATAAATATAAAACATTAACTTTATAAAGCTAACGAATCTTTAA T
1883	*mam3* del verification forward	TCATTGCATTGCATCGCATT
1884	*mam3* del verification reverse	AACATAGCGGACGCTCACAA
1885	*pfl8* del forward	ATCTATTCTTCTAAAACCGAACAGATTTGGAACCACGTTCTAATCAGTGC TAGATTGAATATTTTTCTAAAAAATTTACGTTTTCTTTACTATTGCACTT
1886	*pfl8* del reverse	GCTTTCAATCTATTATAATAATAAATAATTAATAAATTAAAATTCAAAGT GCCGTTTGAGGCTTAAAGGGCCGTAATAATAAAGCTAACGAATCTTTAAT
1887	*pfl8* del verification forward	GCTGGGAAAAAACAAGGAGT
1888	*pfl8* del verification	GAGTCAGACAAAGAATGTGT

	reverse	
1907	*hpm1* verify forward	CTATTTTGTCTACATGAACG
1908	*hpm1* verify reverse	GTTATGTAATGTGGATATGT
1930	*hpm1* deletion reverse	ATCATCTTTAAATAACATATGTTTTGTTTATCTTCTAAATTCGTTTCTGCTT TGAGTCTTTACCCTATAATTAAGAAATGGAATTCGAGCTCGTTTAAAC
1957	*pfl6* del with his forward	AATAATACTATTTTTAATTAATTTTTTTTTTTTTTTTTTTTTTTTTTTTTC AAACGAAATATTTGATATTTTTTCATTTTTTCTTTACTATTGCACTT
1958	*pfl6* del with his reverse	TTCTTGACCTTTGACATATTAGAAATCCGATTCGTAGCTCAAGTACCGAT TTAATTATTTTCTGAAATTTTCAAACAATTAAAGCTAACGAATCTTTAAT
1959	*pfl6* del verify with his forward	CTGATTGACGGGAAAACCGT
1960	*pfl6* del verify with his reverse	AGATGCCCACTATACCTCGC
1961	*map4* del with his forward	TTACTCTATTTTGTGCATACTTTGATTTTTTTTTATCTGCATATTCCATTTG TCATTCATTAATATTAATATTAATAATTTTTTCTTTACTATTGCACTT
1962	*map4* del with his reverse	AATTATGAGACAAAGGGTGATGAGATGAACTAATTTTGAATTAAAAAGA ACGTCCTGCAACTTTTCAGTAGAAATAAAGCAAAGCTAACGAATCTTTAA T
1963	*map4* del verify with his forward	ACTCTCACGTCAATTCGCTG
1964	*map4* del verify with his reverse	AGGGAGGCCACTAAAGTACC
1965	*pfl7* del with his forward	GTTGATTTTTGAAAATCCTTTCACACTCTTCGCGCAATAGAGGTGACTAA AAGTTTAGAACAAACTGACAGTTACGGACATTTTCTTTACTATTGCACTT
1966	*pfl7* del with his reverse	ATTTTTCAATTCAAAATTATATATTAAATTTATTTACAAGGACTTTAAAGT CCAGTAAAAGATGGGATAAATCCTTAAAGAAAGCTAACGAATCTTTAAT
1967	*pfl7* del verify with his forward	GCGACCAGACACCAATTTTAC
1968	*pfl7* del verify with his reverse	CAAATGAAGAAGGCACGGAC
1969	*pfl4* del with His3+ forward	AATTCTTTAATCCCTTCTAATTCTTCTTTTCTATTCTTGCTTATAGCACATC TAATTTATTTAATCATTGGAAGTTCATCTTTTCTTTACTATTGCACTT
1970	*pfl4* del with His3+ forward	AATGATATGTATATAAATATATGTTATAGCTGCAAAAAATGATCCAATTC GTACTCAAATTTTGACGAATCGCTTCAAAAAAAGCTAACGAATCTTTAAT
1971	*pfl4* del verify with His3+ forward	GAAGACCATCCAGAGTTAGTTGC
1972	*pfl4* del verify with His3+ reverse	GCCTCGCGCTATTCAACTCTTC
1973	SPBC1348.08c del his forward	TCTTGGATGAAATAATACTATTTTTAATTAATTTTTTTTTTTTTTTTTTTT CAAACGAAATATTTGATATTTTTTCATTTTTTCTTTACTATTGCACTT

1974	SPBC1348.08c del his reverse	TTCTTGACCTTTGACATATTAGAAATCCGATTCGTAGCTCAAGTACCGATTTAATTATTTTCTGAAATTTTCAAACAATTAAAGCTAACGAATCTTTAAT
1975	SPBC1348.08c del verify his forward	GATTGACGGGAAAACCGTTG
1976	SPBC1348.08c del verify his reverse	AGATGCCCACTATACCTCGC
1990	*map4* del verify reverse	GGTACTTTAGTGGCCTCCCT
2002	*asp1*$^{+}$ 41x and 81X tagging with GFP for	AGTTCATCTTCCCAAAAGGTTTATTCCTGTTAACATTAATCGGATCCCCGGGTTAATTAA
2003	*asp1*$^{+}$41x and 81X tagging with GFP rev	AAGAAAAACCCTAGCAGTACTGGCAAGGGAGACATTCCTTTATTTGTATAGTTCATCCA
2015	*gsf2* promoter with GFP forward	TTTTTTTATTCGTTTGGTTAAATTATCTTAATAATTTTGTTTTTTTCTAATTCACTTACCCGTTTTTGAATATATCAACAATGAGTAAAGGAGAAGAACTTTTC
2016	*gsf2* promoter with GFP reverse	CCAGAAGTCAAGGAGGGAAGAAGAGCAGCCGTGAAAAGTAATGCCCGAGCAGATGTGGATAAAAACCTTCTAACAGACATGAATTCGAGCTCGTTTAAAC
2017	*gsf2* - GFP verify	TCCGCAAGCTCGGTCTTTGG
2032	*met10* deletion reverse	GGCATTTTGCACAACCTAATGTGTAAATAAACCTGAAAAGGTTTTAAATGAGTTTGATTTGACATCTCCTTCTATAAGCTGAATTCGAGCTCGTTTAAAC
2033	*met10* verify forward	GGAAAGCTCGTCAAAACGAA
2034	*met10* verify reverse	AGGCTATTAATGCTGGGCTG
2044	*met10* deletion forward	TTTTGAAACGTTTTGTTAATCAAAATTTTAAATTTCTTTAATTATTTTCTTCCGTTTAATCATTGATTTGTTGGTTCAAAGGCGCGCCACTTCTAAATAA
2088	Luciferase gene in 1053 forward	TTCGTACGCTGCAGGTCGACGGATCCCCGGGTTAATTAACATGGTTAAGAGAGAAAAAAACG
2089	luciferase green gene in 1053 reverse	CATAAATCATAAGAAATTCGCTTATTTAGAAGTGGCGCGCCTTAACCACCAGCTTTTTCC
2091	*gsf2-P-lucG* forward	TTTTTTTATTCGTTTGGTTAAATTATCTTAATAATTTTGTTTTTTTCTAATTCACTTACCCGTTTTTGAATATATCAACAATGGTTAAGAGAGAAAAAAACGTT
2092	*gsf2-P-lucG* verify reverse	TGTGGTTTCGGTTTGACTGA
2093	*cbf11* deletion verify forward	TCAGTCAAACCGAAACCACA
2094	*cbf11* deletion verify reverse	GAGTAGGAAGCCACCGACCTG
2095	*cbf12* deletion verify forward	CGACAGCTCTCGACAGACAC
2096	*cbf12* deletion verify	AAGCTAACCGTCCGAATTTC

	reverse	
2097	NatR verify forward	GCGCACGTCAAGACTGTC
2099	*hpm1*deletion forward	GCAAAAATCCTACACTAGGATCAAGACATACAATTTCTACTAAAGCCAA GACAGGTTGCGAAATCAATCAACTTGCAAATGGCGCGCCACTTCTAAAT AA
2215	*rfl1* deletion verify forward	TCGTCCTTTCACATTCCTCA
2216	*rfl1* deletion verify reverse	AACACGTCAAATTTGCTAGCTG

2.10. Antibodies

Primary antibody α-GFP Roche 1:1000 dilution anti mouse monoclonal

Primary antibody γ-tubulin 1:1000 dilution anti mouse monoclonal

Secondary antibody: anti mouse AP conjugate: Promega- dilution 1:10000

2.11. Media and growth conditions for *S. pombe*

S. pombe strains were grown in solid/liquid full media (YE5S) containing yeast extract and five essential amino acids (adenine, leucine, uracil, lysine, and histidine). For plasmid transformation *S. pombe* strains were grown in full media overnight at 30°C on an shaker and transformed with plasmids and the selected for prototroph on minimal media (MM). To repress the promoter *nmt1* thiamine was added to the minimal media at the concentration of 5µg/ml to both solid and liquid media. Derepression of the promoter is done by cultivating the transformants in thiamine free media for approximately 18-20hours. To solidify one liter of solid media 20 grams of agar was added. Selection for the resistance to the antibiotic, Geneticin disulfate (G418)/ Nourseothricin (NatR)/ Hygromycin (HgR) was carried out on solid full media consisting of G418/NatR/HgR at a final concentration of 100 mg/l.

Full medium (YE5S)

10 g yeast extract
150 ml Adenine stock solution
75 ml Uracil stock solution
20 ml je Histidine-, Lysine-, und Leucine stock solution
40 g Agar (for solid media)
1645 ml ddH_2O was added and aliquoted in 5 x 360 ml portions and autoclaved.

60 g Glucose was added in 200 ml ddH_2O and autoclaved separately and 40ml of glucose solution was added to each bottle after the autoclave.

Minimal medium (MM) or Edinburgh-Minimal medium (EMM)

5,5 g Na_2HPO_4 x 2 H_2O
6 g potassium hydrogen phthalate
2 g Glutamic acid (only for MM)
10 g Ammonium chloride (only for EMM)
40 ml 50 x Salt stock
2 ml 1000 x Vitamin stock
0.2 ml 10000 x Mineral stock
40 g Agar (for solid Medium)

Added 1780 ml ddH_2O, aliquoted 5 x 360 ml portions and autoclaved.
40 g Glucose was added in 100 ml ddH_2O and autoclaved separately. After autoclaving the media, 20ml of autoclaved glucose solution was added to it.
Amino acids were added later at an end concentration of 75mg/L
met10Δ strain in MM: 330 µM cysteine and 140 µM methionine were added additionally

Amino acid stock solution (Sterile autoclaved)

2.7 g/l Adenine stock
2 g/l Uracil stock
7.5 g/l Histidine stock
7.5 g/l Lysine stock
7.5 g/l Leucine stock
7.5 g/l Arginine stock

50x Salt stock:

21.4 g $MgCl_2$ x 6 H_2O
0.29 g $CaCl_2$ x 2 H_2O
20 g KCl
0.8 g Na_2SO_4
Added 400 ml ddH_2O, autoclaved and stored at 4°C.

1000x Vitamin stock:

1 g sodium pantothenic acid
10 g Nicotinic acid
10 g Inositol
10 mg Biotin
In 1 L ddH_2O, sterile filtered and stored at 4°C.

10000x Mineralstock

5 g H_3BO_3
4 g $MnSO_4$

4 g $ZnSO_4$ x 7 H_2O
2 g $FeCl_2$ x 6 H_2O
4 g MoO_3
1 g KI
4 g $CuSO_4$ x 5 H_2O
10 g citric acid
In 1 L ddH_2O, sterile filtered and stored at 4°C.

Thiamin-Stock: 10 mg/ml, sterile filtered, and stored in dark at room temperature

TBZ-Stock: 10 mg/ml in DMF, store at -20°C

Malt extract medium (for mating)
12 g Malt extract
56.25 ml Adenine stock
56.25 ml Uracil stock
3 ml Histidine stock
3 ml Leucine stock
8 g Agar
Added 281.5 ml ddH_2O, adjusted the pH to 5.5 and autoclaved.

2.12. Media and growth conditions for *S. cerevisiae*

S. cerevisiae was grown on solid and liquid full medium (YPD) at 30°C. For plasmid transformation selective minimal medium (SD) was used without selective prototroph marker.

Full medium (YPD)
20 g yeast extract
40 g Peptone
2 ml Adenine stock (2 g/l)
4 ml Tryptophan stock (5 g/l)
40 g Agar (solid medium)
1788 ml ddH_2O was added, 5 x 360 ml portions were aliquoted. Later the media was autoclaved.
40 g Glucose was added in 200 ml ddH_2O and autoclaved separately. Later the autoclaved glucose solution was added to the media.

YPD + G418: G418 was added after the medium reached the room temperature and later the plates are stored at 4°C

SD-Minimal medium

3.4 g yeast nitrogen base (YNB) without amino acids and ammonium sulfate

10 g Ammonium sulfate
4 g Drop-out Mix
40 g Agar (for solid Medium)
1800 ml ddH_2O was added the pH to 6 was adjusted with NaOH. 5 x 360 ml portions were aliquoted. Later the media was autoclaved.
40 g Glucose was added in 100 ml ddH_2O and autoclaved separately. Later the autoclaved glucose solution was added to the media.

For plasmid selection the required supplement is omitted from the mix.

Drop-out Mix: 0.2 g para-Aminobenzoidacid; 0.5 g Adenine; 2 g Alanine, Arginine, Asparaginacid , Cysteine, Lysine, Methionine, Phenylalanine, Proline, Glutamine, Glutamic acid, Glycine, Histidine, Inositol, Isoleucine, Serine, Threonine, Tryptophan, Tyrosine, Uracil, Valine; 10 g Leucine

Media for *E. coli*

E. coli was grown on solid or liquid LB media at 37°C. Antibiotics were added to the media only after the media got cooled to 50°C. Then the plates were stored at 4°C.

LB-Medium

10 g Trypton
5 g yeast extract
5 g NaCl
13.5 g Agar (for solid Medium)
1 L ddH_2O was added, pH was adjusted to 7.5 and 5 x 200 ml portions were aliquoted. Later the media was autoclaved.
LB + Ampicillin: 50 µg/ml, Ampicillin, stored at 4°C.
LB + Kanamycin: 50 µg/ml, Kanamycin, stored at 4°C.
Ampicillin Stock: 200 mg/ml, stored at -20°C
Kanamycin-Stock: 200 mg/ml, stored at -20°C
X-Gal-Stock: 100 mM in DMF, stored at -20°C

2.13. DNA methods

DNA concentrations were measured photo metrically by absorbance at 260nm. The quality of DNA was measured as a ratio between absorbance at 260nm and 280nm. Other DNA methods such as restriction analysis, DNA ligation, were done according to the manufacturer's protocols and recommendations.

DNA precipitation and gel electrophoresis

Two volumes of 96% ethanol were added to the DNA. 1/10th volume of 3M Sodium acetate was added and centrifuged at 13,000 rpm for 20 minutes. Obtained supernatant was carefully discarded and the pellet was washed with 1 volume of 70% ice cold ethanol. Later, the pellet was dried at 65°C or vacuum dried. The pellet was later, dissolved in adequate volume of 1x TE buffer or ddH_2O. 1% Agarose gel was prepared using 1x TBE-buffer and the digested plasmids or PCR product was loaded by adding 6x DNA loading dye. 5µL of gene ruler was added as a reference. DNA gel elution and PCR purification was done according to the manufacturer's recommendations from Qiagen.

2.14. Transformation of *E. coli*

One minute transformation

1 µl of plasmid DNA was mixed with 3 µl DMSO-competent cells in an eppendorf tube and kept on ice. Later the mix was placed at 42°C for 1 minute. Immediately 100 µl LB-Medium was added then platted on desired plates and incubated at 37°C overnight.

Electroporation

40µL electro competent cells were added to 2-10µL of plasmid DNA. This mixture was added to a pre cooled electro cuvette and placed on ice. This cuvette is later electroporated at 2.1 kV, 200 Ω, 25 µF. Immediately, 900µL LB media was added and resuspended then it was incubated at 37°C for one hour on a shaker. Later the cells were centrifuged and resuspended in 100 µl LB media. They were platted on a selective media and incubated at 37°C overnight.

Ultra-competent cells

50-150 µl of plasmid DNA was mixed with 100 µl ultra competent cells in an eppendorf tube and kept on ice. Immediately, 100 µl was platted on desired plates and incubated at 37°C overnight.

2.15. Plasmid isolation from *E. coli*

For the preparation of small quantities of DNA from *E. coli* the procedure following the protocol of the alkaline lysis was (Ish Horowicz & Burke 1981) used. For the preparation of large quantities of DNA a "plasmid Midi kit" from Qiagen was used according to manufacturer's instructions.

2.16 PCR

PCR reactions were performed according to the standard protocols. For colony PCR, gene tagging and gene deletion PCRs, the Taq DNA polymerase was used. For cloning of plasmids pFX or Pfu, proof reading polymerases were used. All PCR´s have an initial denaturation step at 95°C for 5 minutes. Annealing temperature and time was based on the oligo nucleotides used. Usually the extension temperature was 1min /1kb of PCR product and was followed by 35 cycles.

Taq-PCR

5 µl	10x Taq-buffer
3 µl	25 mM $MgCl_2$
2.5 µl	4 mM dNTPs
1 µl	DNA template (10-100 ng)
1 µl	Oligos A and B (50 µM)
1 µl	Taq-Polymerase
35.5µl	ddH_2O
50µl	total volume

Colony PCR

3 µl	10x PCR-buffer
1.8 µl	25 mM $MgCl_2$
1.5 µl	4 mM dNTPs
10µl	ddH_2O + cells
0.3 µl	oligos A and B (50 µM)
0.3 µl	Taq-Polymerase
12.8 µl	ddH_2O
30µl	total volume

Pfx-PCR

5 µl	10 x Pfx-buffer
1.5 µl	10 mM dNTPs
1 µl	50 mM $MgSO_4$
1 µl	DNA template (10-100 ng)
1.5 µl	Oligos A and B (10 µM)
0.4 µl	Pfx-Polymerase
39.6 µl	ddH_2O
50µl	total volume

PCR cycles

1. Initial denaturation: 94/95°C for 5 min
2. Denaturation: 94/95°C for 1 minute
3. Annealing temperature: 45/60°C
4. Elongation temperature: 72°C 1-3 minutes(1 min/1kbp)
5. Final elongation: 72°C 5 minutes
6. Store at12°C

35x

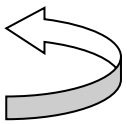

2.17 *In vitro* ligation

In vitro ligation was carried out using T4 DNA ligase. Initially PCR was performed using proof reading polymerase and later the PCR product was digested with desired restriction endonucleases. The plasmid was also digested with the same nucleases. Both PCR

product and the plasmid were pooled in 3:1 molar ratio along with T4 DNA ligase buffer and T4 DNA ligase enzyme in a total volume of 20µl. The reaction was incubated at 22°C for one hour and inactivated by heating it at 65°C for 10 minutes. Later, 5µl of the reaction was electroporated into *E. coli*

DNA sequencing

DNA sequencing was carried out by the Biologisch-Medizinischen Forschungszentrum (BMFZ) of the University of Dusseldorf and GATC.

2.18. Yeast transformation methods: *S. pombe*

Lithium acetate Li-Ac transformation

The transformation of *S. pombe* strains was carried out according to Lithium acetate method by Okazaki (Okazaki et al., 1990). The cells were first incubation at 30°C in 0.1M lithium acetate to destabilize the cell wall. Later 500 ng of plasmid DNA and 50% (w/v) PEG4000 were added to the cells. After one hour of incubation at 30°C, the DNA and cells mixture was heated up to 43°C for 15 minutes. For the transformation of linear DNA fragments for homologous recombination, 5 µl herring sperm DNA (10 mg / ml) was added.

***S. pombe* electroporation**

The *asp1Δ and asp1*^{D333A} strains were unable to be transformed by the Li-Ac transformation method as these strains have a thicker cell wall. So we have to electroporate the strains for transformation.

The cells were grown overnight in 150 ml of minimal media with all required supplements to an OD of 1x10^7 cells per ml. All the steps were carried out on ice including reagents, and centrifugation was carried out at room temperature. Cells were placed on ice for 15 min. 50ml of the cells were centrifuged and the cells were washed for 3 times with ice cold dd$H_2$0. 5 ml of 0.6 M sorbitol / 25 mM DTT / 20 mM HEPES / pH 7.5 was added and resuspended. Later, it was incubated for 15 minutes at 30°C. Centrifugation was done for 5 min at 3500 rpm. Then, it was washed once with ice-cold 1 M sorbitol. Finally, the cell pellet was resuspended in 1M sorbitol in a total volume of 500 µl.

Electroporation

Electroporation cuvettes were precooled. 100 ng plasmid DNA was added to an eppendorf tube and 50µl of the electro competent cells were added. The whole mixture plasmid and cells were added to a cuvette and electroporated at 2.1 kV, 200 Ω, and 25 µF. Immediately, 900 µl of 1M sorbitol was added to the mix and kept on ice until all the electroporation's were performed. The cells were incubated for 10 min at 30°C and 100 µl were platted on MM with the needed supplements. The transformants appeared after 8 days.

Isolation of genomic DNA from *S. pombe*

S. pombe strains were inoculated in 8 ml YE5S and were grown overnight. Centrifugation was done for 5 min at 3500 rpm and resuspended in 1 ml SP1 (1.2 M sorbitol, 50 mM Sodium citrate, 50 mM sodium phosphate, 40 mM EDTA, pH 5.6) with 0.25 mg Zymolyase (freshly prepared). Then the samples were incubated for 45 min-1hr at 37°C. To check for Spheroblast 5 µl cells were mixed with 3 µl of 10% SDS and observed microscopically. The protoplasts were centrifuged at 6000 rpm for 5 min and resuspended in 450 µl 5xTE (50 mM Tris pH 8, 5 mM EDTA). 50 µl of 10% SDS was added to it and incubated for 5 min at room temperature. Later 150 µl of 5M potassium acetate was added and incubated for 10 min on ice. Then Centrifugation was done at 13,000 rpm for 10 min. The supernatant was transferred to a new eppendorf tube.
1 volume of isopropanol was added and centrifuged at 13000 rpm for 3 min. Then the pellet was washed with 70% ethanol and was resuspended in 250 µl 5x TE with 2 µg / ml RNase, 20 min at 37°C. DNA prepared was sufficient for the PCR reactions.

2.19 *S. cerevisiae* plasmid isolation

S. cerevisiae plasmid DNA was isolated using the protocol from Birnboim and Doly, 1979. Overnight cultures were grown in 5ml SD media at 30°C. 2ml of cultures were centrifuged at 3500 rpm and washed with water for two times. The pellet was resuspended in 500µl of P1 (50 mM Tris/ HCl pH 8, 100 mM EDTA, 100 µg/ ml RNase). It was followed by another resuspension step, with 500µl of P2 (200 mM NaOH, 1 % SDS). The suspension was gently mixed by inverting the tubes. 2/3 volume of glass beads were added to it and were lysed in the Precellys at 2x2000 U for 20 seconds and placed them on ice. The lysate was centrifuged at 2000 RPM for two minutes. One ml of supernatant was transferred into a fresh tube and 500µl of P3 (3 M potassium acetate pH 5.5) was added to it. The tubes were gently mixed and incubated on ice for 10 minutes. Then the samples were centrifuged at 13000 RPM for 15 minutes and then 750µl of the supernatant was transferred into fresh tube. 750µl

of isopropanol was added and vortexed. After that, the sample was centrifuged for 30 minutes at 13,000 RPM and precipitated with 70% EtOH. Later the precipitate was air dried and dissolved in 20µl of water and electroporated into *E. coli.*

2.20 Mating of *S. pombe*

S. pombe is a haploid organism, with two mating types; h^+ and h^-. Under unfavorable conditions and presence of other mating type it can undergo karyogamy and form tetrads with four viable spores. This allows creating a combination of genetic traits from both the parents. A small volume of freshly grown cells from both the mating types were mixed together and plated as a drop on the malt medium. After incubating at 25°C for 2-3 days tetrads were observed under the microscope. These tetrads can be further isolated by random spore analysis or tetrad dissection

2.21 Random spore analysis

In this method the walls of the tetrads were digested by enzymes to free the spores. These free spores were platted on full media and later on selective media.

A small amount of material from the mating spot was resuspended in 980µl of H2O. 20µl of 1:10 diluted β-glucuronidase was added and vortexed briefly. Later, it was incubated overnight at 25°C. The spores were visually observed under the microscope for complete lysis of the vegetative cells and tetrads leaving behind the spores intact. The spores were washed twice with ddH_20 and were counted using a cell counting chamber. 100-200 spores were platted on the full media plates and incubated at desired temperatures.

2.22. Tetrad analysis

This method is usually performed when the double mutant phenotype is unknown and the two strains have identical markers. A small volume of cells from the mating spot was resuspended in 1 ml of ddH_20. 50µl of the suspension was placed on a predetermined spot on the agar plate. Using a micromanipulator the spores are separated. The micromanipulator consists of a glass needle which can pick individual tetrads. Using this needle tetrads were picked and placed on the defined grid on the agar plate. Later, the plate was incubated at higher temperatures for a couple of hours. The tetrads burst out leaving 4 individual spores aside. Subsequently, the spores were separated from each other and placed apart. After incubation of 3-4 days each spore germinates into a haploid strain that could be analyzed for genotype. This approach allows us to identify the double mutants using the genotype distribution within a tetrad.

The genotypes of the strains were identified by autotrophy growth on selective minimal medium, adenine markers ade6-M210/M216 ade6-allele by characteristic red color on adenine deficient medium (MM + 5 µg/ml adenine), KanMX6 module growth in G418-containing medium. The mating type PCR was identified by colony PCR using the following oligos.

605, 606 and 607 and the resulting PCR product size determine the mating type.

Mating type h^+ 671 bp

Mating type h^-: 432 bp

Mating type h90: 671 bp and 432 bp

2.23 Invasive growth analysis

Strains were grown in 5 mL full media (YE5S) or minimal media (MM) or Edinburg Minimal Media (EMM) and transformants were grown overnight in 5 mL minimal media containing all essential amino acids with or without thiamine for repressed or de- repressed conditions respectively. Cells were diluted to a concentration of $2x10^6$ cells/ml. 5µL of cells were later patched on appropriate plates. The cell patches were at equal distance from each other and to the circumference of the agar plate.

Plates containing excess iron were made by adding 0.1 M FeCl3 to a final concentration of 1-5mM. The plates were allowed to dry. Later, plates were incubated at required temperatures for a period of 14-21 days. Invasively growing colonies were found after two weeks of incubation. But the quantification was done after incubation for 21 days.

For analyzing invasively growing colonies, initially the plates were photographed by gel documentation system to analyze the surface growth morphology of the colony. Later a small stream of double distilled water was allowed to pass through the top of the colony for approximately 30-60 sec to remove the cells which are non-adhesive and non-invasive. The plates were photographed to display the adhesive ability of the colony. To analyze the invasive growing ability the cells were completely washed under a stream of water and hand rubbed completely to remove cells unable to grow invasively. Later, plates were allowed to dry and photographed using a binocular microscope and digital Sony DSLR camera.

1 M Ferric chloride Stock:

$FeCl_3$ x 6 H2O in ddH2O: 0.2M HCl sterile filter.

2.24. Yeast two hybrid

For two hybrid analyzes the Matchmaker "GAL4 Two Hybrid System 3" from the company Clontech was used and proceeded according to the manufacturer.

2.25 Protein extraction from *S. pombe*

The transformants were grown in minimal media without thiamine in corresponding media and the strains were grown in YE5S media overnight in 300ml flasks. $2x10^8$ cells were centrifuged at 3500 RPM for 5 minutes. Cells were resuspended in 5ml stop buffer (150mM NaCl, 10mM EDTA, 1mM NaN3, and 50mM NaF, pH 8) then centrifuged again at 3500 RPM and resuspended in 5 ml stop buffer. Centrifugation was repeated and the supernatant was discarded. Then the pellet was dissolved in remaining stop buffer. Cells were transferred into 2 ml eppendorf tubes with screw cap. Centrifugation was done for 5 minutes at 10,000 RPM to remove the remaining stop buffer. 500µl HB15 buffer (25mM MOPS, 60 mM β-Glycerophosphate, 15 mM p-nitrophenylphosphate, 15 mM MgCl2, 15 mM EGTA, 1 mM DTT, 0.1 mM Sodium orthovanadate, 1 % Triton X 100, 1 mM PMSF, complete protease inhibitor) and ¾ of eppendorf tubes glass beads(1.5 ml) were added. Cells were lysed with Precellys instrument at 5000 U for ten seconds. Lysis was repeated again for 10 seconds and the samples were placed on ice in between. Tubes were pierced with a heated needle from bottom and placed in 1.5 ml eppendorf tubes and centrifuged for 30 seconds at 3000 RPM. The flow through was collected in the new tubes and centrifuged at 10,000 RPM for 30 minutes. This step was again repeated. These samples were used for Bradford assay and western blotting.

2.26 Determination of protein concentration using Bradford's assay

The protein extracts were diluted 1:800 with ddH2O to a total volume of 800µl. 200µl of Bradford's reagent was added and vortexed. After incubating for 10 minutes at room temperature the OD_{595} is measured and the protein samples were diluted to the lowed OD_{595} measurements of the samples.

Coomassie staining

32,5µl of the diluted protein sample was mixed with 12.5µl of SDS loading buffer and 5µl 1M DTT. The samples were boiled 10 minutes at 100°C and were placed on ice. Two 10% SDS gels were loaded with the same volume of protein and separated by PAGE at 100 V up to the loading buffer reaches the resolving gel. Later the voltage was increased up to 200V. Once the loading gel reaches the end of the resolving gel, the gel was gently removed and put in the coomassie solution and microwaved at 600 watts for 30 seconds until the bands appear.

Western blotting

The second gel used above was used for western blotting. The gel was placed on a PVDF membrane and blotted for 30 minutes at 300mA using the blotting apparatus. After the blotting was finished the PVDF membrane was soaked in 3% milk solution (PBS +0.1% tween) for one hour at room temperature. Later, the membrane was sealed with the primary antibody (1:1000) and incubated over night at 4°C. Then, the membrane was washed gently for 2x15 minutes and 3x5 minutes with PBS tween solution. Further, the membrane was incubated in the milk solution with secondary antibody (1:10000) for 3-4 hours at room temperature. Then the membrane was washed gently for 2x15 minutes and 3x5 minutes with PBS tween solution. The membrane was soaked in (DIG P3+NBT/BCIP) solution and incubated in dark until the bands appear. For stopping the reaction the membrane was washed with ddH_2O.

2.27. Strain construction

Strains were constructed by homologous recombination technique**.** Gene deletions or C- terminal/N-terminal tagging of the desired genes is carried out by *in vivo* by homologous recombination as mentioned by Bahler et al., 1998. The integration cassette was PCR amplified using oligos to 5' and 3' with 80 bp homology to the target gene. This PCR product was later transformed into *S. pombe*. The correct integration of the cassette was verified by PCR. The correct clone was back crossed twice to eliminate further gene mutations. The oligos and cassette used for deletion of different strains were shown in the table below.

Strain number	strain	plasmid template used	Forward oligo	reverse oligo	PCR product length (bp)	verification oligo forward	verification oligo reverse	product length in (bp)
1726	*SPAPB2C8.01* Δ	163	920	921	1800	1873	113	475
						1874	205	551
2459	*pfl4*Δ	163	1969	1970	1700	1971	834	1443
						1972	124	1291
2540	*pfl8*Δ	163	1885	1886	1750	1887	113	554
						1888	205	1900
2511	*pfl3*Δ	163	1867	1868	1500	1869	833	1499

						1870	205	570
1728	*pfl9*Δ	163	1957	1958	1650	1959	205	534
2527	*mam3*Δ	163	1881	1882	1670	1883	113	462
						1884	205	624
2663	*gsf2-P-gfp*	177	2015	2016	2200	1543	1124	1053
						1543	2092	1239
2762	*gsf2-p-lucG*	1053	2090	2016	3500	1543	2092	1239
						2091	827	1754
2649	*hpm1*Δ	177	2099	1930	1800	1907	827	1243
						1908	821	1177
2923	*met10*Δ	177	2032	2044	1800	821	2034	1224
						2033	827	1319
2586	*SPBC725.03*Δ	177	1931	1932	2200	1909	1124	1006
						1910	821	1524
2684	*SPCC4B3.05c*Δ	177	2027	2028	1800	2029	827	950
						821	2034	1200

2.28. Luciferase assays

Sample preparation method by flash lysis

A sample of 100 µl of cells from an *S. pombe* culture was centrifuged and the pellet was resuspended in Glo-Lysis Buffer (Promega). Probes were then briefly frozen in liquid nitrogen and thawed at room temperature before assessing the luciferase activity.

Luciferase reaction

Probes were mixed with Luciferin-EF (Endotoxin-Free; Promega) at an end concentration of 160 µg/ml.

Chroma-Glo reagent

Probes were mixed with an identical volume of the Chroma-Glo reagent before measuring luminescence activity.

Luminescence measurements

After starting the probes and reagent, luminescence was read using Tristar (Berthold) luminometers. Probes were dispatched in a 96 well microtiter plate. The total volume of the reaction was 200 µl in a well of a 96 well plate. Plates were shaken for 10-15 sec at 1 m/s before the first luciferase activity measurement and for 10 sec before each measurement. The reaction temperature was 30°C. For each time point, three measurements were made: No Filter, where no optical filters were used; 510/60, the green optical filter 510/60 (Chroma Technology Corporation) was used; 610LP, the red optical filter 610LP (Chroma Technology Corporation) was used. For all measurements, unless otherwise specified, the exposition time was 1 sec. For measurements with the red and green filters, the luminescence values were corrected as the standard. Unless, otherwise specified, luminescence was measured over time (> 120 min) and the maximal luminescence value (Lmax) was reported.

Initially to evaluate the assay green and red light emitting luciferase strain was used. Cell concentration of $1x10^8$ per ml cells was used for the assay. The luminance measured was extremely high that it surpassed the detection limits of the equipment. So a serial dilution was prepared from the cells containing $1x10^8$ per ml to 1:2, 1:5, and 1:10. Dilution of the 1:2 resulted in adequate amount of luminescence emission and remained within the limits of the equipment (data not shown). Other dilution resulted in the very poor emission and the values stayed lower than the threshold limit. So a concentration of $5x10^7$ cells per ml was used.

2.29. Statistics

The error bars displayed on the graph with the standard deviation was calculated with Microsoft Excel. The stars displayed on graphics illustrate the results of an unpaired t-test (with Microsoft Excel): *, p-values ≤0.05, ** p-values ≤0.01, *** for p-values ≤0.001.

3. Results

S. pombe grow as single cell yeast but can also switch to pseudo hyphae. In the current study, the invasively growing colonies observed are the indicators of the dimorphic switch. It was shown that Asp1 is essential for the switch in context to nutrient limitation (Pöhlmann et al., 2010). The dimorphic switch can be accomplished by different external signals. In this work, the invasive growing ability of *S. pombe* was investigated in the correlation with Asp1. This work encompasses the following segments.

3.1) Extrinsic signals that govern invasive growth

3.2) Inositol pyrophosphates levels and invasive growth

3.3) Potential targets of Asp1 and invasive growth

3.1 Extrinsic signals that govern invasive growth

Previous experiments concerning the *S. pombe* dimorphic switch and invasive growth had been performed at an incubation temperature of 30°C and standard full media or Edinburgh minimal media (Dodgson et al., 2009, Dodgson et al., 2010, Pöhlmann et al., 2010). So far identified environmental factors that led to activation of the dimorphic switch are the nutrient limitation and the presence of toxic substances (excess iron in the media) (Dodgson et al., 2009, Prevorovsky et al., 2009, Dodgson et al., 2010). In the current study, the effect of three diverse external stimuli that indicated a role in the dimorphic switch was studied in three Asp1 variants ($asp1^{+}$, $asp1^{D333A}$, $asp1^{H397A}$ strains).

The first external stimulus to be tested was temperature. The second external stimulus tested was the presence of higher concentrations of toxic substances such as Ferric chloride ($FeCl_{3)}$. $FeCl_3$ was identified as one of the key external stimuli that can trigger the dimorphic switch (Prevorovsky et al., 2009). The third external stimulus reported was a nutrient limitation. Nutrient limitation in particular nitrogen limitation was identified as a major signal required for the dimorphic switch (Amoah-Buahin et al., 2005).

In the current study, the above mentioned three environmental stimuli were tested for the consequences on invasive growth ability of the strains expressing different $asp1^{+}$ variants.

3.1.1. Lower temperatures induce the formation of invasively forming colonies

Asp1 is required for invasive growth and increase in the level of Asp1 generated inositol pyrophosphates increases the number of cells to switch to invasively growing mode at 30°C (Pöhlmann et al., 2010). To answer if the temperature has an influence on invasive growth, the experimental set up for invasive growth was performed between 20°C to 34°C.

To test the effect of various temperatures, the *asp1*$^{+}$, *asp1*^{H397A}, *asp1*^{D333A} and *asp1Δ* strains were used. The wild-type (*asp1*$^{+}$) strain displayed few invasive colonies (9±3) per cell patch at 30°C (Figure 9A lower panel). The wild-type strain displayed 25 fold higher invasive colonies at 25°C (234±21) compared to 30°C (Figure 9A lower panel). The wild-type strain at 20°C, displayed 64 fold higher (577±56) number of invasively growing colonies compared to 30°C (Figure 9A lower panel).). The wild-type strain at 34°C, displayed only one to two invasive colonies (Figure 9A lower panel).

The *asp1*^{H397A} strain displayed 175±17 invasive colonies per cell patch at 30°C (Figure 9B lower panel). The *asp1*^{H397A} strain displayed 2 fold higher invasive colonies (394±28) at 25°C compared to 30°C (Figure 9B lower panel). At 20°C, the *asp1*^{H397A} strain displayed 8 fold higher (1489±100) invasive colonies compared to 30°C (Figure 9B lower panel). Similar to wild-type strain, the *asp1*^{H397A} strain displayed very few invasive colonies (3±1) at 34°C (Figure 9B lower panel). The number of invasively growing colonies at 34°C was significantly lower than the numbers that were observed at 30°C.

The *asp1*^{D333A} and *asp1*Δ strains did not show invasive colonies at any temperature tested (Figure 9 C and D lower panels).

Increase in the number of invasively colonies with a decrease in the temperature has been observed for both *asp1*$^{+}$ and *asp1*^{H397A} strains. But the magnitude of increase in invasively growing colonies is not similar in *asp1*$^{+}$ and *asp1*^{H397A} strains (*Figure 9E).* The wild-type strain displayed 26 fold and 64 fold increase at 25°C and 20°C respectively compared to 30°C (Figure 9E). Whereas, *asp1*^{H397A} strain displayed only an increase of 2 fold and 8 fold at 25°C and 20°C respectively (Figure 9E).

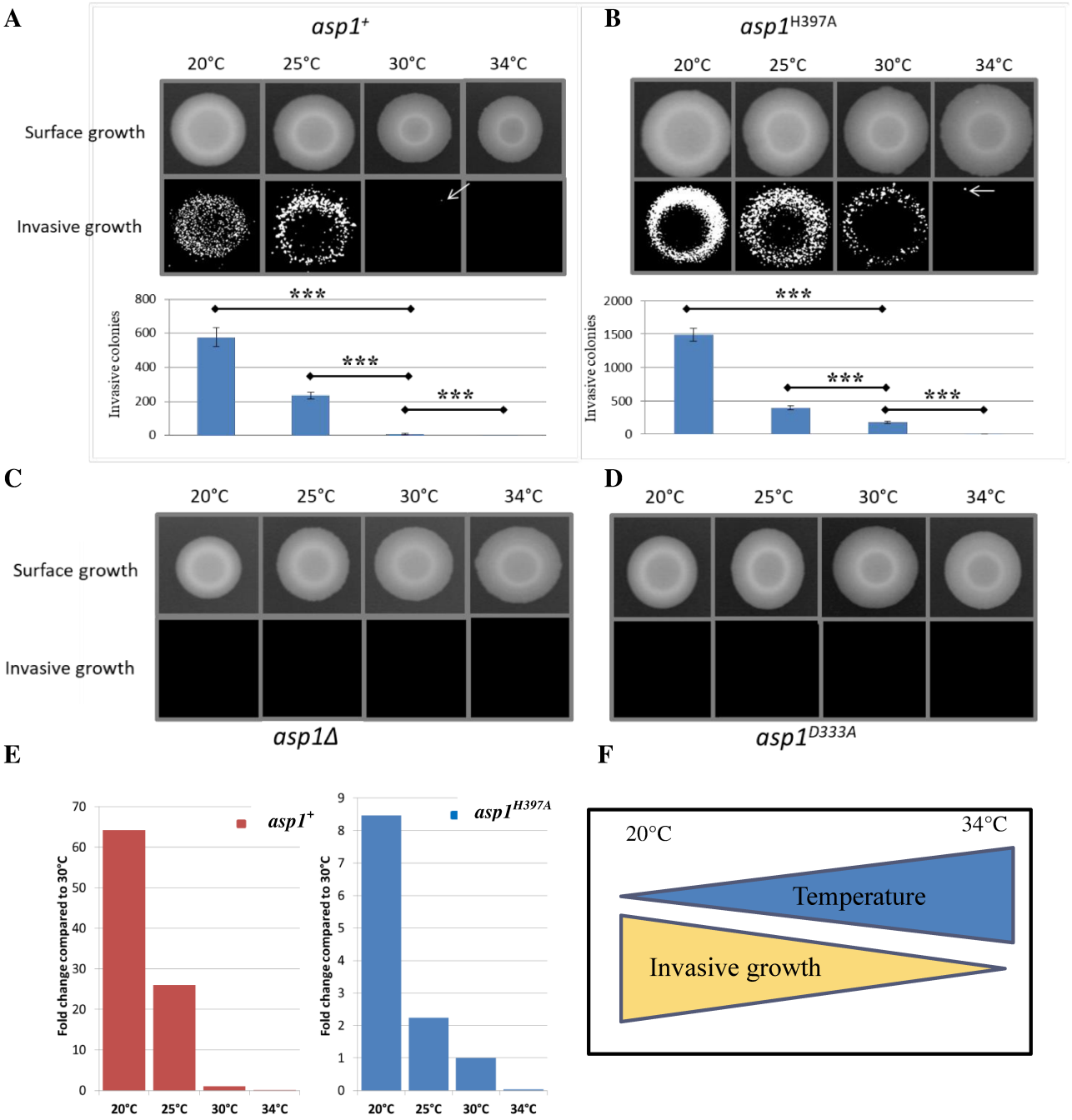

Figure 9: Lower temperatures induce a higher number of invasive colonies and require Asp1 kinase activity. A) Invasive growth assay of wild-type strain at different temperatures tested. The number of invasively growing colonies observed after washing off all the cells under a stream of water and rubbing off all the non-invasive cells were counted. B) Invasive growth of *asp1*^{H397A} strain at different temperatures. C and D) Invasive growth assay of *asp1*Δ and *asp1*^{D333A} strains at different temperatures displayed no invasive growing colonies. The bar charts display the absolute number of invasively growing colonies at different temperatures. The standard deviation represents the variations in numbers of invasive colonies in triplicates in an experiment performed at least three times. Quantification of invasively growing colonies; per strain 3 cultures were analyzed in triplicate, ***P < 0.0005, t-test. E) Fold change in invasively growing colonies of *asp1*$^{+}$ and *asp1*^{H397A} strains at different temperatures. F) Outline of the effect of temperature on invasive growth.

3.1.2. Excess iron induces invasive colonies in the absence of Asp1

Iron has been shown to be a potent stimulant of invasion (Prevorovsky et al., 2009). To investigate the effect of iron in the formation of invasive colonies, *asp1*$^{+}$ variant strains were grown on increasing concentrations of $FeCl_3$ containing media. These concentrations comprise a gradual increase from 1mM to 5mM $FeCl_3$. Wild-type *asp1*$^{+}$, *asp1*^{D333A} and *asp1*^{H397A} strains were analyzed in the current study.

For non-iron media with no additional iron, the total number of invasive colonies observed was similar to previously published results (Figure10A, Pöhlmann et al., 2010). With an increase in the iron concentrations in the media the number of invasively growing colonies increased in the wild-type strain, *asp1*^{D333A} and *asp1*^{H397A} strains compared to the control where no extra iron was added (Figure 10A, B, and 10C).

Interestingly *asp1*^{D333A} strain for the first time exhibited invasively growing colonies in the presence of 2.5mM $FeCl_3$ (Figure 10B lower panels). The numbers of invasive colonies are comparable to the *asp1*$^{+}$ strain but not up to the magnitude of *asp1*^{H397A} strain (Figure 10B). Further increase in the iron concentration to 5mM is toxic to in all strains and led to death (data not shown). As the iron concentration increased the cell patch diameter was decreased due to the increased hydrophobicity of the agar surface by excess iron.

The findings show that the presence of iron increases the invasively growing colonies in *asp1*$^{+}$ variants compared to iron free media. This suggests two independent signaling pathways that control the dimorphic switch may exist. Only one of them depends on 1,5-IP_8 generated by Asp1. The Asp1 mediated dimorphic switching can be bypassed through an unknown mechanism by the presence of excess iron in the nutrient media or environment.

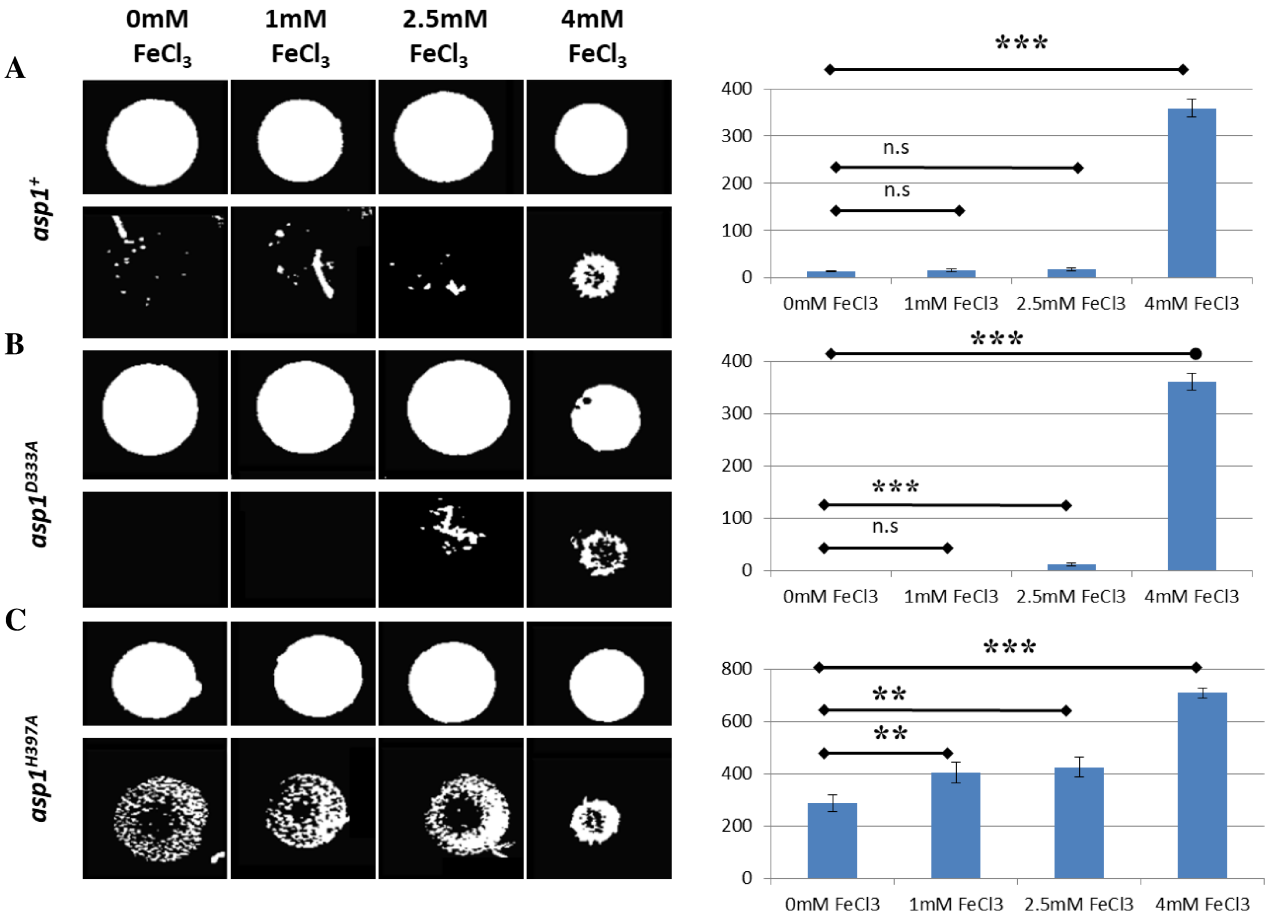

Figure 10: Excess iron in the media induces invasive growth in the absence of functional Asp1 kinase domain. A) Invasive growth of *asp1*$^{+}$ wild-type strain in YE5S media and YE5S media with additional iron. In the absence of $FeCl_3$, *asp1*$^{+}$ led to 12±2 invasive colonies per cell patch. The increase of the $FeCl_3$, to a concentration of 4mM led to 360±20 invasive colonies per cell patch. B) No invasively growing colonies were observed in *asp1*^{D333A} strain on standard media. Addition of 2.5mM $FeCl_3$ initiated the invasive growth of the *asp1*^{D333A} strain. The increase of the $FeCl_3$ concentration to 4mM led to 360±16 invasive colonies. C) Invasive growth of *asp1*^{H397A} strain in YE5S media and YE5S media with additional iron. In the absence of $FeCl_3$, the *asp1*^{H397A}strain was able to make 286 ±31 invasive colonies per cell patch. The increase of the $FeCl_3$, to a concentration of 4mM led to 708±18 invasive colonies. The standard deviation represents the differences of triplicates in an experiment at least performed three times. Quantification of invasively growing colonies; per plasmid 3 transformants were analyzed in triplicate, ***P < 0.0005, **P > 0.0005, n.s - not significant t-test.

3.1.3. Different growth media did not influence the number of invasive colonies

Three different media are generally used to cultivate *S. pombe*. YE5S media contains yeast extract, and essential amino acids are added to it later. In YE5S media the yeast extract itself acts as a nitrogen source. Edinburgh minimal media (EMM) uses ammonium chloride as main nitrogen source whereas, minimal media (MM) used glutamic acid as the main nitrogen source. According to Armstrong et al., 2005, nitrogen limitation is a critical extrinsic signal required for the dimorphic switch. To analyze the effect of various growth media on the ability of the strains to grow invasively the fore mentioned media were used to grow Asp1 variant strains.

The Asp1 variant strains were grown overnight in the corresponding media on which they were tested. Incubation of strains on various media resulted in the similar tendency in all types of media. The *asp1* ^{D333A} strain did not grow invasively in any of the media tested (Figure 11 A, B and C middle lower panels).

Wild-type *asp1*$^{+}$strain exhibited 8±3 invasively growing colonies on all the three kinds of media (Figure 11 A, B, C). No significant difference in the total number of invasive colonies was observed in wild-type strain on different media used.

The *asp1*^{H397A} strain displayed the highest number of invasive colonies on all growth media compared to the wild-type *asp1*$^{+}$ strain. As observed in the wild-type *asp1*$^{+}$ strain no significant differences in the total number of invasive growing colonies were observed in *asp1*^{H397A} strain on all the three kinds of growth media used.

From the above results, it implies that nutrient limitation could be one of the several external stimuli for the dimorphic switch as invasively growing colonies were only formed after initial inoculation with high cell density and growing cells for long periods of incubation (10-14 days). Regardless of the media with different nitrogen sources used the similar number of invasive colonies was observed. It could be interpreted as that nutrient limitation acts as an extrinsic signal to initiate the Asp1 mediated dimorphic switch.

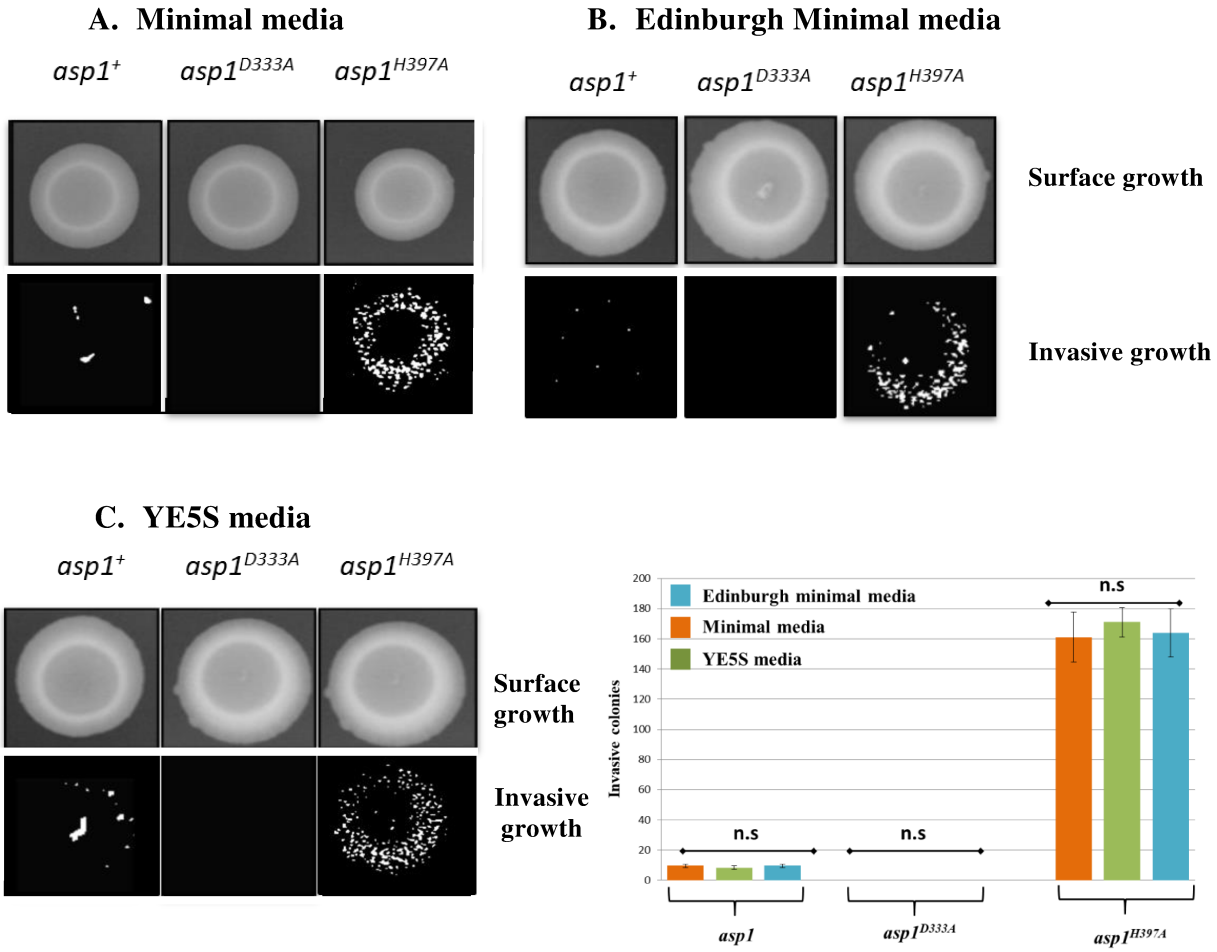

Figure 11: Asp1 variants displayed a similar number of invasively growing colonies irrespective of the media. A) Invasive growth ability of *asp1*$^{+}$, *asp1*^{D333A} and *asp1*^{H397A} strains in minimal media. The wild-type *asp1*$^{+}$ strain displayed 8±3 invasive colonies per cell patch whereas, *asp1*^{H397A} strain displayed 180±20 invasive colonies per cell patch. The *asp1*^{D333A} strain did not display any invasive growing colonies. B) Invasive growth ability of the wild-type *asp1*$^{+}$ strain, *asp1*^{D333A} strain and *asp1*^{H397A} strain in Edinburg minimal media. The wild-type *asp1*$^{+}$ strain displayed 5±2 invasive colonies per cell patch whereas, *asp1*^{H397A} strain displayed 145±15 invasive colonies per cell patch. The *asp1*^{D333A} strain did not display any invasive growing colonies. C) Invasively growing ability of *asp1*$^{+}$ strain, *asp1*^{D333A} strains in YE5S media. The *asp1*$^{+}$ strain displayed 9±5 invasive colonies per cell patch, whereas, *asp1*^{H397A} strain displayed 190±15 invasive colonies per cell patch in four different patches. The *asp1*^{D333A} strain did not display any invasive growing colonies. The standard deviation represents the differences of triplicates at least performed in three different experiments. n.s: not significant t-test.

3.2. Inositol pyrophosphates levels and invasive growth

Functional Asp1 kinase domain is essential for the formation of invasive growing colonies. The functional Asp1 kinase domain can generate 1,5-IP_8 *in vivo*. In this section it was investigated whether the increase in the Asp1 generated IPPs are directly proportional to the increase in the number of invasive colonies.

3.2.1. Intracellular 1,5-IP_8 levels are correlated with the number of invasive colonies

Exogenous expression of *asp1*$^+$ on a plasmid massively enhanced the invasively forming colonies in wild-type and *asp1*Δ strains (Pöhlmann et al., 2010). In an *asp1*Δ strain, exogenous expression of *asp1*$^+$ led to 10 fold higher invasive colonies compared to the *asp1*$^{1-364}$ plasmid expression. 50-60 invasive colonies were observed when *asp1*$^{1-364}$ was expressed in an *asp1*Δ strain whereas, no invasive colonies were found in the vector control. This was surprising as *in vitro* kinase assay indicated that Asp1$^{1-364}$ has twice the amount of IP_7 than that of the full-length Asp1, as Asp1$^{1-364}$ lacks the pyrophosphatase domain that can dephosphorylate the IP_7 generated by the kinase domain back to IP_6 (Pöhlmann et al., 2014, Marina Pascual-Ortiz et al., 2018). In the recent publication from our laboratory, it was demonstrated that these IPPs generated *in vivo* by Asp1 kinase domain are 1,5-IP_8 that uses IP_7 as the substrate (Marina Pascual-Ortiz et al., 2018). Thus the question arose whether 1,5-IP_8 levels have to be upheld to certain levels for efficient invasive growth. To answer this, *asp1*$^+$ and *asp1*$^{1-364}$ were expressed at different levels using variants of *the nmt1*$^+$ promoter (Moreno et al., 2000).

3.2.2 Expression of *asp1*$^+$ and *asp1*$^{1-364}$ by *nmt1*$^+$ promoter variants

To analyze if 1,5-IP_8 levels have to be corrected for certain levels, plasmid-encoded *asp1*$^+$ and *asp1*$^{1-364}$ were expressed at varying levels. This was achieved by expression of *asp1* and *asp1*$^{1-364}$ under variants of thiamine repressible promoter's *nmt1*$^+$*, nmt41, nmt81 (*Moreno et al*., 2000)*. The *asp1*$^+$ variants expression levels are shown in Figure 12A. The *asp1* encoding plasmids variants shown in Figure 12 were transformed into wild-type and *asp1*Δ strains and the resulting transformants were analyzed for their invasive growth ability.

3.2.3 The *asp1*$^+$ and *asp*$^{1-364}$ are differentially expressed by *nmt1*$^+$ promoter variants

To compare Asp1 and Asp1$^{1-364}$ protein levels, the relative protein amounts of Asp1 variants were determined in the *asp1Δ* strain transformants. For this purpose, C-terminal *gfp*

fusion proteins of *asp1*$^{+}$ and *asp1*$^{1\text{-}364}$ variants were constructed. The *asp1*$^{+}$*-gfp* and *asp1*$^{1\text{-}364}$*-gfp* were expressed under the control of the *nmt1*$^{+}$*, nmt41, nmt81* promoters. Subsequently, the protein levels of the GFP fusion proteins were quantified using a western blot.

Figure 12A and B shows the bands corresponding to Asp1-GFP and Asp1$^{1\text{-}364}$-GFP. The expression level of these proteins under various *nmt1*$^{+}$ variants was determined in an *asp1*Δ strain. The endogenous level was measured in an *asp1*$^{+}$*- gfp* strain. As the C-terminal domain of Asp1 can dephosphorylate the IPPs generated by the N-terminal kinase domain, the exogenous expression of Asp1 possibly could influence the physiological levels of IPPs. So it is impractical to measure the expression levels in the same strain and the following numbers are just an approximation by quantification of the western blots.

Expression of Asp1 under the *nmt1*$^{+}$ promoter resulted in approximately 4 fold higher protein level compared to the endogenous Asp1. Expression of Asp1$^{1\text{-}364}$ displayed approximately 17 fold higher protein level compared to endogenously expressed Asp1. Expression of Asp1 and Asp1$^{1\text{-}364}$ under *nmt41* promoter resulted in an increase in 2 fold and 5.6 fold respectively compared to the endogenous Asp1. Expression of the Asp1 by *nmt81* promoter results in a reduction to 0.5 fold compared to endogenously expressed Asp1. Asp1$^{1\text{-}364}$ expression by *nmt81* resulted into 2 fold increase in protein level compared to endogenously expressed Asp1.

Figure 12B shows the expected protein sizes of the C-terminal tagged Asp1 and expressed under various *nmt1* promoters. *In vitro* level of IP_7 by Asp1$^{1\text{-}364}$ domain is almost twice compared to the full-length Asp1 (Pöhlmann et al., 2014). Figure 12B shows the calculated 1,5-IP_8 levels after the expression of Asp1 variants. Plasmid-borne expression of asp1$^{1\text{-}364}$ has an increase of both IP_7 and IP_8, however, the IP_7 was twice the amount of IP_8 (Marina Pascual et al., 2018).

A

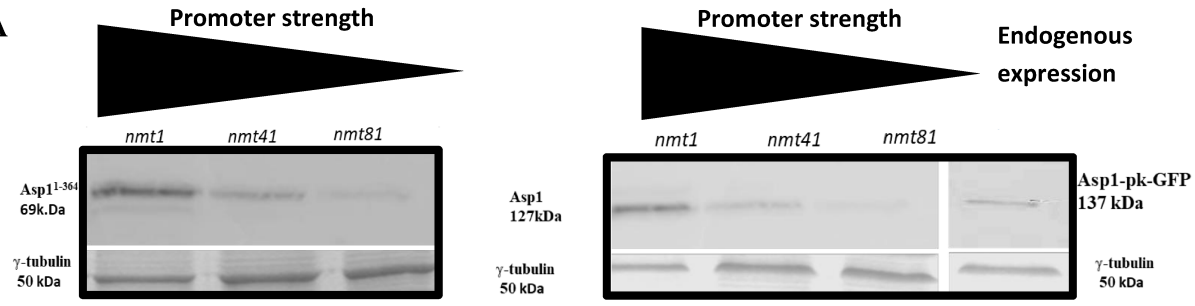

B

Promoter	Plasmid	Protein size (kDa)	*In vitro* IP_7 levels	Plasmid expression	*In vivo* 1,5-IP_8 levels (approx.)	Invasive colonies
Endogenous	Asp1	137	1		1	+
nmt1	Asp1	133	1	4.1x	4	+++++
nmt41	Asp1	133	1	2.2x	2	+++
nmt81	Asp1	133	1	0.5x	0.5	++
nmt1	Asp1-K	69	2	17x	34	++
nmt41	Asp1-K	69	2	5.6x	13	++++
nmt81	Asp1-K	69	2	1x	2	+++

Figure 12: Asp1 and Asp1$^{1-364}$ expression levels by various *nmt1* promoters. A) Total protein extract was isolated from the transformants expressing *asp1*$^+$*-gfp* and *asp1*$^{1-364-}$ *gfp* from *asp1*Δ strain grown in minimal media without thiamine at 30°C for 20 hours. Asp1-GFP runs at a size of 127 kDa and Asp1$^{1-364}$ runs at a band size of 69 kDa. The intensities were normalized to the endogenously expressed Asp1-Pk-GFP (137k.Da). γ/tubulin was used as internal loading control. B) The table shows expression levels of Asp1 and Asp1$^{1-364}$ by variants of the *nmt1* promoter together with the resulting invasive growth after the expression of *asp1*$^+$ and *asp1*$^{1-364}$. Asp1 and Asp1$^{1-364}$ IPP output determined *in vitro*. Factorials of approximate expression levels multiplied by their kinase activity and the outcome of their expression on invasive growth.

3.2.4 IPP levels generated by *asp1*$^{1-364}$ has to be altered for increased invasive growth

The plasmid-encoded *asp1*$^+$ and *asp1*$^{1-364}$ variants were used to examine the invasive growth ability in *asp1*Δ strain. These transformants were patched on the media containing thiamine as a control. No invasively growing colonies were observed (data not shown). As seen in Figure 13, the transformants containing the vector control did not exhibit any invasive colonies. But the expression of the *asp1*$^+$ under the *nmt1*$^+$ promoter exhibited a massive increase in the invasive growth ability.

Exogenous expression of *asp1*$^{+}$ on a plasmid enhanced the number of invasively growing colonies, in accordance to the amount of protein expressed (Figure 12B and 13A). Exogenous expression of the *asp1*$^{+}$ under *nmt41* and *nmt81* promoters resulted in reduced protein levels and furthermore displayed a decline in the total number of invasive colonies (Figure 12B and Figure 13A). Exogenous expression of *asp1*$^{+}$ via *nmt1*$^{+}$ promoter resulted in 735±60 invasive colonies per cell patch whereas, expression through *nmt41* promoter resulted in 180±20 invasive colonies per cell patch (Figure 13A). The expression of the *asp1*$^{+}$ via the weakest promoter *nmt81* resulted in 67±8 invasive colonies per cell patch (Figure 13A). Surprisingly expression of the *asp1*$^{1\text{-}364}$ by strongest promoter *nmt1*$^{+}$ resulted only in approximately 67±8 invasive colonies per cell patch. Asp1$^{1\text{-}364}$ expression was 16 fold higher compared to the endogenous expression. Expression of Asp1$^{1\text{-}364}$ via *nmt41* promoter resulted in approximately 180±20 invasive colonies. The protein level was reduced 3 fold in comparison to full strength *nmt1* promoter. Expression of *asp1*$^{1\text{-}364}$ through the weakest promoter *nmt81* resulted in approximately 135±8 invasive colonies per cell patch, which was twice as observed for the *asp1*$^{1\text{-}364}$ expression through the full strength *nmt1*$^{+}$ promoter.

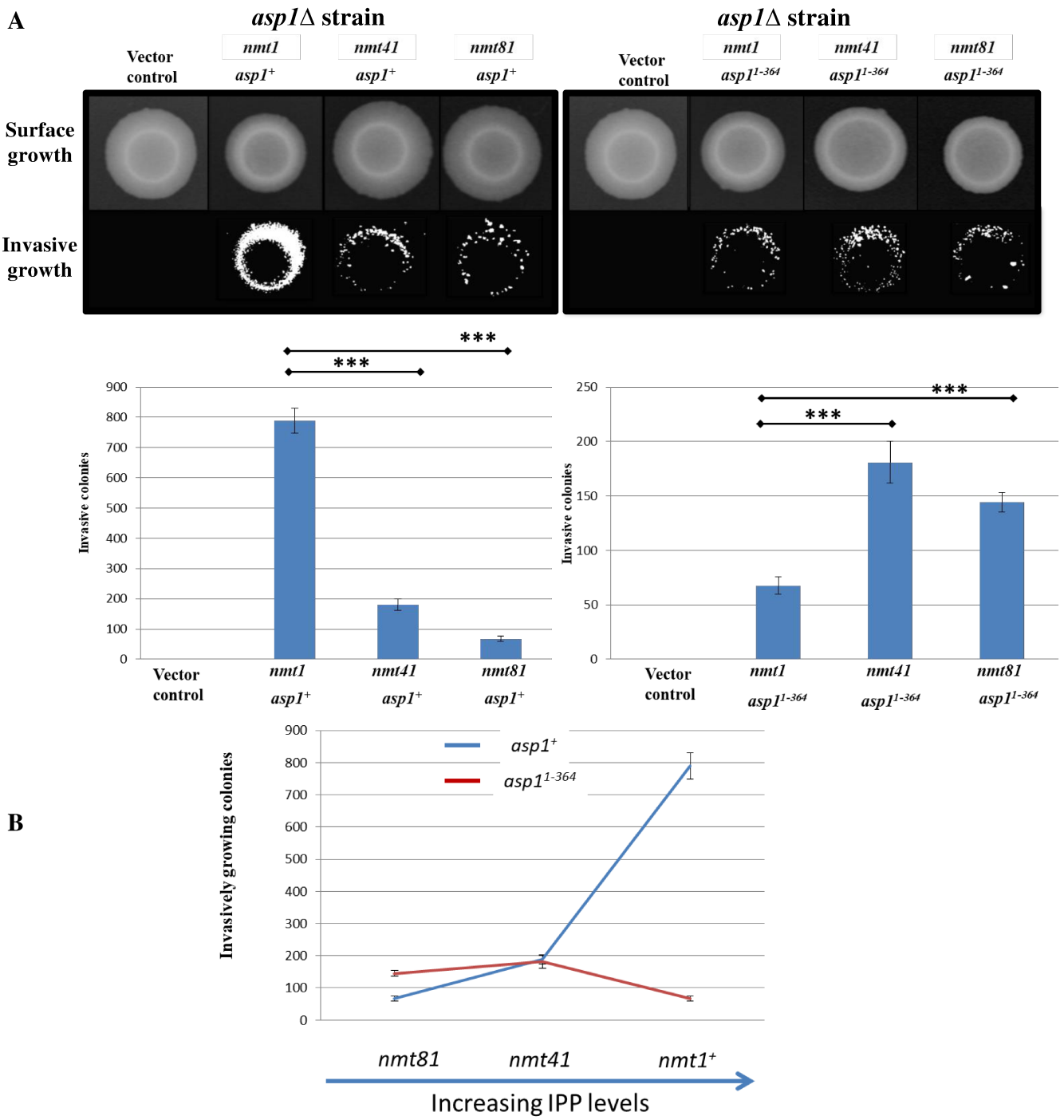

Figure 13: Asp1$^{1\text{-}364}$ levels have to be modulated for the efficient dimorphic switch. The *asp1Δ* transformants, transformed with *asp1*$^{+}$ and *asp1*$^{1\text{-}364}$ plasmids at various levels by different *nmt1*$^{+}$ variants. Expression of *asp1*$^{+}$ under strongest promoter *nmt1*$^{+}$ promoter resulted in the highest number of invasive colonies. Expression of *asp1*$^{+}$ under medium strength *nmt41* and *nmt81* promoter resulted in the reduction of invasive colonies. Expression of *asp1*$^{1\text{-}364}$ under full strength *nmt1*$^{+}$ promoter resulted in invasive colonies but the number increased when the *asp1*$^{1\text{-}364}$ was expressed via a weak *nmt41* promoter. Expression of *asp1*$^{1\text{-}364}$ by *nmt81* also resulted in the increase in invasive colonies approximately twice. These absolute number of invasive colonies for 4 different transformants from a single experiment. Each experiment has been performed at least in triplicates. Quantification of invasively growing colonies; per plasmid 3 transformants were analyzed in triplicate, ***P < 0.0005, t-

test. B) The graph illustrates the trend of invasive growing colonies in relation to *asp1*$^{+}$ and *asp1*$^{1\text{-}364}$ expression.

3.2.5 Invasive growth assay as a dissection of the Asp1 pyrophosphatase function

Vip1 family including Asp1 has an N-terminal kinase domain and C-terminal pyrophosphatase domain with homology to the histidine-acid-phosphatase and contains conserved signature motifs (Fridy PC et al., 2007). The signature motif of histidine-acid-phosphatases RHXXR (Motif M1) and HD (Motif M2) is present in PPIP5Ks/Vip1 family members except for the aspartate next to the second histidine (Rigden at al., 2008). A study by Gokhale et al., 2011 has reported Vip1 proteins had no phosphatase activity. But in contrast the pyrophosphatase domain of Asp1 was shown to negatively regulate the IP_7 output generated by the N-terminal kinase domain in a study by Pöhlmann et al., 2014. The study by Pöhlmann et al., 2014 was the first to demonstrate the pyrophosphatase activity of the Asp1 C-terminal domain *in vitro*. The C-terminal pyrophosphatase activity is inhibited by iron-Sulfur clusters (Wand H et al., 2015). But no iron-sulfur clusters were found in the recombinant Asp1 variants produced bacterially *in vitro* (Marina Pascual et al., 2018).

It was shown in an *in vitro* kinase assay that recombinant Asp1 protein can generate IP_7 using IP_6 as a substrate (Pöhlmann et al., 2014). Addition of Asp1$^{365\text{-}920}$ protein to the kinase assay decreased the amount of IP_7 dependent on the amount of protein used *in* a *vitro* assay. But the addition of Asp1$^{365\text{-}920/H397A}$ to the kinase assay did not show any decrease in the IP_7 levels (Pöhlmann et al., 2014). This shows us that Asp1$^{365\text{-}920/H397A}$ lacks the pyrophosphatase enzymatic activity. It was recently shown in a publication from our lab that Asp1, *in vivo* generates 1,5-IP_8 using 1-IP_7 as a substrate.

To analyze the role of conserved amino acids present in the conserved region motif M1 of Asp1 were exchanged to alanine(Asp1^{R396A}, Asp1^{R400A}) and tested for the ability to dephosphorylate the IP_7 generated *in vitro* (Marina Pascual Ph.D. work) and the ability to form invasive colonies (this work). Asp1^{R396A}, Asp1^{R400A} variants from the first conserved domain were tested through an *in vitro* pyrophosphatase assay weather they can dephosphorylate IP_7 to IP_6. Asp1^{R396A}, Asp1^{R400A} were unable to dephosphorylate IP_7 to IP_6 as no reduction in IP_7 was observed *in vitro* phosphatase assay (Marina Pascual et al., 2018). This demonstrates that these amino acids are essential for the enzymatic activity of the C-terminal domain.

Enzymatic function of histidine acid phosphatases requires a proton donor in the second motif (M2). Aspartic acid acts as a proton donor in this enzymatic reaction (Rigden et al., 2008). But in Vip1 family members of proteins isoleucine is present at this position instead of aspartic acid. So the isoleucine residue was exchanged for aspartic acid. To analyze the role of conserved amino acid present in the second conserved regions M2 of Asp1, histidine was exchanged to alanine ($Asp1^{H807A}$) and isoleucine was exchanged to aspartic acid, valine, and asparagine ($Asp1^{I808D}$, $Asp1^{I808V}$ $Asp1^{I808N}$). $Asp1^{I808D}$ exchange makes it a perfect histidine acid phosphatase as seen in other acid phosphatases (HD instead of HI).

The *asp1*^{I808D} variant was used in an *in vitro* phosphatase assay to analyze if it can dephosphorylate IP_7 and found out that it cannot. But interestingly endogenous exchange (*asp1*^{I808D}) at this position and *in vivo* analysis exhibited increased (approximately twofold) higher levels of 1,5-IP_8 compared to wild-type *asp1*$^{+}$. This shows that the pyrophosphatase domain is not functional in $Asp1^{I808D}$ (Marina Pascual et al., 2018). Exchange of amino acid isoleucine to aspartate, which is the proton donor in classical histidine acid phosphatases, abolished pyrophosphatase function (Marina Pascual et al., 2018). The conserved histidine residue at position 807 was described to be essential for the pyrophosphate function. Addition of the $Asp1^{H807A}$ to the *in vitro* phosphatase assay partially decreased the amount of IP_7 indicating the pyrophosphatase activity is still present (Marina Pascual et al., 2018).

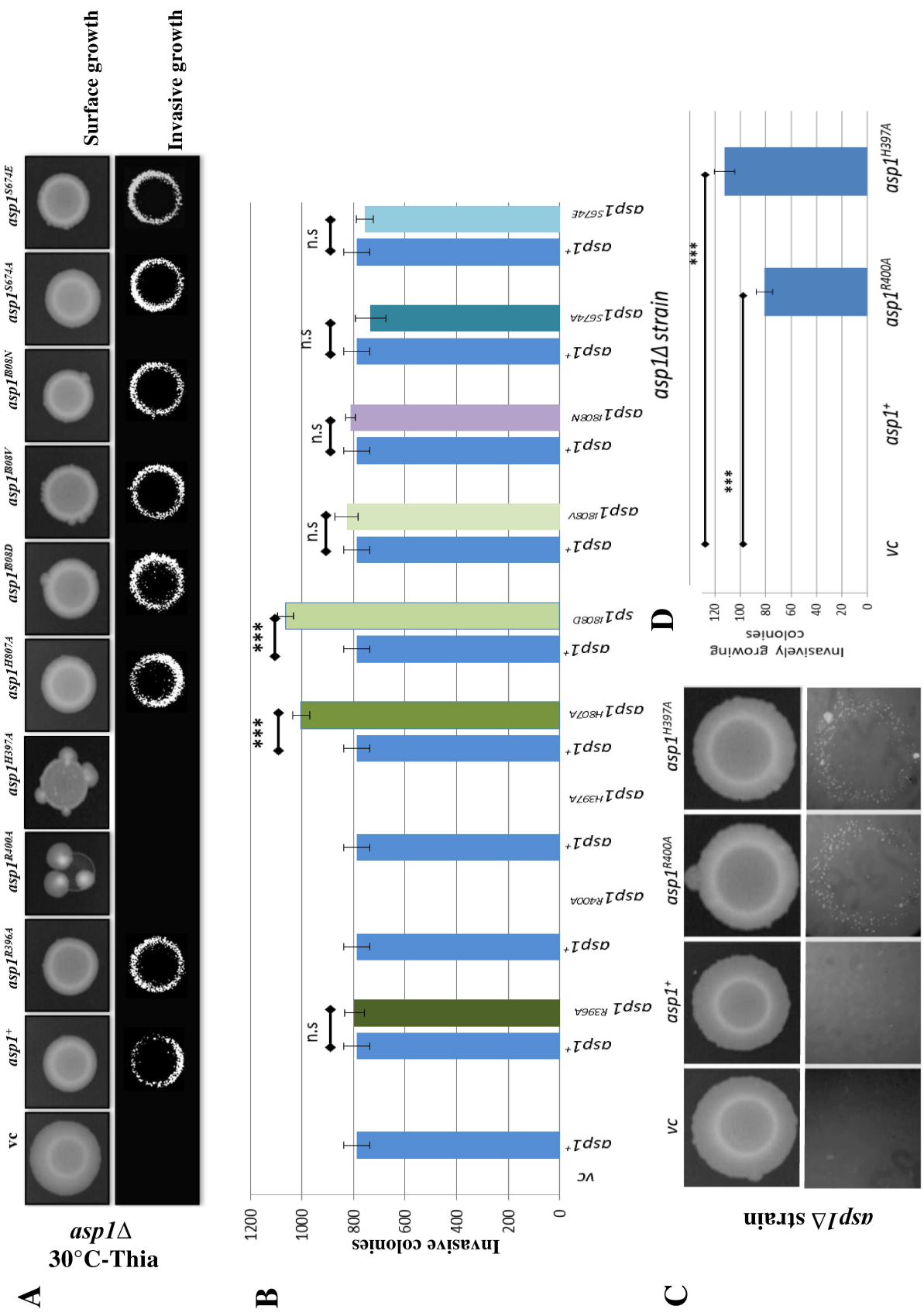
A
Surface growth
Invasive growth
vc
asp1+
asp1R396A
asp1R400A
asp1H397A
asp1H807A
asp1E808D
asp1E808V
asp1E808N
asp1S674A
asp1S674E
asp1Δ
30°C-Thia
B
Invasive colonies
1200
1000
800
600
400
200
0
vc
asp1+
asp1 R396A
asp1R400A
asp1H397A
asp1H807A
sp1E808D
asp1E808V
asp1E808N
asp1S674A
asp1S674E
n.s
***
C
asp1Δ strain
vc
asp1+
asp1R400A
asp1H397A
D
asp1Δ strain
Invasively growing colonies
120
100
80
60
40
20
0
vc
asp1+
asp1R400A
asp1H397A
***

Figure 14: **Loss of pyrophosphatase activity by the exchange of conserved amino acids led to increased invasive growth.** A) The expression of *asp1* variants in *asp1Δ* strain. The expression of a*sp1*^{H397A} and *asp1*^{R400A} displayed no invasive colonies as over-expression of these variants is lethal. The expression of *asp1*^{H807A} and *asp1*^{I808D} led to higher invasively growing colonies compared to *asp1*$^{+}$. B) The total number of invasively growing colonies *in asp1*Δ strain when different variants of *asp1*$^{+}$ are expressed compared to wild-type *asp1*$^{+}$. Statistical analysis using a student T-test displayed significant difference between *asp1*$^{+}$ and *asp1*^{H807A} and *asp1*^{I808D}. The expression of *asp1*^{I808V}, *asp1*^{I808N}, *asp1*^{S674A}, and *asp1*^{S674E} displayed similar number of invasive colonies to *asp1*$^{+}$. Statistical analysis using a student t-test displayed no significant differences between *asp1*$^{+}$ and *asp1*^{I808V}, *asp1*^{I808N}, *asp1*^{S674A}, *asp1*^{S674E}. ***P < 0.0005, n.s - not significant t-test. All the experiments were performed by using 4 different transformants in least in two different experiments. C) Invasive growth assay *of asp1*Δ strain transformed with vector control, *asp1*$^{+}$, *asp1*^{H397A} *and asp1*^{R400A} and grown on medium containing thiamine. D) Quantification of invasive growth assay *of asp1*Δ strain transformed with vector control, *asp1*$^{+}$, *asp1*^{H397A} *and asp1*^{R400A} and grown on medium containing thiamine. Quantification of invasively growing colonies 3 transformants per plasmid used. ***P < 0.0005 t-test.

Koch et al., 2011 has shown that the Asp1 was phosphorylated at the serine position 674 during mitosis. So the amino acid position with serine was mutated to glutamic acid and alanine. The *asp1*^{S674A} and *asp1*^{S674E} plasmids were provided by Natascha Kunzel. Serine is mutated to glutamic acid to mimic the phosphorylation of the serine residue whereas, in contrast mutating to alanine generating the phospho-dead mutant. These mutants were also analyzed for their ability to form invasive colonies.

To investigate the effect of the above mentioned Asp1 variants in invasive growth, the variants were expressed in *asp1*Δ strain. Figure 14A shows that the transformants in the presence of thiamine did not display invasive colonies. Figure 14B shows the transformants grown without thiamine. Expression of Asp1 in *asp1*Δ strain displayed invasively growing colonies. Higher number of invasive colonies was observed through the expression of *asp1*^{R396A} variant in *asp1*Δ strain compared to the vector control. Similar number of invasively growing was observed through the expression of *asp1*^{R396A} and wild-type *asp1*$^{+}$ (Figure14 B). *In vitro* kinase assay indicated no difference in the ability to dephosphorylate IP_7 *in vitro*. Expression of *asp1*^{R400A} displayed no invasive colonies. In fact, the phenotype was similar to the variant *asp1*^{H397A} i.e. overexpression of this variant is lethal (Mulugu et al., 2007) (Figure14B). The Asp1^{H397A} and Asp1^{R400A} displayed higher levels of IP_7 in an *in vitro* kinase assay compared to wild-type Asp1 as the C-terminal phosphatase domain is nonfunctional.

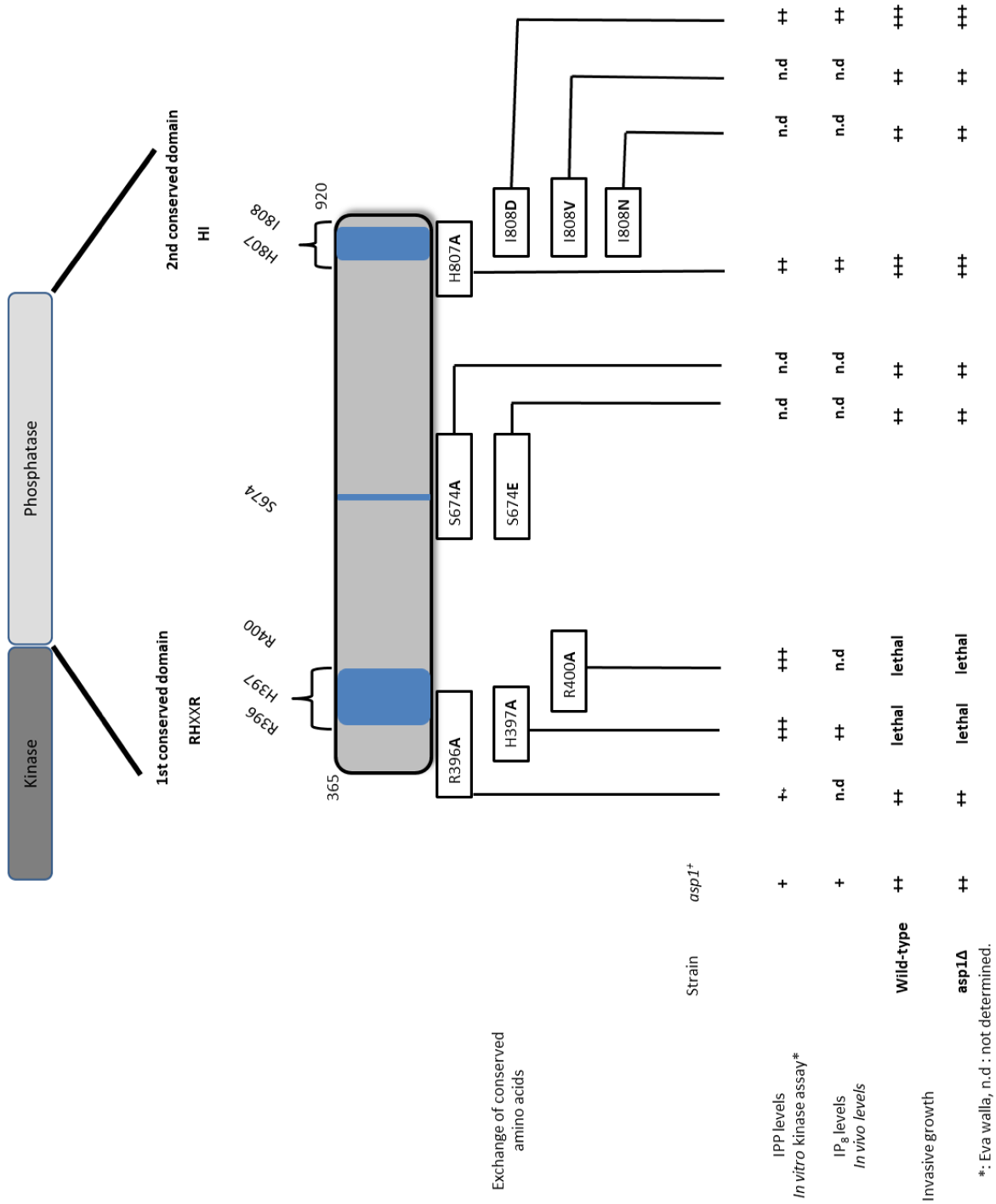

Figure 15: Summary of Asp1 variants and their inositol pyrophosphate output and their growing ability to grow invasively. Asp1 mutants generated via site-directed mutagenesis were expressed in wild-type and *asp1*Δ strains. Expression of variant a*sp1*^{R396A} displayed a similar number of invasively growing colonies compared to *asp1*$^{+}$. Overexpression of *asp1*^{H397A} and *asp1*^{R400A} lysed the cells. Expression of variant *asp1*^{S674A} and *asp1*^{S674E} displayed a similar number of invasively growing colonies compared to *asp1*$^{+}$. Expression of mutant *asp1*^{H807A} displayed an increase in the number of invasively growing colonies compared to *asp1*$^{+}$ by 20%. Expression of *asp1*^{I808V}, *asp1*^{I808N} variants, displayed no significant increase in the number of invasively growing colonies compared to *asp1*$^{+}$.

Expression of mutant *asp1*^{I808D} displayed an increase in the number of invasively growing colonies compared to the *asp1*$^{+}$ by 20%.

The asp1^{S674A} and *asp1*^{S674E} did not show any significant differences in the total number of invasive colonies compared to *asp1*$^{+}$. This implies that the phospho mimicking or change of amino acid residue to alanine at serine at position 674 of Asp1 did not exhibit any differences compared to the wild-type. *In vitro* kinase assay has to be performed on these mutants.

Change in the amino acid residue at position 807 from histidine to alanine in second phosphatase signature motif led to significant increase in the total number of invasive colonies. Approximately 1000 invasively growing colonies per cell patch were observed. This is almost 20% higher compared number of colonies observed for wild-type Asp1 (Figure14B). *In vitro* phosphatase assay displayed no decrease in the amount of IP_7 levels (Figure 14B).

The *asp1*$^{+}$, *asp1*^{H397A} and *asp1*^{R400A} transformants were grown overnight in media without thiamine and patched on media containing thiamine. Later analyzed for invasive colonies *asp1*^{H397A} and *asp1*^{R400A} resulted in increased number of invasive colonies compared to Asp1 (Figure 14 D). We can conclude that Asp1^{R400A} lacks the functional C-terminal.

Overexpression of *asp1*^{I808D} displayed increase in the total number of invasive colonies compared to wild-type. *In vitro* phosphatase assay displayed no decrease in the IP_7 levels demonstrating no functional phosphatase domain (Figure14B). Further changes at amino acid position 808 to valine or asparagine did not lead to differences in the number of invasive colonies compared to wild-type (Figure14B). *In vitro* kinase assay has to be performed on these mutants to show that the pyrophosphatase activity is similar to the wild-type Asp1. The summary of the data above is diagrammatically displayed in Figure 15.

3.3 Potential targets of Asp1 and invasive growth

My analysis demonstrated that IPPs generated by the Asp1 is essential for the formation of invasive colonies. However, how these IPPs regulate invasive colonies are not known up to date. In this chapter, two possible targets through which the invasive colonies might be achieved will be presented.

i) Adhesins
ii) Physical interactors

3.3.1 Adhesins

It was identified that the wild-type *asp1*$^{+}$ and *asp1*^{H397A} strains adhered to the surface and invaded the substrate. Whereas, the *asp1*^{D333A} and *asp1*Δ strains were unable to adhere and invade the substrate without the presence of generate 1,5-IP_8. So in this context, it was investigated if adhesins are responsible for the formation of invasive colonies and if so which adhesins?

3.3.2. Adhesin Gsf2 is a possible target of Asp1

S. pombe encodes 12 potential flocculins and adhesins (Linder T et al., 2007, Kwon et al., 2012). These are designated as Pfl1 (Gsf2), Pfl2, Pfl3, Pfl4, Pfl5, Pfl6, Pfl7, Pfl8, Pfl9, SPAPB2C8.01, Map4, and Mam3. All the Pfl designated genes were identified as flocculins and are required for flocculation (Kwon et al., 2012). Map4 is a protein predicted as cell surface adhesion protein required for mating and conjugation (Sharifmoghadam MR et al., 2006). In this experiment, it was tested if Asp1 can modulate these flocculins and adhesins that are required for formation of invasive colonies. Galactose-specific flocculation Gsf2 was previously identified as the adhesin required for the galactose recognition and mediates the cell to cell adhesion and cell to substrate adhesion as well as the formation of pseudohyphal filamentous growth (Matsuzawa et al., 2011).

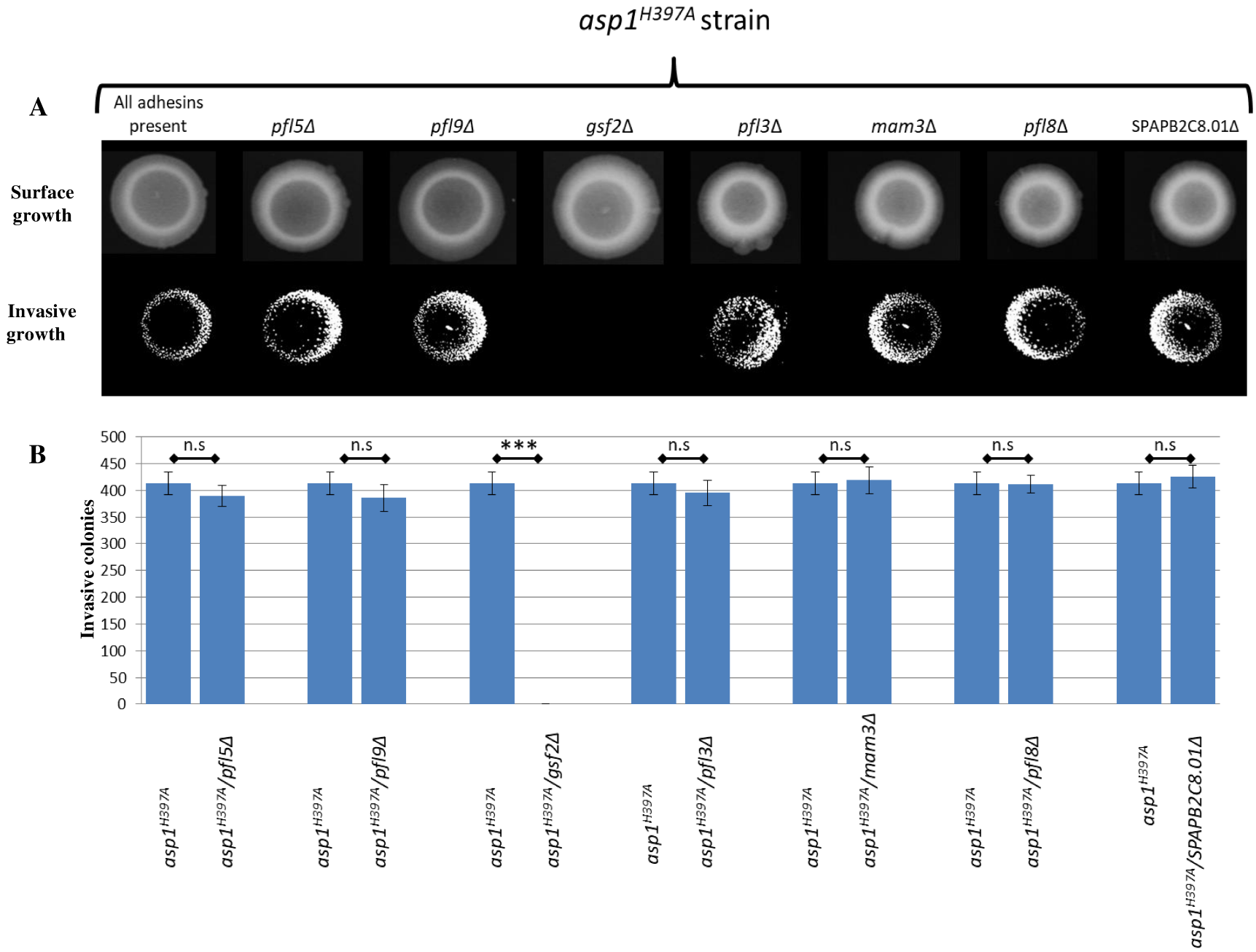
asp1H397A strain
A
All adhesins present
pfl5Δ
pfl9Δ
gsf2Δ
pfl3Δ
mam3Δ
pfl8Δ
SPAPB2C8.01Δ
Surface growth
Invasive growth
B
Invasive colonies
500
450
400
350
300
250
200
150
100
50
0
n.s
n.s
***
n.s
n.s
n.s
n.s
asp1H397A
asp1H397A/pfl5Δ
asp1H397A
asp1H397A/pfl9Δ
asp1H397A
asp1H397A/gsf2Δ
asp1H397A
asp1H397A/pfl3Δ
asp1H397A
asp1H397A/mam3Δ
asp1H397A
asp1H397A/pfl8Δ
asp1H397A
asp1H397A/SPAPB2C8.01Δ

Figure 16: Gsf2 is the essential flocculin required for the Asp1 dependent invasive growth. SPAPB2C8.01*, pfl9, gsf2*, *pfl3, mam3* genes were deleted in the *ap1*^{H397A} background and analyzed for invasive growth on YE5S media. The *asp1*^{H397A} strain with all adhesins intact displayed 412±22 invasively growing colonies per cell patch. Whereas, other mutant strains displayed a similar number of invasively colonies. The *pfl5*Δ strain displayed 390±20 invasive colonies per cell patch. The *pfl9*Δ strain displayed approximately 385±25 invasive colonies per cell patch. The *gsf2*Δ strain did not display any invasive colonies in any of the cell patches. *pfl3*Δ, *mam3*Δ, *pfl8*Δ *and* SPAPB2C8.01Δ strains displayed 395±24, 418±25, 411±16, and 425±21 invasive colonies respectively. There is no significant difference in the total number of invasive colonies compared to the *asp1*^{H397A} strain other than *gsf2*Δ strain. B) The absolute number of invasive colonies compared to *asp1*^{H397A} strain and other adhesin gene deletions. ***P < 0.0005 t-test.

Adhesin	**Deletion in *asp1*^{H397A}**	**Invasive growth**	**Deleted by**
All adhesins present	-	++	-
SPAPB2C8.01	yes	++	- This study
pfl4^{+}	not determined	++	not determined
pfl6^{+}	not determined	not determined	- not determined
SPBC1348.08c	not determined	not determined	not determined -
pfl8^{+}	yes	++	This study
map4^{+}	not determined	not determined	not determined -
pfl3^{+}	yes	++	This study
pfl7^{+}	not determined	not determined	not determined -
pfl9^{+}	yes	++	This study
pfl5^{+*}	yes	++	Pöhlmann J
mam3^{+}	yes	++	This study
Pfl1/gsf2*	**yes**	**abolished**	**Pöhlmann J**

Table 2: Adhesin gene deletion strains together with their invasively growing ability. The adhesin deletion was done in the *asp1*^{H397A} strain background. The ability of the deletion strains was determined using invasive growth assay.

Genes encoding Gsf2 and Pfl5 were previously deleted by Pöhlmann J. These were chosen as Pfl5 has high similarities to the *S. cerevisiae* adhesin FLO11 and Gsf2 is an

important adhesin required for the invasive growth in *S. pombe* (Matsuzawa et al., 2011, Kwon et al., 2012). The 5 adhesins gene deletions (*pfl9+*, *pfl8*$^{+}$, *pfl3*$^{+}$, SPAPB2C8.01, *and mam3*$^{+}$) i.e. one per strain was carried out in *asp1*^{H397A} strain background in the current study. Other deletions were not performed as no significant differences in flocculation were observed in these gene deletion strains (Kwon et al., 2012). Deletion of six potential adhesins revealed no significant difference in the change of the invasive number of colonies compared to the *asp1*^{H397A} strain (Figure 16). The absence of *pfl1*$^{+}$/*gsf2*$^{+}$ completely abolished the ability of *asp1*^{H397A} strain to grow invasively. This demonstrated that Gsf2 adhesin is required for the dimorphic switch.

3.3.3 Increase of *gsf2*$^{+}$ levels alter the number of invasively growing colonies

Gsf2 adhesin is essential for the Asp1 mediated dimorphic switch (Section 3.3.1). In the following experiment, it was analyzed if an increase in the expression of the Gsf2 increases the ability to form invasively growing colonies. To answer this, a strain was used, in which the 3'end of the native *gsf2* promoter was replaced with the *nmt41* promoter at its native locus i.e. the adhesin *gsf2* is now under the control of the *nmt41* promoter (Figure 17). This strain was kindly provided by Matsuzawa group upon request (Tomohiko Matsuzawa et al., 2011). This strain generated higher expression levels of Gsf2 mRNA compared to wild-type (Tomohiko Matsuzawa et al., 2011). To investigate the effect of Asp1, on *gsf2*$^{+}$ expression double mutant strains were constructed between this construct and the *asp1*$^{+}$, *asp1*^{D333A}, and *asp1*^{H397A} variant strains.

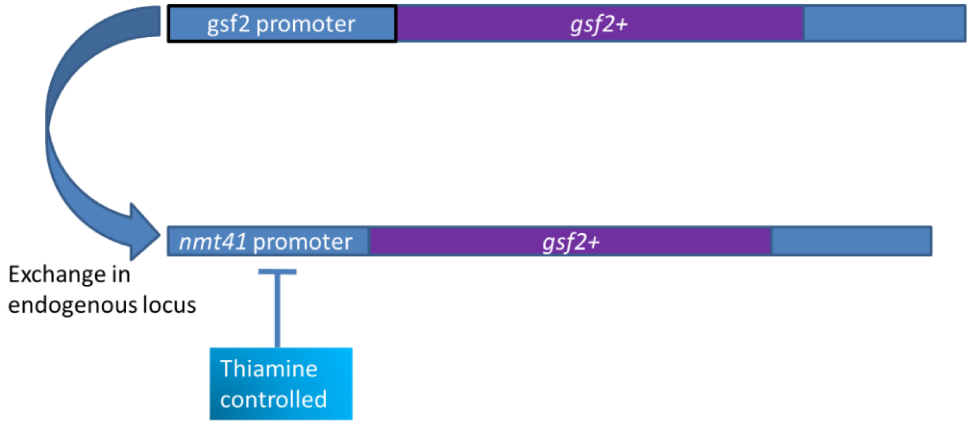

Figure 17: **Strain expressing *gsf2* under the *nmt41* promoter**. The *nmt41* promoter was inserted upstream of *gsf2*$^{+}$ (Matsuzawa T et al., 2011).

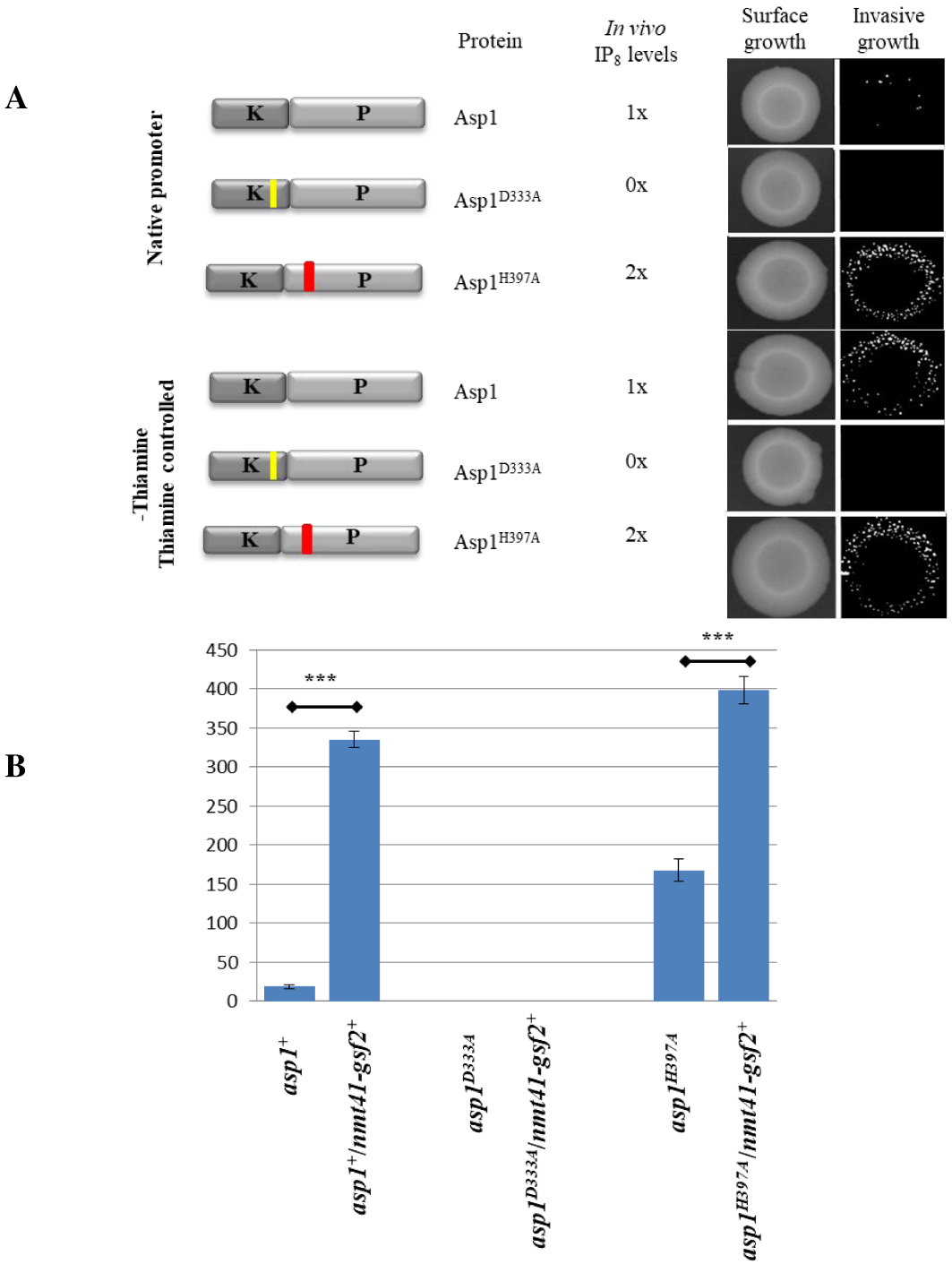

Figure 18: Increased expression of adhesin Gsf2 increases the number of invasively growing colonies but only in the presence of 1,5-IP$_8$. A) Asp1 variants in which Gsf2 is expressed via the native promoter or the *nmt41* promoter were grown in selective minimal media without thiamine. The absolute numbers of invasively growing colonies are shown in the bar chart. The experiment was performed with four individual cultures for three times in three different experiments. ***P < 0.0005 student t-test.

The resulting strain was grown on a liquid minimal media in the presence and absence of thiamine. As a control *asp1*$^{+}$, *asp1*^{D333A} *and asp1*^{H397A} strains were used in which *gsf2* is expressed under native promoter. In control plates containing thiamine, no invasive growing

colonies were observed indicating, *the gsf2* expression is essential for the switch (data not shown). In plates lacking thiamine invasively growing colonies were observed. The *nmt41-gsf2 /asp1*$^{+}$ strain displayed an increase in the number of invasive colonies. The invasively growing colonies were almost 20 fold higher compared to the native promoter (Figure 18B). No invasively growing colonies were observed in the double mutant *nmt41-gsf2/ asp1*^{D333A} strain as seen for *asp1*^{D333A} strain alone (Figure 18A). Thus, uncoupling *gsf2*$^{+}$expression from its normal regulation is not sufficient to induce the invasive growing colonies in the absence of 1,5-IP_8.

The *nmt41-gsf2/ asp1*^{H397A} double mutant strain displayed an additive effect. The *nmt41-gsf2/asp1*^{H397A} strain displayed a threefold increase in the number of invasive colonies compared to the *asp1*^{H397A} strain. This infers higher levels of Gsf2 are sufficient to increase the number of invasive colonies but still requires functional Asp1 kinase domain.

3.3.4 Positive regulators of the adhesin Gsf2 expression are required for invasive growth

The *S. pombe* adhesin Gsf2 and other flocculins expression are regulated by a transcriptional regulatory network consisting of the Mbx2, Rfl1, Cbf11, Cbf12 and Prz1 as key components (Kwon et al., 2012, Kate Chatfield-Reed et al., 2016). These include both transcription activators as well as repressors. Mbx2 and Cbf12 are positive regulators whereas, Rfl1 and Cbf11 are repressors. *cbf11*Δ and *cbf12*Δ strains were a kind gift from Prevorovsky group (Prevorovsky, M. et al., 2009). Double mutants were made between *asp1*^{H397A} strain and deletions of genes coding for transcriptional factors. These *S. pombe* double mutants were analyzed for invasive growing ability.

The deletion of genes encoding the transcription factors *mbx2*Δ and *cbf11*Δ strains completely abolished the invasive phenotype of the *asp1*^{H397A} strain as well as in *asp1*$^{+}$ strain (Figure 19). Kwon et al., 2012 and Prevovrsky et al., 2009 have shown that the invasive phenotype was completely abolished in *mbx2*Δ and *cbf11*Δ strains. Deletion of the repressor *cbf11*Δ had no effect on the number of invasively growing colonies compared to wildtype as well as in *asp1*^{H397A} strain.

WT
asp1H397A
mbx2Δ
mbx2Δ asp1H397A
cbf11Δ
cbf11Δ asp1H397A
cbf12Δ
cbf12Δ asp1H397A
rfl1Δ
rfl1Δ asp1H397A
prz1Δ
prz1Δ asp1H397A
Surface growth
Invasive growth
Invasive colonies
0
50
100
150
200
250
300
350
400
1500
2000
2500
***
n.s
asp1+
asp1+/mbx2Δ
asp1H397A
asp1H397A/mbx2Δ
asp1+
asp1+/cbf11Δ
asp1H397A
asp1H397A/cbf11Δ
asp1+
asp1+/cbf12Δ
asp1H397A
asp1H397A/cbf12Δ
asp1+
asp1+/rfl1Δ
asp1H397A
asp1H397A/rfl1Δ
asp1+
asp1+/prz1Δ
asp1H397A
asp1H397A/prz1Δ

Figure 19: **Positive transcriptional factors (regulators) of the adhesin Gsf2 are required for Asp1 dependent invasive growth.** Genes expressing the positive (marked in green) and negative transcriptional regulators (marked in violet) of *S. pombe* adhesin Gsf2 were deleted. Strains with *asp1*$^{+}$ or *asp1*^{H397A} along with the transcription factor deletion mutants were analyzed by invasive growth assay. Deletion of the transcription factors *mbx2*Δ, *cbf12*Δ completely abolished the invasive growing ability. Deletion of the repressor *cbf11*Δ displayed no significant differences in invasively growing colonies in both *asp1* and *asp1*^{H397A} variants. Deletion of the repressor *rfl1*Δ in *asp1*$^{+}$ background displayed a higher number of invasively growing colonies. Deletion of the *rfl1*Δ in *asp1*^{H397A} strain background displayed an enormous increase in invasively growing colonies that the quantification was highly impossible. Deletion of transcription factor *prz1*Δ resulted in an increase in invasively growing colonies in wild-type *asp1*$^{+}$ *and asp1*^{H397A} strain background. B) Numbers are the absolute number of invasive colonies per strain in 4 different cultures. ***P < 0.0005 student t-test.

	Wild type	***mbx2*Δ**	***cbf11*Δ**	***cbf12*Δ**	***rfl1*Δ**	***prz1*Δ**
asp1^{+}	+	-	+	-	+++	++
asp1^{H397A}	++	-	++	-	++++	+++
***asp1*Δ**	-	**n.d**	**n.d**	**n.d**	+	**n.d**

Table 3: Transcription factor gene deletion strains along with their ability to grow invasively with *asp1* variants. (+) Wild-type like invasive growth, (++) *asp1*^{H397A} strain like, (+++) higher than *asp1*^{H397A}, (n.d) not determined.

Deletion of the repressor *rfl1*Δ led to a different phenotype. Cells flocculated very strongly even under normal culturing conditions. Cells patched formed colonies that were highly invasive. In normal invasive growth assays, invasive colonies are formed at the circumference of the cell patch but whereas, in this strain invasive colonies also formed at the center of the cell patch with highly invasive colonies (marked within red box) compared to wild-type and other mutants (Figure 19). A high number of invasive growing colonies were formed in the *rfl1*Δ compared to *asp1*$^{+}$. In the double mutant *asp1*^{H397A} /*rfl1*Δ strain, invasive colonies were formed so massively that quantification was highly impossible. Deletion of *prz1*, a transcription factor which acts upstream of transcription factor Cbf11 (Chatfield-Reed et al., 2016) led to increased invasively growing colonies compared to wildtype (Figure 19) The strain *prz1*Δ/*asp1*^{H397A} displayed an increased number of invasively growing colonies compared to *asp1*^{H397A} strain alone (Figure 19).

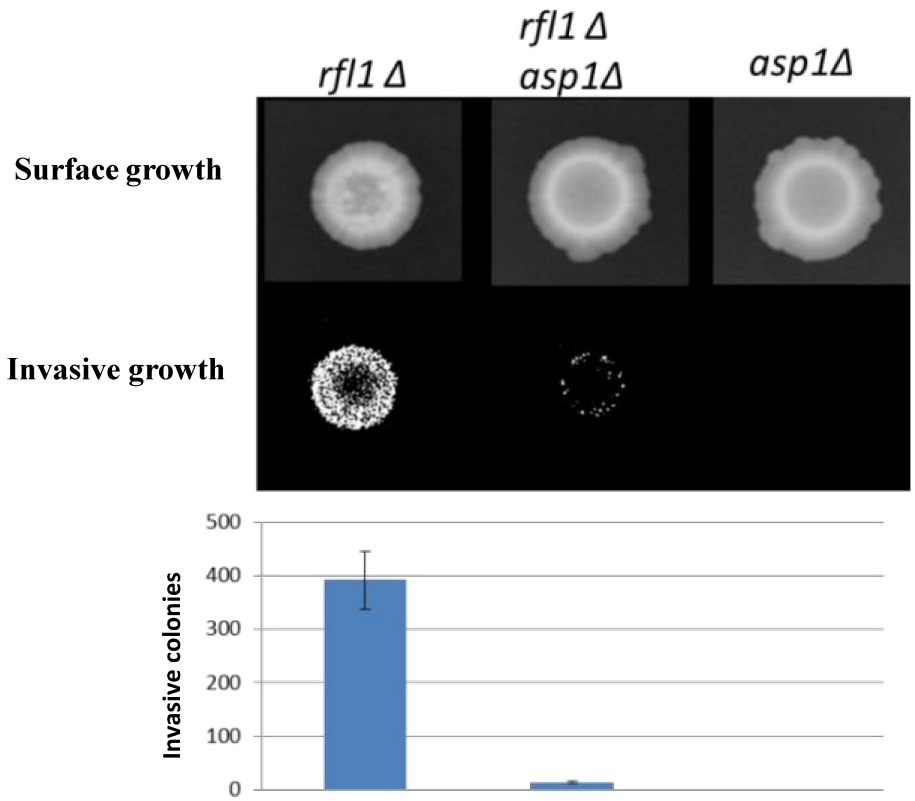

Figure 20: ***rfl1*Δ strain displayed decreased invasively growing colonies in the absence of *asp1*$^{+}$.** Deletion of transcription repressor *rfl1*Δ resulted in massive increase in invasively growing colonies in the wildtype *asp1*$^{+}$. In *rfl1*Δ/*asp1*Δ number of invasively growing colonies number was highly reduced. As expected *asp1*Δ strain did not exhibit any invasively growing colonies. Each experiment was done with at least 4 different cultures and in duplicates.

Next, it was examined whether invasive growth in the strain *rfl1*Δ was lowered in the absence of Asp1. So a double mutant was constructed with *asp1*Δ/*rfl1*Δ. It turned out that the deletion of the *asp1*$^{+}$ in the strain growing extremely invasive *(rfl1*Δ) lowered the total number of invasive colonies (Figure 20). This was the first time ever *asp1*Δ strain exhibited invasive growth under normal testing conditions. The *asp1*Δ strain also exhibited invasive growing colonies in the presence of excess iron in the media (Section 3.1.2). This result gives us an indication that a parallel pathway other than the Asp1 mediated exists that regulates the dimorphic switch. It also suggests that the other transcription repressors and transcriptional activators are still acting upon the adhesins which are essential for invasive growth in the absence of Asp1 generated 1,5-IP_8.

3.3.5 Asp1 generated 1,5-IP$_8$ regulate the Gsf2 expression level.

The above data shows that Pfl1/Gsf2 is possibly the main adhesin required for invasive growth. The increased levels of Gsf2 increased the number of invasive colonies. So the question arose was "Is Gsf2 differentially expressed in the Asp1 variants?" To answer this, the *gfp* ORF was cloned in frame to the native promoter of *gsf2*$^+$ and a selection marker. The constructed strain was verified using colony PCR (Materials and methods, section 2.26). Double mutant's strains were constructed along with the *gsf2*$^+$*-p-gfp* and *asp1*^{D333A} or *asp1*^{H397A}variant. The GFP expression pattern shows that the *gsf2*$^+$ promoter is regulated by Asp1.

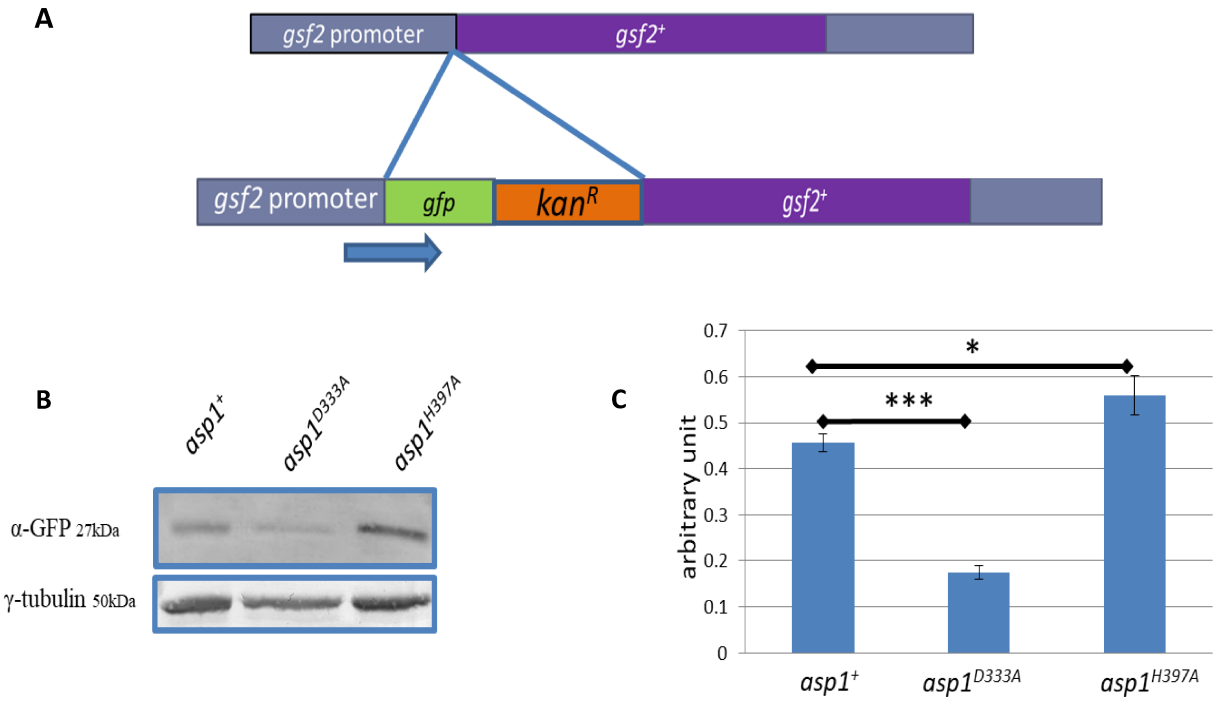

Figure 21: Gsf2 expression levels vary with varying 1,5-IP$_8$ levels. A) The construct of the reporter strain used for GFP reporter assay. A *gfp* ORF was cloned to the 3´ end of the native promoter of the *gsf2*$^+$. B) Double mutants were constructed along with the *gsf2*$^+$*-p-gfp* and *asp1*^{D333A} or *asp1*^{H397A} variants and GFP expression levels were determined. C) The intensity of the bands shown in the western blot was quantified using ImageJ program and the absolute numbers were projected. Numbers from two different western blots were used for statistics. Student t-test: ***P < 0.0005, *P > 0.0005 t-test.

In Figure 21, western blot analyses of *gsf2*$^+$ promoter-driven *gfp* in various Asp1 variant strains are shown. These bands represent the expression of GFP at the size of 27 kDa. GFP is expressed in all the *asp1* variants at different levels. GFP expression level in *asp1*^{D333A} strain had the lowest expression levels compared to *asp1* and *asp1*^{H397A}strains. GFP expression in wild-type *asp1*$^+$ strain is twice the amount as in the *asp1*^{D333A} strain. The

asp1^{H397A} strain has approximately 20% increase compared to *asp1*$^{+}$ and has the highest GFP expression.

The double mutant strain was constructed containing *asp1*Δ and *gsf2*$^{+}$promoter-driven *gfp* construct. The double mutant was transformed with *asp1* variants on a plasmid. The *asp1* variants used were *asp1*$^{+}$, *asp1*$^{1-364}$, *asp1*$^{365-920}$, and *asp1*$^{365-92/\ H397A}$.

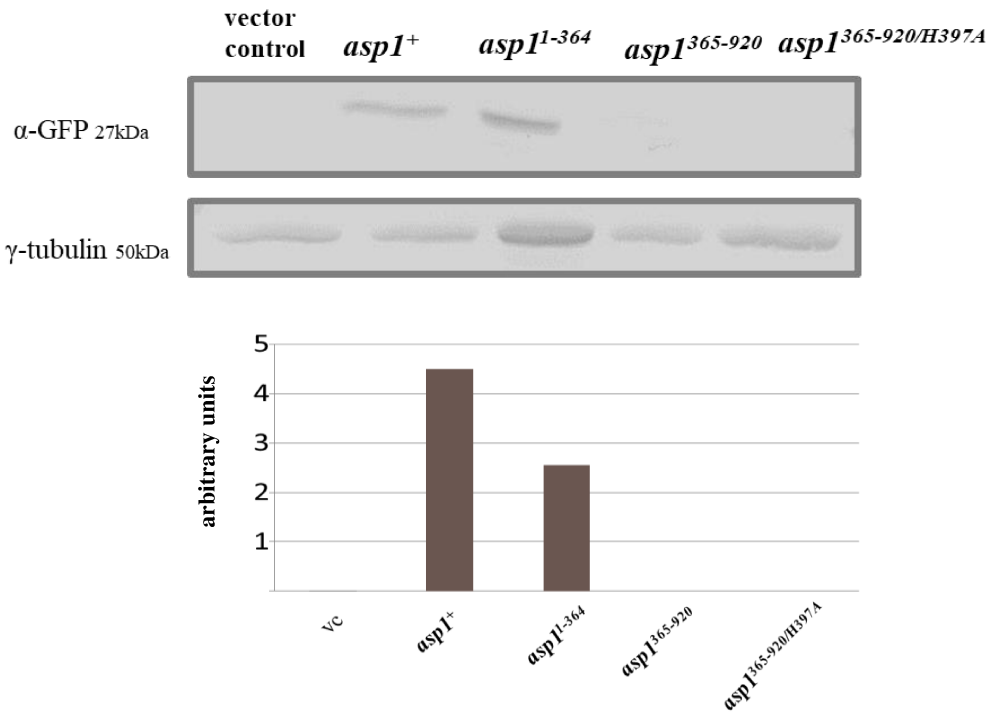

Figure 22: The *gsf2*$^{+}$ promoter activity is varied with varying 1,5-IP$_8$ levels. The *asp1*Δ/ *gsf2-p-gfp* strain double mutant strain was transformed with *asp1* expression plasmids and GFP expression levels were detected. The intensity of the bands shown in the western blot was quantified using ImageJ program and the absolute numbers were used. Expression of vector control does not activate *gsf2*$^{+}$ promoter and thereby no GFP was expressed. Expression of *asp1*$^{+}$ can activate the *gsf2*$^{+}$promoter and thereby GFP was expressed. Expression of *asp1*$^{1-364}$ can also activate the *gsf2*$^{+}$promoter and thereby GFP was expressed. The expression of *asp1*$^{365-920}$ and *asp1*$^{365-920H397A}$ do not active the *gsf2*$^{+}$promoter. The arbitrary units are the values obtained by normalization of GFP expression to the internal control γ-tubulin by quantification using ImageJ software. It can be proved that 1,5-IP$_8$ generated by Asp1 kinase domain is essential for the activation of *gsf2*$^{+}$promoter.

Figure 22 shows the expression of GFP in *asp1*Δ and *gsf2* promoter-driven *gfp* construct strain transformed with *asp1*$^{+}$ and other variants expression with plasmids. GFP expression is completely repressed in this strain (Figure 22 vector control). GFP expression is regained when any plasmid containing functional Asp1 kinase domain is expressed. The *asp1*$^{365-920}$ and *asp1*$^{365-920}$/H397A expression did not activate the *gsf2*$^{+}$ promoter. GFP expression level was induced when *asp1*$^{+}$ and *asp1*$^{1-364}$ were expressed. This implies *asp1*$^{+}$

and *asp1*$^{1-364}$ generated 1,5-IP_8 and these molecules are essential for the activation of *the gsf2*$^{+}$ promoter. As seen in chapter 2.2 the expression of *asp1*$^{+}$ led to increased invasive growth compared to *asp1*$^{1-364}$. Here it can be explained as *asp1* full-length expression leads to higher levels of *gsf2*$^{+}$ promoter activity and thereby higher levels of GFP expression compared to the *asp1*$^{1-364}$. This result shows a completely new role/function of 1,5-IP_8 in activation or upregulation of the target genes.

3.3.6 The *gsf2*$^{+}$ promoter is inactive by the expression of *asp1*$^{365-920}$

Next, it was analyzed if the expression of the *asp1*$^{365-920}$ in the wildtype strain could diminish the activity of *the gsf2*$^{+}$ promoter. In parallel, wild-type strain was also transformed with the *asp1* variants to analyze the invasive growth phenotype. The transformants were patched at 20°C as the difference in the invasively growing colonies between vector control and others expression plasmids is significantly high at this temperature than that observed at 30°C in an invasive growth assay. The influence of expression of these *asp1*$^{+}$ variants on the invasive growth and *gsf2*$^{+}$ promoter activity was analyzed.

As seen in Figure 23A, the wild-type strain transformed with the vector control displayed invasively growing colonies at 20°C. As numbers of invasively colonies are higher at a lower temperature such as 20°C, this temperature was used to increase the difference between vector control and asp1$^{365-920}$. Expression of *asp1*$^{+}$ and *asp1*$^{1-364}$ can further increase the number of invasive growing colonies. Expression of the *asp1*$^{365-920}$ abolished the wild-type cells to grow invasively. The transformant containing the vector control shows approximately 120 invasively grown colonies per cell patch. The number of invasive colonies is transformants that express Asp1$^{365-920/H397A}$ is similar to the vector control.

The *gsf2*$^{+}$*-p-gfp* reporter strain exhibited a similar trend as observed for the invasive growth experiment. The *gsf2*$^{+}$*-p-gfp* strain was transformed with *asp1* $^{365-920}$ and *asp1* $^{365-920}$/^{H397A} plasmids. As shown in the Figure 23 B expression of the *asp1* $^{365-920}$ diminished the *gsf2*$^{+}$ promoter activity and thereby we see a reduction in the expression of GFP. The *asp1*$^{365-920/H397A}$ expression led to the expression of GFP, denoting an active *gsf2*$^{+}$ promoter. Thus, these results indicate that the 1,5-IP_8 are required to activate the promoter, here, in this case, the *gsf2*$^{+}$ promoter and thereby express the genes required for invasive growth. Expression of *asp1*$^{365-920}$ can dephosphorylate the 1,5-IP_8 back to IP_7 and this results in the diminished activity of the *gsf2*$^{+}$ promoter.

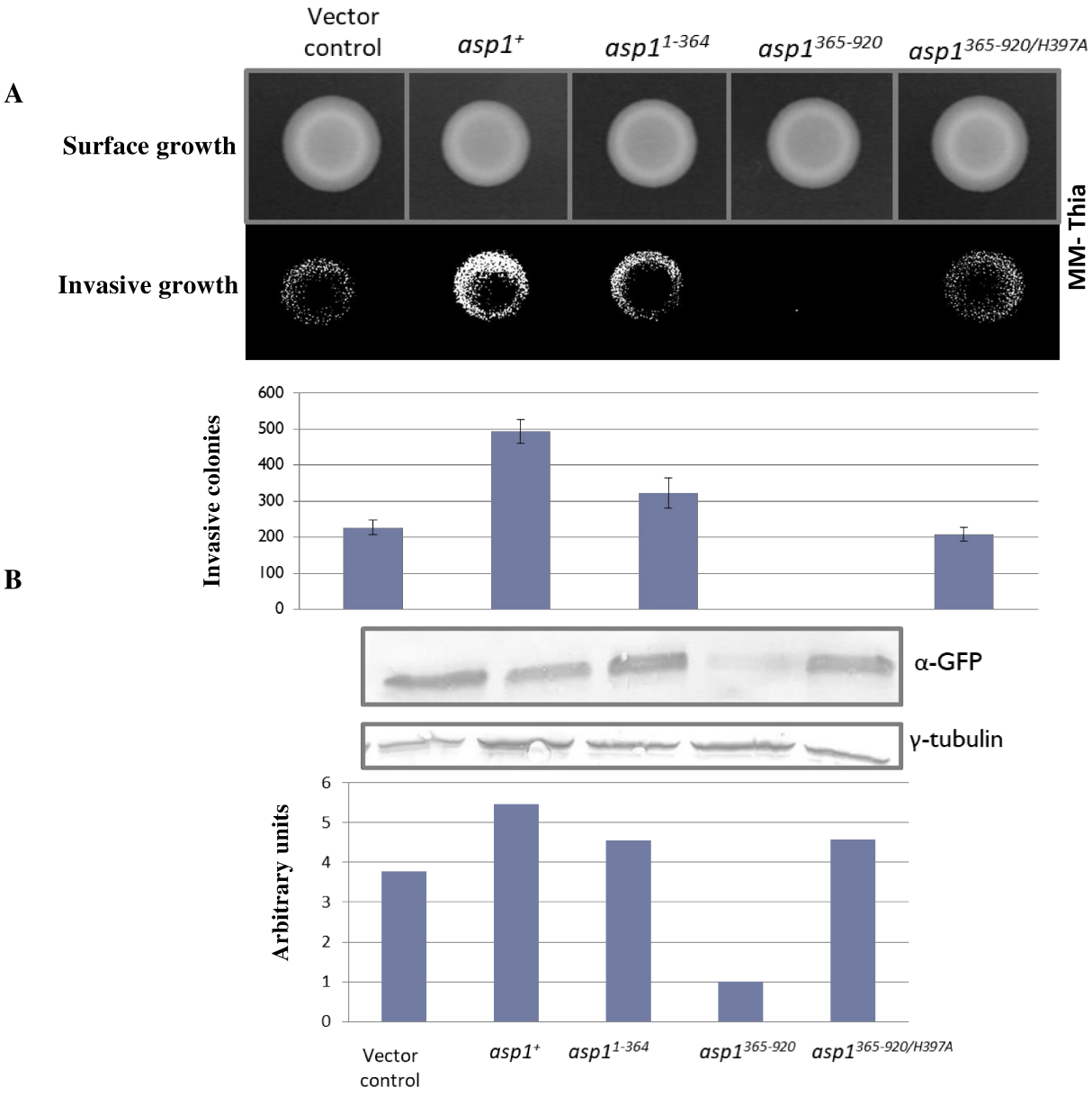

Figure 23: The *gsf2*$^{+}$ promoter activity is varied with varying 1,5-IP$_8$ levels analyzed by GFP reporter assay. A) Wild-type strain transformed with different *asp1* variant plasmids. Expression of *asp1*$^{365-920}$ completely abolished the invasive growth ability of the wild-type strain at 20°C. B) Transformants were grown in media lacking thiamine at 30°C and GFP expression level was determined. Expression of *asp1*$^{+}$ can activate the *gsf2*$^{+}$promoter and thereby GFP was expressed. Expression of *asp1*$^{1-364}$ can also activate the *gsf2*$^{+}$promoter and thus GFP was expressed. The expression of *asp1*$^{365-920}$ can diminish the activity of the *gsf2*$^{+}$ promoter. Expression of *asp1*$^{365-920/H397A}$ shows no difference in the *gsf2*$^{+}$promoter activity compared to the vector control. The arbitrary units are the values obtained by normalization of GFP expression to the internal control γ-tubulin by quantification using ImageJ software. It can be shown that 1,5-IP$_8$ generated by Asp1 kinase domain is essential for the activation of *gsf2*$^{+}$promoter.

3.3.7 Asp1 regulate the *gsf2*$^+$ expression level analyzed by Luciferase assay

The benefit of luciferase assay is more sensitive measurements from the assay and more dynamic range and more accuracy when analysis promoter activity. The assay is quite easy (basically lyse the cells and use the supernatant with the substrate and measure the light using a luminometer). Luciferase assay is an extremely sensitive allowing quantification of even small changes in expression levels and provides results instantaneously within minutes. It was mentioned in previous studies that for promoter analysis, luciferase is the best system (Francisca Alcaraz-Pérez et al., 2008, Nina Solberg et al., 2013). The dual system with Firefly and Renilla luciferases allow for the correct data for the promoter activity.

The previously used GFP reporter system is great, as it does not require any specific substrate not it does require a fluorometer. It is a bit also a time-consuming process as it involves growing the strains and isolation of total protein from the cells and running in the SDS gels and blotting and later with detection. So a more sensitive system was used to analyze the *gsf2* promoter activity i.e. luciferase assay system. The *asp1*^{D333A} and *asp1*Δ strains have a thicker cell wall and these strains were also resistant to cell wall degrading enzymes such as zymolase (Pöhlmann Ph.D. thesis 2010).To reduce this hindrance and to give assurance to the result obtained above via GFP reporter assay and as an alternative method to show that Asp1 generated 1,5-IP_8 regulate the *gsf2*$^+$ promoter activity luciferase assay was used.

A green light emitting luciferase gene (*CBGluc:* **C**lick **B**eetle **G**reen **L**uciferases) ORF was cloned behind the 3' end of the *gsf2*$^+$ native promoter (Figure 24). The *gsf2*$^+$ was also kept intact as the first 80 bp of the *gsf2* was used for homologous recombination. The constructed strain was verified using colony PCR (Materials and methods, section 2.26). As an internal control in the same strain, a red light emitting luciferase gene (*CBRluc:* **C**lick **B**eetle **R**ed **L**uciferases) is expressed at the *leu1*$^+$ locus. This strain emitting red luciferase was a kind gift from Marc Bühler group (Yukiko Shimada et al., 2012).

The strains were analyzed for luciferase emittance until the reaction reached saturation. All the strains emitted an equal amount of red light depicting the internal control is equal (Figure 24). The green light emittance was varied as the promoter activity was different for different *asp1* variants. The ratio of the green light emission to that of the red light emission gives the normalized values for each strain. Thus obtained R_{max} ratio (green

luciferase/red luciferase) of the *asp1* variants were normalized to the R_{max} ratio of *asp1*Δ strain Figure 24.

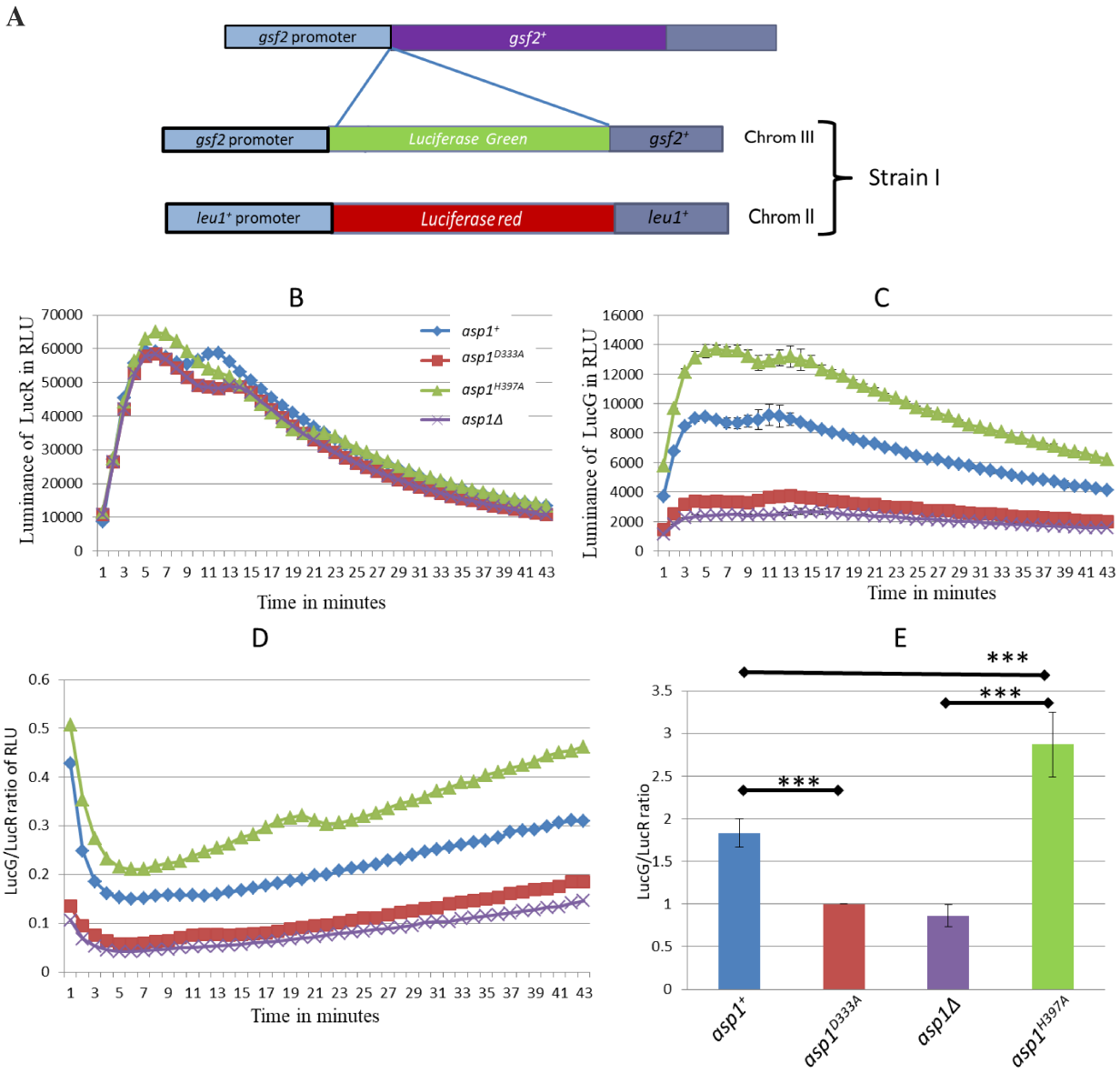

Figure 24: Gsf2 promoter activity is varied with varying 1,5-IP_8 levels analyzed by luciferase assay A) The construct of the reporter strain used for luciferase assay. The green light emitting Luciferase ORF was cloned 3' to the native promoter of the *gsf2*$^+$. The red light emitting luciferase gene was used as an internal control. The red light emitting luciferase was cloned to the *leu1*$^+$ native promoter and at the *leu1*$^+$ locus. B) The mutants constructed were analyzed for the luciferase expression. The red light emittance by red luciferase was detected for one-minute time interval until the reaction reached saturation. The points determine the detection at several time points in triplicates. C) The green light emittance by green luciferase was detected for one-minute time interval until the reaction reached saturation. The points determine the detection at several time points in triplicates. D) The values obtained by detecting green light were normalized to the red light and the R_{max} ratio was determined. The ratio of green to red at the maximum light detection was used for the quantification. Each sample was done in triplicates using a 96 well plate. E) The bar chart represents the

normalized R_{max} values compared to that of *asp1*Δ strain. Student t-test: ***P < 0.0005, t-test.

The R_{max} ratio of the strain harboring the wild-type *asp1*$^{+}$ has two-fold increases in the R_{max} ratio compared to the *asp1*Δ or *asp1*^{D333A}strains. The *asp1*^{H397A} strain displayed a threefold increase in the R_{max} ratio in comparison to *asp1*Δ or *asp1*^{D333A}strains. The R_{max} ratio of *asp1* ^{H397A} strain was significantly high in comparison to the wild-type *asp1* Figure 24. The strains *asp1*Δ and *asp1*^{D333A} displayed almost similar values which were in accordance to state that 1,5-IP_8 generated by Asp1 kinase domain is essential to activate *gsf2* promoter. This data suggests the loss of Asp1 kinase activity decreases the activity of the *gsf2* promoter.

Both the reporter assays showed that Asp1 generated 1,5-IP_8 are required for the activity of *the gsf2* promoter, thereby regulating the expression of *gsf2* an adhesin essential for the dimorphic switch and invasive growth.

3.4 Asp1 interacts with four proteins in a yeast two-hybrid screen

Asp1 was suggested to exist as a dimer, as *S. cerevisiae* orthologue Vip1 was reported to bind to other Vip1 molecules (Feoktistova et al., 1999, Krogan et al., 2004). Thus in a yeast two-hybrid analysis, the interaction of Asp1 with itself was tested. Previous studies of Asp1 dimerization analysis by co-immunoprecipitation using a diploid strain expressing *asp1-pk- gfp* and *asp1-HA* fusion proteins did not reveal interaction (unpublished data by Pöhlmann J).

3.4.1 Asp1 does not interact with Asp1$^{1-364}$ and Asp1$^{365-920}$ domain

For further understanding interactions of the Asp1 domains, *asp1*$^{1-364}$ and *asp1*$^{365-920}$ domains were expressed as individual molecules and tested whether these can interact with each another or with itself. To answer this *asp1*$^{1-364}$ and *asp1*$^{365-920}$ are cloned to activation and the binding domain of yeast two-hybrid vectors and expressed in reporter strain.

Asp1 did not interact with itself as identified before by Pöhlmann J (unpublished data). The Asp1$^{1-364}$ domain did not interact either to itself or to the Asp1. No interaction was identified between Asp1$^{1-364}$ and Asp1$^{365-920}$. The Asp1$^{365-920}$ did not interact with Asp1, Asp1$^{1-364}$ and with itself Figure 25. These proteins were expressed as seen a western blot (data not shown).

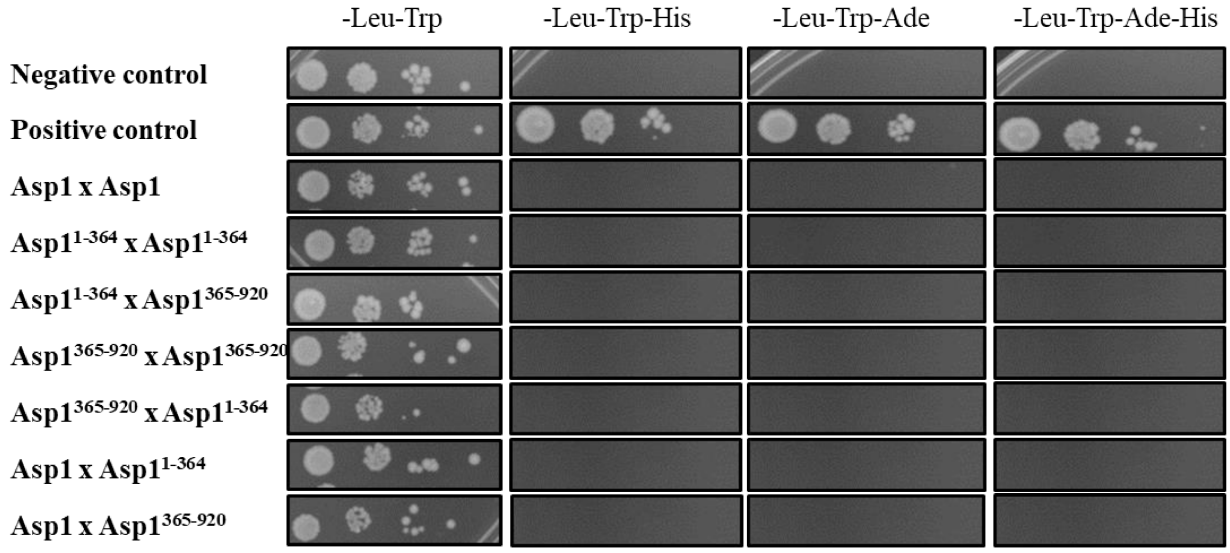

Figure 25: Asp1 does not interact with itself in a yeast two-hybrid assay. Asp1, Asp1$^{1\text{-}364,}$ and Asp1$^{365\text{-}920}$ do not interact with itself and also with Asp1$^{1\text{-}364}$ and Asp1$^{365\text{-}920}$ analyzed via yeast two-hybrid. Yeast two-hybrid vectors were cloned with *asp1*$^{+}$ and *asp1*$^{1\text{-}364}$ and *asp1*$^{365\text{-}920}$. Thus constructed vectors were transformed into *S. cerevisiae* reporter strain. If there is an interaction the reporter genes can be expressed. Here the reporter genes are Histidine and Adenine. As seen the positive controls can grow on all selective plates and the others interactions are similar to negative control depicting that there is no interaction between any of these Asp1 variants.

3.4.2 Yeast two-hybrid screen identified four potential interactors

To identify further interactions a genome-wide screen was performed by Dr.Visnja Jakopec using full-length Asp1 as bait. Four potential interactors were identified. None of the identified proteins had been previously studied. Table no 4 shows the list of the interactors and their systemic ID's and their predicted function. The predicted function was derived from the Pombase database.

Gene	Predicted function	Homologous Protein in *S. cerevisiae*
SPAC1071.05	Histidine protein methyltransferase	Hpm1
SPCC584.01c	Sulfite reductase NADPH flavo protein subunit	Met10
SPBC725.03	Pyridoxamine 5'- phosphate oxidase	YGR017W
SPCC4B3.05c	Uroporphyrinogen decarboxylase Hem12	Hem12

Table 4: Asp1 interactors identified via yeast two-hybrid screen

Homologous proteins for the identified potential interactors where found in *S. cerevisiae* implying a conservation of these proteins. The potential functions of the identified proteins in yeast are described below.

In this part of the chapter the identified interactors were analyzed for two different roles:

i) If the identified proteins interact with Asp1 via the kinase domain or the pyrophosphatase domain
ii) Role of the interactors in invasive growth

3.4.3 SPAC1071.05: histidine protein methyltransferase

The biological role of this protein is not characterized but inferred as ribosome methyltransferase that is involved in ribosome assembly (Hpm1). Hpm1 the homolog of SPAC1071.05 (Hpm1) in *S. cerevisiae* encodes a protein, AdoMet-dependent methyltransferase that is involved in a novel 3-methylhistidine modification of ribosomal protein Rpl3p (Webb et al., 2010). Hpm1 gene deletion in *S. cerevisiae* resulted in abnormal interactions between Rpl3 (Ribosomal 60S subunit protein) and the 25S ribosomal RNA (Webb et al., 2010). The Asp1 interacted with Hpm1 identified by a yeast two-hybrid screen and it was further identified that N-terminal of Hpm1 (amino acids from 1-291) are essential for binding to Asp1 and $Asp1^{1-364}$. C-terminal of Hpm1 was unable to interact with Asp1 and $Asp1^{1-364}$.

Hpm1 interacts with Asp1 analyzed via yeast two-hybrid screen. Does this interaction occur through one specific domain or does it need the whole Asp1 protein? To answer this $Asp1^{1-364}$ and $Asp1^{365-920}$ domains that were previously cloned into yeast two-hybrid vectors were used. This analysis revealed a unique interaction between Asp1 and Hpm1 through $Asp1^{1-364}$ domain only (Figure 26, marked in the red box). No interaction was observed with the $Asp1^{365-920}$domain (Figure 26). The interaction was observed very weak as colonies were only formed on plates with low stringency (-leu-trp-his). On other plates, a weak interaction was observed as very tiny colonies were seen.

To elucidate the role of Hpm1 in invasive growth gene $hpm1^{+}$ was deleted. The *hpm1*Δ strain was analyzed for its ability to form invasive colonies. The constructed strain was verified using colony PCR (Materials and methods, section 2.26).To analyze the role of Hpm1 in relationship to Asp1 and invasive growth double mutants were constructed either

with *asp1*^{D333A} or *asp1*^{H397A} variant strains. The constructed strains were analyzed for the invasive growth ability.

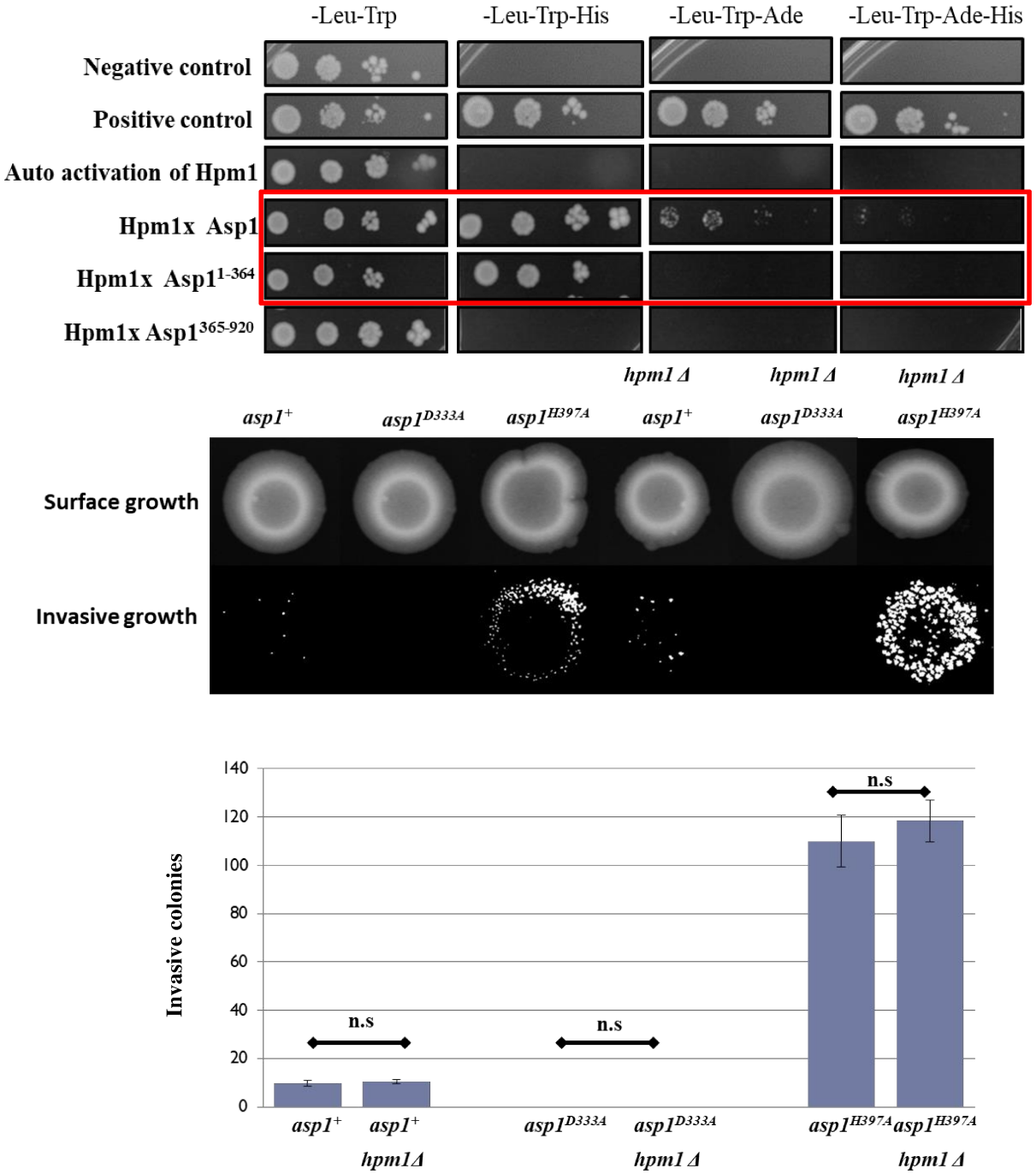

Figure 26: Interaction of Hpm1 to Asp1 via the N-terminal domain A) Asp1 interaction with Hpm1 through its N-terminal Kinase domain. The *asp1*$^{+}$ and *hpm1*$^{+}$ expression plasmids were transformed into reporter yeast strain supplied with the kit (Clontech). The patch test also includes both positive and negative controls for the interactions. The *hpm1*$^{+}$ plasmid was also analyzed for the auto activation of the reporter genes. The patch test revealed the unique interaction of Hpm1 to Asp1 through its N-terminal Kinase domain (marked in the red box).

B) The *hpm1*Δ strain exhibited a very slight increase in the number of invasively growing colonies which is not significant.

The double mutant *hpm1*Δ*/asp1*^{D333A} strain and *hpm1*Δ*asp1*^{H397A} strain did not exhibit any significant differences to *asp1*^{D333A} strain and *asp1*^{H397A} strain alone. Each experiment was performed at least with 4 different cultures in duplicates. Student t-test: n.s not significant t-test. The absence of *hpm1*$^{+}$ resulted in no significant difference in the increase in the number of invasive growing colonies compared to the wild-type strain (Figure 26B). In combination along with the Asp1 variants, no difference was observed. The *hpm1*Δ/*asp1*^{D333A} strain did not exhibit any invasive colonies as seen in *asp1*^{D333A} strain alone. The *hpm1*Δ/*asp1*^{H397A} strain exhibited an equal number of invasive colonies as seen for the *asp1*^{H397A} strain alone. This implies Hpm1 has no significant role as a regulator for Asp1 dependent invasive growth.

3.4.4 Met10 interacts with Asp1 and *met10Δ* strain displayed increased invasive growth

The *met10* gene product was also identified as an interactor in the Asp1 screen. *met10*$^{+}$ encodes a 111.3 kDa protein with a predicted function as sulfite reductase NADPH flavor protein subunit (Met10) (Pombase). Met10 a homolog of SPCC584.01c in *S. cerevisiae* encodes a subunit alpha of assimilatory sulfite reductase involved in methionine and cysteine synthesis (Masselot M and De Robichon-Szulmajster H, 1975, Hansen J, et al., 1994). This data gives us evidence that Met10 could be involved in the dimorphic switch process and could be a crosstalk with Asp1.

Met10 interacted with Asp1 analyzed via yeast two-hybrid screen (Figure 27). Does this interaction occur through one specific domain or does it need the whole Asp1? This analysis revealed a unique interaction between Asp1 and Met10 through Asp1$^{365\text{-}920}$ domain only (Figure 27). No interaction was observed through the expression of the Asp1$^{1\text{-}364}$ domain (Figure 27).

To elucidate the role of Met10 in invasive growth the gene encoding Met10 was deleted and constructed strain was verified using colony PCR (Materials and methods, section 2.26). The *met10Δ* strain constructed can grow as wild-type in full media but when minimal media was used no growth was observed. The growth behavior of *S. pombe met10Δ* strain was similar to *S. cerevisiae MET10* deletion strain and requires cysteine and methionine in the media for growth (Marina Pascual et al., 2018). To analyze the role of

Met10 in correlation to Asp1, double mutants were constructed with *asp1*^{D333A} and *asp1*^{H397A}variants. The constructed strains were analyzed for the invasive growing ability.

The *met10*Δ strain had more invasively growing colonies compared to the wild-type strain. The *met10*Δ strain exhibited approximately 120 invasively growing colonies whereas, wild-type strain only displayed approximately 10 invasively growing colonies. This difference in the number of invasive colonies is significantly high and up to 10 folds higher (Fig 27B). The strain *met10*Δ/*asp1*^{D333A} did not exhibit any invasively growing colonies. In the strain *met10*Δ/*asp1*^{H397A}, approximately 500 invasively growing was observed. In *asp1*^{H397A} strain, approximately 200 invasively growing colonies were observed. An additive effect was observed in the combination of *asp1*^{H397A} and *met10*Δ. But the invasive colony size seems to be much smaller in *met10*Δ than the *asp1*^{H397A} strain alone.

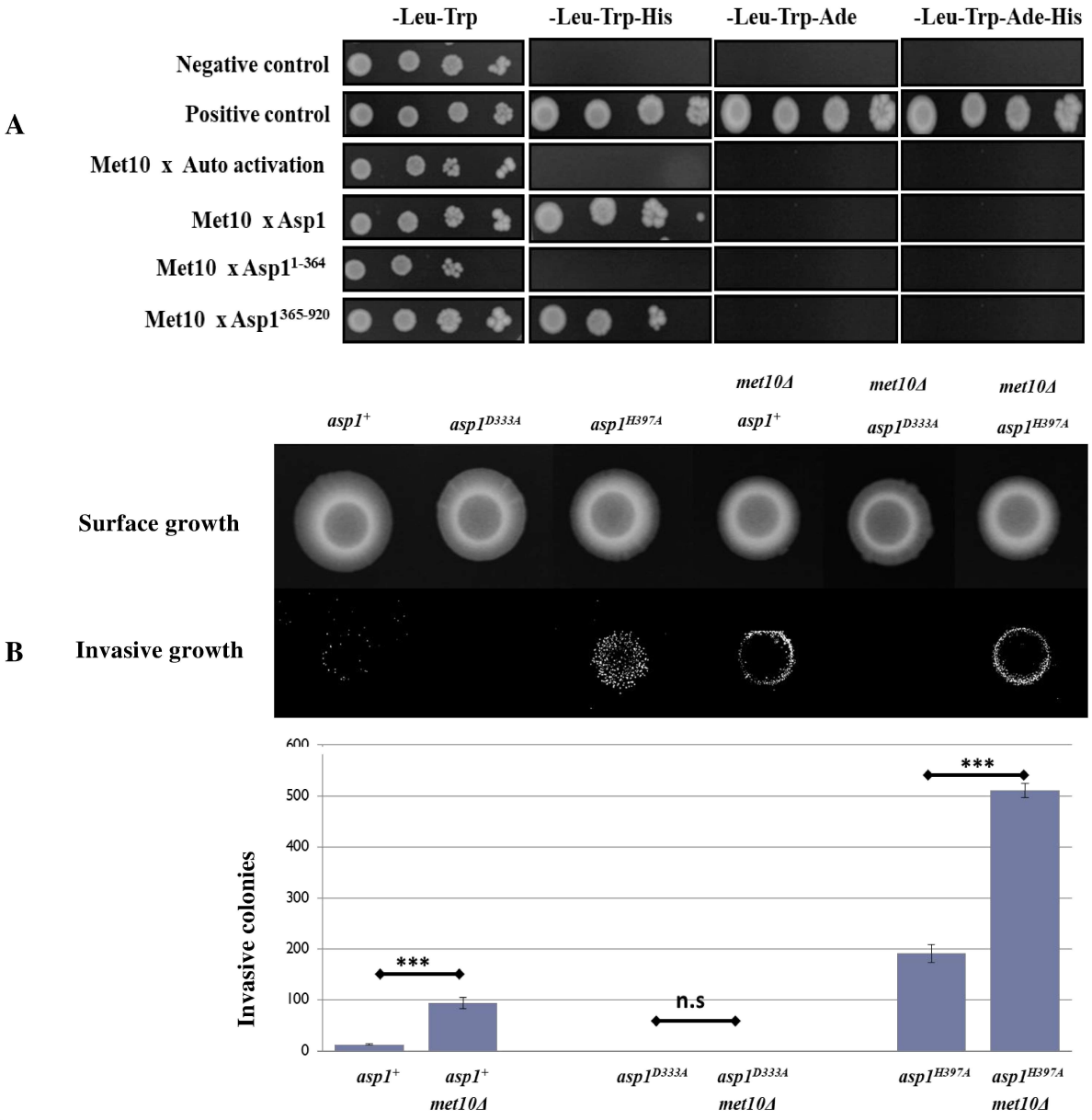

Figure 27: Asp1 interaction with Met10 through its C-terminal pyrophosphatase domain. A) *asp1*$^{+}$ and *met10*$^{+}$ two-hybrid plasmids were transformed into reporter yeast strain supplied with the kit (Clontech). The patch test also includes both positive and negative controls for the interactions. The *met10*$^{+}$ plasmid was also analyzed for the auto activation of the reporter genes. The patch test revealed the unique interaction of Met10 to Asp1 through its C-terminal pyrophosphatase domain (marked in red box). B) The *met10*Δ strain exhibited a significant increase in the number of invasively growing colonies compared to the wild-type strain but the colonies appear very small compared to the colonies of *asp1*$^{+}$ and *asp1*^{H397A} strains. The double mutant strain *met10*Δ/*asp1*^{D333A} did not exhibit any invasively growing colonies similar to *asp1*^{D333A} strain. The *met10*Δ/*asp1*^{H397A} strain exhibited a significant increase in the total number of invasively growing compared to *asp1*^{H397A} strain and appeared to be an additive effect. Each experiment was performed at least with 4 different cultures in duplicates. Student t-test: ***P < 0.0005, t-test.

3.4.5 Absence of Asp1 generated 1,5-IP$_8$ increase the heat tolerance

Endogenous *asp1*$^{1\text{-}364}$ is possibly localized to the mitochondria (Marina Pascual Ortiz unpublished data). Increased number of invasively growing colonies was observed for the *asp1*$^{1\text{-}364}$*-gfp* strain compared to the wild-type *asp1*$^{+}$ strain (Figure 28). The numbers of invasively growing colonies exhibited by *asp1*$^{1\text{-}364}$*-gfp* strain are higher than number of observed for the *asp1*^{H397A} strain (Figure28). Approximately 200 invasive colonies were observed in the *asp1*^{H397A} strain whereas; *asp1*$^{1\text{-}364}$ strain exhibited approximately 550 invasively growing colonies (Figure 28A). Subcellular localization of Met10-GFP was shown to be colocalized with mitochondria. Asp1 interacts with Met10 and therefore Asp1 is associated with a protein that co-localizes with mitochondria (Marina Pascual et al., 2018).

This above data implies Asp1 could localize and might exert its function in close proximity with mitochondria or by interfering with the function of mitochondria. In *S. cerevisiae* cAMP pathway regulates FLO11 an adhesin required for the morphogenesis and adhesion. Anu Aun et al., 2013 has shown that dysfunctional mitochondria in *rho* mutants (dysfunctional mitochondrial genome) can retain the complete functionality of the MAP Kinase pathway but cAMP-PKA was downregulated. This down-regulated cAMP-PKA pathway thereby decreased the ability of the *rho* mutants to perform the morphogenetic switch. Now the question arose was if Asp1 generated 1,5-IP$_8$ can regulate the cAMP-PKA pathway and thereby affecting the ability to switch to other morphogenetic forms. It was shown that *S. pombe* dimorphic switch require functional cAMP-PKA pathway (Pöhlmann et al., 2010).

In *S. cerevisiae,* cAMP-PKA pathway suppresses stress tolerance (Shin et al.,. 1987; Thevelein and de Winde 1999, Hlavatá et al., 2003). To analyze the stress tolerance of *rho*

mutants Anu Aun et al., 2013 exposed *S. cerevisiae* to extreme heat stress at 52°C for a period of 4-12 min and analyzed physiological reporters of the cAMP-PKA pathway, such as heat resistance. If cells are able to tolerate extreme temperatures it implies mitochondria are not functional as heat shock proteins are not expressed and vice versa. The heat-shock tolerance of *rho*$^{-}$ mutants was increased compared to the respective *rho*$^{+}$ strains corresponding to the downregulated of cAMP-PKA pathway.

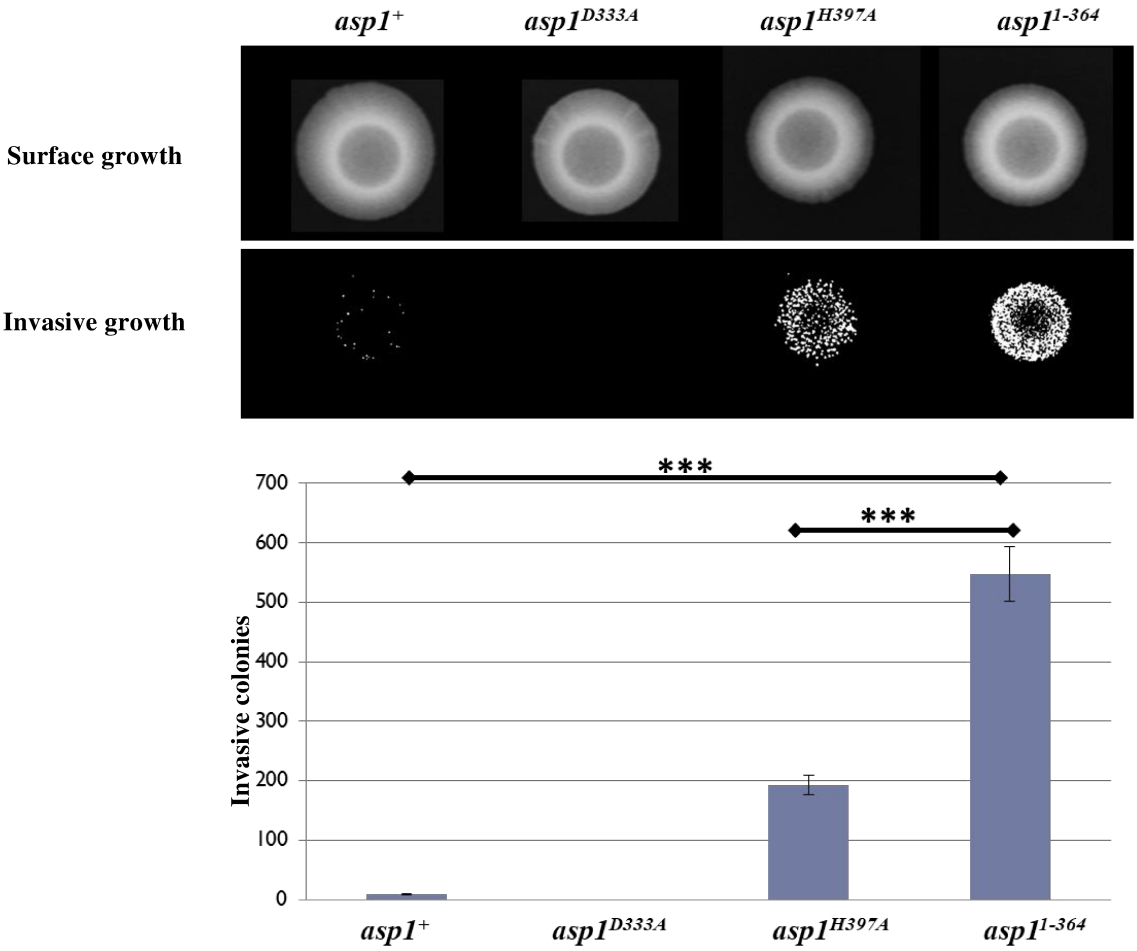

Figure 28: Invasive growth analysis of endogenously expressing *asp1*$^{1-364}$ strain. The strains were grown in full media for a period of 21 days and washed off. The *asp1*$^{1-364}$ strain displayed a higher number of invasively growing colonies compared to the wild-type strain. The *asp1*$^{1-364}$ displayed ≈450 invasively growing colonies per cell patch whereas, *asp1*^{H397A} strain displayed ≈200. Student t-test: ***P<0.005

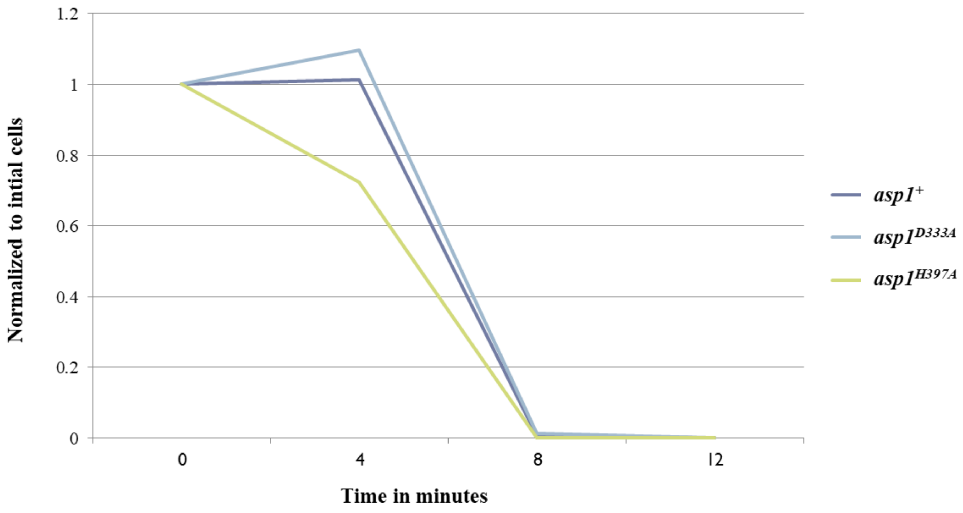

Figure 29: Heat shock tolerance of Asp1 strains. The Asp1 strains were subjected to heat shock at 52°C for the time period indicated. The total number of cells able to form colonies was counted. The colony forming units were normalized to the number of colonies forming units before heat shock.

The experimental set up used by Anu Aun et al., 2013 was used for analyzing the mitochondrial functionality by exposing the exponentially grown cells to high temperature at 52°C. The Asp1 variants were grown overnight in YE5S and diluted to a concentration of 1000 cells per ml. Cells were exposed to 52°C for 4, 8 and 12 minutes and then plated. After the incubation of 5 days at 30°C, the total colony forming units were counted. The number of colony forming units after the heat shock compared to the number of colony forming units in the untreated sample gives the viability ratio (Hlavatá et al., 2003, (Figure 29).

The *asp1*^{H397A} variant strain displayed the steepest decrease (20%) in the number of colonies formed after an incubation time of four minutes compared to the cells that were not treated at 52°C. The *asp1*$^{+}$ and *asp1*^{D333A} strains were able to tolerate heat even after 4 minutes of exposure to 52°C. After 8 minutes of incubation at 52°C, none of the strains were able to form a significant number of colonies other than in *asp1*^{D333A} strain (Figure 29). The *asp1*^{D333A} strain even after incubation for a period of 12 minutes they were able to make few colonies per plate (approximately 3-4) (Figure 29). This implies *asp1*^{D333A} strain has more endurance to heat suggesting, decrease in cAMP-PKA kinase pathway and consequently reduced expression of heat shock proteins by mitochondria.

3.4.6 SPBC725.03 pyridoxamine 5'- phosphate oxidase

The third interactor of Asp1 was SPBC725.03 which has a predicted function as a pyridoxamine 5'- phosphate oxidase. SPBC725.03 has a homolog in *S. cerevisiae* YGR017W. The homolog in *S. cerevisiae* was not characterized. Huh WK, et al., (2003) revealed that it was localized to both nucleus and cytoplasm. Anne-Claude Gavin et al., 2006 has shown TAP tag of Vip1 an ortholog of Asp1 was co-purified with *S. cerevisiae* YGR017W.

SPBC725.03 interacts with Asp1 analyzed via yeast two-hybrid system. Does this interaction occurs through one specific domain or does it need the whole Asp1? To answer, the strategy was adopted as for the previous potential interactors. This analysis revealed a unique interaction between Asp1 and SPBC725.03 through $Asp1^{365-920}$ domain only (Figure 30A). No interaction was observed through the expression of the $Asp1^{1-364}$ domain (Figure 30A).

To elucidate the role of SPBC725.03 in invasive growth the gene encoding SPBC725.03 was deleted. The constructed strain was verified using colony PCR (Materials and methods, section 2.26). SPBC725.03Δ strain was further analyzed for its ability to grow invasively. To analyze SPBC725.03 in relationship to Asp1 double mutants were constructed either with $asp1^{D333A}$ or $asp1^{H397A}$ variant strains. The constructed strains were analyzed for the invasive growth ability.

Deletion of SPBC725.03 resulted in no significant difference in the number of invasive growing colonies compared to the wild-type strain. In combination along with the Asp1 variants, no difference was observed. This implies SPBC725.03 has no significant role as a regulator in invasive growth (Figure 30B).

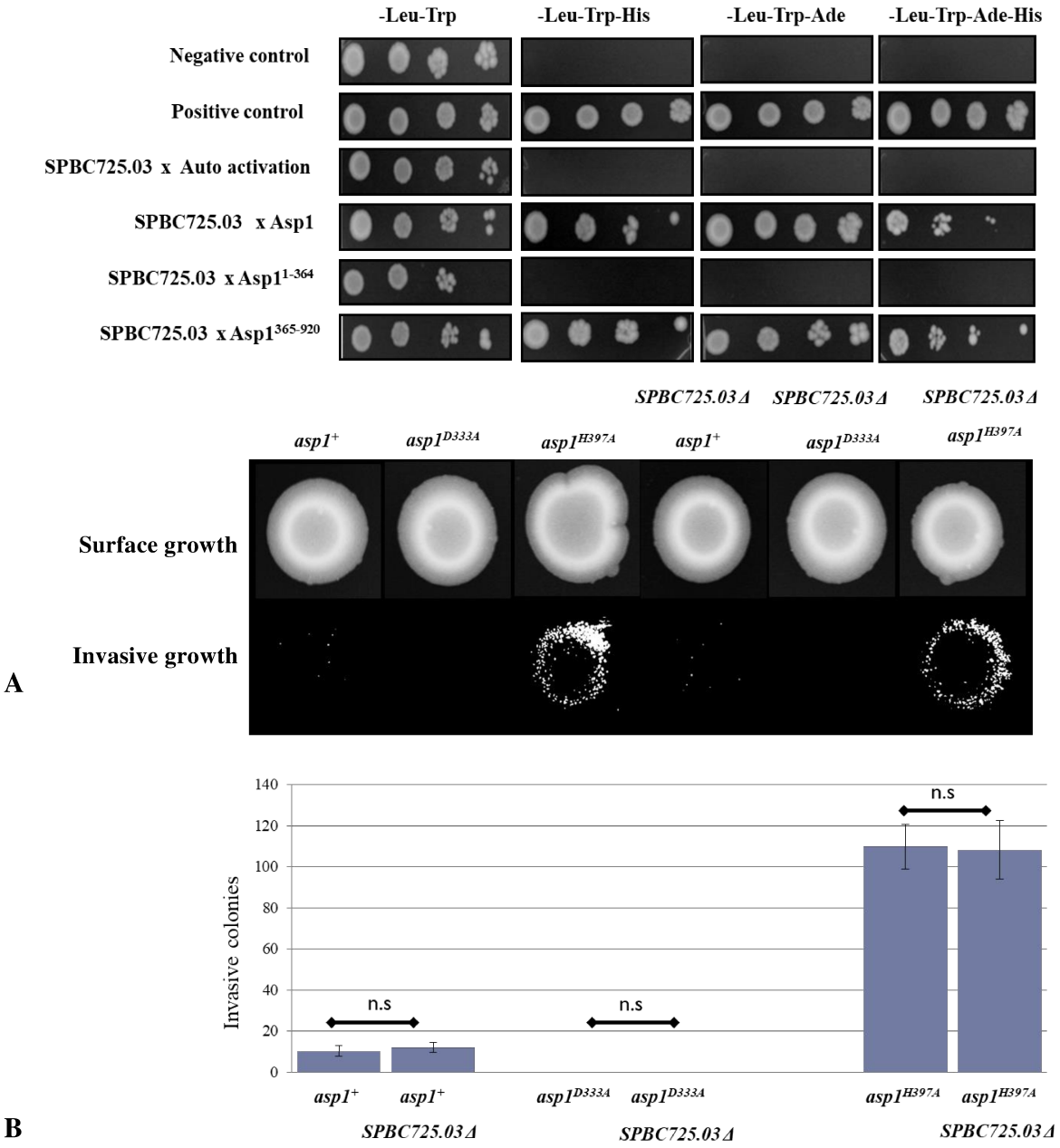

Figure 30: Asp1 interaction with SPBC725.03 through its N-terminal Kinase domain. A) *asp1*$^{+}$ and SPBC725.03 expression yeast two-hybrid plasmids were transformed into reporter yeast strain supplied with the kit (Clontech). The patch test also includes both positive and negative controls for the interactions. The SPBC725.03 plasmid was also analyzed for the auto activation of the reporter genes. The patch test revealed the unique interaction of SPBC725.03 to Asp1 through its N-terminal kinase domain. B) SPBC725.03Δ strain exhibited no increase in the number of invasively growing colonies. Double mutants strain SPBC725.03Δ/*asp1*^{D333A} and SPBC725.03 Δ/*asp1*^{H397A} strains did not exhibit any significant differences between ***asp1***^{D333A} and ***asp1***^{H397A} strains respectively. Each experiment was performed at least with 4 different cultures in duplicates. Student t-test: n.s: not significant.

3.4.7 SPCC4B3.05c uroporphyrinogen decarboxylase (Hem12)

The fourth interactor of Asp1 is Hem12 which has a predicted function as an uroporphyrinogen decarboxylase. Hem12 has a homolog is *S. cerevisiae* Hem12 which catalyzes the fifth step in the heme biosynthetic pathway (Diflumeri C et al., 1993).

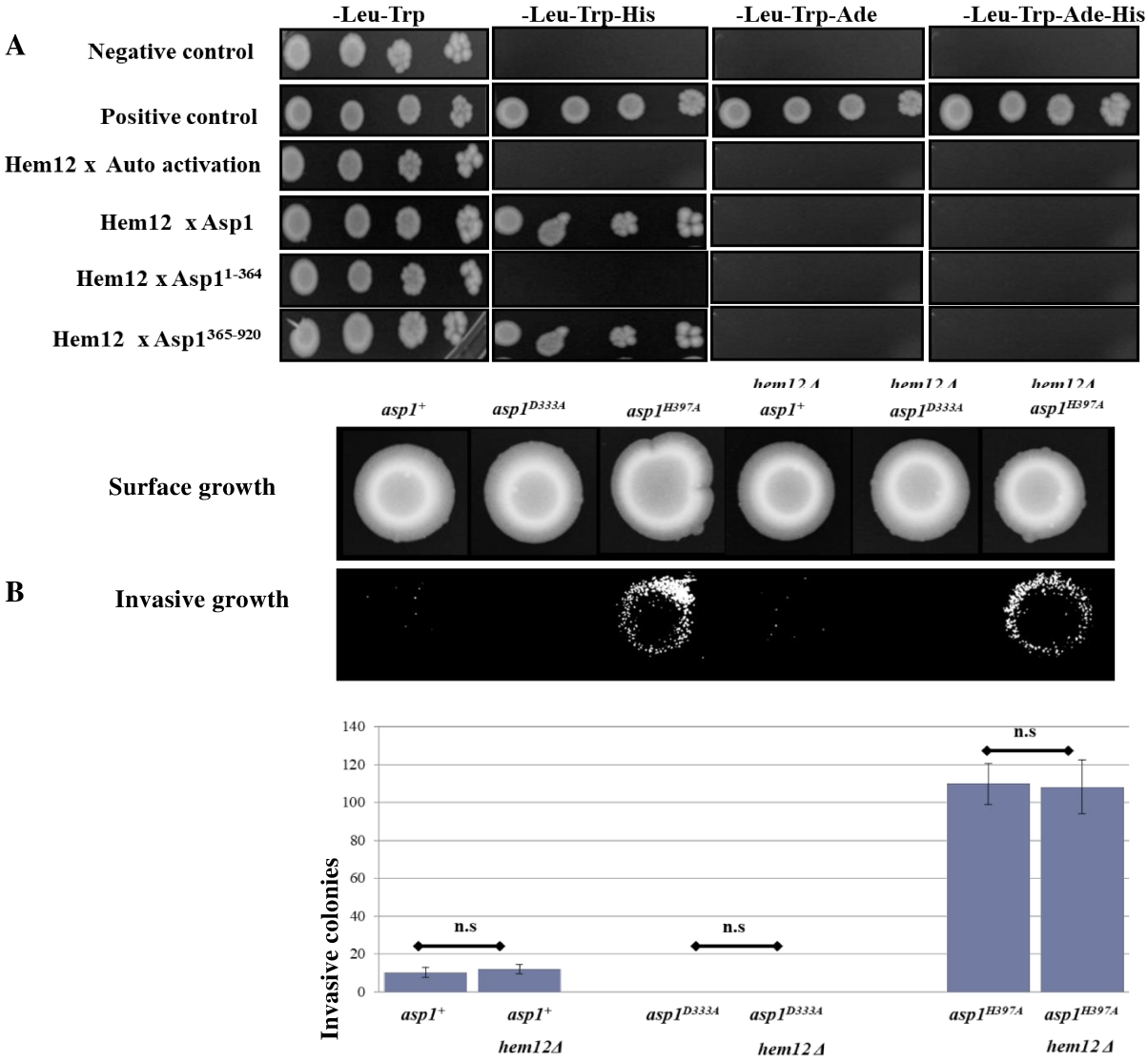

Figure 31: Asp1 interacts with Hem12 through its N-terminal Kinase domain. A) Asp1 and Hem12 yeast two-hybrid plasmids were transformed into reporter yeast strain supplied with the kit (Clontech). The patch test also includes both positive and negative controls for the interactions. The Hem12 was also analyzed for the auto activation of the reporter genes. The patch test revealed the unique interaction of Hem12 to Asp1 through its C- terminal pyrophosphatase domain. B) The *hem12*Δ strain exhibited invasively growing colonies but no significant difference to the *asp1*$^{+}$. Double mutants strain *hem12*Δ/*asp1*^{D333A} *hem12*Δ/*asp1*^{H397A} strain did not exhibit any significant differences in *asp1*^{D333A} and *asp1*^{H397A} strains respectively. Each experiment was performed at least with 4 different cultures in duplicates. Student t-test: n.s: not significant.

Analyzes to identify with which domain of Asp1, Hem12 binds was performed. This revealed a positive interaction between Asp1-pyrophosphatase domain and Hem12. To elucidate the role of Hem12 in invasive growth in *S. pombe* gene deletions were performed. The constructed strain was verified using colony PCR (Materials and methods, section 2.26). The *hem12*Δ strain was analyzed for its ability to grow invasively together with the double mutant with $asp1^{D333A}$ or $asp1^{H397A}$variant strains. The constructed strains were analyzed for the invasive growth ability.

The absence of $hem12^{+}$ gene resulted in no significant difference in the total number of invasive growing colonies compared to the wild-type strain (Figure 31). Both wild-type and *hem12*Δ strains displayed almost similar number of invasively growing colonies. In the double mutant strain *hem12*Δ/$asp1^{D333A}$ no invasively growing colonies were observed. In the double mutant strain *hem12*Δ/$asp1^{H397A}$ invasively growing colonies were observed with no significant differences to the $asp1^{H397A}$ strain (Figure 31B).

4. Discussion

This current work demonstrated that the kinase activity of the *S. pombe* Vip1 family member Asp1 protein, which generates specific 1,5-IP_8 is essential for the dimorphic switch. The morphogenetic switch occurs in response to the environmental signals like low temperatures, toxic substances, and nutrient limitation. In the current study, it was shown that nutrient limitation triggered the dimorphic switch but combination of nutrient limitation and additional stress such as cold stress and toxic stress enhanced the invasiveness. The Asp1 mediated dimorphic switch requires an external signal as a trigger to regulate the adhesin genes expression. Deletion of the dominant adhesin gene $gsf2^+$ can completely abolish the Asp1 mediated dimorphic switch. It was also demonstrated that Asp1 generated 1,5-IP_8 levels influence the expression levels of $gsf2^+$.

4.1 Inositol pyrophosphates are essential for morphogenesis

In *S. pombe,* it was shown that Vip1 family member generated inositol pyrophosphates are essential for the switch in response to nutrient limitations and later in 2018 these inositol pyrophosphates was identified to be 1,5-IP_8 (Pöhlmann et al., 2010, Marina Pascual et al., 2018). In *C. neoformans,* it was demonstrated that another class of inositol pyrophosphates (5-IP_7) are essential for the metabolic response to a nutrient-poor environment which is essential for the pathogenicity of the fungus. The absence of 5-IP_7 made *C. neoformans* susceptible to grow in low carbon source and also its inability to benefit from other carbon sources (Lev S et at., 2015). Similarly, parasitic kinetoplastid *Trypanosoma brucei* possesses one enzyme, an *IP6K (TbIP6K),* that synthesizes inositol pyrophosphates and this protein can complement *S. cerevisiae* ortholog. Conditional knockdown of *TbIP6K* revealed that this kinase is essential for the bloodstream form of this parasite and also has displayed reduced infectivity (Cordeiro et al., 2017*)*. From the above studies, it can be shown that inositol pyrophosphates are essential for survival under nutrient-poor environment and morphogenesis similar to *S. pombe*. Still, research has to be done to elucidate the role of inositol pyrophosphates induced pathogenicity in other pathogenic fungi.

4.2 Environmental stress govern the dimorphic switch in fungi

The primary external stimulus required for *S. pombe* to switch to pseudo-hyphal invasive growth is lack of nitrogen source, with the presence of good carbon source (Amoah-Buahin et al., 2005). This can be elucidated as the invasive colonies were observed after prolonged incubation i.e. for at least two weeks and inoculated with high cell numbers. Addition of nitrogen-containing supplements lysine, adenine and uracil inhibited the

formation of invasive colonies (Martin Prevorovsky et al., 2008). The absence of other nutrient sources like phosphorous, sulfur was unable to trigger this morphogenetic switch (Amoah Buahin et al., 2005). It was shown in a starch degrading *S. cerevisiae* strain plated on starch-containing medium, developed pseudo hyphae and grew invasively into the starch-containing medium (Melane A. Vivier et al., 1997). Mata and Bähler in 2006 has shown that nitrogen starvation has led to large changes in the gene expression pattern of almost all genes where majority of the genes induced and repressed belong to the core environmental stress response. In another recent study conducted by Irma M. H. van Rijswijck et al., 2015 has demonstrated three yeast species *S. cerevisiae, Pichia fabianii and Pichia kudriavzevii* displayed changes in the morphogenetic form in response to nutrient limitation. So in fungi, morphogenetic switch in response to starvation leads to upregulation of stress response gene and activate genes responsible for the switch. Morphogenetic switching is a widely spread phenomenon in fungi, and this was identified in *S. pombe* and it requires Asp1 generated 1,5-IP_8.

The absence of 1,5-IP_8 generated by Asp1 in *asp1*Δ and *asp1*^{D333A} strains abolished the invasive growth in standard cultivation media. However, the addition of excess iron (a toxic substance) to the standard media at lower concentrations than 2.5mM $FeCl_3$ was unable to trigger the switch; whereas, a further increase in the iron concentration at 5mM $FeCl_3$ is lethal (excess iron in the media is toxic). So excess iron can be tolerated at particular concentrations (3-4mM $FeCl_3$) and this can trigger the invasive colonies in the absence of Asp1. Previously, Martin Prevorovsky et al., 2008 has shown in *S. pombe* that presence of excess iron in the media can trigger the formation of invasive colonies but, in the current study it was analyzed in correlation to Asp1. The morphogenetic switch in response to excess iron was also reported in *S. cerevisiae (*Martin Prevorovsky et al., 2008). The dimorphic switch can occur as excess iron in the media can influence other metal ions (redox-active copper and redox-inactive zinc). Depletion of the iron in the media by ferrozine chelator and deletion of iron uptake regulator (*feb1*Δ) has resulted in the reduction of invasive colonies implying that iron is required for the switch at sub-toxic concentrations (Pelletier et al., 2002). Sub-toxic concentrations of iron increased the intracellular iron concentrations and upregulated the genes involved in iron uptake (Martin Prevorovsky et al., 2008). In support of this, a study in *C. albicans* has shown a sub-toxic concentration of H_2O_2 induced pseudo-hyphae. However, H_2O_2 is an oxidative stress molecule, and displayed differential gene expression at a sub-toxic and toxic concentration of H_2O_2 (Srinivasa K et al., 2012). In

another study, *S. cerevisiae* was demonstrated that the deletion of FOL1 a gene essential for the folinic acid synthesis strain was grown on folinic acid supplements resulted in the generation of filamentous pseudo hyphae. This folinic acid supplements media was known to suppress invasive growth but filamentous pseudo hyphae appeared. This suggests alternative signaling pathways could activate the adhesin genes (Güldener U et al., 2004).

Pathogenic fungi have been shown that exposure to toxic levels of micronutrients like iron, zinc, and copper display differential gene expression (Elizabeth RBallou et al., 2016). One hypothesis could be that the cells someway can direct multiple stresses into a single response and the fungi opt whether to switch to the branching state or not. Transcriptional programming in *S. pombe* known as the core environmental stress response (CESR) is common to all, or most, stresses (Chen D et al., 2003). This system can directly and indirectly calculate the total stress of the cell and responds by activation of genes essential for the switch. In *S. cerevisiae,* it was shown that core environmental stress response pathway is triggered in response to severe environmental challenges (Kron SJ et al., 1994). In mammalian PPIP5K1, the enzyme responsible for 1,5-IP_8 synthesis from 5-IP_7, upregulated fourfold upon osmotic stress (Pesesse X, et al., 2004). In *A. thaliana,* it was demonstrated that the stress hormone abscisic acid led to a twofold increase in the levels of both 1-IP_7 and 1,5-IP_8, and plant defense hormone jasmonate led to a twofold increase in 1,5-IP_8 but did not affect 1-IP_7 levels (Laha D et al., 2015). However, the increases in the intracellular inositol pyrophosphate levels were not measured under stress conditions such as reduced temperature or toxic amounts of iron.

In *S. pombe* addition of an inhibitor of calcineurin, Cyclosporine A impairs normal cell division. It displayed impaired cell division at 22°C but not at higher temperatures. This implies that cold stress at 22°C in the combination of another stress (cyclosporine in that study) pushed *S. pombe* into branching state (Yoshida T et al., 1994). Briefly, it can be stated as; in *S. pombe* an external stress by an excess toxic substance at sub-toxic concentrations, and the nutrient limitation can trigger the morphogenetic switch via an alternative pathway in the absence of 1,5-IP_8.

In the current study, it was observed that *S. pombe* can switch to pseudo hyphae at all the temperatures tested in response to nutrient limitation. But increase in the number of invasive colonies at lower temperatures was observed. In the current study, combination of two environmental stimuli i.e. nutrient limitation together with lower temperatures can

further increase the ability to switch. In contrast, to it, pathogenic fungi are capable of performing the switch at higher but only at specific temperatures (37°C). Activation of several genes involved in transcription and translation was observed in *S. cerevisiae* with a decrease in temperature. It was shown in *S. cerevisiae* that, exposure to low temperatures shields the cells against freeze injury and occurs through cold-induced accumulation of trehalose, glycerol and heat-shock proteins. It is also to be noted that in *S. cerevisiae* at lower temperatures was shown to change the membrane fluidity, and it is the primary signal triggering the cold shock response. In *S. pombe*, the stress associated protein kinase (SAPK) is involved in the cold-shock response (Soto et al., 2002). But in a publication from our lab, it was demonstrated that deletion of Sty1, a component of the stress response pathway did not abolish the switch at 30°C. This could be explained that at lower temperatures a different stress response pathway could be activated. In a study by Evgeny Kanshin et al., 2015, the phosphoproteome dynamics under heat shock and cold stress have shown that several kinases and phosphatases were dynamically affected by changes in temperatures. It also displayed altered kinetic profiles and distinct temporal regulatory activities such as stress response, cell cycle and nutrient sensing. The above study by Evgeny Kanshin et al., 2015, also pointed out that cell responds to low temperatures appears to be complex and encompasses a network of proteins interactions involved in cytokinesis, cell morphogenesis, and cycle regulation, and the changes in phosphorylation are consistent with the response to temperature stress. This group also demonstrated in *S. cerevisiae*, that few phosphorylation sites in a key catalytic subunit of Cdc28, a key regulator of morphogenesis and mitosis are probably involved in stress response by triggering the signaling pathway. In *S. cerevisiae,* it was shown that the transcriptional response to lower temperatures involves both general stress and cold-specific mechanisms. It is highly probable that multiple other physiological alterations in cellular processes regulated at the translational and/or posttranslational level contribute to survival and growth in cold conditions (Babette Schade et al., 2002). It can be stated that in model fungi *S. cerevisiae* and *S. pombe* at lower temperature induce differential gene expression.

The Asp1 sub-cellular localization studies revealed an interesting aspect. Feoktistova et al., 1999 has stated that Asp1 did not display any specific sub-cellular localization and is equally distributed all over the cell. However, observations from our lab have demonstrated a temperature dependent localization (unpublished data). When the cells were grown at lower temperatures (25°C and 20°C) Asp1 localized predominantly in the nucleus compared to cells grown at 30°C where, Asp1 is distributed all over the cell. In another study from our lab, it

was identified that the temperature dependent localization of Asp1 is dependent on other proteins (Hpm1) (Patrick Fischbach master thesis, 2016). This shows Asp1 is dependent on other proteins for their temperature dependent localization. It can be hypothesized that core environmental stress genes like adhesins can be upregulated at lower temperatures and Asp1 might be a key player in the regulation of this gene expression, as the absence of Asp1 did not lead to invasive colonies at any temperatures tested.

Data from the current study revealed that in *S. pombe* the external stimuli such as temperature and nutrient limitation can trigger the formation of invasive colonies whereas, addition of two different stimuli (temperature and nutrient limitation in the current study) enhances the ability to switch into pseudohyphal form only in the presence of 1,5-IP_8 generated by Asp1. In accordance to this, it was also shown in *S. cerevisiae* that multiple and simultaneous environmental changes like temperature together with hypo-osmotic shock resulted in the gene expression that is almost the sum of gene expression in response to individual transitions (Gasch et al., 2000). Inositol pyrophosphates were shown to serve as sensors that sense the environment clues and regulate several cellular processes as a response to these external clues. These external clues trigger changes in the intracellular inositol pyrophosphate concentrations and thereby varied levels affect various cellular responses (Lee et al., 2007, Luo et al., 2003, Pesesse et al., 2004).

4.3 Intracellular inositol pyrophosphate levels regulate the frequency of invasive colonies

A recent study from our lab has shown *in vivo* that the wild-type $asp1^{+}$ strain has both IP_7 and IP_8 (Marina Pascual, 2018). The $asp1^{H397A}$ strain generated twice the amount of 1,5-IP_8 than a wild-type strain (Marina Pascal et al., 2018). Physiological levels of 1,5-IP_8 (wildtype Asp1) are sufficient to initiate the invasive growing colonies whereas, an increase in the amount of 1,5-IP_8 ($Asp1^{H397A}$) two-fold increased approximately 25 fold higher number of invasive colonies.

Inositol pyrophosphates were demonstrated to serve as transmitters for environmental clues as the levels of these molecules are upregulated in order to counteract hyperosmotic stress in *Dictyostelium* (Pesesse et al., 2004, Luo et al., 2003). Similarly, inositol pyrophosphates generated by the Vip1 were shown to serve as secondary signaling molecules and activate the environmental stress response genes to counteract osmotic, heat and

oxidative stress in *S. cerevisiae* (Jeremy Worley et al., 2013). This infers that inositol pyrophosphates can act as signaling molecules.

Exogenous expression *asp1*$^{+}$ and *asp1*$^{1\text{-}364}$ plasmids revealed that both *asp1*$^{+}$ and *asp*$^{1\text{-}364}$ can increase the number of invasive colonies compared to the control. However, exogenous expression of *asp1*$^{+}$ led to an enormous increase in the number of invasive colonies when expressed via *nmt1*$^{+}$ promoter (750 invasive colonies). Exogenous expression of *asp1*$^{+}$ *by nmt41* (180 invasive colonies) and *nmt81* promoter (80 invasive colonies) displayed a decrease in the number of invasive colonies. As a surprise expression of *asp1*$^{1\text{-}364}$ via *nmt1*$^{+}$ promoter displayed the lowest number of invasive colonies (70 invasive colonies) compared to *nmt41* (180 invasive colonies) and *nmt81* (145 invasive colonies). The expression of *asp1*$^{1\text{-}364}$ via *nmt1* promoter displayed 4 fold higher protein levels compared to *asp1*$^{+}$ expressed by *the nmt1*$^{+}$ promoter.

In vivo analysis of wild-type strain displayed two classes of inositol pyrophosphates (IP_7 and 1,5-IP_8). Whereas, expression of *asp1*$^{1\text{-}364}$ by *the nmt1*$^{+}$ promoter in a wild-type strain led to increase in IP_7 and 1,5-IP_8 inositol pyrophosphates classes and generated higher amounts of IP_7 (3.5 fold than IP_6) compared to 1,5-IP_8 (2 fold than IP_6). *S. pombe* cells overexpressing Asp1 kinase domain probably generated a mixture of 1-IP_7 and 5-IP_7 because, the peak in the elution profile slightly shifted to the left (anticipated when 1-IP_7 is present instead of 5-IP_7) in comparison to the control implying that IP_7 generated are probably 1-IP_7 (unpublished data from Marina Pascual Ortiz Ph.D. thesis). Thus Asp1 might utilize IP_6 as a substrate and generate 1-IP_7 under non-physiological circumstances such as over-expression of Asp1-kinase domain. Unveiling the crystal structure of PPIP5K2 kinase domain, displayed that the active site of the enzyme would permit IP_6 and 5-IP_7 only. As these molecules pocesses the phosphates and di-phosphates configuration/orientation required around the inositol ring (Wang H et al., 2011). The presence of lysine at position 214 (K224 in *S. pombe* Asp1) interacts with the 5 β phosphate of 5-IP_7 which exemplifies the preference for 5-IP_7 over IP_6 as a substrate (Wang et al., 2011). However IP_6 pyrophosphorylation can occur when the natural substrate becomes inadequate, and still has to be shown *in vivo*.

The *in vivo* data from the wild-type strain and *asp1*^{H397A} strain illustrates that specific 1,5-IP_8 inositol pyrophosphates are required for the invasive growth. Assuming that overexpression of *asp1*$^{1\text{-}364}$ led to generation of 1-IP_7 that is usually not present in the cell and the presence of these molecules negatively influences the formation of invasive colonies.

Reduced expression levels of the *asp1*$^{1\text{-}364}$ domain with the *nmt41* promoter resulted in increase in the number of invasive colonies. This can be due to reduction in 1-IP_7 that negatively influences the invasive colonies. Further reduction in the expression level of *asp1*$^{1\text{-}364}$ domain by *nmt81* promoter led to decrease in the number of invasive colonies compared to *nmt41* promoter and this can be due to reduced 1,5-IP_8 levels. But the numbers of invasive colonies were still higher than *nmt1*$^{+}$ promoter and this can be due to reduced 1-IP_7 levels.

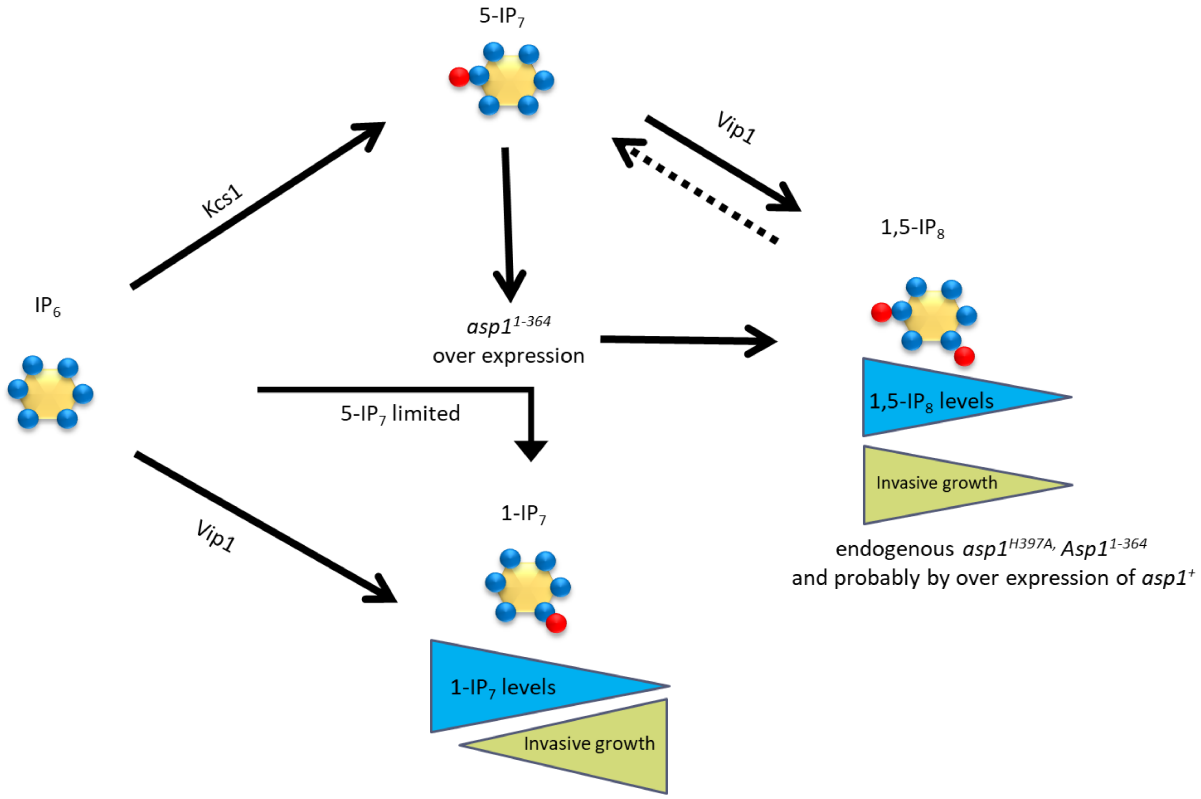

Figure 32: Model for the regulatory mechanism of Asp1 kinase generated different classes of inositol pyrophosphates. Overexpression of Asp1-kinase domain led to increase in IP_7 levels and 1,5-IP_8. It is likely that these IP_7 are specifically 1-IP_7 as a shift in the peak was detected in HPLC elution profile. When Asp1-Kinase domain is overexpressed, all of the substrate is converted to 1,5-IP_8. The Asp1 kinase is present in excess and uses IP_6 as a substrate and generates 1-IP_7. Thus generated 1-IP_7 appears to be the negative regulator of invasive growth.

At present no *in vivo* data of the amount of inositol pyrophosphates present in the cell of *asp1*$^{+}$ overexpressing in wild type is available. So it can be assumed that by over expressing *asp1*$^{+}$, 1,5-IP_8 levels in the cells are at higher levels and the amount of 1-IP_7 is less or completely absent. In addition to it, an increased level of pyrophosphatase domain is present in the cell by over expression of wild-type *asp1*$^{+}$. This domain can dephosphorylate

the 1,5-IP_8 back to 5-IP_7 and this enzymatic activity does not make the substrate a limiting factor for the kinase domain. Whereas, in the *asp1*$^{1-364}$ over expression situation this dynamic activity of kinase and pyrophosphatase domains is absent and makes the substrate a limiting factor. The aforementioned explanations make it understand why overexpression of *asp1*$^{+}$ led to higher invasive colonies compared to the *asp1*$^{1-364}$ overexpression.

In accordance with the hypothesis that 1-IP_7 acts as a negative regulator, *asp1*$^{1-364}$ expression at physiological levels via endogenous promoter led to increase in the number of invasive colonies compared to wildtype and *asp1*^{H397A} strains. At physiological levels, no abundant Asp1-kinase is present and furthermore no pyrophosphatase domain. So assuming that the 1-IP_7 level is low or completely absent an increase in 1,5-IP_8 levels, an increase in the number of invasive colonies was observed. Interestingly, the negative regulation of 1-IP_7 on other analysis such as resistance to microtubule depolymerizing drugs (TBZ), temperature sensitivity was not identified it seems to be specific for the invasive growth. In the other analysis overexpression of *asp1*$^{1-364}$ always displayed enhanced phenotypes compared to *asp1*$^{+}$ and *asp1*$^{365-920}$ (Topolski et al., 2015, Pöhlmann et al., 2014, unpublished data from the lab).

Invasive growth analysis was done with *asp1* variants at the first and second conserved motifs where 1,5-IP_8 levels were determined during the course of work to support the *in vivo* measurements. The conserved amino acids of the histidine acid phosphatase motif **RH**XX**R** are essential for Asp1 pyrophosphatase activity and exchange of these amino acids to alanine lost the pyrophosphatase activity. Expression of Asp1^{R400A} and Asp1^{H397A} are lethal at high levels but displayed invasive colonies when expressed at lower levels (Marina Pascual et al., 2018). Exchange of conserved amino acids at second motif displayed invasive colonies in accordance to the *in vitro* and *in vivo* data. *In vivo* analysis of endogenous *asp1*^{I808D} strain displayed increased 1,5-IP_8 levels and invasive growth assays by overexpressing the *asp1*^{I808D} displayed an increased number of invasive colonies. Similarly, *asp1*^{H807A} overexpression displayed a higher number of invasive colonies and *in vitro* analysis has shown loss of the pyrophosphatase activity. Hence, it can be stated as the loss of pyrophosphatase activity increases the cellular amount of 1,5-IP_8 and thereby increases the number of invasive colonies

4.4 Gsf2 adhesin promoter activity is regulated by the intracellular levels of 1,5-IP_8

Invasive growth analysis of few of the adhesin gene deletions done in the current study identified Gsf2 as the sole and essential adhesin required for the Asp1 mediated dimorphic switch. These adhesins in *S. pombe* are imagined to contain galactosyl groups as presence of galactose inhibits flocculation in liquid media and cells adhere to the agar which is a polymer of galactose (Tanaka et al., 1999, Kim et al., 2001). The adhesin genes are not constitutively expressed instead; adhesions are under the secure transcriptional control of several interacting regulatory pathways and are induced by environmental factors (Verstrepen et al., 2003, Sampermans et al., 2005). In *S. cerevisiae,* activation of FLO11 an adhesin, upon nitrogen starvation, is an example (Kron, 1997; Gagiano et al ., 2002).

In the *in silico* studies conducted by Linder T et al., 2008 identified that all adhesin including Mam3 and Map4 contain a conserved tandem repeats that were found in Als family of adhesins found in *C. albicans* agglutinins. Mam3 and Map4 are cell type-specific agglutinins and the initial adhesins to be identified in *S. pombe.* Deletion of the gene encoding $mam3^{+}$ did not abolish invasive growth in $asp1^{H397A}$ strain and this may due to Mam3 being a cell surface agglutinin is essential for mating rather than stress response.

All the other adhesin gene deletion strains analyzed in the current study did not exhibit any differences in the number of invasive colonies other than the *gsf2*Δ strain in comparison to $asp1^{H397A}$ strain. Similarly in another study done by Eun-Joo Gina Kwon et al., 2012 have identified other adhesin gene deletion strains exhibited flocs in the flocculation inducing medium other than *gsf2*Δ strain. This indicates Gsf2 as a dominant adhesin. Whereas, over-expression of two different adhesins in the wild-type strain exhibited increased flocculation and had an additive effect (Eun-Joo Gina Kwon et al., 2012).

Interestingly only $gsf2^{+}$ does not contain any similarities to the other cell surface glycoproteins found in *S. pombe*. In contrast, all the other adhesins were found to contain amino acid sequence homology to other members of fungal adhesins (Linder T et al., 2008). In support of this in another study by strain Matsuzawa T et al., 2011, Pfl1/Gsf2 was identified as a dominant adhesin required for the dimorphic switch and it was found to be upregulated by *S. cerevisiae* transcription factor FLO8. Gsf2 contains a signal sequence at the N-terminal and a GPI anchor at the C-terminal. It also consists of 16 putative N-glycosylation sites together with two tandem repeats of 78 and 44 amino acids. From the above studies, it

can be proposed that *S. pombe* encodes several adhesins but, among them Gsf2 is essential for the formation of flocculation and invasive colonies which is dependent on galactose.

Several positive and negative transcription factors that regulate adhesins genes were identified in *S. pombe*. Deletion of positive regulator genes did not display any invasive colonies whereas, deletion of the negative regulator genes led to increased invasive colonies in an *asp1*^{H397A} strain background. In another study by Martin Prevorovsky et al., 2008, it was shown that Cbf11 and Cbf12 transcription factors play an antagonistic role in adhesion and invasion. Imbalance of any of these transcription factors can lead to cellular defects and cell density dependent. This result demonstrates that 1,5-IP_8 is essential for the switch, together with the positive regulators to display invasive colonies.

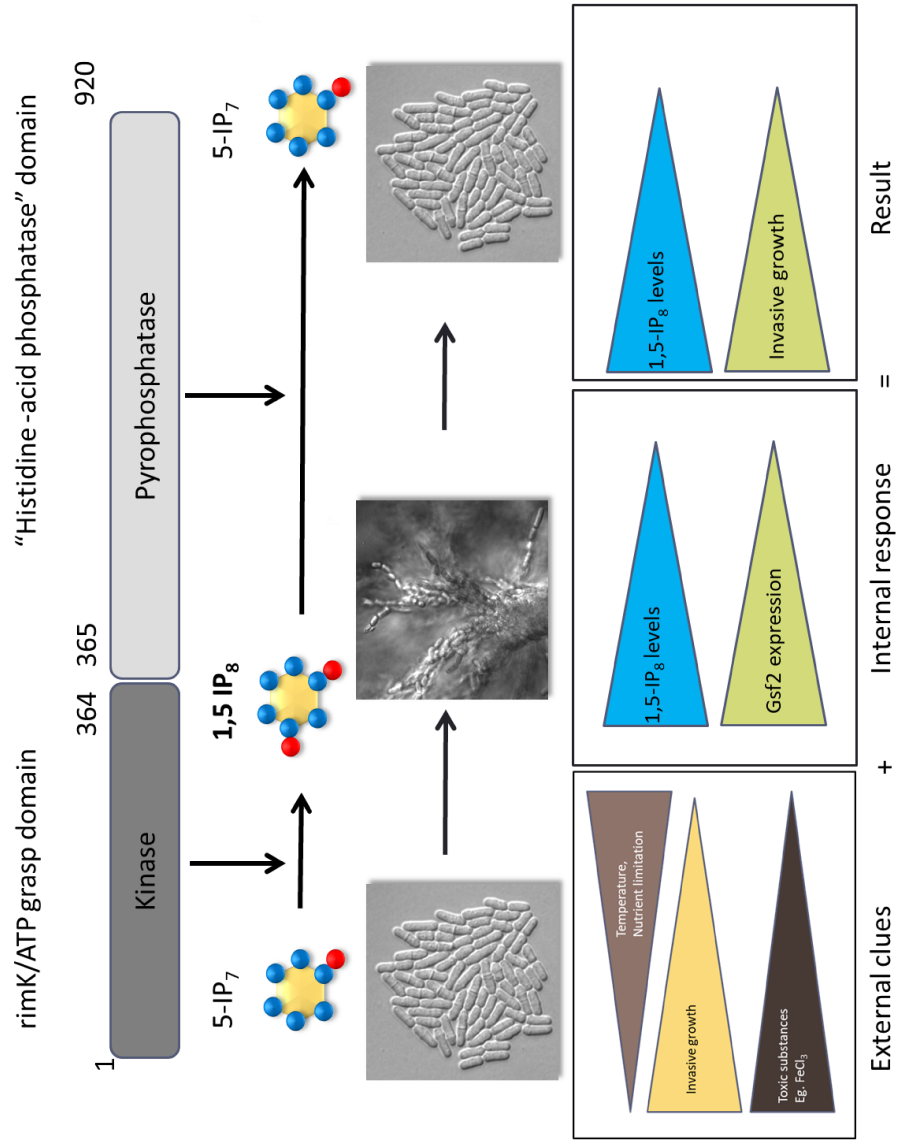

Figure 33: Model for the mechanism of Asp1 induced invasive colonies. Asp1 generates 1,5- IP_8. External stimuli induced the expression of adhesin Gsf2 that is essential for the

formation of invasive colonies. Increase in the intracellular levels of 1,5-IP_8 increase the expression of Gsf2 and form invasive colonies.

Modulation of *gsf2*$^+$ levels by using the *nmt41* promoter resulted in the increase in the number of invasive colonies but, only in the presence of 1,5-IP_8. It was demonstrated that expression of Gsf2 by *nmt41* promoter resulted in higher expression levels than the wild-type strain (Matsuzawa T et al., 2011). Expression levels of Gsf2 were higher than the wild-type strain and an increase in invasive colonies was observed. Whereas, no invasive growing colonies were observed in the *asp1*^{D333A} strain although Gsf2 levels were increased. This implies 1,5-IP_8 is essential and Gsf2 adhesin is the possible target for the formation of invasive colonies. Still, studies have to be performed to elucidate the mechanisms that govern this regulation.

Formation of pseudohyphal colonies was not observed only due to the expression of adhesin molecules but also due to septation and cytokinesis defects (Sipiczki M et al., 1993). It could also be speculated that Asp1 is essential for other cellular function such as cell separation and cytokinesis. Taken together all the data it can be noted that inositol pyrophosphates play a crucial role in several cellular processes.

Interestingly the presence of 1,5-IP_8 also led to increased activity of the *gsf2*$^+$ promoter analyzed via both GFP and luciferase reporter genes. The activity of the *gsf2*$^+$ promoter is regulated by several transcriptional factors like Mbx2, Rfl1, Cbf11, Cbf12, and Prz1. One possibility is transcriptional activators that induce *gsf2*$^+$ promoter could be modulated or altered by 1,5-IP_8. As seen in the transcriptional regulatory network that regulates adhesins in *S. pombe*, several players could act in synchronously or alternatively to express adhesin genes. The activity level of *the gsf2*$^+$ promoter in the absence of multiple transcription regulators still has to be studied. Of all the transcriptional regulators, Rfl1 seems to be a major negative regulator of adhesins because, *rfl1*Δ strain formed a large number of invasive colonies and also flocculated immediately without any stimuli. In the current study, the *rfl1*Δ strain formed massive invasive colonies but only in the presence of 1,5-IP_8. Whereas, in the absence of Asp1, the *rfl1*Δ strain, lost the ability to form such a high number of invasive colonies. The current study is the first to show the *asp1*Δ strain displayed invasive colonies in standard experimental conditions. The result from this study implies that a secondary pathway might exist apart from Asp1 that regulates invasive growth in *S. pombe*.

1-IP_7 generated by the kinase activity of IPPK, PPIP5K1, and PPIP5K2 are essential for induction, phosphorylation and activation of IRF3, a transcription factor for interferon via RIG-I signaling pathway in human cell lines (Pulloor N.K et al., 2014). Inositol pyrophosphate (IP_7) synthesized by inositol hexakisphosphate kinase 1 (IP6K1) in mice was shown to be associated with chromatin and it was shown that these molecules interact with Jumonji domain containing 2C (JMJD2C) a histone lysine demethylase and thus control the number of crucial epigenetic modifications important for gene expression. Furthermore, this study demonstrated that the pyrophosphate signaling influences nuclear function by regulating histone modifications (Adam Burtona et al., 2013). Studies in *S. cerevisiae* has also elucidated that IP_7 regulate transcription to regulate major metabolic pathways Pho80–Pho85 cyclin-cyclin-dependent kinase complex. From the above studies, it can be speculated that inositol pyrophosphates can activate genes through an unidentified signaling pathway in *S. pombe.*

4.5 The *hpm1Δ, hem12Δ* strains displayed no difference in number of invasive colonies

The first physical interactor of Asp1 to be identified was Hpm1. Analysis, via subcloning of different Asp1-variants and Hpm1variants, could show a small interaction region on Asp1. It was identified by localization studies that both Asp1 and Hpm1 needed for localization dependency. Hpm1 also exhibited negative influence on the mitotic spindle, and an increase in the microtubule dynamics was identified. The *hpm1*Δ strain was found to be TBZ resistance and an influence on the microtubules was found. Hpm1 was also identified to have an antagonistic function compared to Asp1 and plays as a negative regulator of the microtubule cytoskeleton (Unpublished data from Fischbach P). Hpm1 in *S. cerevisiae* displayed negative genetic interaction with proteins involved in septum assembly that are required for cytokinesis (Costanzo M, et al. 2010). Hpm1 exhibited genetic interaction with Ira2 a GTPase-activating protein, required for reducing cAMP levels under nutrient limiting conditions (Costanzo M, et al. 2010). These data implied Hpm1 as a potential candidate involved in invasive growth. In contrast deletion of this gene encoding Hpm1 did not show any significant difference in the ability to form invasive colonies. The other physical interactors with Asp1 are SPBC725.03 and Hem12 and strains with gene deletions, encoding these proteins did not show any significant differences in the ability to form invasive colonies. Further studies have to be done to elucidate the role and function of these proteins together with Asp1.

4.5.1 The *met10*Δ strain exhibited an increased in the number of invasive colonies

The *met10*Δ strain displayed increase number of invasively growing colonies. Met10 interacts with the pyrophosphatase domain and inhibited the pyrophosphatase activity in an *in vitro* assay (Marina Pascual et al., 2018). So theoretically in *met10*Δ strain, the amount of IP_8 has to be lower than the wild-type strain. However, the IP_8 levels in the *met10*Δ strain were not affected *in vivo* (Marina Pascual et al., 2018). It can be due to, Asp1 is ubiquitously distributed all over the cell and loss of Met10 can only influence the local concentrations of 1,5-IP_8 but do not interrupt the overall concentration in the cell. Absence of inositol pyrophosphates disrupts the mitochondrial distribution in *S. pombe* and Met10 was shown to be associated with mitochondria (Marina Pascual et al., 2018). However, it was shown that the $Asp1^{1-364}$-GFP is associated with mitochondria and full-length Asp1 is ubiquitously distributed all over the cell (Unpublished results from Marina Pascual Ortiz Ph.D. thesis). So in the absence of pyrophosphatase domain with which Met10 interact, $Asp1^{1-364}$ can localize to mitochondria. Studies still have to elucidate the mitochondrial distribution in the absence of Met10. Absence of active kinase domain of Asp1 inhibited the Asp1 mediated dimorphic switch in the *met10*Δ strain. It can be hypothesized based on the aforementioned data that Met10 might negatively influence the invasive growth and act upstream of Asp1, in the similar pathway that regulate invasive growth. Hence, the loss of Met10 enhanced the ability to grow more invasively.

The structural disruption of mitochondria due to the absence of inositol pyrophosphates might partially influence the functionality of the mitochondria. Mitochondrial activity was shown to be crucial for flocculation and invasive growth in *S. cerevisiae* (C.J. Strausset al., 2007, Rui Jin et al., 2008). It was also demonstrated by Iung AR et al., 1999 that abruption of the mitochondrial function changes the structure of cell wall by interrupting the interactions between adhesins and their substrates. As adhesion and invasion are both dependent on adhesin and substrate interactions it is highly possible that mitochondrial function can influence adhesion and invasive growth. But how the mitochondrial functions influence the *S. pombe* flocculation and invasive growth is still elusive. But, it has been shown that cAMP-PKA pathway is required for the dimorphic switch in *S. pombe* (Pöhlmann et al 2012 and Amoah-Buahin et al., 2005). Previous studies have revealed that cAMP-PKA pathway is modulated by mitochondria using *rho* mutants in *S.cerevisiae* (Shin et al. 1987, Thevelein and de Winde 1999, Hlavatá et al. 2003). To analyze the stress tolerance of *rho*

mutants Anu Aun et al., 2013 exposed *S. cerevisiae* to extreme heat stress at 52°C for a period of 4-12 min and analyzed physiological reporters of the cAMP-PKA pathway, such as heat resistance. If cells are able to tolerate extreme temperatures it implies mitochondria are not functional as heat shock proteins are not expressed and vice versa. Similarly, in the current study, it was shown that partially disrupted mitochondrial function in the $asp1^{D333A}$ strain displayed higher heat tolerance compared to wild-type and $asp1^{H397A}$ strains. This data gives us a clue that Asp1 together with Met10 could work in close proximity to mitochondria and potentially influence the proper functioning of the mitochondria and thereby, regulating other cellular processes downstream of the mitochondria such as morphogenesis.

5. References

References

Ahne F, Merlos-Lange AM, Lang BF, Wolf K. (1984). The mitochondrial genome of the fission yeast *Schizosaccharomyces pombe* : 5. Characterization of mitochondrial deletion mutants Curr Genet. 1984 Sep;8(7):517-24.

Aimanianda V, Bayry J, Bozza S, Kniemeyer O, Perruccio K, Elluru SR, Clavaud C, Paris S, Brakhage AA, Kaveri SV, Romani L, Latgé JP.(2009). Surface hydrophobins prevents immune recognition of airborne fungal spores. Nature 460: 1117–1121.

Albert C, Safrany ST, Bembenek ME, Reddy KM, Reddy K, Falck J, Brocker M, Shears SB, Mayr GW (1997) Biological variability in the structures of diphosphoinositol polyphosphates in *Dictyostelium discoideum* and mammalian cells. Biochem J 327(Pt 2): 553-560

Amoah-Buahin E, Bone N, Armstrong J (2005) Hyphal Growth in the Fission Yeast *Schizosaccharomyces pombe*. Eukaryot Cell 4(7): 1287-1297

Andrew H Limper, Antoine Adenis, Thuy Le, Thomas S Harrison. (2017). Fungal infections in HIV/AIDS Lancet Infect Dis 2017;17: e334–43

Alspaugh JA, Cavallo LM, Perfect JR, Heitman J. (2000). RAS1regulates filamentation, mating and growth at high temperature of *Cryptococcus neoformans*. Mol Microbiol 36:352–365.

Anu Aun, Tiina Tamm, and Juhan Sedman (2013). Dysfunctional Mitochondria Modulate cAMP-PKA Signaling and Filamentous and Invasive Growth of *Saccharomyces cerevisiae*. Genetics, Vol. 193, 467–481

Azevedo, C., Burton, A., Ruiz-Mateos, E., Marsh, M., and Saiardi, A. (2009). Inositol pyrophosphate mediated pyrophosphorylation of AP3B1 regulates HIV-1 Gag release. Proc Natl Acad Sci U S A 106, 21161-21166.

B. Maresca, A. M. Lambowitz, V. B. Kumar, G. A. Grant, G. S. Kobayashi, and G. Medof, (1981). "Role of cysteine in regulating morphogenesis and mitochondrial activity in the dimorphic fungus *Histoplasma capsulatum*," Proceeding of the National Academy of Sciences, USA, vol. 78, no. 7, pp. 4596–4600, 1981.

Babette Schade, Gregor Jansen, Malcolm Whiteway, Karl D. Entian,¶ and David Y. Thomas (2004). Cold Adaptation in Budding Yeast. Molecular Biology of the Cell. December 2004. Vol. 15, 5492–5502.

Bahler J, Nurse P (2001) Fission yeast Pom1p kinase activity is cell cycle regulated and essential for cellular symmetry during growth and division. Embo J 20(5): 1064-1073

Bahler J, Pringle J (1998) Pom1p, a fission yeast protein kinase that provides positional information for both polarized growth and cytokinesis. Genes and Development 12: 1356-1370

Bahn YS, Sundstrom P. (2001). CAP1, an adenylate cyclase associated protein gene, regulates bud-hypha transitions, filamentous growth, and cyclic AMP levels and is required for virulence of *Candida albicans*. J Bacteriol 183: 3211 3223.

Banuett F (1995) Genetics of *Ustilago maydis*, a fungal pathogen that induces tumors in maize. Annu Rev Genet 29: 179–208.

Barker CJ, Illies C, Gaboardi GC, Berggren PO. (2009). Inositol pyrophosphates: structure, enzymology and function. Cell Mol Life Sci. 2009 Dec;66(24):3851-71

Batanghari JW, Deepe GS Jr, Di Cera E, Goldman WE. (1998). *Histoplasma* acquisition of calcium and expression of CBP1 during intracellular parasitism. Mol Microbiol 27: 531–539.

Bayly, J.C., Douglas, L.M., Pretorius, I.S., Bauer, F.F., and Dranginis, A.M. (2005) Characteristics of Flo11-dependent flocculation in *Saccharomyces cerevisiae*. *FEMS Yeast Res* 5: 1151–1156.

Becker W, Joost HG (1999) Structural and functional characteristics of Dyrk, a novel subfamily of protein kinases with dual specificity. Prog Nucleic Acid Res Mol Biol 62: 1-17

Behrens R, Nurse P (2002) Roles of fission yeast tea1p in the localization of polarity factors and in organizing the microtubular cytoskeleton. J Cell Biol 157(5): 783-793.

Beinhauer, J.D., Hagan, I.M., Hegemann, J.H., and Fleig, U. (1997). Mal3, the fission yeast homologue of the human APC-interacting protein EB-1 is required for microtubule integrity and the maintenance of cell form. J Cell Biol 139, 717-728.

Bellocchio S, Montagnoli C, Bozza S, Gaziano R, Rossi G, Mambula SS, Vecchi A, Mantovani A, Levitz SM, Romani L. (2004) The contribution of the Toll-like/IL-1 receptor superfamily to innate and adaptive immunity to fungal pathogens *in vivo*. *J* Immunol 4;172:3059–69.

References

Bennett, M., Onnebo, S.M., Azevedo, C., and Saiardi, A. (2006). Inositol pyrophosphates: metabolism and signaling. Cell Mol Life Sci 63, 552-564.

BermanJ (2006) Morphogenesis and cell cycle progression in *Candida albicans*. Curr Opin Microbiol9(6): 595-601

Bhandari R, Chakraborty A, Snyder SH (2007a) Inositol pyrophosphate pyrotechnics. Cell Metab 5(5): 321-323

Bhandari R, Saiardi A, Ahmadibeni Y, Snowman AM, Resnick AC, Kristiansen TZ, Molina H, Pandey A, Werner JK, Jr., Juluri KR, Xu Y, Prestwich GD, Parang K, Snyder SH (2007b) Protein pyrophosphorylation by inositol pyrophosphates is a posttranslational event. Proc Natl Acad Sci U S A 104(39): 15305-15310

Bi E, Park HO. 2012. Cell polarization and cytokinesis in budding yeast. Genetics 191: 347–387.

Bignell EM.(2012). Conservation in *Aspergillus fumigatus* of pH-signaling seven transmembrane domain and arrest in proteins, and implications for drug discovery. Ann NY Acad Sci 1273: 35–43

Bony, M., Thines- Sempoux, D., Barre, P. and Blondin, B. (1997) Localization and cell surface anchoring of *the Saccharomyces cerevisiae* flocculation protein Flo1p. J Bacteriol 179, 4929–4936

Boyce KJ and Alex Andrianopoulos (2015). Fungal dimorphism: the switch from hyphae to yeast is a specialized morphogenetic adaptation allowing colonization of a host. FEMS Microbiology Reviews, fuv035, 39, 2015, 797–811

Boyce KJ, Chang H, D'Souza CA, Kronstad JW. 2005. An *Ustilago maydis* septin is required for filamentous growth in culture and for full symptom development on maize. Eukaryot Cell. 2005;4:2044–56.

Brand A, Gow NA (2009) Mechanisms of hypha orientation of fungi. Curr Opin Microbiol 12(4): 350- 35

Browning, H., Hayles, J., Mata, J., Aveline, L., Nurse, P., and McIntosh, J.R. (2000). Tea2p Is a Kinesin-like protein required to generate polarized growth in Fission Yeast. J Cell Biol 151, 15-28.

Brunner, D., and Nurse, P. (2000). CLIP170-like tip1p spatially organizes microtubular dynamics in fission yeast. Cell 102, 695-704.

Bryant DM, Mostov KE (2008). From cells to organs: building polarized tissue. Nat Rev Mol Cell Biol 9(11): 887-901

Burton A, Hu X, Saiardi A (2009) Are inositol pyrophosphates signalling molecules? *J Cell Physiol* 220(1): 8-15

Busch KE, Brunner D (2004). The microtubule plus end-tracking proteins mal3p and tip1p cooperate for cell-end targeting of interphase microtubules. Curr Biol 14(7): 548-559

Busch KE, Hayles J, Nurse P, Brunner D (2004) Tea2p kinesin is involved in spatial microtubule organization by transporting tip1p on microtubules. Dev Cell 6(6): 831-843

Busscher HJ, Rinastiti M, Siswomihardjo W, van der Mei HC. (2010). Biofilm formation on dental restorative and implant materials. J. Dent. Res. 89:657– 665.

Byrne, S. M., and C. S. Hoffman. (1993). Six *git* genes encode a glucose induced adenylate cyclase activation pathway in the fission yeast *Schizosaccharomyces pombe*. J. Cell Sci. 105:1095–1100.

C S Hoffman and F Winston(1991). Glucose repression of transcription of the *Schizosaccharomyces pombe* fbp1 gene occurs by a cAMP signaling pathway Genes & Dev. (1991) 5: 561-571

C.J. Strauss, P.W.J. van Wyk, E.J. Lodolo, P.J. Botes, C.H. Pohl, S. Nigam and J.L.F. Kock (2007) Mitochondrial Associated Yeast Flocculation – The Effect of Acetylsalicylic Acid. J. Inst. Brew. 113(1), 42–47, 2007

Castilla R, Passeron S, Cantore ML. (1998). N-acetyl-D-glucosamine induces germination in *Candida albicans* through a mechanism sensitive to inhibitors of cAMP dependent protein kinase. Cell Signal 10: 713–719

Cecilia Li1, Sophie Lev, Adolfo Saiardi, Desmarini, Tania C. Sorrell& Julianne T. Djordjevic (2016). Identification of a major IP5 kinase in *Cryptococcus neoformans* confirms that PP-IP5/IP7, not IP6, is essential for virulence. Scientific Reports 6:23927

Chakraborty A, Kim S, Snyder SH (2011) Inositol pyrophosphates as mammalian cell signals. Sci Signal. 2011 Aug 23; 4(188):re1.

References

Chakraborty A, Kim S, Snyder SH. (2011). Inositol pyrophosphates as mammalian cell signals. Sci Signal. 2011 Aug 23;4(188).

Chakraborty A, Koldobskiy MA, Bello NT, Maxwell M, Potter JJ, Juluri KR, Maag D, Kim S, Huang AS, Dailey MJ, Saleh M, Snowman AM, Moran TH, Mezey E, Snyder SH (2010) Inositol pyrophosphates inhibit Akt signalin, thereby regulating insulin sensitivity and weight gain. Cell. 2010 Dec 10;143(6):897-910

Chakraborty, A., Koldobskiy, M.A., Bello, N.T., Maxwell, M., Potter, J.J., Juluri, K.R., Maag, D., Kim, S., Huang, A.S., Dailey, M.J., *et al.* (2010). Inositol pyrophosphates inhibit Akt signaling, thereby regulating insulin sensitivity and weight gain. Cell *143*, 897-910.

Chang EC, Barr M, Wang Y, Jung V, Xu HP, Wigler MH. (1994). Cooperative interaction of S. pombe proteins requiredfor mating and morphogenesis. Cell 79: 131–141.

Chang F (2001) Establishment of a cellular axis in fission yeast. *Trends Genet* 17(5): 273-278

Chang F, Martin SG (2009) Shaping fission yeast with microtubules. Cold Spring Harb Perspect Biol 1(1): a001347

Chant J. (1999). Cell polarity in yeast. Annu Rev Cell Dev Biol 15: 365–391.

Chen D, Toone WM, Mata J, Lyne R, Burns G, Kivinen K, Brazma A, Jones N, Bahler J. Global transcriptional responses of fission yeast to environmental stress. Mol Biol Cell 2003; 14:214-29.

Choi JH, Williams J, Cho J, Falck JR, Shears SB (2007) Purification, sequencing, and molecular identification of a mammalian PP-InsP5 kinase that is activated when cells are exposed to hyperosmotic stress. J Biol Chem 282(42): 30763-30775

Christophe d'Enfert and Bernhard Hube (2007) Candida*:* Comparative and Functional Genomics.Book

Contag, C.H. (2006) Molecular imaging using visible light to reveal biological changes in the brain. Neuroimaging Clin N Am 16: 633-654, ix.

Cormack BP, Ghori N, Falkow S. (1999). An adhesin of the yeast pathogen *Candida glabrata* mediating adherence to human epithelial cells. Science 285, 578–582.

Costanzo M, Baryshnikova A, Bellay J, Kim Y, Spear ED, Sevier CS, Ding H, Koh JL, Toufighi K, Mostafavi S, Prinz J, St Onge RP, VanderSluis B, Makhnevych T, Vizeacoumar FJ, Alizadeh S, Bahr S, Brost RL, Chen Y, Cokol M, Deshpande R, Li Z, Lin ZY, Liang W, Marback M, Paw J, San Luis BJ, Shuteriqi E, Tong AH, van Dyk N, Wallace IM, Whitney JA, Weirauch MT, Zhong G, Zhu H, Houry WA, Brudno M, Ragibizadeh S, Papp B, Pal C, Roth FP, Giaever G, Nislow C, Troyanskaya OG, Bussey H, Bader GD, Gingras AC, Morris QD, Kim PM, Kaiser CA, Myers CL, Andrews BJ, Boone C (2010) The genetic landscape of a cell. Science 327(5964):425-31

Cottier F, Muhlschlegel FA. (2009). Sensing the environment: Response of *Candida albicans* to the X factor. FEMS Microbiol Lett 295: 1–9.

d'Enfert C, Hube B (2007) Introduction. In *Candida.* Comparative and functional genomics. d'Enfert Ch, Hube B, eds, pp 1–5. Caister Academic Press, Norfolk.

Davis D,Wilson RB, Mitchell AP. (2000). RIM101-dependent and -independent pathways govern pH responses in *Candida albicans*. Mol Cell Biol 20: 971–978.

de Groot PW1, Bader O, de Boer AD, Weig M, Chauhan N. *(2013).* Adhesins in human fungal pathogens: glue with plenty of stick. *Eukaryot Cell. 2013 Apr;12(4):470-81.*

Debabrata Laha, Philipp Johnen, Cristina Azevedo, Marek Dynowski, Michael Weiß, Samanta Capolicchio, Haibin Maof Tim Iven, Merel Steenbergen Marc Freyer, Philipp Gaugler, Marília K.F. de Campos, Ning Zheng, Ivo Feussner Henning J. Jessen, Saskia C.M. Van Wees, Adolfo Saiardi, and Gabriel Schaafa. (2015) VIH2 Regulates the Synthesis of Inositol Pyrophosphate InsP8 and Jasmonate-Dependent Defenses in *Arabidopsis.* Plant Cell. 2015 Apr; 27(4): 1082–1097.

Di Paolo G, De Camilli P (2006) Phosphoinositides in cell regulation and membrane dynamics. Nature 443(7112): 651-657

Diflumeri C, Larocque R, Keng T (1993) Molecular analysis of HEM6 (HEM12) in *Saccharomyces cerevisiae*, the gene for uroporphyrinogen decarboxylase. Yeast 9(6):613-23

Dodgson J, Anatole Chessel, Miki Yamamoto, Federico Vaggi, Susan Cox, Edward Rosten, David Albrecht, Marco Geymonat, Attila Csikasz-Nagy, Masamitsu Sato & Rafael E. Carazo-Salas (2013). Spatial segregation of polarity factors into distinct cortical clusters is required for cell polarity control. Nat Commun 4: 1834.

References

Dranginis, A.M., Rauceo JM, Coronado JE, Lipke PN.., (2007). A biochemical guide to yeast adhesins: glycoproteins for social and antisocial occasions. Micro biol. Mol. Biol. Rev. 71, 282–294

Draskovic, P., Saiardi, A., Bhandari, R., Burton, A., Ilc, G., Kovacevic, M., Snyder, S.H., and Podobnik, M. (2008). Inositol hexakisphosphate kinase products contain diphosphate and triphosphate groups. Chem Biol 15, 274-286.

Drummond DR, Cross RA (2000) Dynamics of interphase microtubules in *Schizosaccharomyces pombe*. Current Biology 10: 766-775

Drutz DJ, Frey CL (1985) Intracellular and extracellular defenses of human phagocytes against Blastomyces dermatitidis conidia and yeasts. J Lab Clin Med 1985, 105:737-750.

Dubois E, Scherens B, Vierendeels F, Ho MM, Messenguy F, Shears SB (2002) In *Saccharomyces cerevisiae*, the inositol polyphosphate kinase activity of Kcs1p is required for resistance to salt stress, cell wall integrity, and vacuolar morphogenesis. *J* Biol Chem 277(26): 23755-23763

Eckert SE, Sheth CC, Muhlschlegel FA (2007) Regulation of morphogenesis in *Candia* species. Caister Academic Press , March 2007

Elizabeth A. Steidle, Lucy S. Chong, Mingxuan Wu, Elliott Crooke, Dorothea Fiedler, Adam C. Resnick, and Ronda J. Rolfes (2016). Siw14 protein selectively cleaves the-phosphate from 5-diphosphoinositol pentakisphosphate (5PP-IP_5). J Biol Chem. 2016 Mar 25; 291(13): 6772–6783.

Eun-Joo Gina Kwon, Amy Laderoute, Kate Chatfield-Reed, Lianne Vachon, Jim Karagiannis, Gordon Chua (2012)Deciphering the Transcriptional-Regulatory Network of Flocculation in *Schizosaccharomyces pombe*. PLoS Genet. 2012 Dec; 8(12)

Europe-Finner, G.N., Gammon, B., and Newell, P.C. (1991). Accumulation of [3H]-inositol into inositol polyphosphates during development of *Dictyostelium.* Biochem Biophys Res Commun 181, 191-196.

Fan, F. & Wood, K.V. (2007). Bioluminescent assays for high-throughput screening. Assay Drug Dev Technol 5: 127-136.

Fantes PA, Hoffman CS, A Brief History of *Schizosaccharomyces pomb*e Research: A Perspective over the Past 70 Years Genetics. 2016 Jun; 203(2):621-9. Doi: 10.1534/genetics.116.189407.

Faty M, Fink M, Barral Y.(2002). Septins: a ring to part mother and daughter. Curr Genet. 2002;41:123–31.

Feierbach B, Chang F (2001) Roles of the fission yeast formin for3p in cell polarity, actin cable formation and symmetric cell division. Curr Biol 11(21): 1656-1665

Feierbach B, Verde F, Chang F (2004) Regulation of a formin complex by the microtubule plus end protein tea1p. J Cell Biol 165(5): 697-707

Feoktistova, A., McCollum, D., Ohi, R., and Gould, K.L. (1999). Identification and characterization of *Schizosaccharomyces pombe asp1(*$^{+}$*),* a gene that interacts with mutations in the Arp2/3 complex and actin. Genetics *152*, 895-908.

Finkel-Jimenez B, Wuthrich M, Klein BS. (2002). BAD1, an essential virulence factor of Blastomyces dermatitidis, suppresses host TNF-a production through TGF-b-dependent and -independent mechanisms. J Immunol 168: 5746 5755

Fischer R, Zekert N, Takeshita N (2008) Polarized growth in fungi--interplay between the cytoskeleton, positional markers and membrane domains. Mol Microbiol 68(4): 813-826

Freisinger T, Klunder B, Johnson J,Muller N, Pichler G, Beck G, Costanzo M, Boone C, Cerione RA, Frey E, et al. 2013. Establishment of a robust single axis of cell polarity by coupling multiple positive feedback loops. Nat Commun 4: 1807.

Fridy PC, Otto JC, Dollins DE, York JD (2007) Cloning and characterization of two human VIP1-like inositol hexakisphosphate and diphosphoinositol pentakisphosphate kinases. J Biol Chem 282(42): 30754-30762

Frieman, M.B. et al., (2002). Modular domain structure in the *Candida glabrata* adhesin Epa1p, a beta1,6 glucan-cross-linked cell wall protein. Mol. Microbiol. 46, 479–492.

Fuchs U, Manns I, Steinberg G. (2005). Microtubules are dispensable for the initial pathogenic development but required for long-distance hyphal growth in the corn smut fungus *Ustilago maydis*. Mol Biol Cell. 2005;16:2746–58.

G. M. Gauthier, “Dimorphism in fungal pathogens of mammals, plants, and insects,” PLoS Pathogens, vol. 11, no. 12, article e1004608, 2015.

Galperin MY, Koonin EV (1997) A diverse superfamily of enzymes with ATP-dependent carboxylateamine/thiol ligase activity. *Protein Sci* 6(12): 2639-2643

Gancedo JM (2001) Control of pseudohyphae formation in *Saccharomyces cerevisiae*. FEMS Microbiol Rev 25(1): 107-123

Gantner BN, Simmons RM, Canavera SJ, Akira S, Underhill DM. (2003) Induction of inflammatory responses by dectin-1 and Toll-like receptor 2. J Exp Med;197:1107–17.

Gantner BN, Simmons RM, Canavera SJ, Akira S, Underhill DM. (2003). Collaborative induction of inflammatory responses by dectin-1 and Toll-like receptor 2. *J Exp Med* 2003;197:1107–17.

Gantner BN, Simmons RM, Underhill DM. (2005). Dectin-1 mediates macrophage recognition of *Candida albicans* yeast but not filaments. EMBO J 24: 1277–1286

Gasch A, Spellman P, Kao C, Carmel-Harel O, Eisen M, Storz G, Botstein D, Brown P (2000) Genomic Expression Programs in the Response of Yeast Cells to Environmental Changes. Mol Biol Cell. 2000 Dec; 11(12): 4241–4257

Gauthier GM, Klein BS (2008) Insights into fungal morphogenesis and immune evasion. Microbe 3: 416–423. PMID: 20628478

Gilmore SA, Naseem S, Konopka JB, Sil A (2013) N-acetylglucosamine (GlcNAc) triggers a rapid, temperature-responsive morphogenetic program in thermally dimorphic fungi. PLoS Genet 9(9): e1003799. doi:10.1371/journal.pgen.1003799

Gimeno CJ, Ljungdahl PO, Styles CA, Fink GR (1992). "Unipolar cell divisions in the *yeast S. cerevisiae* lead to filamentous growth: regulation by starvation and RAS." Cell 68(6): 1077-90.

Girbardt M. 1957. Der Spitzenkörper von Polystictus versicolor The Spitzenkorper of Polystictus versicolor. Planta 50: 47–59.

Glennon MC, Shears SB (1993) Turnover of inositol pentakisphosphates, inositol hexakisphosphate and diphosphoinositol polyphosphates in primary cultured hepatocytes. *Biochem J* 293 (Pt 2): 583-590

Glynn JM, Lustig RJ, Berlin A, Chang F (2001) Role of bud6p and tea1p in the interaction between actin and microtubules for the establishment of cell polarity in fission yeast. Curr Biol 11(11): 836-845

Gokhale NA, Zaremba A, Shears SB (2011) Receptor-dependent compartmentalization of PPIP5K1, a kinase with a cryptic polyphosphoinositide binding domain. *Biochem J*. 2011 Mar 15;434(3):415-26.

Gregory M. Gauthier(2017).. Fungal dimorphism and virulence: molecular mechanisms for temperature adaptation, immune evasion, and *in Vivo* Survival. Mediators of Inflammation Volume 2017, Article ID 8491383.

Gu, C., Nguyen, H.N., Hofer, A., Jessen, H.J., Dai, X., Wang, H., and Shears, S.B. (2017). The significance of the bifunctional kinase/phosphatase activities of diphosphoinositol pentakisphosphate kinases (PPIP5Ks) for coupling inositol pyrophosphate cell signaling to cellular phosphate homeostasis. J Biol Chem *292*, 4544-4555.

Gunasekera A, Alvarez FJ, Douglas LM, Wang HX, Rosebrock AP, Konopka JB. (2010). Identification of GIG1, a GlcNAc-induced gene in *Candida albicans* needed for normal sensitivity to the chitin synthase inhibitor nikkomycinZ. Eukaryot Cell 9: 1476–1483.

Guo B, Styles CA, Feng Q, Fink GR (2000) A *Saccharomyces* gene family involved in invasive growth, cell-cell adhesion, and mating. Proc Natl Acad Sci U S A 97(22): 12158-12163

Gutz, H. and F. J. Doe (1973). "Two Different h Mating Types in *Schizosaccharomyces pombe*." Genetics 74(4): 563-9.
Hagan IM, Hyams JS (1988) The use of cell division cycle mutants to investigate the control of microtubule distribution in the fission yeast *Schizosaccharomyces pombe*. J Cell Sci 89(Pt 3): 343-357

Hansen J, Cherest H, Kielland-Brandt MC(1994). Two divergent MET10 genes, one from *Saccharomyces cerevisiae* and one from Saccharomyces carlsbergensis, encode the alpha subunit of sulfite reductase and specify potential binding sites for FAD and NADPH. J Bacteriol 176(19):6050-8

Harris SD, Read ND, Roberson RW, Shaw B, Seiler S, Plamann M, Momany M. (2005). Polarisome meets spitzenkorper: Microscopy, genetics, and genomics converge. Eukaryot Cell 4: 225–229.

Harris SD. (1999).Morphogenesis is coordinated with nuclear division in germinating *Aspergillus nidulans* conidiospores. Microbiology 145: 2747–2756.

Hlavatá, L., H. Aguilaniu, A. Pichová, and T. Nyström, (2003). The oncogenic RAS2(val19) mutation locks respiration, independently of PKA, in a mode prone to generate ROS. EMBO J. 22: 3337–3345.

Hoffman, C. S. and F. Winston (1991). "Glucose repression of transcription of the *Schizosaccharomyces pombe* fbp1 gene occurs by a cAMP signaling pathway." Genes Dev 5(4): 561-71.

Hogan DA, Sundstrom P. (2009). The Ras/cAMP/PKA signaling pathway and virulence in *Candida albicans*. Future Microbiol 4: 1263–1270

Holbrook ED, Rappleye CA (2008) *Histoplasma capsulatum* pathogenesis: making a lifestyle switch. Curr Opin Microbiol 11(4): 318-324

Howell AS, Lew DJ. (2012).Morphogenesis and the cell cycle. Genetics 190: 51–77.

Hoyer, L.L., (2001). The ALS gene family *of Candida albicans*. Trends Microbiol. 9, 176–180.

Huang D, Friesen H, Andrews B (2007) Pho85, a multifunctional cyclin-dependent protein kinase in budding yeast. *Mol Microbiol* 66(2): 303-314

Huh WK, Falvo JV, Gerke LC, Carroll AS, Howson RW, Weissman JS, O'Shea EK (2003). Global analysis of protein localization in budding yeast. Nature 425(6959):686-91

Iden S, Collard JG (2008) Crosstalk between small GTPases and polarity proteins in cell polarization.Nat Rev Mol Cell Biol 9(11): 846-859

Ilse D Jacobsen, Duncan Wilson,Betty Wächtler,Sascha Brunke, Julian R Naglik and Bernhard Hube (2012). *Candida albicans* dimorphism as a therapeutic target *Expert Rev. Anti Infect. Ther.* 10(1), 85–93 (2012)

Ingram SW, Safrany ST, Barnes LD (2003) Disruption and overexpression of the *Schizosaccharomyces pombe aps1* gene, and effects on growth rate, morphology and intracellular diadenosine 5',5"'-P1,P5-pentaphosphate and diphosphoinositol polyphosphate concentrations. Biochem J 369(Pt 3): 519-528

Isshiki T, Mochizuki N, Maeda T, Yamamoto M (1992) Characterization of a fission yeast gene, gpa2, that encodes a G alpha subunit involved in the monitoring of nutrition. Genes Dev 6(12B): 2455-2462

Iung AR1, Coulon J, Kiss F, Ekome JN, Vallner J, Bonaly R. (1999). Mitochondrial function in cell wall glycoprotein synthesis in *Saccharomyces cerevisiae* NCYC 625 (Wild type) and [rho(0)] mutants. Appl Environ Microbiol. 1999 Dec;65(12):5398-402.

Jessie Fernandez and Kim Orth (2017). Rise of a cereal Killer:The Biology of *Magnaporthe oryzae* Biotrophic Growth Trends in Microbiology,2017.12.007

Johnson JM, Jin M, Lew DJ.(2011). Symmetry breaking and the establishment of cell polarity in budding yeast. Curr Opin Genet Dev 21: 740–746.

Jung WH, Sham A, White R & Kronstad JW (2006) Iron regulation of the major virulence factors in the AIDS associated pathogen *Cryptococcus neoformans*. PLoS Biol 4:e410.

Justyna Karkowska-Kuleta, Maria Rapala-Kozik and Andrzej Kozik (2009). Fungi pathogenic to humans: molecular bases of virulence of *Candida albicans, Cryptococcus neoformans and Aspergillus fumigatus*. Vol. 56 No. 2/2009, 211–224.

Kamasaki T, Arai R, Osumi M, Mabuchi I (2005) Directionality of F-actin cables changes during the fission yeast cell cycle. Nat Cell Biol 7(9): 916-917

Kanetsuna F, Carbonell LM. (1971). Cell wall composition of the yeast like and mycelial forms of *Blastomyces dermatitidis*. J Bacteriol 106: 946–948.

Karkowska-Kuleta J, Rapala-Kozik M, Kozik A (2009). Fungi pathogenic to humans: molecular bases of virulence of *Candida albicans, Cryptococcus neoformans and Aspergillus fumigatus*. Acta Biochim Pol. 2009;56 (2):211-24.

Kate Chatfield-Reed, Lianne Vachon, Eun-Joo Gina Kwon, and Gordon Chua (2016). Conserved and Diverged Functions of the Calcineurin-Activated Prz1 Transcription Factor in Fission Yeast. doi: 10.1534/genetics.115.184218

Kaur, R.Domergue R, Zupancic ML, Cormack BP. (2005). A yeast by any other name: *Candida glabrata* and its interaction with the host. Curr. Opin. Microbiol. 8, 378–384.

Kawamukai M, Ferguson K, Wigler M, Young D (1991) Genetic and biochemical analysis of the adenylyl cyclase of *Schizosaccharomyces pombe*. *Cell Regul* 2(2): 155-164

Kim H, Yang P, Catanuto P, Verde F, Lai H, Du H, Chang F, Marcus S (2003) The kelch repeat protein, Tea1, is a potential substrate target of the p21-activated kinase, Shk1, in the fission yeast, Schizosaccharomyces pombe. J Biol Chem 278(32): 30074-30082

Klein BS, Tebbets B (2007) Dimorphism and virulence in fungi. Curr Opin Microbiol 10(4): 314-319

Klengel T, Liang WJ, Chaloupka J, Ruoff C, Schröppel K, Naglik JR, Eckert SE, Mogensen EG, Haynes K, Tuite MF, Levin LR, Buck J, Mühlschlegel FA. (2005). Fungal adenylyl cyclase integrates CO2 sensing with cAMP signaling and virulence. Curr Biol 15: 2021– 2026.´

Kobayashi O, Hayashi N, Kuroki R, Sone H (1998). Region of FLO1 proteins responsible for sugar recognition. J Bacteriol. 1998 Dec;180(24):6503-10.

Kobayashi O, Suda H, Ohtani T, Sone H (1996) Molecular cloning and analysis of the dominant flocculation gene FLO8 from *Saccharomyces cerevisiae*. Mol Gen Genet 251(6): 707-715

Kobayashi, O., Hayashi, N., Kuroki, R., and Sone, H. (1998) Region of FLO1 proteins responsible for sugar recognition. *J Bacteriol* 180: 6503–6510.

Kristofor J. Webb , Cecilia I. Zurita-Lopez , Qais Al-Hadid , Arthur Laganowsky , Brian D. Young , Rebecca S. Lipson , Puneet Souda , Kym F. Faull, Julian P. Whitelegge, and Steven G. Clarke. (2010). A Novel 3 Methylhistidine Modification of Yeast Ribosomal Protein Rpl3 Is Dependent upon the YIL110W Methyltransferase (2010). The journal of biological chemistry vol. 285, NO. 48, pp. 37598 –37606

Kron SJ, Styles CA, Fink GR. Symmetric cell division in pseudohyphea of the yeast *Saccharomyces cerevisiae*. Mol Biol Cell 1994; 5:1003-22.

Kulkarni RK & Nickerson KW (1981) Nutritional control of dimorphism in *Ceratocystis ulmi*. Exp Mycol 5: 148–154.

Kuramae, E. E., V. Robert, et al. (2006). "Conflicting phylogenetic position of *Schizosaccharomyces pombe*." Genomics 88(4): 387-93.

Kwon E-JG, Laderoute A, Chatfield-Reed K, Vachon L, Karagiannis J, et al. (2012) Deciphering the Transcriptional-Regulatory Network of Flocculation in *Schizosaccharomyces pombe*. PLoS Genet 8(12): e1003104. doi:10.1371/journal.pgen.1003104

La Carbona S, Le Goff C, Le Goff X (2006) Fission yeast cytoskeletons and cell polarity factors: connecting at the cortex. Biol Cell 98(11): 619 631

Lambrechts, M.G., Bauer, F.F., Marmur, J., and Pretorius, I.S. (1996) Muc1, a mucin-like protein that is regulated by Mss10, is critical for pseudohyphal differentiation in yeast. *Proc Natl Acad Sci USA* 93: 8419–8424.

Laussmann T, Eujen R, Weisshuhn CM, Thiel U, Vogel G (1996) Structures of diphospho-myo-inositol pentakisphosphate and bisdiphospho-myo-inositol tetrakisphosphate from *Dictyostelium* resolved by NMR analysis. *Biochem J* 315 (Pt 3): 715-720

Laussmann T, Pikzack C, Thiel U, Mayr GW, Vogel G (2000) Diphospho-myo-inositol phosphates during the life cycle of Dictyostelium and Polysphondylium. Eur J Biochem 267(8): 2447-2451

Lee YS, Huang K, Quiocho FA, O'Shea EK (2008) Molecular basis of cyclin-CDK-CKI regulation by reversible binding of an inositol pyrophosphate. *Nat Chem Biol* 4(1): 25-32

Lee YS, Mulugu S, York JD, O'Shea EK (2007) Regulation of a cyclin-CDK-CDK inhibitor complex by inositol pyrophosphates. *Science* 316(5821): 109-112

Lev S, Li C, Desmarini D, Saiardi A, Fewings NL, Schibeci SD, Sharma R, Sorrell TC, Djordjevic JT. (2015). Fungal inositol pyrophosphate IP7 is crucial for metabolic adaptation to the host environment and pathogenicity. mBio 6(3):e00531-15. doi:10.1128/mBio.00531-15.

Li C, Lev S, Saiardi A, Desmarini D, Sorrell TC, Djordjevic JT (2016). Identification of a major IP5 kinase in *Cryptococcus neoformans* confirms that PP-IP5/IP7, not IP6, is essential for virulence. Sci Rep. 2016 Apr 1;6:23927

Li W and Mitchell, A.P. (1997). Proteolytic activation of Rim1p, a positive regulator of yeast sporulation and invasive growth. Genetics 145, 63-73.

Lin H, Fridy PC, Ribeiro AA, Choi JH, Barma DK, Vogel G, Falck JR, Shears SB, York JD, Mayr GW (2009) Structural analysis and detection of biological inositol pyrophosphates reveal that the family of VIP/diphosphoinositol pentakisphosphate kinases are 1/3-kinases. J Biol Chem 284(3): 1863-1872

Lin, H., Fridy, P.C., Ribeiro, A.A., Choi, J.H., Barma, D.K., Vogel, G., Falck, J.R., Shears, S.B., York, J.D., and Mayr, G.W. (2009). Structural analysis and detection of biological inositol pyrophosphates reveal that the family of VIP/diphosphoinositol pentakisphosphate kinases are 1/3-kinases. J Biol Chem *284*, 1863-1872.

Linder T, Gustafsson CM (2008) Molecular phylogenetics of ascomycotal adhesins--a novel family of putative cell-surface adhesive proteins in fission yeasts. Fungal Genet Biol 45(4): 485-497

Lindner P (1893) *Schizosaccharomyces pombe* n. sp., ein neuer Gährungserreger. Wochenschr Brauerei 10: 1298-1300

Lindsey R, Momany M. (2006). Septin localization across kingdoms: three themes with variations. Curr Opin Microbiol. 2006;9:559–65

Lonetti A, et al. (2011) Identification of an evolutionarily conserved family of inorganic polyphosphate and polyphosphatases. J Biol Chem 286(37):31966–31974.

Lorenz MC, Bender JA, Fink GR. (2004). Transcriptional response of *Candida albicans* upon internalization by macrophages. Eukaryot Cell 3: 1076–1087.

Luo G, Ibrahim AS, Spellberg B, Nobile CJ, Mitchell AP, Fu Y. (2010). *Candida albicans* Hyr1p confers resistance to neutrophil killing and is a potential vaccine target J InfectDis 201: 1718–1728.

Luo HR, Huang YE, Chen JC, Saiardi A, Iijima M, Ye K, Huang Y, Nagata E, Devreotes P, Snyder SH (2003) Inositol pyrophosphates mediate chemotaxis in Dictyostelium via pleckstrin homology domain- PtdIns(3,4,5)P3 interactions. Cell 114(5): 559-572,

Luo, H. R., Y. E. Huang, J. C. Chen, A. Saiardi, M. Iijima, K. Ye, Y. Huang, E. Nagata, P. Devreotes, and S. H. Snyder. (2003). Inositol pyrophosphates mediate chemotaxis in Dictyostelium via pleckstrin homology domain- PtdIns(3,4,5)P3 interactions. Cell 114:559–572.

Luo, H.R., Huang, Y.E., Chen, J.C., Saiardi, A., Iijima, M., Ye, K., Huang, Y., Nagata, E., Devreotes, P., and Snyder, S.H. (2003). Inositol pyrophosphates mediate chemotaxis in *Dictyostelium* via pleckstrin homology domain-PtdIns(3,4,5)P3 interactions. Cell *114*, 559-572.

Madhani HD, Fink GR (1998) The control of filamentous differentiation and virulence in fungi. Trends Cell Biol 8(9): 348-353

Maeda T, Watanabe Y, Kunitomo, H, Yamamoto M, (1994). Cloning of pka1 gene encoding the catalytic subunit, of the cAMP-dependent protein kinase in *Schizosaccharomyces pombe.* J Biol Chem 269:9632-9637

Magditch DA, Liu TB, Xue C, Idnurm A. 2012. DNA mutations mediate microevolution between host-adapted forms of the pathogenic fungus *Cryptococcus neoformans*. PLoS Pathog 8: e1002936.

Maidan MM, De Rop L, Serneels J, Exler S, Rupp S, Tournu H, Thevelein JM, Van Dijck P. (2005a). The G protein coupled receptor Gpr1 and the Ga protein Gpa2 act through the cAMP-protein kinase A pathway to induce morphogenesis in *Candida albicans*. Mol Biol Cell 16: 1971–1986.

Maidan MM, Thevelein JM, Van Dijck P. Carbon source induced yeast-to-hypha transition *in Candida albicans* is dependent on the presence of amino acids and on the G-protein-coupled receptor Gpr1. Biochem Soc Trans. 2005 Feb;33(Pt 1):291-3.

Marks J, Hagan IM, Hyams JS (1986) Growth polarity and cytokinesis in fission yeast: the role of the cytoskeleton. J Cell Sci Suppl 5: 229-241

Martin SG (2009) Microtubule-dependent cell morphogenesis in the fission yeast. Trends Cell Biol 19(9): 447-454

Martin SG, Arkowitz RA. (2014). Cell polarization in budding and fission yeasts. FEMS Microbiol Rev 38: 228–253.

Martin SG, Chang F (2005) New end take off: regulating cell polarity during the fission yeast cell cycle.Cell Cycle 4(8): 1046-1049

Martin SG, Rincon SA, Basu R, Perez P, Chang F (2007) Regulation of the formin for3p by cdc42p and bud6p. Mol Biol Cell 18(10): 4155-4167

Martin-Cuadrado AB, Morrell JL, Konomi M, An H, Petit C, Osumi M, Balasubramanian M, Gould KL, Del Rey F, de Aldana CR (2005) Role of septins and the exocyst complex in the function of hydrolytic enzymes responsible for fission yeast cell separation. Mol Biol Cell 16(10): 4867-488

Masselot M and De Robichon-Szulmajster H (1975). Methionine biosynthesis in *Saccharomyces cerevisiae*. I. Genetical analysis of auxotrophic mutants. Mol Gen Genet 139(2):121-32

Mata J, Nurse P (1997) tea1 and the microtubular cytoskeleton are important for generating global spatial order within the fission yeast cell. Cell 89(6): 939-949

McLennan AG (2006) The Nudix hydrolase superfamily. Cell Mol Life Sci 63(2): 123-143

Medoff G, Kobayashi GS, Painter A, Travis S (1987): Morphogenesis and pathogenicity of Histoplasma capsulatum. Infect Immun 1987, 55:1355-1358.

Melane A. Vivier, Marius G. Lambrechts, and lsak S. Pretorius (1997). Coregulation of Starch Degradation and Dimorphism in the yeast *Saccharomyces cerevisiae.* Critical Reviews in Biochemistry and Molecular Biology, 32(5):405435 (1997)

Menniti FS, Miller RN, Putney JW, Jr., Shears SB (1993) Turnover of inositol polyphosphate pyrophosphates in pancreatoma cells. J Biol Chem 268(6): 3850-3856

Mikoshiba K1, Furuichi T, Miyawaki A, Yoshikawa S, Nakagawa T, Yamada N, Hamanaka Y, Fujino I, Michikawa T, Ryo Y, et al. (1993) Inositol trisphosphate receptor and Ca^{2+} signalling. Philos Trans R Soc Lond B Biol Sci. 1993 Jun 29;340(1293):345-9.

Mitchison JM, Nurse P (1985) Growth in cell length in the fission yeast *Schizosaccharomyces pombe*. J Cell Sci 75: 357-376

Mochizuki, N. and M. Yamamoto (1992). "Reduction in the intracellular cAMP level triggers initiation of sexual development in fission yeast." Mol Gen Genet 233(1-2): 17-24.

Moseley JB, Goode BL. The yeast actin cytoskeleton: from cellular function to biochemical mechanism. Microbiol Mol Biol Rev. 2006;70:605–45.

Moseley JB, Nurse P (2009) Cdk1 and cell morphology: connections and directions. Curr Opin Cell Biol 21(1): 82-88

Motegi F, Arai R, Mabuchi I (2001) Identification of two type V myosins in fission yeast, one of which functions in polarized cell growth and moves rapidly in the cell. Mol Biol Cell 12(5): 1367-1380

Mullaney EJ, Ullah AH (2003) The term phytases comprises several different classes of enzymes. Biochem Biophys Res Commun 312(1): 179-184

Mulugu S, Bai W, Fridy PC, Bastidas RJ, Otto JC, Dollins DE, Haystead TA, Ribeiro AA, York JD (2007) A conserved family of enzymes that phosphorylate inositol hexakisphosphate. Science 316(5821): 106-109

Nadal M, Garcia-Pedrajas MD, Gold SE (2008) Dimorphism in fungal plant pathogens. FEMS Microbiol Lett 284(2): 127-134

Nicholls S, Leach MD, Priest CL, Brown AJ. (2009). Role of the heat shock transcription factor, Hsf1, in a major fungal pathogen that is obligately associated withwarm-blooded animals. *MolMicrobiol* 2009;74:844–61

Nichols CB, Perfect Z, Alspaugh JA. 2007. A Ras1-Cdc24signal transduction pathway mediates thermotolerancein the fungal pathogen *Cryptococcus neoformans*. MolMicrobiol 63: 1118–1130.

Odds, F. C. (1985). "Morphogenesis in *Candida albicans*." Crit Rev Microbiol 12(1): 45-93.

Odom, A.R., Stahlberg, A., Wente, S.R., and York, J.D. (2000). A role for nuclear inositol 1,4,5-trisphosphate kinase in transcriptional control. Science *287*, 2026-2029.

Oliver Stehling, Ajay A. Vashish, Judita Mascarenhas1, Zophonias O. Jonsson, Tanu Sharma, Daili J. A. Netz, Antonio J. Pierik1, James A. Wohlschlegel , Roland Lill, (2012)MMS19 Assembles Iron-Sulfur Proteins Required for DNA Metabolism and Genomic Integrity Science 13 Jul 2012: Vol. 337, Issue 6091, pp. 195-199

Onnebo SM, Saiardi A (2009) Inositol pyrophosphates modulate hydrogen peroxide signalling. Biochem J 423(1): 109-118

Ostanin K, Harms EH, Stevis PE, Kuciel R, Zhou MM, Van Etten RL (1992). Overexpression, site-directed mutagenesis, and mechanism of *Escherichia coli* acid phosphatase. J Biol Chem. 1992 Nov 15;267(32):22830-6.

References

Ostanin K, Van Etten RL (1993) Asp304 of *Echerichia coli* acid phosphatase is involved in leaving group protonation. J Biol Chem. 1993 Oct 5;268(28):20778-84

Palecek SP, Parikh AS, Kron SJ (2002) Sensing, signalling and integrating physical processes during *Saccharomyces cerevisiae* invasive and filamentous growth. Microbiology 148(Pt 4): 893-907.

Pascual-Ortiz M, Saiardi A, Walla E, Jakopec V, Künzel NA, Span I, Vangala A, Fleig U. Asp1 Bifunctional Activity Modulates Spindle Function via Controlling Cellular Inositol Pyrophosphate Levels in *Schizosaccharomyces pombe*. Mol Cell Biol. 2018 Apr 16;38(9).

Pasricha S, Payne M, Canovas D, Pase L, Ngaosuwankul N, Beard S, Oshlack A, Smyth GK, Chaiyaroj SC, Boyce KJ, Andrianopoulos A. (2013). Cell-type-specific transcriptional profiles of the dimorphic pathogen *Penicillium marneffe*i reflect distinct reproductive, morphological, and environmental demands. G3: Genes, Genomes, Genet. 2013; 3:1997–2014.

Pasricha S, Schafferer L, Lindner H, Joanne Boyce K, Haas H, Andrianopoulos A. (2016). Differentially regulated high-affinity iron assimilation systems support growth of the various cell types in the dimorphic pathogen *Talaromyces marneffei*. Mol Microbiol. 2016; 102:715–737.

Pelletier B, Beaudoin J, Mukai Y & Labbe S (2002) Fep1, an iron sensor regulating iron transporter gene expression in *Schizosaccharomyces pombe*. J Biol Chem 277: 22950–22958.

Pennisi, E.(2010)Armed and dangerous. Science 327, 804–805

Perfect JR , Arturo Casadevall (2006). Chapter 1: Fungal Molecular Pathogenesis: What can it do and why do we need it? Fungal Molecular Pathogenesis:

Perfect JR, Casadevall A (2006) Fungal molecular pathogenesis: what can it do and why do we need it? In *Molecular principles of fungal pathogenesis*. Heitman J, Filler SG, Edwards JE Jr, Mitchell AP, eds, pp 3–11. ASM Press, Washington DC.

Pesesse X, Choi K, Zhang T, Shears SB (2004) Signaling by higher inositol polyphosphates. Synthesis of bisdiphosphoinositol tetrakisphosphate ("InsP8") is selectively activated by hyperosmotic stress. *J Biol Chem* 279(42): 43378-43381

Peter A. Fantes and Charles S. Hoffman, (2016). A Brief History of *Schizosaccharomyces pombe* Research: A Perspective Over the Past 70 Years. Genetics. 2016 Jun; 203(2): 621–629.

Piel M, Tran PT (2009) Cell shape and cell division in fission yeast. *Curr Biol* 19(17): R823-827

Pöhlmann J, Fleig U (2010) Asp1, a conserved 1/3 Inositol polyphosphate kinase, regulates the dimorphic switch in *Schizosaccharomyces pombe*. Mol Cell Biol. 2010 Sep;30 (18):4535-47

Pöhlmann J, Risse C, Seidel C, Pohlmann T, Jakopec V, et al. (2014) The Vip1 Inositol Polyphosphate Kinase Family Regulates Polarized Growth and Modulates the Microtubule Cytoskeleton in Fungi. PLoS Genet 10(9): e1004586. doi:10.1371/journal.pgen.1004586

Pulloor, N.K., Nair, S., Kostic, A.D., Bist, P., Weaver, J.D., Riley, A.M., Tyagi, R., Uchil, P.D., York, J.D., Snyder, S.H., *et al.* (2014). Human genome-wide RNAi screen identifies an essential role for inositol pyrophosphates in Type-I interferon response. PLoS Pathog *10*, e1003981.

Quinn CC, Wadsworth WG (2008) Axon guidance: asymmetric signaling orients polarized outgrowth.Trends Cell Biol 18(12): 597 603

Ramage G, Martinez JP, Lopez-Ribot JL. (2006). *Candida* biofilms on implanted biomaterials: a clinically significant problem. FEMS Yeast Res.6:979 –986.

Rhind, N., Z. Chen, et al. (2011). "Comparative functional genomics of the fission yeasts." Science 332(6032): 930-6

Richardson MD (2005) Changing patterns and trends in systemic fungal infections. *J Antimicrob Chemother* 56: 5–11.

Rigden, D.J. (2008). The histidine phosphatase superfamily: structure and function. Biochem J *409*, 333-348.

Riquelme M, Fischer R, Bartnicki-Garcia S (2003) Apical growth and mitosis are independent processes in Aspergillus nidulans. Protoplasma 222(3-4): 211-215

Riquelme M. (2013). Tip growth in filamentous fungi: A road trip to the apex. Annu Rev Microbiol 67: 587–609.

Rocha CR, Schroppel K, Harcus D, Marcil A, Dignard D, Taylor BN, Thomas DY, Whiteway M, Leberer E. (2001). Signaling through adenylyl cyclase is essential for hyphal growth and virulence in the pathogenic fungus *Candida albicans*. Mol Biol Cell 12: 3631–3643

Roeder A, Kirschning CJ, Rupec RA(2004) Toll-like receptors as key mediators in innate antifungal immunity. *Med Mycol* 2004;42:485–98.

Rui Jin, Craig J. Dobry, Phillip J. McCown, and Anuj Kumar (2008). Large-Scale Analysis of Yeast Filamentous Growth by Systematic Gene Disruption and Overexpression. Molecular Biology of the Cell Vol. 19, 284–296.

Rupp S, Summers E, Lo HJ, Madhani H, Fink G (1999) MAP kinase and cAMP filamentation signaling pathways converge on the unusually large promoter of the yeast FLO11 gene. Embo J 18(5): 1257-1269

Safrany ST, Caffrey JJ, Yang X, Bembenek ME, Moyer MB, Burkhart WA, Shears SB (1998) A novel context for the 'MutT' module, a guardian of cell integrity, in a diphosphoinositol polyphosphate phosphohydrolase. *Embo J* 17(22): 6599-6607

Safrany ST, Ingram SW, Cartwright JL, Falck JR, McLennan AG, Barnes LD, Shears SB (1999) The diadenosine hexaphosphate hydrolases *from Schizosaccharomyces pombe* and *Saccharomyces cerevisiae* are homologues of the human diphosphoinositol polyphosphate phosphohydrolase. Overlapping substrate specificities in a MutT-type protein. *J Biol Chem* 274(31): 21735-21740

Saiardi A (2012) How inositol pyrophosphates control cellular phosphate homeostasis?

Saiardi A, Bhandari R, Resnick AC, Snowman AM, Snyder SH (2004) Phosphorylation of proteins by inositol pyrophosphates. Science 306(5704): 2101-2105

Saiardi A, Caffrey JJ, Snyder SH, Shears SB (2000) The inositol hexakisphosphate kinase family. Catalytic flexibility and function in yeast vacuole biogenesis. J Biol Chem 275(32): 24686-24692

Saiardi, A., Bhandari, R., Resnick, A.C., Snowman, A.M., and Snyder, S.H. (2004). Phosphorylation of proteins by inositol pyrophosphates. Science *306*, 2101-2105.

Saiardi, A., Erdjument-Bromage, H., Snowman, A.M., Tempst, P., and Snyder, S.H. (1999). Synthesis of diphosphoinositol pentakisphosphate by a newly identified family of higher inositol polyphosphate kinases. Curr Biol *9*, 1323-1326.

Saiardi, A., Nagata, E., Luo, H.R., Sawa, A., Luo, X., Snowman, A.M., and Snyder, S.H. (2001). Mammalian inositol polyphosphate multikinase synthesizes inositol 1,4,5-trisphosphate and an inositol pyrophosphate. Proc Natl Acad Sci U S A *98*, 2306-2311.

Sanna ML, Zara S, Zara G, Migheli Q, Budroni M, Mannazzu I. *Pichia fermentans* dimorphic changes depend on the nitrogen source. Fungal Biol-Uk. 2012;116(7):769–77. pmid:22749163

Schuchardt I, Assmann D, Thines E, Schuberth C, Steinberg G. (2005). Myosin-V, Kinesin-1, and Kinesin-3 cooperate in hyphal growth of the fungus Ustilago maydis. Mol Biol Cell. 2005;16:5191–201.

Seider K, Heyken A, Luttich A, Miramon P, Hube B. (2010). Interaction of pathogenic yeasts with phagocytes: Survival, persistence and escape. Curr Opin Microbiol 13: 392–400.

Seitz-Mayr G, Wolf K. (1982) Extrachromosomal mutator inducing point mutations and deletions in mitochondrial genome of fission yeast. Proc Natl Acad Sci U S A. 1982 Apr;79(8):2618-22.

Sharifpoor S, Van Dyk D, Costanzo M, Baryshnikova A, Friesen H, Douglas AC, Youn JY, VanderSluis B, Myers CL, Papp B, Boone C, Andrews BJ (2012) Functional wiring of the yeast kinome revealed by global analysis of genetic network motifs. Genome Res 22(4):791-801

Shears SB (2009) Diphosphoinositol polyphosphates: metabolic messengers? Mol Pharmacol 76(2):236-252

Sheppard DC, Yeaman MR, Welch WH, Phan QT, Fu Y, Ibrahim AS, Filler SG, Zhang M, Waring AJ, Edwards JE Jr. (2004). Functional and structural diversity in the Als protein family of *Candida albicans*. J. Biol. Chem. 279, 30480–30489.

Shimoda, C. (2004). "Forespore membrane assembly in yeast: coordinating SPBs and membrane trafficking." J Cell Sci 117(Pt 3): 389-96

Shin, D. Y., K. Matsumoto, H. Iida, I. Uno, and T. Ishikawa, 1987 Heat shock response of *Saccharomyces cerevisiae* mutants altered in cyclic AMP-dependent protein phosphorylation. Mol. Cell. Biol. 7: 244–250.

Siegrist SE, Doe CQ (2007) Microtubule-induced cortical cell polarity. Genes Dev 21(5): 483-496

Simonetti N, Strippoli V, Cassone A (1974). Yeast-mycelial conversion induced by N-acetyl-D-glucosamine in *Candida albicans*. Nature. 1974 Jul 26;250(464):344-6.

Sipiczki M, Grallert B, Miklos I. (1993) . Mycelial and syncytial growth in *Schizosaccharomyces pombe* induced by novel septation mutations. J Cell Sci 1993; 104:485-93.

Sipiczki, M., K. Takeo, et al. (1998). "Environmentally controlled dimorphic cycle in a fission yeast." Microbiology 144 (Pt 5): 1319-30.

Sipiczki, M., K. Takeo, et al. (1998). "Growth polarity transitions in a dimorphic fission yeast." Microbiology 144 (Pt 12): 3475-85.

Snaith HA, Sawin KE (2003) Fission yeast mod5p regulates polarized growth through anchoring of tea1p at cell tips. Nature 423(6940): 647-651

Snaith HA, Thompson J, Yates JR, Sawin KE. (2011). "Characterization of Mug33 reveals complementary roles for actin cable-dependent transport and exocyst regulators in fission yeast exocytosis." J Cell Sci 124:2187-2199 2011

Srinivasa K1, Kim J, Yee S, Kim W, Choi W (2012). A MAP kinase pathway is implicated in the pseudohyphal induction by hydrogen peroxide in *Candica albicans*. Mol Cells. 2012 Feb;33(2):183-93.

Staab JF, Bradway SD, Fidel PL, Sundstrom P. (1999). Adhesive and mammalian transglutaminase substrate properties of *Candida albicans* Hwp1. Science 283: 1535–1538.

Steinberg G (2007) Hyphal growth: a tale of motors, lipids, and the Spitzenkorper. Eukaryot Cell 6(3): 351-360

Steinberg G. (2007). Tracks for traffic: microtubules in the plant pathogen Ustilago maydis. New Phytol. 2007;174:721–33

Stephens L, Radenberg T, Thiel U, Vogel G, Khoo KH, Dell A, Jackson TR, Hawkins PT, Mayr GW (1993). The detection, purification, structural characterization, and metabolism of diphosphoinositol pentakisphosphate(s) and bisdiphosphoinositol tetrakisphosphate(s). J Biol Chem. 1993 Feb 25;268(6):4009-15

Stratford, M. (1989) Evidence for two mechanisms of flocculation in *Saccharomyces cerevisiae*. *Yeast* 5 (Spec No.): S441–S445.

Sudbery P. 2011a. Fluorescent proteins illuminate the structure and function of the hyphal tip apparatus. Fungal Genet Biol 48: 849–857.

Szijgyarto Z, Garedew A, Azevedo C, Saiardi A (2011) Influence of inositol pyrophosphates on cellular energy dynamics. Science 334:802–805

Szijgyarto Z, Garedew A, Azevedo C, Saiardi A (2011) Influence of inositol pyrophosphates on cellular energy dynamics. Science 334(6057):802–805.

Tanaka N, Awai A, Bhuiyan MS, Fujita K, Fukui H, Takegawa K (1999) Cell surface galactosylation is essential for nonsexual flocculation in *Schizosaccharomyces pombe*. *J Bacteriol* 181(4): 1356-1359

Tatebe H, Nakano K, Maximo R, Shiozaki K (2008) Pom1 DYRK regulates localization of the Rga4 GAP to ensure bipolar activation of Cdc42 in fission yeast. Curr Biol 18(5): 322-330

Tatebe H, Shimada K, Uzawa S, Morigasaki S, Shiozaki K (2005) Wsh3/Tea4 is a novel cell-end factor essential for bipolar distribution of Tea1 and protects cell polarity under environmental stress in *S. pombe*. Curr Biol 15(11): 1006-1015

Terenna CR, Makushok T, Velve-Casquillas G, Baigl D, Chen Y, Bornens M, Paoletti A, Piel M, Tran PT (2008) Physical mechanisms redirecting cell polarity and cell shape in fission yeast. Curr Biol 18(22): 1748-1753

Teunissen AW, Steensma HY (1995). The dominant flocculation genes of *Saccharomyces cerevisia*e constitute a new subtelomeric gene family. Yeast. (1995) Sep 15;11(11):1001-13.

Thevelein, J. M., and J. H. de Winde, 1999 Novel sensing mechanisms and targets for the cAMP-protein kinase A pathway in the yeast *Saccharomyces cerevisiae*. Mol. Microbiol. 33: 904–918.

Thota, S.G., and Bhandari, R. (2015). The emerging roles of inositol pyrophosphates in eukaryotic cell physiology. J Biosci *40*, 593-605

References

Thota, S.G., Unnikannan, C.P., Thampatty, S.R., Manorama, R., and Bhandari, R. (2015). Inositol pyrophosphates regulate RNA polymerase I-mediated rRNA transcription in *Saccharomyces cerevisiae*. Biochem J *466*, 105-114.

Tomee JF, Kauffman (2000). Putative virulence factors of *Aspergillus fumigatus*. Clin Exp Allergy. 2000 Apr;30(4):476-84.

Tomohiko Matsuzawa, Tomotake Morita, Naotaka Tanaka, Hideki Tohda and Kaoru Takegawa (2011) Identification of a galactose-specific flocculin essential for non-sexual flocculation and filamentous growth in *Schizosaccharomyces pombe*, Molecular Microbiology (2011) 82(6), 1531–1544

Topolski B, Jakopec V, Künzel NA, Fleig U. Inositol Pyrophosphate Kinase Asp1 Modulates Chromosome Segregation Fidelity and Spindle Function in *Schizosaccharomyces pombe*. Molecular and Cellular Biology. 2016;36(24):3128-3140. doi:10.1128/MCB.00330-16.

Veelders, M., Bruckner, S., Ott, D., Unverzagt, C., Mosch, H.U., and Essen, L.Q. (2010) Structural basis of flocculin mediated social behavior in yeast. *Proc Natl Acad Sci USA* 107: 22511–22516.

Verdin J, Bartnicki-Garcia S, Riquelme M. 2009. Functional stratification of the Spitzenkorper of *Neurospora crassa*.Mol Microbiol 74: 1044–1053.

Verstrepen KJ, Klis FM (2006) Flocculation, adhesion and biofilm formation in yeasts. Mol Microbiol 60(1): 5-15

Verstrepen, K.J., Derdelinckx, G., Verachtert, H., and Delvaux, F.R. (2003) Yeast flocculation: what brewers should know. *Appl Microbiol Biotechnol* 61: 197–205.

Verstrepen, K.J., Klis, F.M., (2006). Flocculation, adhesion and biofilm formation in yeasts. Mol. Microbiol. 60, 5–15.

Volling K, Thywissen A, Brakhage AA, Saluz HP.(2011). Phagocytosis of melanized Aspergillus conidia by macrophages exerts cytoprotective effects by sustained PI3K/ Akt signalling. Cell Microbiol 13: 1130–1148.

Wang L, Lin X (2012) Morphogenesis in Fungal Pathogenicity: Shape, Size, and Surface. PLoS Pathog 8(12): e1003027. doi:10.1371/journal.ppat.1003027

Wang Y. (2009). CDKs and the yeast–hyphal decision. Curr Opin Microbiol 12: 644–649.

Wedlich-Soldner R, Altschuler S,Wu L, Li R. (2003). Spontaneous cell polarization through actomyosin-based delivery of the Cdc42 GTPase. Science 299: 1231–1235.

Wendland J (2001) Comparison of morphogenetic networks of filamentous fungi and yeast. Fungal Genet Biol 34(2): 63-82

Wilson, M.S., Livermore, T.M., and Saiardi, A. (2013). Inositol pyrophosphates: between signalling and metabolism. Biochem J *452*, 369-379.

Wolf K1, Del Giudice L.(1980) Effect of ethidium bromide on transmission of mitochondrial genomes and DNA synthesis in the petite negative yeast Schizosaccharomyces pomhe. Curr Genet. 1980 Apr;1(3):193-7.

Wood V, Bähler J.(2002).Hhow to get the best from fission yeast genome data. Comparative and Functional Genomics Volume 3 (2002), Issue 3, Pages 282-288

Wood, K.V., Lam, Y.A. & McElroy, W.D. (1989) Introduction to beetle luciferases and their applications. *J Biolumin Chemilumin* 4: 289-301.

Wood, K.V., Lam, Y.A., McElroy, W.D. & Seliger, H.H. (1989) Bioluminescent click beetles revisited. *J Biolumin Chemilumin* 4: 31-39.

Wood, V., R. Gwilliam, et al. (2002). "The genome sequence of *Schizosaccharomyces pombe*." Nature 415(6874): 871-80.

Wundenberg T1, Mayr GW. (2012). Synthesis and biological actions of diphosphoinositol phosphates (inositol pyrophosphates), regulators of cell homeostasis. Biol Chem. 2012 Sep;393(9):979-98

Xiaorong Lin, J. Andrew Alspaugh,Haoping Liu, and Steven Harris (2015). Fungal Morphogenesis Cold Spring Harb Perspect Med. 2015 Feb; 5(2): a019679.

Yamamoto M., Imai Y,.and Watanabe Y (1997).Mating and sporulation in *shizosaccharomyces pombe*.In *The* Molecular and Cellular Biology of the Yeast *Saccharomyces spp*.1037–1106

Yang L, Reece JM, Cho J, Bortner CD, Shears SB (2008) The nucleolus exhibits an osmotically regulated gatekeeping activity that controls the spatial dynamics and functions of nucleolin. *J Biol Chem* 283(17): 11823-11831

York JD, Hunter T (2004) Signal transduction. Unexpected mediators of protein phosphorylation. *Science* 306(5704): 2053-2055

York, J.D. (2006). Regulation of nuclear processes by inositol polyphosphates. Biochim. Biophys. Acta 1761: 552–559.

York, J.D., Odom, A.R., Murphy, R., Ives, E.B., and Wente, S.R. (1999). A phospholipase C-dependent inositol polyphosphate kinase pathway required for efficient messenger RNA export. Science *285*, 96-100.

York, S.J., Armbruster, B.N., Greenwell, P., Petes, T.D., and York, J.D. (2005). Inositol diphosphate signaling regulates telomere length. J Biol Chem *280*, 4264-4269.

Yoshida T, Toda T, Yanagida M. A calcineurin-like gene *ppb1*$^{+}$ in fission yeast: Mutant defects in cytokinesis, cell polarity, mating and spindle pole body positioning. J Cell Sci 1994; 107:1725-35.

Zarnack K, Feldbrugge M (2007) mRNA trafficking in fungi. Mol Genet Genomics 278(4): 347-359

Zou H, Fang HM, Zhu Y, Wang Y.(2009). *Candida albicans* Cyr1, Cap1 and G-actin form a sensor/effector apparatus for activating cAMP synthesis in hyphal growth. Mol Microbiol 75: 579–591.

Zhao Z-S, Leung T, Manser E, Lim L. 1995. Pheromone signalling in Saccharomyces cerevisiae requires the small GTP-binding protein Cdc42p and its activator CDC24.Mol Cell Biol 15: 5246–5257.

Zuin A, Gabrielli N, Calvo IA, Garcı´a-Santamarina S, Hoe K-L, et al. (2008) Mitochondrial Dysfunction Increases Oxidative Stress and Decreases Chronological Life Span in Fission Yeast. PLoS ONE 3(7): e2842. doi:10.1371/journal.pone.0002842

6. Abbreviations

IP_6	Inositolhexakisphosphate
IP_7	Diphosphoinositolpentakisphosphate (1-IP_7)
IP_8	1,5-bisdiphosphoinositol tetrakisphosphate (1,5-IP_8)
ATP	Adenosine triphosphate
PKA	Protein kinase A
MAP	mitogen activated protein
bp	base pairs
C-terminal	carboxy-terminus
N-terminal	Amino terminal
DNA	desoxyribonucleinacid
GFP	green fluorescent protein
dH_2O	distilled water
ddH_2O	double distilled water
dNTPs	deoxy nucleotides
EtOH	ethanol
g	gram
h	hours
kb	kilo base pairs
kDa	kilo Dalton
L	liter
M	molar
mA	milliampere
min	minute
mg	milligram
ml	milliliter
mM	mill molar
µg	microgram
µl	microliter
µM	micro molar
ms	milliseconds
nm	nanometer
OD	optical density
ORF	open reading frame
PCR	polymerase chain reaction
pH	potential of hydrogen
pmol	pikomole
x^R	resistance
rpm	revolutions per minute
RT	room temperature
U	units
V	volume

Δ	gene deletion
VC	Vector control
cAMP	Cyclic Adenosinmonophosphate
NETO	new end take off
YE5S	Full medium (*S. pombe)*
EMM	Edinburgh-Minimal medium
MM	Minimal media
Thia	Thiamine
kann	kanamycin
amp	ampicillin
lucG	Green light emitting luciferase
lucR	Red light emitting luciferase
Rmax	Maximum light intensity
C. neoformans	*Cryptococcus neoformans*
A. fumigatus	*Aspergillus fumigatus*
S. cerevisiae	*Saccharomyces cerevisiae*
A. nidulans	*Aspergillus nidulans*
C. albicans	*Candida albicans*
D. discoideum	*Dictyostelium discoideum*
E. coli	*Escherichia coli*

7. List of Figures **Page number**

Figure 1: The cell cycle and polarized growth of *S. pombe* during the cell cycle…….…..6

Figure 2: The organization of an *S. pombe* growth zone and the role of actin and microtubule skeleton.....12

Figure 3: Dimorphic switch in *S. pombe*……...16

Figure 4: A model depicting the transcriptional regulatory network regulating adhesins in *S. pombe*……...……..20

Figure 5: Generation of inositol pyrophosphates. ..……...23

Figure 6: Diagrammatic representation of functions of inositol pyrophosphates in different organisms and their diverse cellular process …….…….....8

Figure 7: Diagrammatic representation of the structure of Vip1 inositol polyphosphates kinase family.....29

Figure 8: Asp1 generated inositol pyrophosphates regulated cellular processes in *S. pombe*…….……...……..34

Figure 9: Lower temperatures induce a higher number of invasive colonies and require Asp1 kinase activity…….....72

Figure 10: Excess iron in the media induces invasive growth in the absence of functional Asp1 kinase domain……74

Figure 11: Asp1 variants displayed a similar number of invasively growing colonies irrespective of the media……..76

Figure 12: Asp1 and Asp1$^{1-364}$ expression levels by various *nmt1* promoters…..……79

Figure 13: Asp1$^{1-364}$ levels have to be modulated for the efficient dimorphic switch…….....81

Figure 14: Loss of pyrophosphatase activity by the exchange of conserved amino acids led to increased invasive growth. …….…….....85

Figure 15: Summary of Asp1 variants and their inositol pyrophosphate output and their growing ability to grow invasively. ……86

Figure 16: Gsf2 is the essential flocculin required for the Asp1 dependent invasive growth.90

Figure 17: Strain expressing *gsf2* under the *nmt41* promoter…….....91

Figure 18: Increased expression of adhesin Gsf2 increases the number of invasively growing colonies but only in the presence of 1,5-IP_8 . …….....92

Figure 19: Positive transcriptional factors (regulators) of the adhesin Gsf2 are required for Asp1 dependent invasive growth…….……94

Figure 20: *rfl1*Δ strain displayed decreased invasively growing colonies in the absence of *asp1*$^+$…….96

Figure 21: Gsf2 expression levels vary with varying 1,5-IP_8 levels…….97

Figure 22: The *gsf2*$^+$ promoter activity is varied with varying 1,5-IP_8 levels. …….98

Figure 23: The *gsf2*$^+$ promoter activity is varied with varying 1,5-IP_8 levels analysed by GFP reporter assay……...…...100

Figure 24: Gsf2 promoter activity is varied with varying 1,5-IP_8 levels analyzed by luciferase assay…….....102

Figure 25: Asp1 does not interact with itself in a yeast two-hybrid assay……..104

Figure 26: Interaction of Hpm1 to Asp1 via the N-terminal domain..……107

Figure 27: Asp1 interaction with Met10 through its C-terminal pyrophosphatase domain..109

Figure 28: Invasive growth analysis of endogenously expressing *asp1*$^{1\text{-}364}$ strain……111

Figure 29: Heat shock tolerance of Asp1 strains……...112

Figure 30: Asp1 interaction with SPBC725.03 through its N-terminal Kinase domain …..114

Figure 31: Asp1 interacts with Hem12 through its N-terminal Kinase domain…….....115

Figure 32: Model for the regulatory mechanism of Asp1 kinase generated different classes of inositol pyrophosphates…….....124

Figure 33: Model for the mechanism of Asp1 induced invasive colonies……128

8. List of Tables

Table 1: Levels of inositol pyrophosphates in Asp1 variants strains in *vivo* and *in vitro*…..35

Table 2: Deletion of potential adhesins and their ability of to grow invasively ……88

Table 3: Summary of the genes deletions encoding transcription regulators and their invasive growth ability……..……..…93

Table 4: Asp1 interactors identified via yeast two-hybrid screen……104

9. Publications

Pascual-Ortiz M, Saiardi A, Walla E, Jakopec V, Künzel NA, Span I, **Vangala A,** Fleig U. (2018). Asp1 Bifunctional Activity Modulates Spindle Function via Controlling Cellular Inositol Pyrophosphate Levels in *Schizosaccharomyces pombe*. Molecular and Cellular Biology 2018 Apr 16;38(9). doi: 10.1128/MCB.00047-18.

10.Acknowledgements

I would like to express my gratitude to all the people who have given me support for the past few years to encourage me to finish this project.

First and foremost, I would like to thanks a million my “Doktormutter” Prof. Dr. Ursula Fleig for giving me an opportunity to peruse my PhD. I am indebted for her never ending encouragement during my tough times especially at the beginning and end of my PhD. She taught me how research works and fed me with a lot of insightful discussions. She was supportive in several ways that she is something more than just a “Doktormutter”

I am grateful to my co-supervisor Prof. Dr. Johannes Hegemann to co-supervise me and for his supportive advices and comments during the follow-up meetings and lab seminars. I would also further extend my gratitude to Prof. Dr. Joachim Ernst, for allowing me to perform the luciferase assays in his laboratory, which was a great help for my thesis.

I whole heartedly thank all the former and current members of the lab for providing such a work friendly environment. I thank Dr.Visnja Jakopec, for her support during my PhD with injecting me with her invaluable suggestions and lab experience. I would specially thank Eva Walla for her never ending support in the lab as well as smooth running of the laboratory. I cannot imagine the lab without “two beautiful roses” Marina and Natascha. Their presence made the lab a lovely place and working with them has given me life time memories and made me forget my home. I am grateful for bringing the lab fun to my flat too. I thank “Mother Nature” for gifting you as friends (Philosophy ☺). I also thank Laase, Patrick for supporting me in the lab and extending the fun further. I am thankful to all the members of the Hegemann lab for their invaluable support and discussion in the seminars, nice talks and games during barbeque and Christmas parties. I would specially like to thank Coco and Alison for their support and especially for her delicious tiramisu.

Thanks to the MOI graduate school and the colleagues for having a good time during the MOI meetings. I would also like to thank Dr.Inge Krümpelbeck for being supportive and intimating me with the curriculum and final dates for several reports.

This could have not been possible without my “Oldenburg family members” especially Veera, Maya, Veeya, Pratik, Chinmay, Lisa, Chui, Preseela, and Vinay and also friends from Müncheberg Bianka, Eileen, Rene, Caro, Gabriele, Muqit, Tamanna and Aahil for having fun during the weekends and making me forget home.

నన్ను కష్ట పడి చదివించినందుకు మా అమ్మ నాన్నలకి ఏమి చెప్పాలో తెలియటం లేదు. వాళ్ళు ఎన్నో సుఖాలు వదులుకొని, త్యాగాలు చేసి, వాళ్ళకి దూరంగా వున్నా పర్వాలేదు అనుకోని, మమ్మలిని చదివించారు. మా అమ్మ నాన్న లు వెనక ఉండీ నన్ను ప్రోత్సహించక పోతే ఇది సాధించే వాడిని కాదు. వారి త్యగానికి నా నమస్కారములు. మా అక్కలు బావలు అన్నయ వదిన, తేజ మరియు ప్రణవ్, ప్రేమ ప్రోత్సాహం లేనిదే ఇది సాధించే వాడిని కాదు. వాళ్ళ ప్రేమ అభిమానం వల్లే నేను ఇవాళ ఇది సాధించ గలిగాను. ఇలా నన్ను ఎల్లప్పుడూ నన్ను వెనక ఉండీ ప్రోత్సహించినందుకు కృతజ్ఞతలు. నన్ను ప్రోత్సహించిన మామయ్య గారికి అత్తయ్యగారికి మరదలకి నా కృతజ్ఞతలు. నా సంతోషం కోసం నిరంతరం కోరుకునే మా కుటంబ సభ్యులకి స్నేహితులకి నా కృతజ్ఞతలు.

I have no words to express my love, to the wonderful person in my life who entered my life as a friend, and now became an inseparable part of me i.e. my lovely wife. This could not have been possible without her support and patience. Thank you for sharing life with me and I will never be exhausted in cheering you up. We fought together a lot of hurdles in life and with your love and support we can achieve anything in this world. As I always say “You cannot stop anything from happening, so we will better be happy”

11.Statutory Declaration

I declare under oath that I have compiled my dissertation independently and without any undue assistance by third parties under consideration of the 'Principles for the Safeguarding of Good Scientific Practice at Heinrich Heine University Düsseldorf'.

I declare that I have not used sources or means without declaration in the text. All the passages taken from other works in the wording or in the meaning have been clearly indicated with sources. This thesis has not been used in the same or similar version to achieve an academic grading or is being published elsewhere.

Düsseldorf,

Anand Babu Vangala